Applications of Hydrogen Borrowing in the Synthesis of Carbocycles and Novel Dopamine Transporter Inhibitors

Francisco Oscar Battiti

St. Peter's College

A thesis submitted for the degree of Doctor of Philosophy in the

University of Oxford Hillary Term 2026

Abstract

This thesis is comprised of two projects conducted at Oxford University and the National Institute on Drug Abuse – Intramural Research Program. The first project focused on developing methodology using Hydrogen borrowing (HB) which has been shown to be a useful tool for the construction of poly-substituted cyclohexane and 1-acyl-cyclohexenes starting from an ortho-disubstituted aryl methyl ketone and 1,5-pentanediols. Herein we report a method for the one-pot HB-mediated cyclization of an ortho-disubstituted aryl methyl ketone and 1,5-pentanediols and subsequent aromatization of the resulting cyclic system to generate arenes in modest to good yields. Furthermore, controlling chirality at the α-stereocenter in the cyclohexanes formed under HB is a difficult challenge due to epimerization under basic conditions. We investigated the feasibility of controlling the α-stereocenter in 2,3-disubstituted 1-acyl-cyclohexane. However, this effort was ultimately unsuccessful.

The second project focused on the design, synthesis and in vitro evaluation of a series of modafinil analogues as novel atypical dopamine transporter (DAT) inhibitors. Psychostimulant use disorder (PSUD) is a public health crisis for which there remains no effective medical treatment. Psychostimulants such as cocaine and methamphetamine target the DAT and block the reuptake of dopamine (DA). The resulting rapid increase in synaptic DA, particularly in the mesolimbic brain region, effects the subjective feelings of "high" that for some can lead to the development of addiction. Although these classic DAT inhibitors are highly addictive, another class of DAT inhibitors that do not share this psychostimulant behavioral profile have emerged as potential medications for the treatment for PSUD. These "atypical" DAT inhibitors also block DA reuptake into the dopaminergic neuron, but the increase in DA is neither rapid nor nearly as high as that produced by cocaine or methamphetamine. Importantly, these compounds do not demonstrate any addictive liability in laboratory animals. Furthermore, these atypical DAT inhibitors can prevent cocaine or methamphetamine from binding DAT and thus block their psychostimulant actions, in vivo.

Modafinil is an FDA-approved drug for the treatment of narcolepsy that functions as a weak DAT inhibitor (K_i = 2.52 ± 0.2 μM) and demonstrates some atypical DAT inhibitor properties.

Nevertheless, its poor solubility and low DAT binding affinity preclude it from being effective in treating PSUD. In an attempt to improve its pharmacological profile, we report a series of modafinil-like analogues wherein we replace the primary amide of the parent compound with a triazole and substitute one of the terminal phenyl rings with a 3-Br, creating a chiral benzylic center. Our lead compound reported is compound **217** (K_i = 78.3 ± 14 nM) with higher affinity for DAT than the parent compound or typical DAT inhibitors such as cocaine, and excellent selectivity over other monoamine transporters (e.g., ~100-fold selective for DAT over SERT). We further identified the most active stereoisomer of **217** to be **217C**, with a DAT K_i = 22.3 ± 3 nM and over 1000-fold selectivity over SERT.

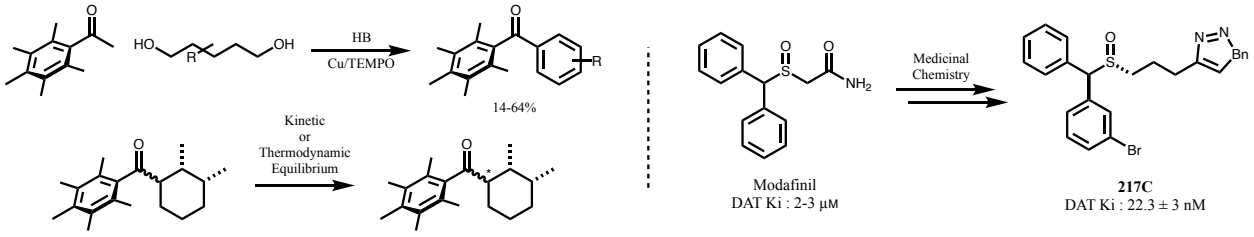

Acknowledgements

I'd like to first thank my two advisors Prof. Tim Donohoe and Dr. Amy Newman for their guidance and support. To Tim I'll always be grateful for the opportunity I was given, for ensuring I was always more than welcome in the lab, that even though life through some curve balls my way you treated me with compassion and understanding. To Amy, it's hardly fair to try and encompass everything I'm grateful to you for after working together for so many years, I can only hope to do it justice in person before I head on to my next adventure.

I have been blessed to have worked with so many incredible people in two different groups in two different countries in two different continents. At Oxford, I couldn't be more grateful to Jess, Lydia, Andrew, little Tim and Teddy for making me feel at home away from home. I'm grateful to Bruno, Nik, Ciaran, Hannah, Dana, Lewis, Dani, Mo, Sam, Matt, and Aaron for their friendship and for making the TJD lab just a great place to work. You all helped me in countless ways, I can only hope you all know that.

I've worked with so many people at the NIH it's starting to feel like the village Amy always refers to when discussing how many people it takes to make scientific research work. Immense thank you to the entire NIH OxCam program, for their unwavering support, and for giving me the opportunity to be a part of this undertaking. To Prof. Alessandro Bonifazi, I can't thank you enough for everything you did for me early on in my career. I am forever grateful to all that you did for me and once again it feels almost unfair to try and put it all together here, I look forward to working together again one day. Thank you to Emma and to Gisela whose friendships I value immensely still. To Renata who's been with me through absolutely everything, I don't know where one could find a better friend. To Marta who makes me laugh more than anyone else. Thank you Laia, Miguel, Nick, Victoria, Diego, y Jazon…you all know just how much you mean to me and how I

can never come close to thanking you enough for all you've done. Thank you to Renee for keeping me humble and to Khorshada for keeping me entertained. Thank you, Brad, for not only being a friend but for saving my life with binding more than once. To Caleb for every bit of help, advice, interesting conversation, and for painstakingly double checking every CNMR in this thesis. To Kuo Hao for being a guiding light in the lab and *in silico*. Also huge thank you to Brenna, I would probably be out of a job because of some super important thing that I didn't realize I had to right away if it wasn't for you.

Thank you to Olivia for all the emotional support you've been, sitting next to me day in and day out, while I was writing. Lastly, thank you to my mom and dad, never has anyone supported me and believed in me quite like you, I carry that with me always.

Declaration

All the work described herein is my own unless otherwise specified, no portion of this work has been previously used, partially or in full, for another qualification in this or other institute.

Excluding figure captions, references, diagrams, and the appendix, the text of this thesis contains approximately 49857 words.

Francisco Battiti

January 2026

Table of Contents

ABSTRACT I

ACKNOWLEDGEMENTS III

DECLARATION V

TABLE OF CONTENTS VI

ABBREVIATIONS IX

1 INTRODUCTION: HYDROGEN BORROWING 1

1.1 Introduction to Hydrogen Borrowing 1
1.1.1 Introduction to Hydrogen Borrowing Concept 1
1.1.2 Early C-N bond forming Hydrogen Borrowing 4
1.1.3 Early C-C bond forming Hydrogen Borrowing 7
1.2 Hydrogen Borrowing coupled to Aldol Condensation 8
1.2.1 Early attempts to Aldol Condensation in HB 8
1.2.2 Control of carbonyl reduction 9
1.3 Hydrogen Borrowing employing ortho disubstituted aryl methyl ketone 12
1.3.1 Identification of optimal ortho disubstituted aryl methyl ketone 12
1.3.2 Acyclic Systems 14
1.3.3 Cyclic Systems 17
1.4 Acceptorless Dehydrogenation 20
1.5 Ph* Cleavage 22

2 HYDROGEN BORROWING CYCLIZATION AND AROMATIZATION 24

2.1 Introduction to Cyclization and Aromatization Design 24
2.2 Aerobic Palladium mediated cyclization and aromatization 26
2.3 Palladium mediated aromatization 30
2.3.1 Optimization of Palladium aromatization 30
2.3.2 Substrate scope of the palladium mediated aromatization 33
2.3.3 One-pot Ph* ketone-diol cyclization and aromatization 34
2.4 Copper and TEMPO mediated Aromatization 35
2.4.1 Introduction to Copper and TEMPO dehydrogenation 35
2.4.2 Application of Copper and TEMPO system to cyclohexenes 37
2.5 Ph* Cleavage of diaryl ketone substrates. 45
2.6 Conclusion 46

3 STEREOCHEMICAL CONTROL OF ALPHA-STEREOCENTERS IN POLYSUBSTITUTED CYCLOHEXANES 47

3.1 INTRODUCTION TO STEREOCHEMICAL CONTROL IN HB (5+1) ANNULATION 47
3.1.1 GENERAL CONSIDERATIONS 47
3.1.2 STEREOCONTROL OF THE GAMMA-STEREOCENTER 48
3.1.3 ISSUES WITH DIOL CYCLIZATION 49
3.2 CONTROL OF THE ALPHA-STEREOCENTER IN 75 AND 76 53
3.2.1 THERMODYNAMIC CONTROL 54
3.2.2 KINETIC CONTROL AND SILYL ENOL ETHERS AS ENOLATE PRECURSOR 57
3.2.3 PH* REMOVAL 60
3.2.4 FORMATION OF KETENE AND INTERCEPTION 61
3.3 SUBSTRATES BEYOND 2,3-DIMETHYL-CYCLOHEXANE 62
3.4 CONCLUSIONS 64

4 INTRODUCTION: DAT AND DAT INHIBITORS 66

4.1 INTRODUCTION TO DAT AND DAT INHIBITORS 66
4.1.1 INTRODUCTION TO DOPAMINE 66
4.1.2 DA AND DRUG ABUSE 67
4.1.3 DA AND DAT 69
4.1.4 DRUGS OF ABUSE AS DAT INHIBITORS 71
4.2 ATYPICAL DAT INHIBITORS 73
4.2.1 RISE OF ATYPICAL DAT INHIBITORS 73
4.2.2 WHAT MAKES A DAT INHIBITOR ATYPICAL? 75
4.2.3 ATYPICAL DAT INHIBITORS AS TREATMENT FOR PSUD 78
4.3 SAR OF MODAFINIL ANALOGUES 80
4.3.1 FIRST GENERATION OF MODAFINIL ANALOGUES 80
4.3.2 SECOND GENERATION OF MODAFINIL ANALOGUES AND JJC-COMPOUNDS 84
4.3.3 NEW APPROACH AT MODAFINIL ANALOGUES 86

5 SYNTHESIS OF MODAFINIL ANALOGUES AS DAT INHIBITORS 90

5.1 INITIAL DRUG DESIGN 90
5.2 FIRST SYNTHETIC APPROACH FOR MAKING MODAFINIL ANALOGUES 92
5.2.1 PROPARGYL THIOL AS A BUILDING BLOCK AND FIRST SERIES OF ANALOGUES 92
5.2.2 CHANGING PROPARGYL THIOL FOR ALKENYL-TIPS PROPARGYL THIOL 95
5.2.3 COMPUTATIONAL PREDICTIONS AND SHIFT TO N-BENZYL TRIAZOLES 99
5.3 FIRST GENERATION OF MODAFINIL ANALOGUES 101
5.3.1 NEW PROPOSED SYNTHETIC ROUTE 101
5.3.2 RADIOLIGAND BINDING STUDIES RESULTS FOR FIRST GENERATION OF MODAFINIL ANALOGUES 107
5.4 SECOND GENERATION OF MODAFINIL ANALOGUES 111
5.4.1 SYNTHESIS OF EXTENDED CHAIN THIOLS AND IMIDAZOLE THIOLS 111
5.4.2 SYNTHESIS OF SECOND GENERATION OF ANALOGUES 116
5.4.3 RADIOLIGAND BINDING STUDIES ON SECOND GENERATION OF MODAFINIL ANALOGUES 119
5.5 STEREOISOMERS OF 217 123

5.6 Computational Studies of 217 124
5.7 Conclusions 128

6 CONCLUSION AND FUTURE WORK 131

7 REFERENCES 133

8 EXPERIMENTAL PROCEDURES AND METHODS 162

8.1 General Considerations 162
8.2 Experimental Methods 164
8.2.1 Radioligand Binding Studies 164
8.2.2 General Procedures 164
8.2.3 Data for Chapter 2 169
8.2.4 Data for Chapter 3 194
8.2.5 Data for Chapter 5 219
8.2.4 Computational Methods 288
8.2.5 References for Experimental section 289

9 APPENDIX 292

Abbreviations

Ac	acetyl
acac	acetylacetone
Ar	aryl
aq	aqueous
BHT	butylated hydroxytoluene
Bn	benzyl
Bu	butyl
°C	degree(s) Celsius
cm-1	wavenumber(s)
cod	1,5-cyclooctadiene
COSY	Correlation Spectroscopy
Cp*	pentamethylcyclopentadienyl
Cy	cyclohexyl
DA	dopamine
DAT	dopamine transporter
DBU	1,8-diazabicyclo[5.4.0]undec-7-ene
DCM	dichloromethane
DIBAL-H	diisobutylaluminium hydride
DMAP	4-dimethylaminopyridine
DMF	N,N-dimethylformamide
DMSO	dimethyl sulfoxide
dppb	1,4-Bis(diphenylphosphino)butane
d.r.	diastereomeric ratio
DTBM	3,5-di-tert-butyl-4-methoxyphenyl
eq.	equivalent(s)
e.r.	enantiomeric ratio
ESI	electrospray ionisation
Et	ethyl
EWG	electron-withdrawing group
FCC	Flash Column Chromatography
g	gram(s)
h	hour(s)
[H]	hydride
HFIP	hexafluoroisopropanol
HPLC	high performance liquid chromatography
HRMS	high resolution mass spectrometry
HSQY	Heteronuclear Single Quantum coherence Spectroscopy
IR	infrared spectroscopy
J	coupling constant (Hz)
L	ligand
LA	Lewis acid
LDA	lithium diisopropylamide
M	molarity, mol dm-3

mCPBA	meta-chloroperoxybenzoic acid
m.p.	melting point
Me	methyl
MeCN	acetonitrile
Mes	mesityl
min	minute(s)
mL	millilitre(s)
mol	mole(s)
MPV	Meerwein-Pondorf-Verley
Ms	methanesulfonyl
NET	Norepinephrine Transporter
NMR	Nuclear Magnetic Resonance spectroscopy
nOe	Nuclear Overhauser effect
NOESY	Nuclear Overhauser Effect Spectroscopy
Nuc	nucleophile
o	ortho
[ox]	oxidation
p	para
PG	protecting group
Ph	phenyl
Ph*	pentamethylphenyl
PhMe	toluene
PMP	4-methoxyphenyl
ppm	parts per million
Pr	propyl
PSUD	psychostimulant use disorder
q	quartet
Quant.	quantitative
R	generic substituent
[red]	reduction
r.t.	room temperature
sat.	saturated
SERT	serotonin transporter
t	tertiary alkyl group, tert-alkyl
TBAF	tetra-n-butylammonium fluoride
Temp	temperature
TFA	trifluoroaceticacid
THF	tetrahydrofuran
Tol	4-methylphenyl
Ts	toluenesulfonyl
UV	ultraviolet
νmax	infrared absorption maximum
X	generic halide

1 Introduction: Hydrogen Borrowing

1.1 Introduction to Hydrogen Borrowing

1.1.1 Introduction to Hydrogen Borrowing Concept

Hydrogen Borrowing (HB) is a powerful methodology for the formation of new carbon-carbon and carbon-nitrogen bonds. Conceptually, HB consists of a traditional transfer hydrogenation, wherein the substrate that undergoes the original oxidation (loss of H2) undergoes an intermediate reaction, and then is subsequently reduced (gain of H2). (Figure 1) Traditionaly, HB will use an alcohol as an alkylating agent, exploiting the richer chemistry available to it's corresponding carbonyl. With the use of transition metal catalysis, the alcohol (**I**, Figure 1) is dehydrogenated to the more reactive ketone or aldehyde (**II**), concomitantly generating a metal-hydride species. This carbonyl species may then undergo an intermediate reaction (i.e. aldol condensation) to generate an unsaturated intermediate (**III**) which can be reduced by the metal hydride species generated in the first step thereby "returning" the "borrowed" hydrogen and generating a saturated product (**IV**). The irreversibility of the final step serves to drive the reaction equilibrium forward.[1] Importantly, a wide variety of intermediate reactions may be achieved within the HB paradigm, highlighting the versatility of this method: Wittig, amination, conjugate addition, and Friedel-Crafts reactions.[2–8]

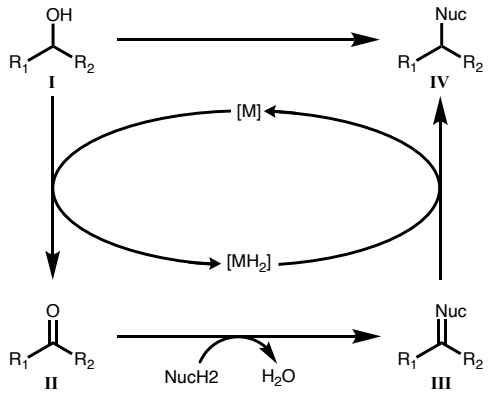

Figure 1: General HB reaction pathway.

By enabling the use of simple alcohols as reactive electrophiles, this methodology replaces traditional electrophiles (i.e. alkyl halides) in alkylation reactions, which often produce toxic waste and side-products.[7] In fact, the sole byproduct of HB reactions is water, resulting in excellent atom economy and the minimization of chemical waste, providing a sustainable and green alternative to classic methods.[10]

The term "borrowing of hydrogen" (borrowing hydrogen and HB are used interchangeably and denote the same process) was first coined in 2004 by Jonathan Williams who reported the alkylation of benzylic alcohols through a ruthenium-complex mediated HB reaction coupled with an intermediate Wittig reaction, a sample reaction from that paper is shown below, where thiophenemethanol **1** undergoes a [Ru] mediated oxidation, Wittig, and reduction to afford thiophene derivative **2**.[20] (Figure 2A) Though the term was not used prior to 2004, functional HB reactions have been employed for decades. The first known example of this reactivity is the Guebert Reaction.[11] Reported in 1899, Guebert reported the dimerization of 1-butanol under basic conditions and heat (200 °C). Shown in Figure 2B, following oxidation of alcohol **I** under atmospheric oxygen, the resulting butaldehyde **II** dimerizes through an intermediate

intramolecular aldol condensation to reveal the enone **III**. Under reaction conditions the enone is subsequently reduced by two equivalents of the butanol alkoxide *via* a Meerwein-Ponndorf-Verley (MPV)-like hydride transfer to afford the dimerized product **IV**.

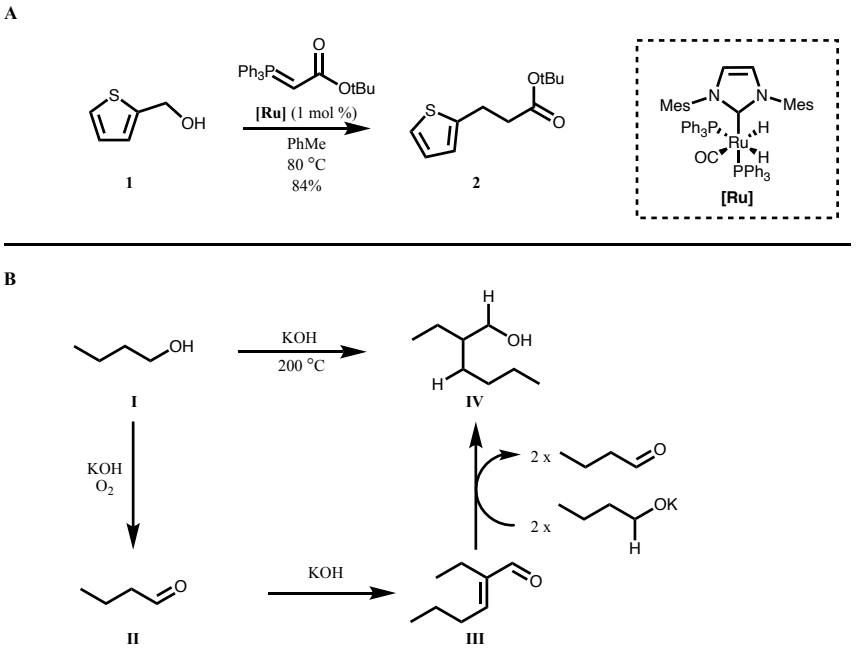

Figure 2: A) Sample reaction from Edwards *et al*. (2004).[20] B) Guebert Reaction and reaction pathway.

Early developments in HB methodologies centered around the formation of carbon-nitrogen bonds. Within the context of HB, the known condensation of amines with carbonyls to form an intermediate imine poses a good opportunity as it can be consequently reduced by the metal hydride. Traditional amine alkylating methods require conventional alkylating agents (i.e. alkyl halides) or aldehydes for reductive amination which are traditionally less commercially available and less stable than their corresponding alcohol. HB allows for the *in situ* formation of a carbonyl from alcohols, which can undergo the desired condensation, and subsequently reduce the resulting imine in a single multi-step sequence.[2] Though the use of HB in the formation of carbon-nitrogen

bonds is beyond the scope of the current work, we briefly highlight the developments in this area insofar as they predate the use of HB in carbon-carbon bond formation methodologies and as such contributed to their eventual development. Discussed below are key examples of early carbon-nitrogen forming reactions where the authors propose a HB reaction pathway, examples where a different reaction pathway is proposed are not included.

1.1.2 Early C-N bond forming Hydrogen Borrowing

Grigg and coworkers are largely cited as the first to report a homogenous catalytic system of amine alkylation through a HB strategy. They reported in 1981 the alkylation of a series of primary and secondary amines with primary alcohols in excellent yields with a series or iridium and rhodium catalysts[12] (select example in Figure 3A). They also showed the power of this technique to form nitrogen heterocycles through an intermolecular cyclization with 1,4-amino alcohols (Figure 3A). The reaction is described as proceeding through a HB sequence of oxidation and formation of a metal-hydride complex, imine formation, and subsequent reduction of the imine by the metal-hydride species to regenerate the catalyst. This work was followed in 1982 by the Murahashi lab, mindful of the potential of this approach for the construction of N-heterocycles, they describe the synthesis of a series of intramolecular cyclizations of amino acids to construct saturated N-heterocycles (such as piperazine **3**) and the construction of tetrahydroisoquinolines (i.e. **4**) in excellent yields. They also show this methodology can be used to access the 1,2,3,4,6,7,12,12b-Octahydroindolo[2,3-a]quinolizine (**5**) scaffold (backbone to a myriad of natural products) from tryptamine and 1,5-pentanediol in albeit a low yield (Figure 3B). Note that two C-N bonds and one C-C bond are formed in this reaction. They postulate the reaction pathway to be consistent

with the modern conception of HB.[13] That same year the lab of Antonio Arcelli in Bologna would similarly report their own amine alkylation with saturated alcohols using $RuCl_2(PPh_3)_3$ and postulating a HB reaction pathway.[14]

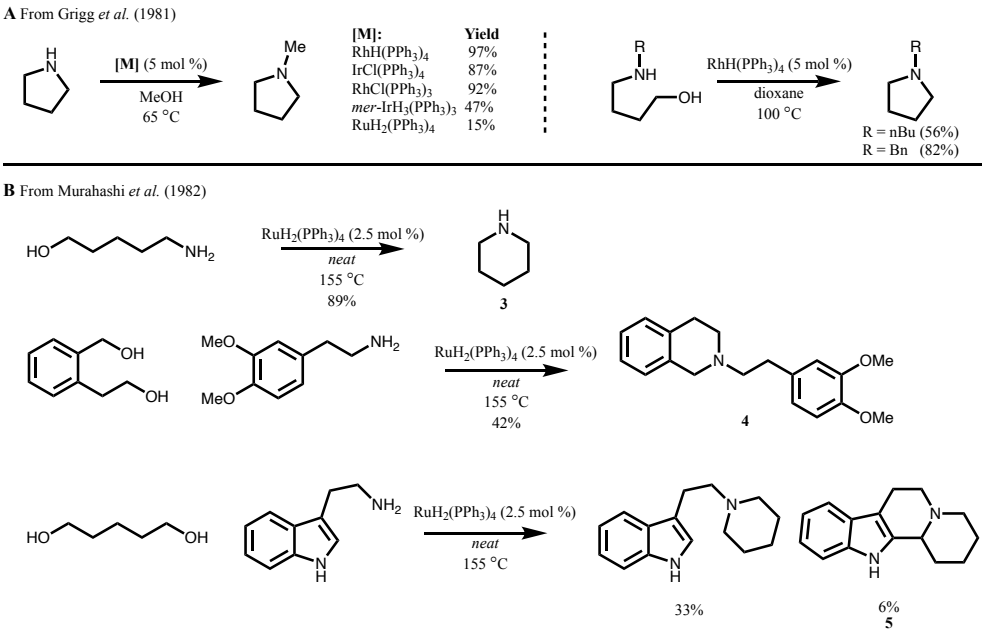

Figure 3: A) Sample of the first Hydrogen Borrowing report. B) Select examples from Murahashi *et al*. (1982) using HB for the synthesis of heterocycles.

The Watanabe group played an important role in expanding this chemistry in a series of papers spanning the 1980's. As early as 1981 they reported a $RuCl_2(PPh_3)_3$ catalyzed system for the alkylation of anilines with alcohols. Of particular interest, they show this chemistry can be employed using 2,3-unsaturated alcohols to yield a series of 2,3-alkylquinolines (Figure 4).[15] The reaction is reported as indeed proceeding through oxidation of the alcohol by the ruthenium catalyst, followed by formation of the Schiff base, and reduction of the imine by the Ru-H_2 species.

The Watanabe group would expand their $RuCl_2(PPh_3)_3$ catalyzed HB system for both the alkylation of anlines with a series of unactivated alcohols,[16.] and more interestingly the synthesis of piperidines, morpholines (**6**), and piperazines (**7**) from the corresponding diols and aniline in excellent yields (Figure 4).[17] They explicitly point to a hydrogen borrowing pathway in both studies, in the later their RuCl2(PPh3)3 catalyst first oxidizes one hydroxyl end of the diol, following condensation with aniline the ruthenium-hydrogen reduces the imine, and then the cycle repeats intermolecularly with the second hydroxy group. Their group later extended this methodology to alkylate aminopyridines as well.[18]

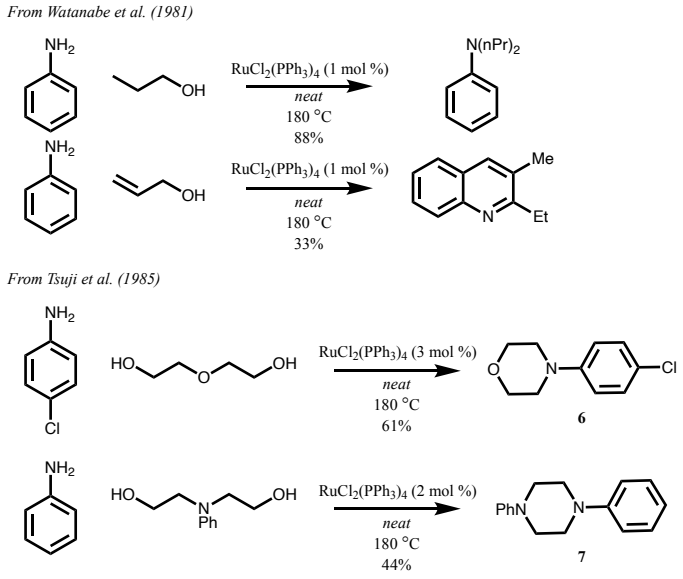

Figure 4: Select examples of early HB development by the Watanabe group.

1.1.3 Early C-C bond forming Hydrogen Borrowing

Perhaps the earliest example of deliberately generating C-C bonds by means of a HB strategy also came from Ronald Grigg's group in 1981, wherein they report the alkylation of arylacetonitriles with primary alcohols in modest to good yields (Figure 5). They note that ruthenium, rhodium, and iridium catalysts could all afford this transformation and propose that it indeed went through a HB pathway, where in the aldehyde formed from dehydrogenation by the metal catalyst would undergo a Knoevenagel condensation with benzyl cyanide, the α,β-unsaturated nitrile is subsequently reduced by the metal-hydrogen species.[19] Despite this early example, HB as a strategy to form C-C bonds wouldn't gain momentum until in the early 2000's.

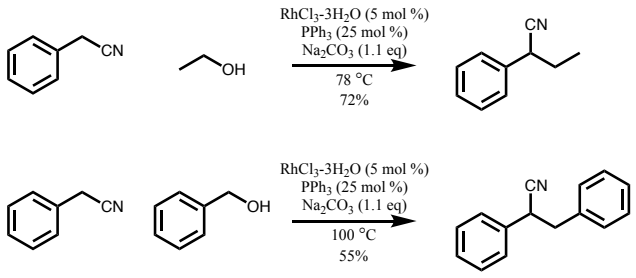

Figure 5: First example of C-C bond formation via HB.

An early strategy which had some success came from the lab of Jonathan Williams who reported an "indirect Wittig reaction of alcohols".[7] Using an $[IrCl(cod)]_2$/dppp system, they demonstrated that a series of benzylic alcohols (**I**) could be oxidated in situ to the aldehyde (**II**), this could undergo a traditional Wittig reaction with β-carbonyl phosphonates, and the resulting α,β-unsaturated system (**III**) subsequently reduced to yield the saturated product (**IV**). (Figure 6) The group would continue to develop a ruthenium-based system using $Ru(IMes)(PPh_3)_2(CO)H_2$ which would allow for milder conditions (80C vs 150C when using $[IrCl(cod)]_2$/dppp).[20]

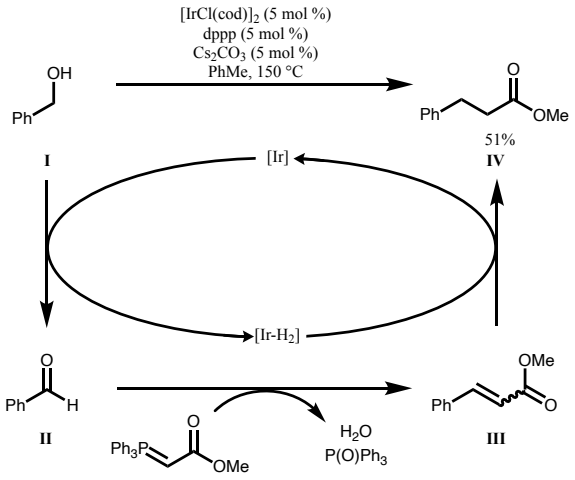

Figure 6: Original HB-Wittig reaction reported by the Williams group.

1.2 Hydrogen Borrowing coupled to Aldol Condensation

1.2.1 Early attempts to Aldol Condensation in HB

Alpha alkylation of ketones with alcohols, via HB couple to an intermediate aldol condensation, was shown by Cho *et al*. to be a promising new C-C bond forming transformation as early as 2001.[21] They report the alpha alkylation of acetophenone with a series of primary alcohols under relatively mild conditions using $RuCl_2(PPh_3)_3$, often the catalyst of choice for HB since the 1980's. At this point, it was not possible to prevent the reduction of the resulting ketone (**I**) (Figure 7) which would be further reduced to the racemic alcohol (**II**). By increasing the reaction temperature, they could drive the reduction of the carbonyl intermediate **I** to completion. They report the reaction as being feasible (albeit at slightly lower yields) at 25 °C but at the expense of having a mixture of carbonyl **I** and alcohol **II** products. The reaction also requires three equivalents of the starting alcohol substrate to ensure full reduction of the carbonyl **I** product. They would require

the addition of 1 eq of 1-dodecene as a sacrificial hydrogen acceptor to prevent over reduction of the product.[22]

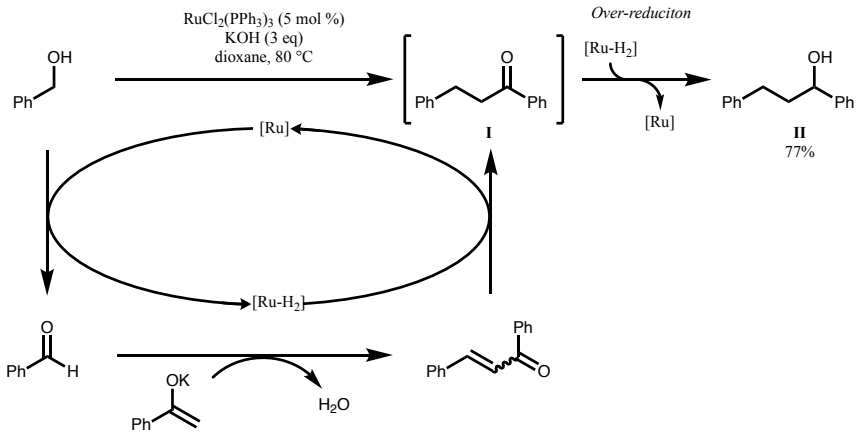

Figure 7: First HB-Aldol condensation reaction reported by Cho *et al*. (2001).[21]

1.2.2 Control of carbonyl reduction

Preventing overreduction of the resulting ketone is usually desirable, as the carbonyl is a more versatile functional handle for further manipulation. Taguchi *et al*. described the first hydrogen-acceptor free HB process for the α-alkylation of methyl ketones.[23] Inspired by their earlier work using $[Ir(cod)Cl]_2$ as a transfer hydrogenation catalyst, they realized an $[Ir(cod)Cl]_2$/dppp/Cs_2CO_3 system would readily facilitate the selective transfer hydrogenation of 2-propanol (as H_2 source) to the alkene of α,β-unsaturated carbonyls.[24] Importantly, they noticed that the system selectively reduces the olefin of the enones tested, leaving the carbonyl untouched. They speculate this reactivity is largely due to preferential coordination of the iridium hydride complex to the olefin double bond over the carbonyl, noting that reduction of the saturated ketone is significantly slower than the olefin under reaction conditions. The group further postulated that this system would work

under a HB paradigm to alkylate methyl ketones: it could effectively oxidize an alcohol (**I** in Figure 8) and, following an intermediate aldol condensation with aldehyde **II**, selectively reduce the enone **III** to the ketone (**IV**). (Figure 8)[23] They would show that a $[Ir(cod)Cl]_2/PPh_3/KOH$ system was optimal to afford the desired reactivity. Shown in Figure 8 are the two alcohol substrates (butanol and benzyl alcohol) tested with acetophenone. However they tested a series of aromatic and aliphatic methyl ketones with great success (yields ranging between 47-96%) as well as a an extensive series of primary alcohols.

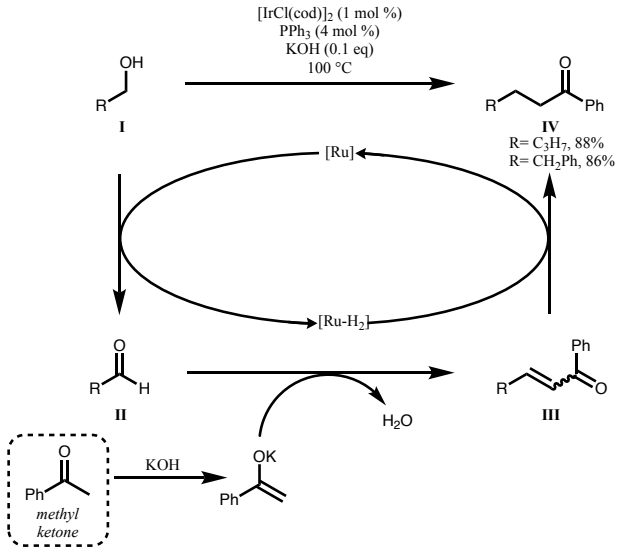

Figure 8: First efficient HB-aldol condensation reported by Taguchi *et al*. (2004),[23] acetophenone was selected as the sample methyl ketone for this general example.

A series of catalytic system with such reductive selectivity would then be developed in quick succession. The Yus lab reported extensive work using $RuCl_2(DMSO)_4$ for the α-alkylation of methyl ketones (though primarily acetophenone), where the extent of the final reduction [ketone vs alcohol] could be controlled by the equivalents of alcohol substrate used.[25–27] A system utilizing aluminum hydroxide-supported palladium was developed by the Park group in 2005 and showed

excellent versatility in facilitating the mono α-alkylation of a wide range of aryl- and aliphatic-methyl ketones with both benzyl and aliphatic alcohols with excellent yields.[28] The same year, Chan Sik Cho reported the same reaction can be catalyzed by palladium on carbon to similar effect, with admittedly lower yields.[29] The decade that follow would see increased interest in the area and a plethora of new catalysts would be explored seeking to use more inexpensive and readily available metals such as iron,[30] nickel,[31,32] manganese,[33] cobalt,[34] among others.[9]

Despite continued work and interest in the area, a major limitation to this methodology remained largely unresolved. These alkylation methods were largely limited to methyl ketones and using primary alcohols as the electrophile source, limiting accessible substrates to linear mono alpha-substituted ketones. This would be a challenging obstacle to overcome: branched ketones (as opposed to methyl ketones) showed significantly lower alkylation yields due to the increased steric bulk at the enolate. In addition, using secondary alcohols as electrophiles requires an aldol condensation with a ketone instead of an aldehyde; which is less preferred electronically and sterically, prone to undergo retro-aldol, and self-condensation with a second unit of the ketone substrate becomes a competing pathway. Attempts at addressing this key limitation saw varying levels of success though ultimately were largely limited to the α-methylation of ketones (Figure 9).[35–39]

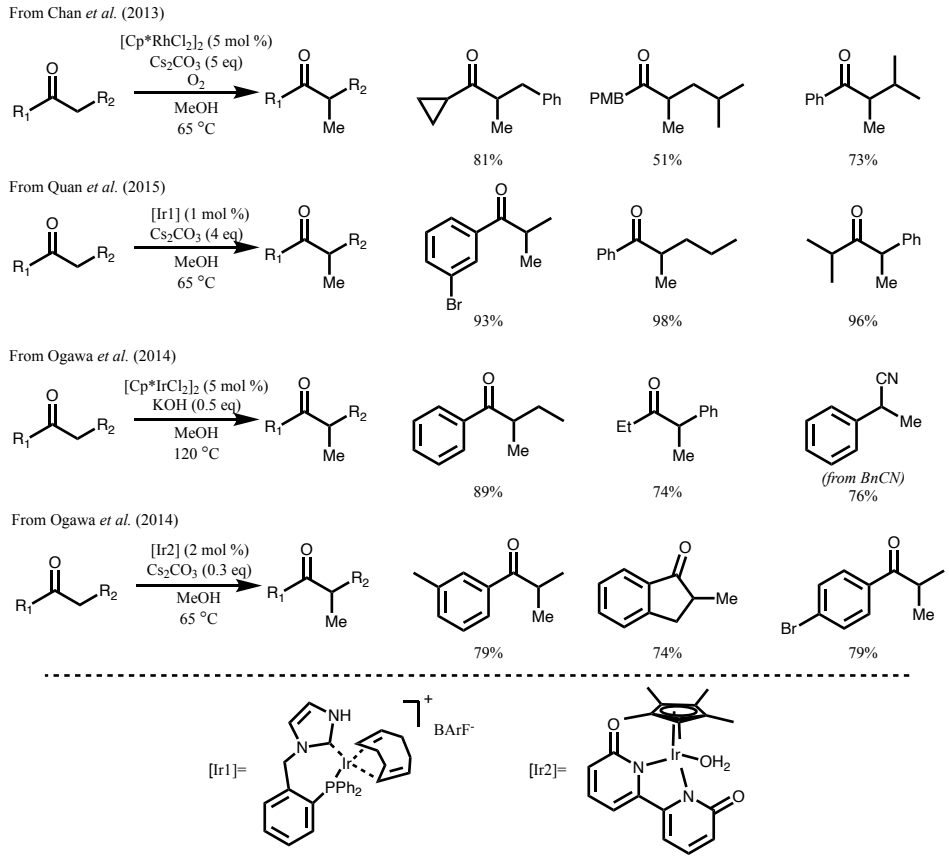

Figure 9: Selected examples of HB used in the synthesis of α-branched ketones.

1.3 Hydrogen Borrowing employing ortho disubstituted aryl methyl ketone

1.3.1 Identification of optimal ortho disubstituted aryl methyl ketone

The first major breakthrough would come from the Donohoe lab and their insight that an *ortho*-disubstituted aryl methyl ketone could solve this issue.[40] The result of an *ortho*-disubstitution pattern in the aryl methyl ketone (Figure 10) is the aryl ring becomes twisted out of conjugation from the carbonyl. This altered conformation has a drastic effect on the reactivity of the ketone and was the key to solve the problem of forming branched ketones. They noted the two key

obstacles in these alkylations preventing the formation of branched ketones are: a) destabilized intermediate aldol adduct due to steric clash leading to retro-aldol, and b) competing reactivity of the ketone towards nucleophilic attack and reduction. By twisting the aromatic ring perpendicular to the plane of the ketone, this reduces the steric hindrance about the alpha carbon stabilizing the intermediate aldol adduct. Furthermore, the *ortho* methyl substituents can now shield the carbonyl from nucleophilic attack and reduction.

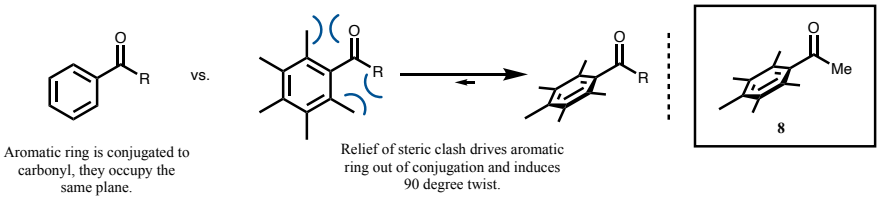

Figure 10: Key structural consequence to *ortho* disubstitution.

The optimal ortho disubstituted ketone was identified to be pentamethylphenyl (Ph*) methyl ketone, **8** (Figure 10). The twisted conformation of the Ph* ketones is due to the otherwise steric clash between the *ortho*- methyl substituents and the ketones. This conformation has since been proven extensively by X-ray crystallography as well as being visible using infrared spectroscopy, where the C=O stretch band for Ph* methyl ketone is 1697 cm^{-1}, compared to the carbonyl in acetophenone 1680 cm^{-1}, revealing a lack of conjugation.[41] The pentamethyl substitution pattern was found to be superior to other *ortho* disubstituted ketones (Figure 11), note that a single *ortho*-methyl substituent grants a significant improvement (69%) relative to the unsubstituted phenyl ketone (< 5%), and the pentamethylbenzene analogue resulted in near quantitative yield. (Figure 11).[41]

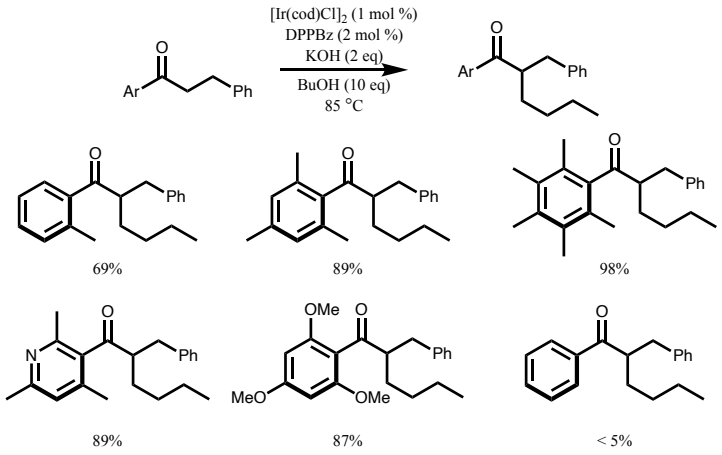

Figure 11: Optimization of aromatic ketone for ketone alkylation. Data from Armstrong *et al*.[41]

1.3.2 Acyclic Systems

In first instance, the versatility of the Ph* methyl ketone **8** in HB reactions was highlighted in the context of it's ability to engender a diverse array of α-branched ketones. Using $[Ir(cod)Cl]_2$ and DPPBz as the system of choice to catalyze the HB process, Frost *et al*. showed an array of branched ketones that could be accessed, including scaffolds bearing protected alcohols and amines (Figure 12).[40] In 2017, the Donohoe group subsequently showed this methodology could be readily extended to alkylating **8** with secondary alcohols, a feat that had hitherto been largely elusive.[42] A few reports of HB involving a secondary alcohol had been published at the time but these were limited in scope; limited to Friedel-Crafts-type alkylations,[43] intramolecular crotonization of the ketone,[44] lactonization of diols and malonates.[45] These lack the breadth of chemical diversity accessible through the alkylation of a methyl ketone with a secondary alcohol. The conditions required for this transformation were altered slightly from the original report on α-branched ketones, switching to $[IrCp^*Cl_2]_2$ in place of $[Ir(cod)Cl]_2$ and lower alcohol loading. This new methodology led to a series of complex α-substituted ketones (**9**, **10**, **11**, **12**), tolerant of protected

amines (**13**, **14**), alcohols (**15**, **16**), and ketones (**17**) as well as heterocycles such as pyridines (**18**) and thiophenes (not shown) (Figure 12). It is noteworthy that when subjecting 1,4-pentane diol to the reaction conditions they could access substituted cyclopentanes (**19**) (Figure 12) in good yields with excellent diastereoselectivity.[42]

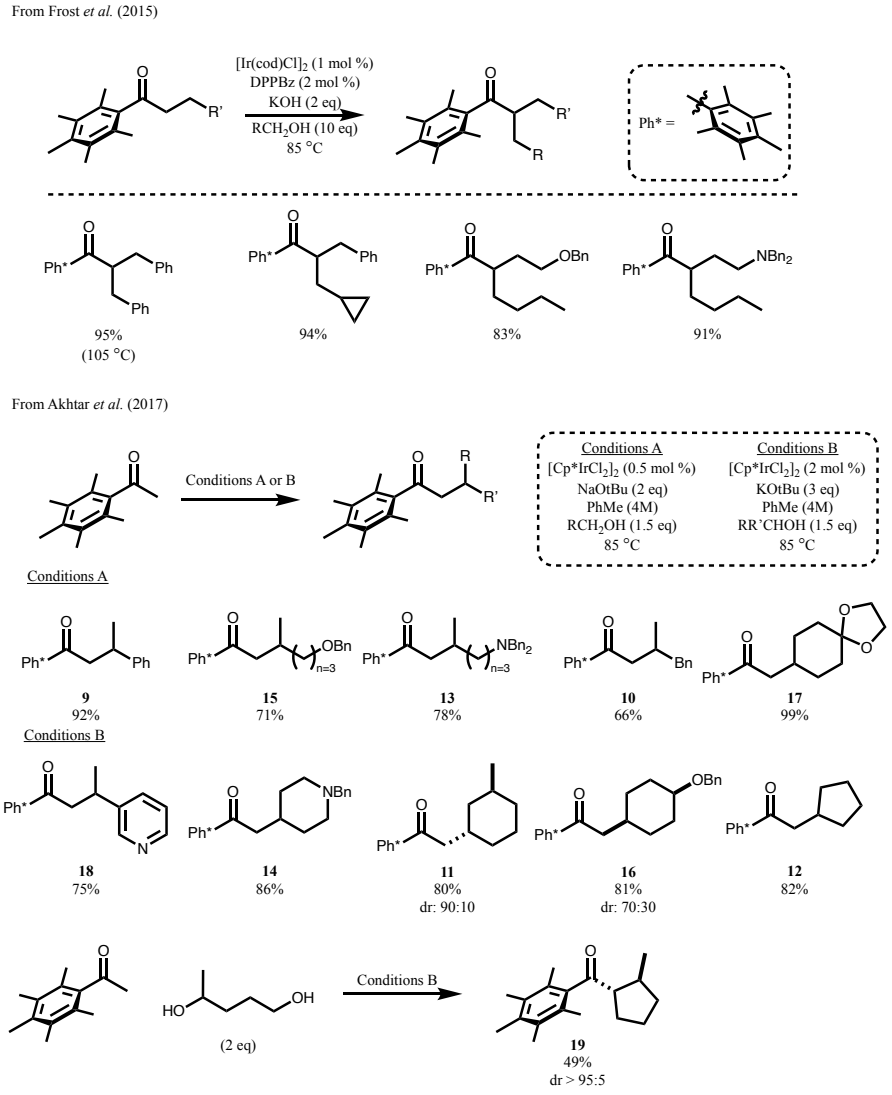

Figure 12: Construction of α-branched ketones through HB enabled by use of Ph*.

Subsequent work from the Donohoe group would focus on making this transformation enantioconvergent, realizing that stereocontrol of the branched ketones formed remained a limitation of the methodology (methods shown above yield racemic products unless specified). To this end, Cheang *et al*. (2020) developed a method wherein substituting the catalytic system to Ir(cod)acac and chiral ligand (*R*)-DTBM-SEGPHOS would selectively reduce the prochiral intermediate enone from the *si*-face.[46] The resulting process was an effective α-alkylation of **8** with a diverse array of racemic secondary alcohols to yield enantioenriched β-branched ketones, including linear branched chains (**20**, **21**, **22**) and carbocycles of various sizes (**23**, **24**, **25**). (Figure 13) As visible in the select examples provided, the larger the R group used the better the enantiomeric ratio of the product obtained. The enantiomeric excess and yield decrease as R gets smaller (for instance **22**, 54% 48:42 e.r.; **21**, 91%, 10:10 e.r.) Nonetheless this proved a significant step forward in this methodology. The use of **8** would prove pivotal to achieve this type of reactivity and would continue to be expanded upon by other groups.[47–49]

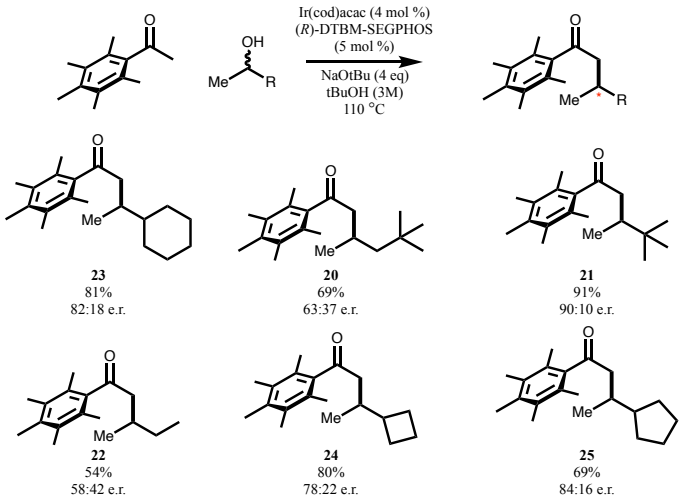

Figure 13: Enantioconvergent alkylation of Ph* methyl ketone with racemic secondary alcohols, data from Cheang *et al*. (2020).[46]

1.3.3 Cyclic Systems

More relevant to the current work were subsequent studies by the Donohoe group which explored the use of 1,5-diols as precursors to synthesize 6 membered cyclohexanes. Analogous to the work done by the Watanabe group in the 1980's to synthesize N-heterocycles, the Donohoe group postulated that they could employ **8** to undergo a double alkylation with these diols to afford six-membered carbocycles in a (5+1) cyclization strategy. (Figure 14) They hypothesized that an initial oxidation/aldol condensation/reduction cycle could be followed by a second oxidation/intramolecular aldol condensation/reduction (Figure 14) to afford the desired cyclohexane.

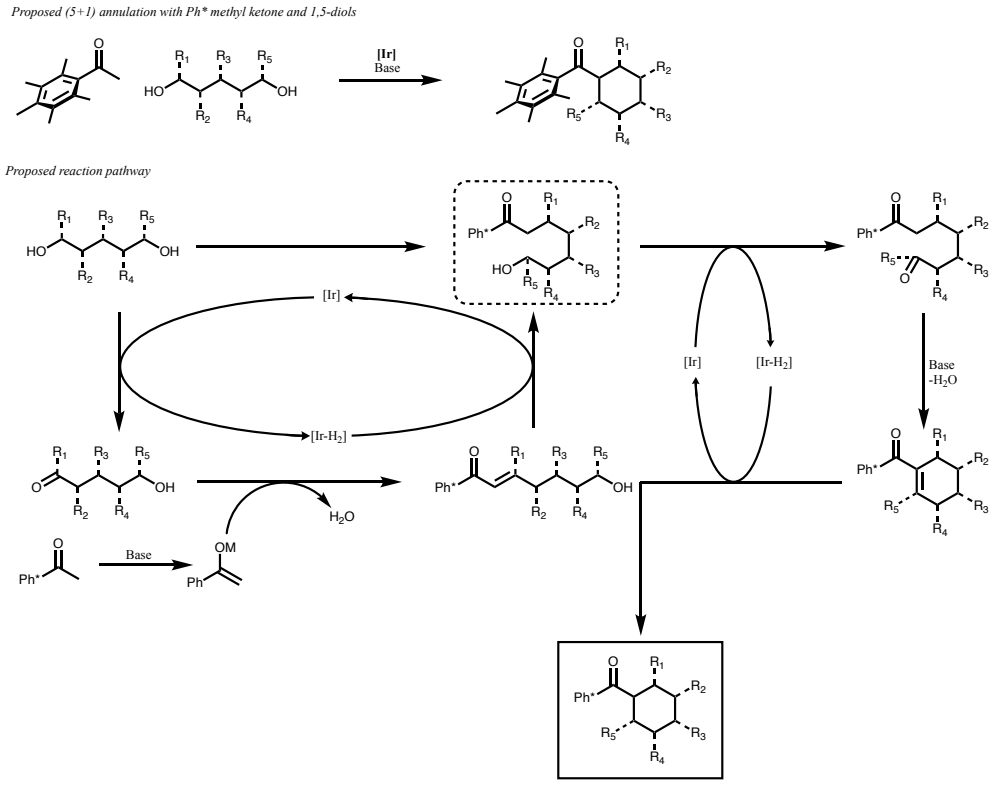

Figure 14: Proposed (5+1) annulation with 1,5-diols and Ph* methyl ketone as well as proposed reaction pathway.

This methodology proved to be very successful, effectively being employed to generate a series of 2, 3, and 4-substituted cyclohexanes, often with good diastereoselectivity (Figure 15).[50] For 4-substituted cyclohexanes (**26**, **27**, **28**) the product will yield exclusively the trans diastereomer, similarly 2-substituted cyclohexanes (**29**, **30**, **31**) yield *trans* diastereomer with high d.r. Substitution at the 3 position (**32**) yields the *cis*-diastereomer similarly in high d.r. (91:9). Diastereoselectivity is similarly excellent in polysubstituted substrates (**28**, **30**, **31**). Unfortunately the functional group tolerance in this study suffered slightly from harsh conditions but aryl chlorides (**27**) and aryl fluorides (not shown) were well tolerated as well as aryl methoxy ethers (**31**). Spirocyclic substrates can similarly be synthesized (**32**).

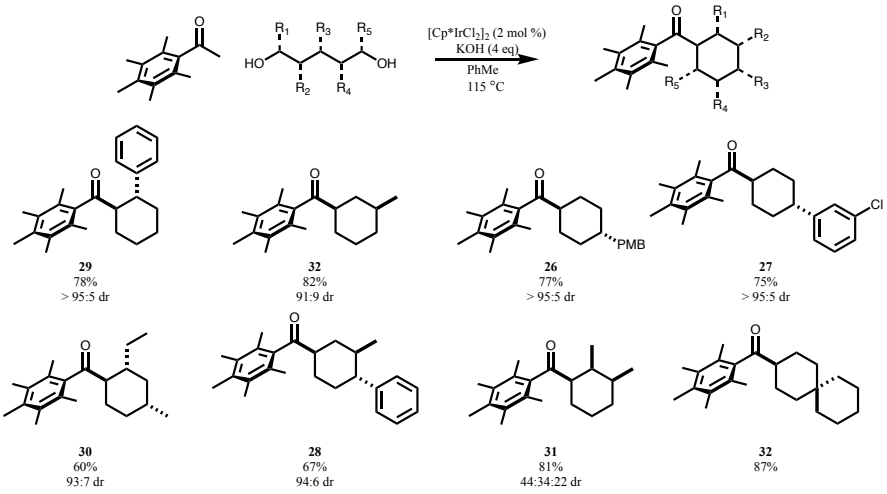

Figure 15: Selected examples of cyclohexanes synthesized via (1+5) annulation through HB with Ph* methyl ketone and 1,5-diols.

The synthetic utility of this transformation largely hinges on the ability to control the stereochemical outcome of the final product; this has traditionally been a challenge in HB methodologies due to the relatively harsh conditions used (high temperatures and strong basic

conditions favoring epimerization).[51] Significant strides have been made in this undertaking: early on it was found the relative stereochemistry about the α-stereocenter results from thermodynamic equilibration under reaction conditions due to epimerization, furthermore it was observed that stereochemistry about the *δ*-stereocenter is set in the starting material (i.e. using a chiral diol) and is retained through the reaction.[50] Analogous to the work preparing enantioenriched β-branched ketones cited earlier, control of the β-stereocenter was achieved through catalyst control; Ir(cod)(acac) and DTBM-SEGPHOS were found to be optimal and enable selective reduction of the enone to establish the β-stereocenter.[52] The last remaining challenge was controlling the stereochemistry about the γ-stereogenic center, which is known to racemize under reaction conditions via the formation of extended enolates. This challenge was solved, albeit with slightly less stereo-control, by Cheang *et al*. by means of dynamic kinetic resolution, judiciously exploiting the different rates of reduction induced by the stereochemistry at the γ-carbon when employing an Ir(cod)(acac) and [R_P,*S*]-PPF-NH_2 catalytic system. (Figure 16) This specific method will be expanded upon in a future chapter.[53]

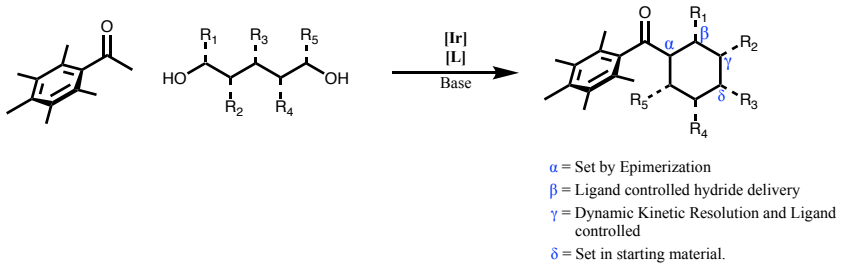

Figure 16: Control of stereochemistry in cyclohexane synthesis *via* methods reported by the Donohoe Lab.

1.4 Acceptorless Dehydrogenation

Evidently the sensible choice of iridium source and ligand has allowed for the advancement of the Donohoe group's hydrogen borrowing (1+5) annulation strategy. This insight led to the realization that if it were possible to interrupt the final enone reduction, the resulting product would be a cyclohexene which is a valuable functional motif, better poised for further chemical manipulation, and removes stereochemical considerations about the α- and β-stereocenters. Smith *et al*. posited that sterically bulkier ligands may continue to allow access of a primary alcohol to the metal center necessary for the initial alcohol dehydration, but be sufficiently bulky to hinder reduction of the sterically congested enone olefin. Indeed, employing CataCXium A in conjuction with $[Ir(cod)Cl]_2$ under comparatively dilute (0.25M) conditions effected the desired transformation in remarkable yields for a diverse range of substrates (Figure 17), giving access to synthetically useful tetra- and tri-substituted olefins.[54] This transformation deviates from HB in that the hydrogen is no longer "returned", instead it dissociates from the iridium catalyst and is released as hydrogen gas, making this an acceptorless dehydrogenation coupled to an aldol condensation and subsequent cyclization. Indeed this method provided access to 1-acyl cyclohexenes in excellent yields (Figure 17). Tetrasubstituted (**33**, **34**, **35**) olefins could be prepared readily and in high yields. The reaction was amenable to be scaled up (**36**; 1.6 g scale). Functional groups such as aryl chlorides (**37**) as well as methoxy ethers (**78**) (and methoxy thioethers, not shown) were well tolerated as well. The transformation also resulted in excellent yields to substrates bearing a range of unsubstituted aliphatic (**38**, **39**, **34**, **36**, **35**) and aryl substituents (**39**).

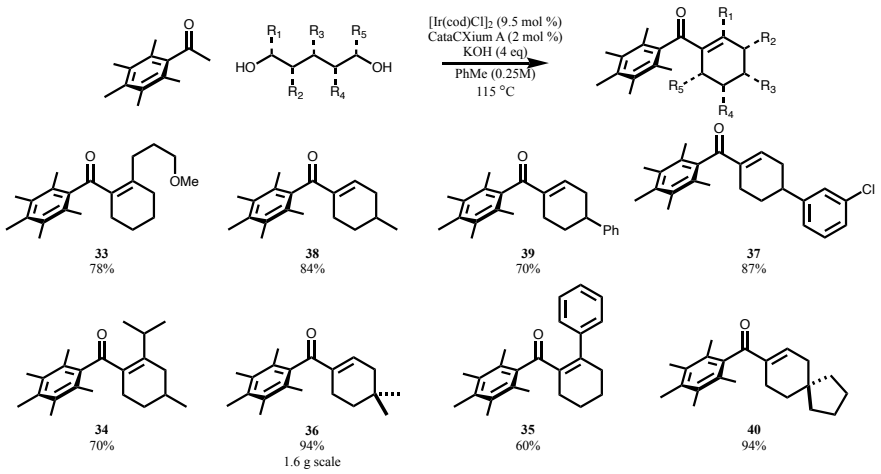

Figure 17: Acceptorless dehydrogenation of 1,5-diols with Ph* methyl ketone

This new transformation proved illuminating, as it brought forth a new understanding of how these (5+1) annulations proceed. The working hypothesis had been these annulations rely on back-to-back aldol condensations enabled by back-to-back oxidations of the two alcohols of the diol (Figure 14). This mechanistic proposal would require the formation of dash-boxed intermediate in Figure 14 as the result of the first HB cycle, which was never observed. This led to the discovery of a new pathway as a result of a holistic mechanistic study: following initial oxidation of diol **I** (Figure 18) to the corresponding aldehyde (**II**), and an aldol condensation with **52**, intermediate alcohol **III** is formed. Under traditional HB conditions, the olefin in **III** would be reduced but when using a bulky ligand and dilute conditions hydrogen gas dissociates from the iridium metal center. Deprotonation of **III** leads to alkoxide **IV**, which is poised to undergo a [1,5]-hydride shift to generate intermediate **V**. This intermediate subsequently undergoes an aldol condensation with the aldehyde to afford the desired cyclohexene **VI**. Once again, under these reaction conditions, reduction of the enone is too slow and is not further reduced. This is the currently accepted mechanism for the (5+1) anulations between **8** and 1,5-diols summarized above, in the synthesis

of cyclohexanes, the resulting cyclohexene is reduced by the iridium hydride to release the cyclohexane.

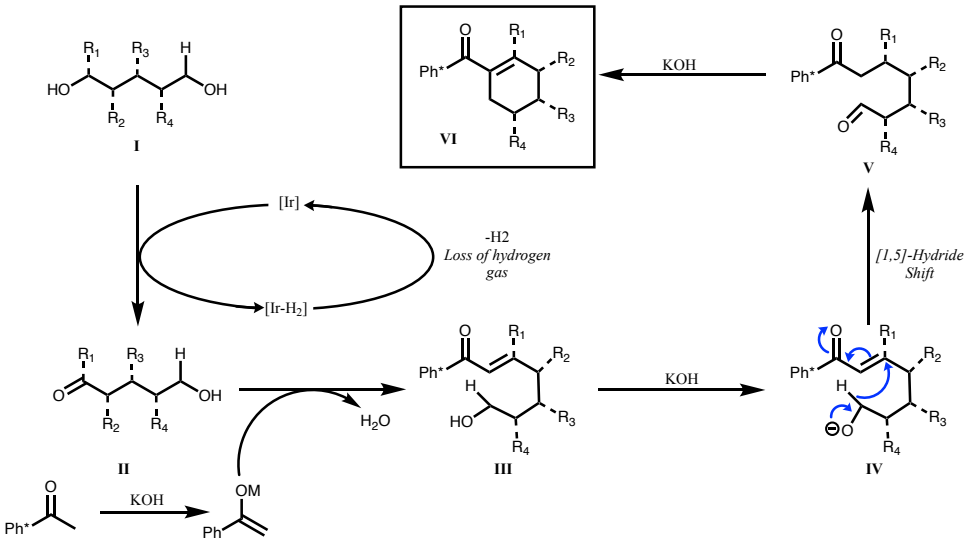

Figure 18: New proposed reaction pathway for formation of cyclohexenes from 1,5-diols and Ph* methyl ketones under acceptorless dehydrogenation conditions.

1.5 Ph* Cleavage

The synthetic utility of the aforementioned transformations is reliant on the straightforward removal of the Ph* group to unveil the desired carbonyl moiety. Ph* ketones serve as placeholders for carboxylic acids, the aromatic ring is electron-rich due to the twisted conformation of Ph* (Figure 10) and the pentamethyl substitution, making the Ph* readily cleavable via retro-Friedel-Crafts acylation.[41] Due to the electron-rich nature of the Ph* ring, it is prone to *ipso*-addition to a variety of electrophiles (Figure 19). Upon electrophilic addition to the Ph*, the Wheland intermediate undergoes fragmentation to for the acylium ion (Figure 19) which can then be

captured with a nucleophile. For linear acyclic and cyclohexane systems, this cleavage is best achieved with 2 equivalents of bromine at -17 °C, where the acyl bromide is rapidly generated and can be further functionalized with a wide variety of nucleophiles as shown in the selected examples below. (Figure 6) As is seen in the examples shown, the Ph* ketones prepared via HB can be readily converted to amides (**41**, **42**), esters (**43**, **44**), thioesters (**45**), as well as alcohols (not shown).[41]

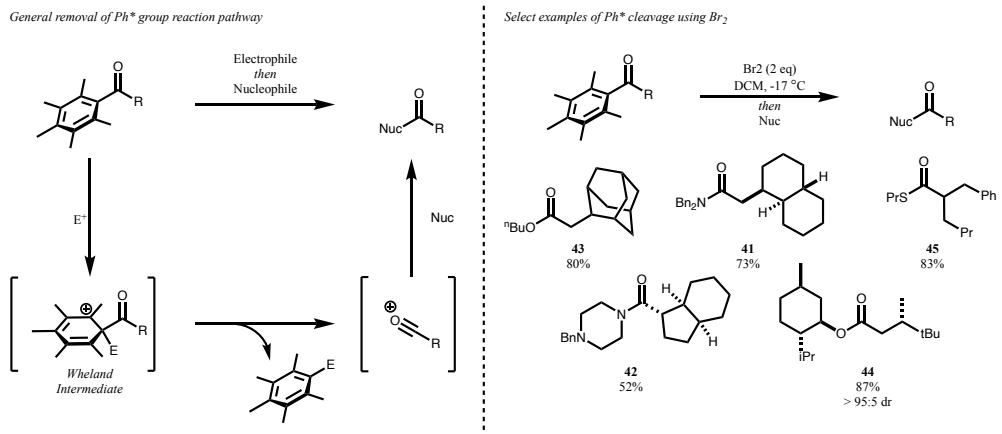

Figure 19: Mechanism for Ph* removal via retro-Friedel Craft and select examples of Ph* cleavages using variety of nucleophiles.

For the cyclohexenes discussed above, bromine would inevitably react with the olefin, and as such a method where cleavage is achieved in high yields with 2M HCl in HFIP was developed, which installs a carboxylic acid in place of the Ph*. Under these conditions acid proton serves as the electrophile and water from the aqueous HCl serves as the nucleophile, yielding the corresponding acid.

2 Hydrogen Borrowing Cyclization and Aromatization

2.1 Introduction to Cyclization and Aromatization Design

As described in the previous chapter, the Donohoe group has developed methods for the formation of cyclohexanes and cyclohexenes (Figure 20A) *via* hydrogen borrowing[50,52] and acceptorless dehydrogenation.[54] We envisioned the natural progression of the methodology to involve the formation of benzene rings from the precursor Ph*COMe (**8**) and diols (Figure 20B). To this end it upon formation of the cyclohexene through established means, only two further oxidations of the ring would be required to enable access to a series of highly decorated benzene rings.

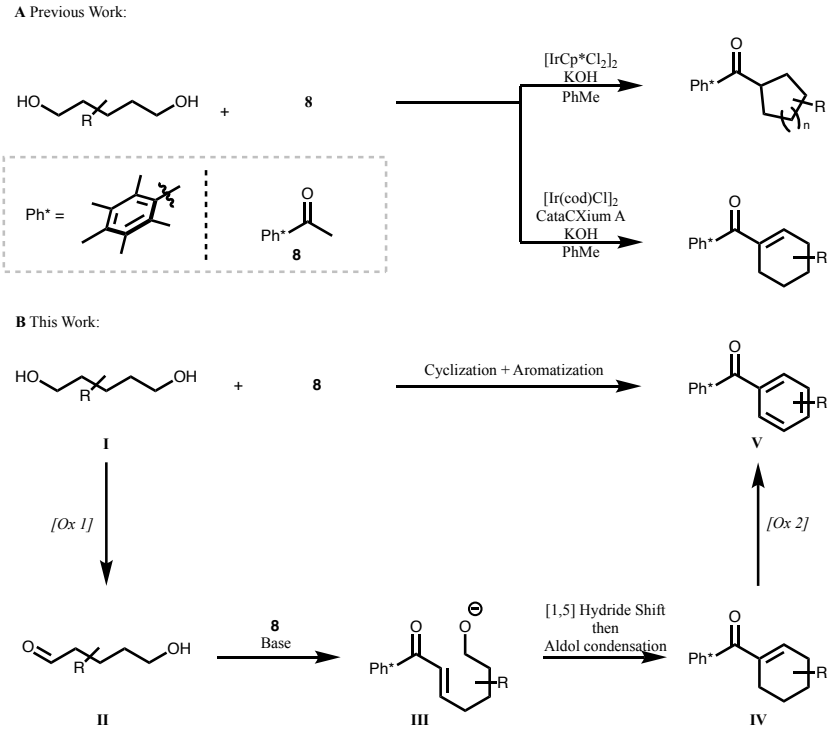

Figure 20: A) Methods to synthesize saturated and unsaturated carbocycles. B) New proposed transformation to generate arenes.

Depicted in Figure 20B, this transformation requires an initial oxidation (Ox 1) of the diol starting material **I** followed by an aldol elimination with **8** and **II**. This sets the stage for the necessary [1,5]-hydride shift and concomitant aldol condensation for the formation of the intermediate cyclohexene **IV**. Lastly, two successive oxidations (Ox 2) of cyclohexene **IV** would provide aromatized product **V**.

We were encouraged by the fact that there is significant literature precedent for both Ox 1 and Ox 2 processes being facilitated by palladium catalysis. A series of papers reporting the palladium-catalyzed aerobic oxidation of aliphatic alcohols by Nishimura *et al*.[55] and the oxidation of various cyclohexenes to their aromatic counterparts by Iosub *et al*.[56,57] showed compatible oxidative conditions which we hypothesized could be exploited to effect Ox 1 and Ox 2 as illustrated by the general pathway shown in Figure 21 below. Both Ox 1 and Ox 2 transformations are known to proceed independently, however to run them concomitantly in a single reaction vessel would be challenging.

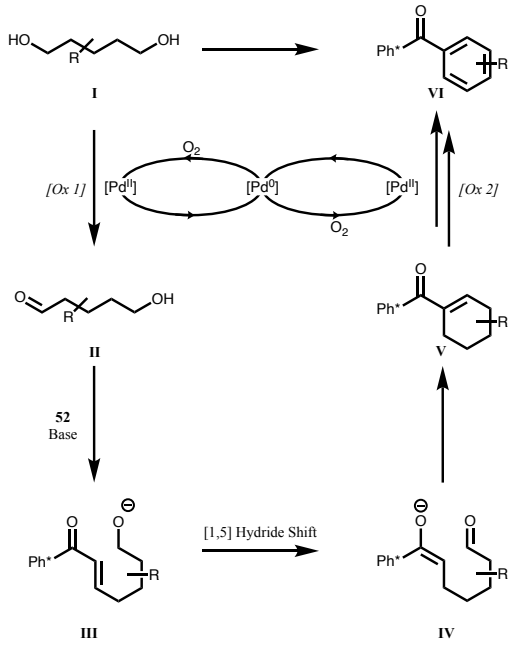

Figure 21: Proposed mechanistic pathway for [Pd] catalyzed cyclization and aromatization pathway.

2.2 Aerobic Palladium mediated cyclization and aromatization

To test our proposed transformation, 3-methyl-1,5-pentanediol was chosen as the model substrate due to its commercial availability and known reactivity under previous 1,5-diol cyclizations by our group. Common palladium(II) salts such as $Pd(OAc)_2$ and $PdCl_2$ were reported to facilitate both the oxidation of inactivated alcohols[55] and the aromatization of enones and cyclohexenes[58] and therefore served as a starting point to test the feasibility of this palladium mediated acceptorless dehydrogenation and tandem aromatization. Lastly, Ox1 and Ox2 are the first and last steps in the overall transformation, oxidizing **I** and **V** (Figure 21). Reaction conditions must also ensure the three intermediate steps can proceed, namely: deprotonation of **8** and subsequent aldol condensation with the newly formed **II**, [1,5]-hydride shift of alkoxy-enone **III** to engender the enolate-aldehyde intermediae **IV**, intramolecular aldol elimination of the enolate and aldehyde will afford cyclohexene **V** poised for aromatization to **VI**. This series of intermediate reactions necessitates basic conditions to promote the aforementioned aldol condensations and, importantly, high temperatures (115 °C) relative to the temperatures required by Ox 1 and Ox 2 (80 °C), to promote the pivotal [1,5]-hydride shift.[54]

Table 1 below reports a selection of preliminary results observed with our model system. Treatment of 3-methyl-1,5-pentanediol and **8** in the presence of $Pd(OAc)_2$ under an oxygen atmosphere in basic conditions afforded the desired product A (Table 1) in 9% yield (Entry 1,

Table 1). This initial hit was encouraging and led to further effort to optimize the reaction. Changing the palladium source to $Pd(Cl)_2$ had a minor effect on the yield of A but did lead to improved conversion. It was noted that this reaction had the potential to yield every oxidation stage of the cyclized product: product A through the desired reaction pathway, cyclohexene B through stopping reaction pathway prior to Ox2 (Figure 21), and cyclohexane C potentially through a hydrogen borrowing where the palladium hydride species reduces enone B too before being recycled.

Table 1:

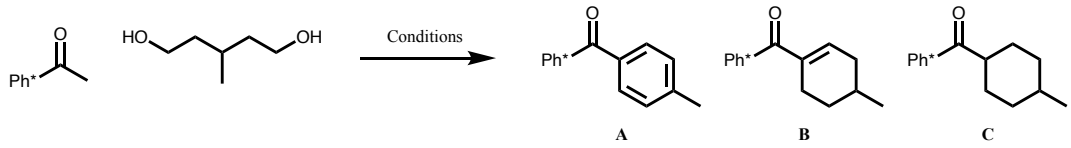

Entry	PdX_2 (x mol%)	Oxidant (x eq)	Ligand (x mol%)	Additive (x eq)	1HNMR Yield A	1HNMR Yield B	1HNMR Yield C	Conversion (%)
1	$Pd(OAc)_2$ (1)	O_2 (g)	n/a	n/a	9	3	32	44
2	$PdCl_2$ (1)	O_2 (g)	n/a	n/a	10	15	44	69
3	$PdCl_2$ (1)	O_2 (g)	n/a	Neohexene (2 eq)	7	19	37	63
4	$Pd(OAc)_2$ (2.5)	O_2 (g)	Xantphos (2.5)	Neohexene (2 eq)	10	16	44	70
5	$Pd(OAc)_2$ (2.5)	O_2 (g)	DPPE (2.5)	Neohexene (2 eq)	12	3	38	53
6	$PdCl_2$ (1)	O_2 (g)	cataCXium A (2)	n/a	19	16	n/a	n/a
7	$PdCl_2$ (1)	O_2 (g) + $CuCl_2$ (0.5eq)	n/a	n/a	10	15	44	69

Conditions: Ph*COMe (0.3 mmol, 1 eq), diol (2 eq), KOtBu (2 eq), PhMe (1M), 115 °C, 24 hrs. Neohexene refers to 3,3-dimethylbut-1-1ene

The increased conversion to cyclized product (69 vs 44%, Entry 2 vs Entry 1) of $PdCl_2$ was seen as a positive step yet the undesired cyclohexane was clearly being favored. To counteract this issue, 3,3-dimethylbut-1-1ene (neohexene) was added to serve as a sacrificial hydrogen acceptor however this had no significant effect in the ratio of A to B+C. A series of bulky ligands were then tested such that the increased steric bulk about the metal center may mask the reductive reactivity observed, however no major effect was observed on reaction outcome (Entries 4-6). Addition of substoichiometric copper(II) as a co-oxidant to facilitate the recycling of the palladium catalyst was tested but also led to no significant improvement in the yield of the desired aromatic product. A series of other conditions were tested (i.e. additives, catalyst loadings, oxidants) yet the highest yield of desired product A measured was 19% (Entry 6), for a complete table of conditions tested see Appendix Table A1.

These results indicate that the first oxidation step (Ox1), along with the intermediate aldol condensations and [1,5]-hydride shift, proceed well as evidenced by the good conversion rates to cyclized product. The key obstacle to this transformation is final oxidation step, from cyclohexene **V** to arene **VI** (Ox2, Figure 21). It was unclear what element of the final aromatization step was failing. We hypothesized that the final aromatization may be occurring slowly and therefore outcompeted disproportionation of the cyclohexene, conversely the palladium hydride species generated from the first oxidation step (Ox1) may be responsible for the rapid reduction of **V**. In fact, palladium has been shown to engage in hydrogen borrowing, which would indeed explain the formation of C.[29]

Due to the complexity of the reaction, we decided to optimize the final oxidation in isolation. Indeed, when subjecting cyclohexene **46** to the rection conditions (i.e. $Pd(OAc)_2$ and an oxygen

atmosphere) the starting material remained largely untouched and there was no trace of the aromatic product **47** formed. (Figure 22) This result suggests that the aromatized product A in the reaction shown on Table 1 may have been forming through an independent reaction pathway. The addition of a catalytic (0.25 eq) amount of acid proved sufficient to allow the reaction to proceed (26% yield; Figure 22), it is possible that addition of acid contributed to make the palladium catalyst more electrophilic through the exchange of coordinating counterions which led to the increased reactivity (as will be discussed in better detail below, the electron-deficient nature of the olefin in these adducts makes this reaction particularly challenging). At this juncture we believed it likely that the palladium catalyst was decomposing to palladium black under the aerobic conditions, hindering reaction progress. 2-amino-pyridine, a ligand commonly employed in these reactions to stabilize palladium from decomposition, was tested under the reaction conditions for this purpose but had no major effect in reaction yield. (Figure 22)

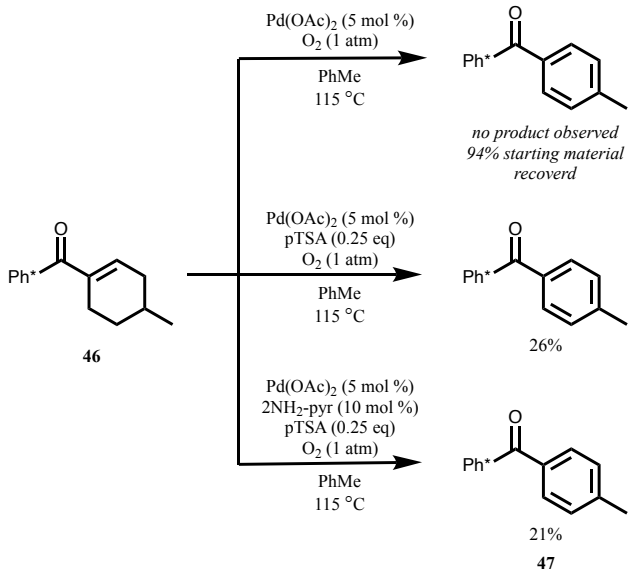

Figure 22: Early results of aerobic oxidation of **46** to **47**.

Exchanging toluene for DMSO as the reaction solvent would facilitate these aerobic, for instance treatment of **46** with Pd(TFA)2 (5 mol %) in an oxygen atmosphere yielded **47** in 45% yield. However, this yield could not be improved upon further, addition of copper(II) salts as co-oxidant led to a lower yield, as did the addition of a sacrificial hydrogen acceptor (norbornene) (See Table in Appendix Table A1). At this point we decided to test copper(II) salts as oxidant, as the aerobic conditions being tested were conducive to catalyst degradation.

2.3 Palladium mediated aromatization

2.3.1 Optimization of Palladium aromatization

A screen of palladium sources revealed $Pd(TFA)_2$ to yield the most promising results, compared to other palladium sources (Entries 1-3 Table 2), which in conjunction with $CuCl_2$ as an oxidant afforded **47** in 63% isolated yield (Entry 3 Table 2). Next we tested a series of pyridine-based ligands, as these are common in analogous transformations.[59] With the exception of 2-nitro-pyridine (entry 9), all other ligands had a detrimental effect in yield relative to Entry 3. The use of 2-nitro-pyridine resulted in a ^{1HNMR} yield comparable to the reaction without ligands. Common additives employed in palladium chemistry were tested.[56,57] The use of silver salts as additives resulted in interesting results, the addition of silver fluoride (AgF) to the reaction mixture showed no improvement for substrate **46** however was observed to improve the yield in reactions with more difficult substrates.

Table 2:

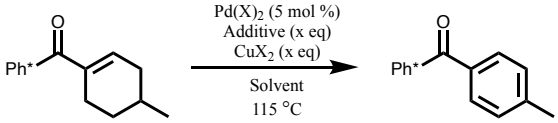

Entry	PdX_2 (x mol%)	Oxidant (x eq)	Ligand (x mol%)	Additive (x eq)	Solvent (x M)	^{1HNMR} Yield (Isolated)
1	$Pd(OAc)_2$ (5)	$CuCl_2$ (2 eq)	n/a	n/a	DMF (2 M)	57
2	$PdCl_2$ (5)	$CuCl_2$ (2 eq)	n/a	n/a	DMF (2 M)	50
3	$Pd(TFA)_2$ (5)	$CuCl_2$ (2 eq)	n/a	n/a	DMF (2 M)	83 (63)
4	$Pd(TFA)_2$ (5)	$CuCl_2$ (3 eq)	n/a	n/a	DMF (2 M)	37
5	$Pd(TFA)_2$ (5)	$CuCl_2$ (2 eq)	2-NH_2-py (10)	n/a	DMF (2 M)	66
6	$Pd(TFA)_2$ (5)	$CuCl_2$ (2 eq)	2-Me-py (10)	n/a	DMF (2 M)	40
7	$Pd(TFA)_2$ (5)	$CuCl_2$ (2 eq)	2-COOH-py (10)	n/a	DMF (2 M)	44
8	$Pd(TFA)_2$ (5)	$CuCl_2$ (2 eq)	2-F-py (10)	n/a	DMF (2 M)	50
9	$Pd(TFA)_2$ (5)	$CuCl_2$ (2 eq)	2-NO_2-py (10)	n/a	DMF (2 M)	85
10	$Pd(TFA)_2$ (5)	$CuCl_2$ (2 eq)	n/a	NaTFA (0.2)	DMF (1 M)	60
11	$Pd(TFA)_2$ (5)	$CuCl_2$ (2 eq)	n/a	AgF (0.2)	DMF (0.5M)	(60)
12*	$Pd(TFA)_2$ (5)	$CuCl_2$ (2 eq)	n/a	n/a	DMF (2 M)	(25)
13*	$Pd(TFA)_2$ (5)	$CuCl_2$ (4 eq)	n/a	n/a	DMF (0.5M)	31

*substrate used was unsubstituted Ph*CO cyclohexene.

As seen in Entry 4, increasing the equivalents of copper salts from 2 to 3 equivalents resulted in a significant decrease in yield (83 to 37% ^{1HNMR} yield). This effect was accredited to the poor solubility and high concentration these reactions are run in; as the copper salts would not homogenize and rather form suspensions which had trouble stirring. Based on the proposed

mechanism for this reaction, where **I** Figure 23 forms an intermediate π-allyl complex with the palladium species, beta hydride elimination yields diene **II**, and the process repeats itself to form **III**.

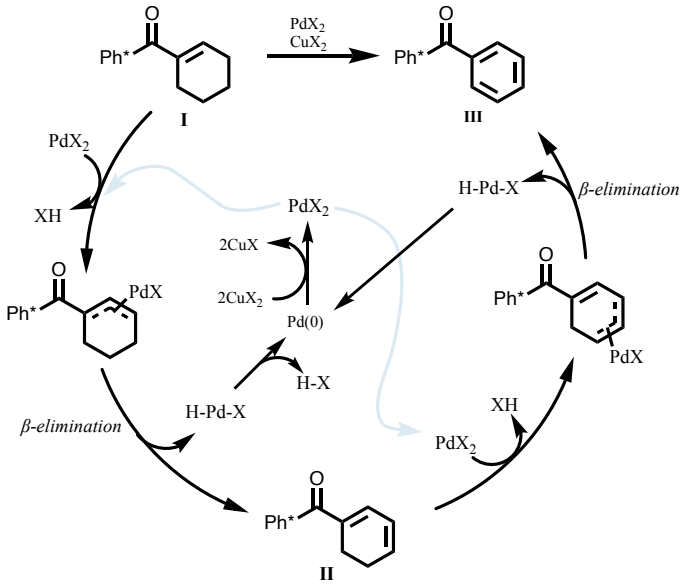

Figure 23: Proposed mechanistic pathway for the aromatization reaction.

This reaction mechanism would suggest 4 equivalents of copper(II) would be required for the reaction to reach completion, as two equivalents of copper(II) are required to oxidize Pd(0) back to Pd(II) and the palladium catalyst undergoes two Pd(II)-Pd(0)-Pd(II) cycles per substrate. Attempts to homogenize the reaction mixture by using more dilute conditions (0.5M vs 2M) with the higher copper(II) loadings (Entries 12 and 13) however proved inefficient.

2.3.2 Substrate scope of the palladium mediated aromatization

Figure 24 below shows the substrate scope tested under optimized conditions. Substrate screen of cyclohexenes prepared previously through the acceptorless dehydration procedure reported in Smith *et al*.[54] reveals substitutions in positions 3 and 4 are well tolerated as seen by **47**, **48**, **49**, **50**, **51**, **52**, and **53**, which have moderate yields ranging from 42-63%. Substitution in the 2-position is detrimental to the reaction yield however (**54**, **55**, **56**) resulting in low yields (25-30%). It is likely the increased steric hindrance about the tetrasubstituted olefin for the 2-substituted substrates obstructs initial coordination to the palladium catalyst. Substrate **57** similarly had a low (25%) yield despite bearing no substituents.

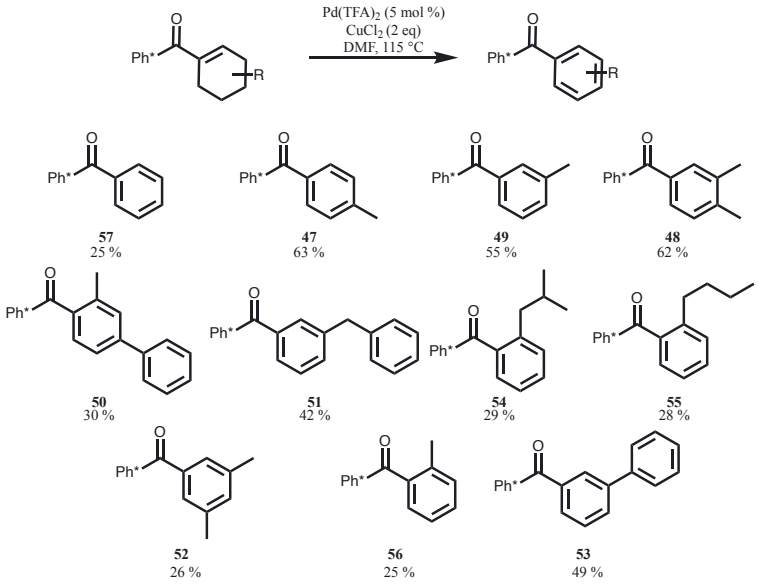

Figure 24: Substrates tested under aromatization conditions.

Furthermore, we hypothesized that the electron-deficient nature of the olefin may be responsible for the low reactivity observed and harsh conditions required. This was likely the reason sources

of more electrophilic palladium showed increased yields. To test this idea, we set out to test two analogous systems under our aromatization conditions (Figure 25). Starting from acid **58** (which was prepared by HFIP/HCl Ph* removal of **46**), the Weinreb amide **59** was prepared in 20% yield and later utilized to prepare the two substrates **60** and **61** through corresponding Grignard addition in 15 and 16% yields respectively.

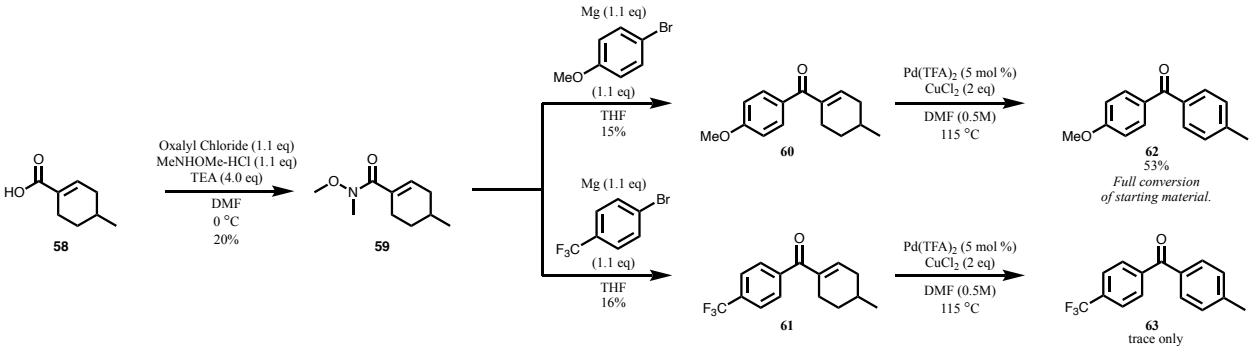

Figure 25: Test of electron-rich vs electron-deficient olefin role in aromatization.

Compound **60** was seen as the "electron-rich" analogue to **46** and **61** as the "electron-poor". As expected, our aromatization system proceeded as expected with the electron rich analogue to yield **62**, where full conversion of the starting material was observed. On the other hand only trace of **63** was seen and the starting material was largely untouched.

2.3.3 One-pot Ph* ketone-diol cyclization and aromatization

Unfortunately, the conditions necessary to perform the aromatization reaction in conjunction (one-pot) with the cyclization step ultimately proved unsuccessful. (Figure 26) Adding the $Pd(TFA)_2$ and $CuCl_2$ to the reaction mixture simultaneously with the [Ir]/[L] and KOH resulted in no reaction, while addition of the [Pd]/[Cu] after 24 hours before stirring for an additional 24 hours saw 62%

of intermediate cyclohexene **46** but no aromatized product formed. Seeing as the toluene solvent was known to be detrimental to the aromatization with $Pd(TFA)_2$ and $CuCl_2$, switching the solvent to *tert*-butanol (known to work with the HB chemistry employed during the cyclization step) also resulted in no aromatized product observed. Ultimately these reactions proved to be too orthogonal to be coupled together.

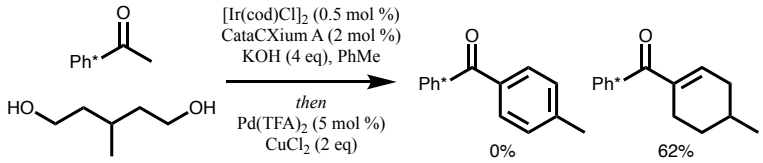

Figure 26: One-pot Ir-catalyzed cyclization and Pd-catalyzed aromatization.

2.4 Copper and TEMPO mediated Aromatization

2.4.1 Introduction to Copper and TEMPO dehydrogenation

In a final attempt to realize the desired one-pot tandem cyclization and aromatization, we were intrigued by a paper from Shang *et al*. who reported a copper-catalyzed dehydrogenation of a series of carbonyl-bearing substrates with 2,2,6,6-tetramethylpiperidine-N-oxyl (TEMPO) to afford their corresponding alpha-beta unsaturated analogues.[60] Most notably, they reported the oxidation of phenyl cyclohexyl ketone to the corresponding benzophenone and cyclohexane carboxaldehyde to benzaldehyde in good yields (Figure 27A). Shang *et al*. claim the reaction from ketones/aldehydes to their α,β- unsaturated counterparts begins through the formation of a copper enolate (**I**; Figure 27B), the homolysis of which yields the α-radical (**II**) which is captured by TEMPO (**III**). This intermediate then undergoes TEMPO elimination through β-H abstraction with another molecule of TEMPO to release the α,β- unsaturated carbonyl (**IV**) along with one equivalent of TEMPO and

TEMPOH (Figure 27B). They propose TEMPOH then proceeds to oxidize the Cu(I) species formed during the homolysis of C-Cu to regenerate the Cu(II) catalyst (Figure 27B).[60,61]

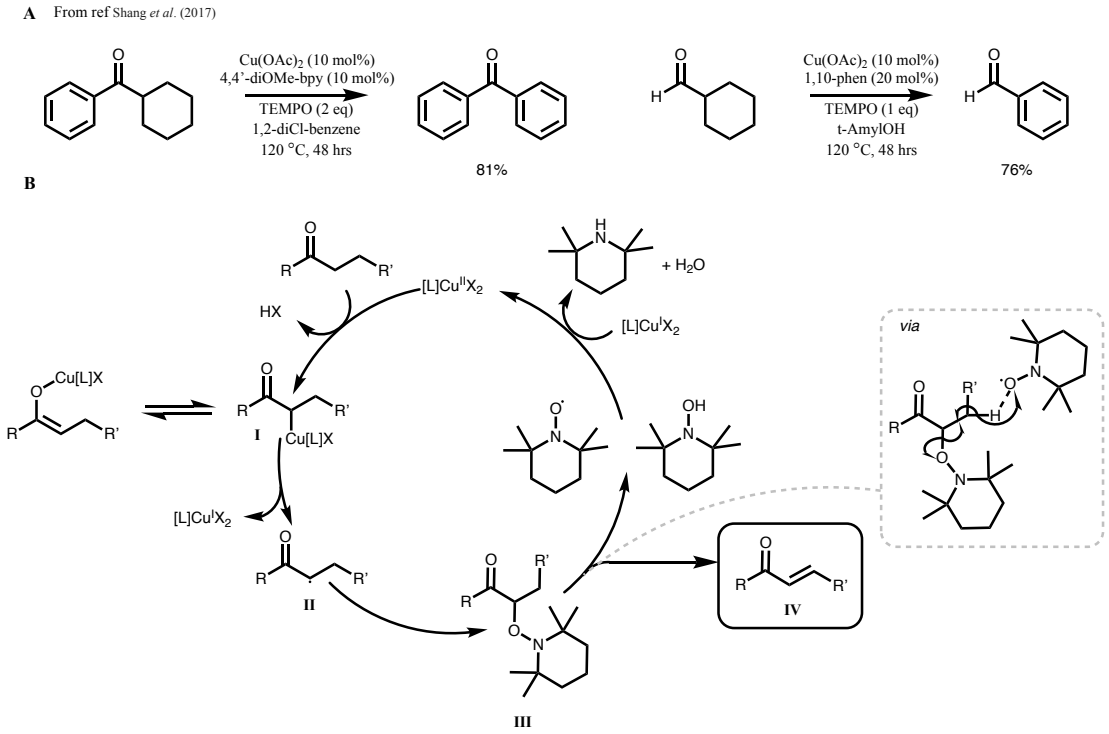

Figure 27: A) Sample aromatizations from Shang *et al*. (2017).[60] B) Proposed mechanism for TEMPO mediated oxidation of ketones.

Specially significant to our reaction development, this methodology would ensure successive dehydrogenations where possible (Figure 28A), as they claim complexation of the α,β- unsaturated carbonyl to the Cu(II) metal (**I**) would polarize the γ-C-H bond to enable deprotonation and generation of the Cu-dienolate (**II**). Subsequent homolysis of the Cu-O bond could unveil a γ-radical (**III**) that is sufficiently stabilized by the 5-center-π-electron system. A TEMPO molecule then traps the γ-radical (**IV**) and the reaction continues in analogous fashion to the previously described, to generate poly-unsaturated conjugated systems.

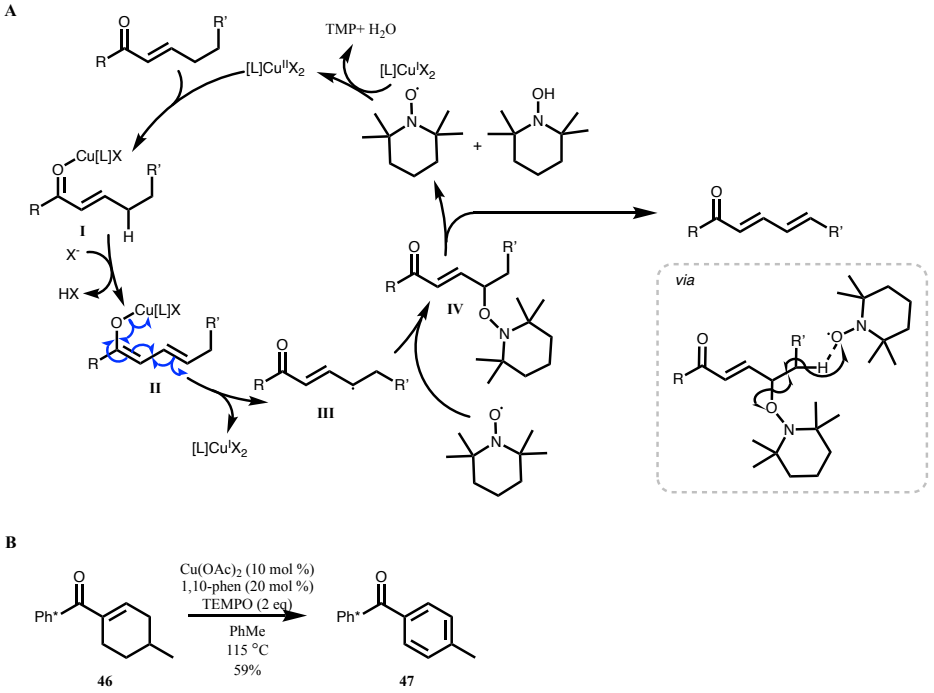

Figure 28: A) Subsequent dehydration of α,β- unsaturated carbonyls. B) TEMPO mediated aromatization of **46**.

2.4.2 Application of Copper and TEMPO system to cyclohexenes

We therefore hypothesized we could potentially exploit this Cu(II)/TEMPO system to induce our desired aromatization. Notably, the Cu(II)/TEMPO system used conditions analogous to the conditions required for the 1,5-diol and Ph*COMe (i.e. tert-amyl-OH or PhMe solvent, base-tolerant, high temperatures) and as such could be used in a one-pot reaction design. Testing the conditions of Shang *et al.* revealed that indeed cyclohexene **46** could be fully oxidized to **47** in good yield (59%). We hypothesized that a merger of our group's [1,5] annulation with the Cu/TEMPO oxidation conditions (Figure 29) would have the highest chance of success.

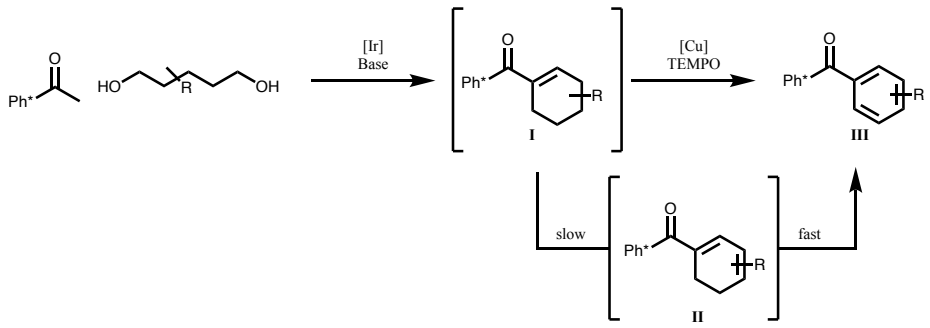

Figure 29: New proposed one-pot cyclization/aromatization strategy.

By employing the acceptorless dehydrogenation conditions reported by Smith *et al*.,[60] we could access cyclohexene **I** (Figure 29), from that point we the first oxidation step to **II** would likely be the least favorable, with the final oxidation from **II** to **III** likely proceeding due to the aromatization driving force.

Initial attempts to run this reaction in a one pot fashion by adding both cyclization and aromatization reagents in a single step (Figure 30A) were unsuccessful and led to no product formation and significantly reduced conversion of the cyclization product. Instead it was decided to add reagents in a stepwise fashion (Figure 30B): starting the reaction under conventional conditions found by our group to promote the desired cyclization via either hydrogen borrowing (to access the intermediate cyclohexane, Condition A) or acceptorless dehydrogenation (to access the intermediate cyclohexene, Condition B), and subsequently add $Cu(OAc)_2$, 1,10-phenanthroline, and TEMPO to the flask 24 hours later.

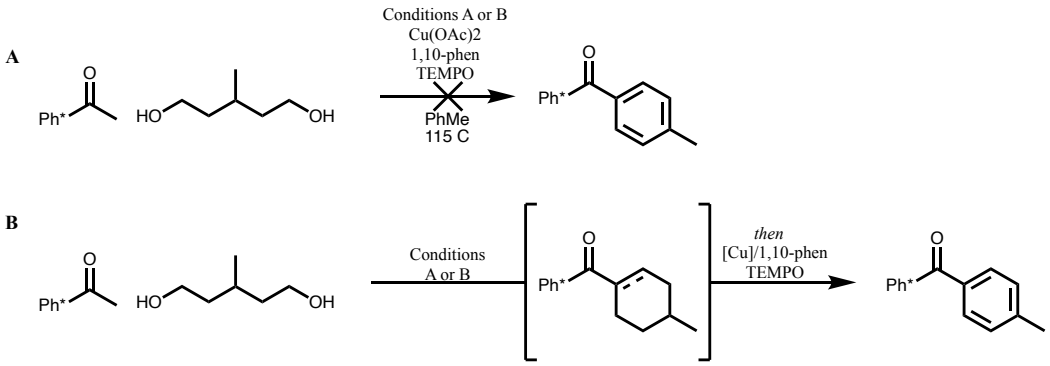

Figure 30: A) General schematic of all reagents added together during initial reaction set up. B) General schematic of stepwise addition of reagents, first reagents of Conditions A or B, followed by [Cu]/1,10-phen and TEMPO 24 hours later. Conditions A: Ph*COMe (1 eq), diol (1.1 eq), , KOtBu (0.5 eq), $[IrCp^*Cl_2]_2$ (2 mol %), tert-amyl-OH (1M), 115 °C. Conditions B: Ph*COMe (1 eq), diol (1.5 eq), , KOtBu (1 eq), $[Ir(cod)Cl]_2$ (0.5 mol %), catacXium A(2 mol %) toluene (0.25M), 115 °C.

Initial studies in this reaction tested the compatibility of the $Cu(OAc)_2$/phenanthroline/ TEMPO system with Conditions A (conditions used to generate intermediate cyclohexane) as well as Conditions B (conditions used to generate intermediate cyclohexene). Although logically starting from the cyclohexene intermediate would facilitate the overall aromatization by circumventing the first oxidation step, relative to the cyclohexane, it remained plausible that the slightly milder conditions A would be most compatible with the subsequent aromatization.

2.4.2.1 Optimization of Copper and TEMPO dehydrogenation coupled to cyclization step

A series of conditions were tested using 3-methyl-1,5-diol to ascertain the feasibility of this method, these are summarized in Table 3 below, for full list of optimization experiments conducted see Appendix Table A3. Using the hydrogen borrowing conditions A, subsequently followed by the conditions reported by Shang and co-workers (10 mol % of copper(II) acetate, 10 mol % of 1,10-phenanthroline, and 3.0 equivalents of potassium acetate) with 4.0 equivalents of TEMPO to

compensate for the additional oxidation steps required, led to 41% isolated yield of the desired product (Entry 1). A reduction in equivalents of TEMPO used (3.0 eq) resulted in a notable decrease in yield (Entry 2).

Table 3

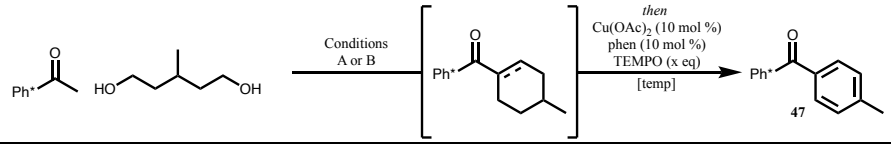

Entry	Condition A or B	[M] (x mol %) [L] (x mol %)	Additive (x eq)	TEMPO (eq)	Temp (C)	NMR yield of **47** (isolated)
1[a]	A	$Cu(OAc)_2$ (10) 1,10-phen(10)	KOAc (3)	4	115	(41)
2	A	$Cu(OAc)_2$ (10) 1,10-phen (10)	KOAc (3)	3	115	33 (11)
3	A	$Cu(OAc)_2$ (10) 1,10-phen (10)	n.a	4	115	63
4	A	$Cu(OAc)_2$ (10) 4,4'-$(CF_3)_2$bpy (10)	KOAc (3)	4	115	40
5	A	$Cu(OAc)_2$ (10) 1,10-phen (10)	n.a	4	125	68
6	A	$Cu(OAc)_2$ (10) 1,10-phen (10)	n.a	4	135	72 (47)
7	A	$Cu(OAc)_2$ (10) 1,10-phen (10)	tert-amyl-OH (0.1M)	4	125	31
8	A	$Cu(OAc)_2$ (15) 1,10-phen (15)	NHIP (4 eq) + O2	0	125	0
9	B	$Cu(OAc)_2$ (10) 1,10-phen (10)	n.a	4	125	70 (53)
10[b]	B	$Cu(OAc)_2$ (10) 1,10-phen (10)	n.a	6	125	48
11	B	Cu(OAc)2 (10) Phen(10)	n.a	6	125	(64)
12	B	$Cu(OAc)_2$ (10) 1,10-phen (10)	ABNO (6 eq)	0	125	19
13	B	$Cu(OAc)_2$ (10) 1,10-phen (10)	NHIP (5 eq) + O2	0	125	0
14	B	$Cu(OAc)_2$ (10) 1,10-phen (10)	NBS (4 eq)	0	125	0
15	B	$Cu(OAc)_2$ (10) 1,10-phen (10)	n.a	6	140	67

16[c]	B	$Cu(OAc)_2$ (10) 1,10-phen (10)	n.a	6	125	34
17[d]	B	$Cu(OAc)_2$ (10) 1,10-phen (10)	n.a	6	125	56

Conditions A: Ph*COMe (1 eq), diol (1.1 eq), , KOtBu (0.5 eq), $[IrCp^*Cl_2]_2$ (2 mol %), tert-amyl-OH (1M), 115 °C. Conditions B: Ph*COMe (1 eq), diol (1.5 eq), , KOtBu (1 eq), $[Ir(cod)Cl]_2$ (0.5 mol %), CataCXium A(2 mol %) toluene (0.25M), 115 °C. For reactions utilizing Conditions A for cyclization, reaction was subsequently diluted to 0.5M during aromatization step. Copper(II) acetate, 1,10-phenanthroline, TEMPO, and any additive used were added in one portion at room temperature to the reaction vessel, the vessel was then sealed, and placed in hot bath and stirred for 48 hrs.

[a] Aromatization done at 1M.

[b] Used 4 equivalents of KOH instead of KOtBu for cyclization step.

[c] Used 2 equivalents of KOtBu during cyclization step.

[d] Condition B and aromatization done with 1,2-dichlorobenzene as solvent.

When removing the potassium acetate additive (Entry 3), NMR yield showed in improvement relative to Entry 1, this is more likely due to the improved solubility and general stirring within the reaction. Generally, these reactions form very concentrated suspensions which leads to difficulty in generating a homogenous reaction mixture, it is likely the addition of excess salts contributes to this negatively. We hypothesized that increasing the Lewis acid character would increase the acidity of the γ-proton and thereby increase the rate of formation of the intermediate copper dienolate (Figure 28A), to that end we replaced 1,10-phenanthroline with the analogous, more electron withdrawing, 4,4'-$(CF_3)_2$bpy, however this had a negative impact on the overall yield (40% NMR yield, Entry 4). It was noted that a common side product observed from this reaction was the TEMPO substituted enone, analogous to the one shown in Figure 28A, though this could not be isolated. The subsequent step to this reaction is the hydrogen abstraction by a second TEMPO molecule to generate TEMPOH and eliminate the γ-TEMPO to generate the desired olefin. Hence we postulated that increasing the temperature of the aromatization would positively affect the reaction by means of increasing the rate of β-H abstraction. Pleasingly, increasing the temperature of the reaction to 125 and 135 °C indeed had a positive effect on the yield observed

(Entries 5 and 6) with Entry 6 showing the best yield obtained when using Conditions A, 72% NMR yield and 47% isolated yield. As the NMR yield difference (68 at 125 °C vs 72 at 135 °C) between these was deemed to be small the reactions were continued to be carried at 125 °C which was practically more feasible. As mentioned above, a practical hindrance to these reactions is the difficulty in generating homogenous reaction mixtures due to the substantial number of reagents engaged. As such we attempted to dilute the reaction to homogenize the reaction but this decreased the overall yield to 31%. Lastly, unlike the substrates reported by Shang and co-workers, the cyclohexane/hexene systems treated here are inherently bulkier. The Ph* ring itself provides substantial steric hindrance about the ring, more importantly our aim is to apply this methodology to poly-substituted six membered rings, with every substituent adding additional steric hindrance to the system. This poses a considerable challenge, as TEMPO is an already sterically hindered agent, thereby creating a considerable steric barrier to overcome. We attempted to take advantage of known N-hydroxyphthalimide (NHPI) reactivity under aerobic conditions to generate phthalimide-N-oxyl radical (PINO), which could serve as a less hindered analogue to TEMPO. Unfortunately, replacing TEMPO in our reaction for NHIP (4 eq) in an oxygen atmosphere and saturating the solvent with oxygen gas did not produce any of the desired product (Entry 8).

As expected, utilizing Conditions B to enable the cyclization step and produce the intermediate cyclohexene resulted in greater yields relative to when using Conditions A. When utilizing unchanged conditions to Entry 5, the standard 10 mol % $Cu(OAc)_2$, 10 mol % phenanthroline, and 4 equivalents of TEMPO at 125 °C following cyclization under Conditions B yielded our desired product in 53% isolated yield (70% HNMR yield) as shown in Entry 9. Increasing the TEMPO used increased the isolated yield of the product to 64% and was the highest yield obtained (Entry 11). Conditions B were slightly altered to utilizing 4 equivalents of KOH, as these were the original

conditions reported by Smith *et al*.,[54] however this had a detrimental effect on the final yield (48%, Entry 10). As the potential yield of the reaction using TEMPO appeared to reach a plateau, we once more looked for potential alternatives. The first alternative tested was naturally 9-azabicyclo[3.3.1]nonane N-oxyl (ABNO), a commonly used TEMPO analogue with significantly less steric hindrance about the N-oxyl radical and as a result significantly more reactive.[62] We hypothesized this lower steric hindrance would be perfectly poised to work in our system, however replacement of TEMPO for ABNO led to a significant decrease in yield (Entry 12). Once again the system with NHPI under aerobic conditions in place of TEMPO was tested, now under the Conditions B the reaction is run in toluene as opposed to *tert*-amyl alcohol and this could lead to better dissolution of the oxygen gas into the reaction mixture thus allowing the initiation of the NHPI to PINO, however this did not work and no product was formed (Entry 13). Lastly, we posited that NBS could be used as a source of bromine radicals, which could participate in an analogous fashion to TEMPO, but this also led to no formation of desired product (Entry 14). Of note, the large discrepancy in HNMR vs isolated yields most likely due to issues with work up and purification which were later largely fixed. The original workup reported by Shang *et al*. involved filtering with silica plug followed by column. Unfortunately, TEMPO had very close retention time to our aromatized product, as a result a method had to be devised to remove most of the TEMPO during workup to avoid it interfering during purification, see Experimental.

2.4.2.2 Substrate scope of One pot cyclization aromatization reaction

Optimized conditions were subsequently tested with a series of 1,5-diols to ascertain the generalizability of this transformation. (Figure 31) As shown below, yields of the aromatized

product are largely consistent. Simple methyl and aromatic substitutions were well tolerated (compounds **47**, **64**, **65**) and suggest this could be a useful transformation in synthesizing biphenyl compounds. Substrates **66**, **67**, and **68** bear longer aliphatic chains stemming from the ring constructed and yield insight into a key limitation to the methodology.

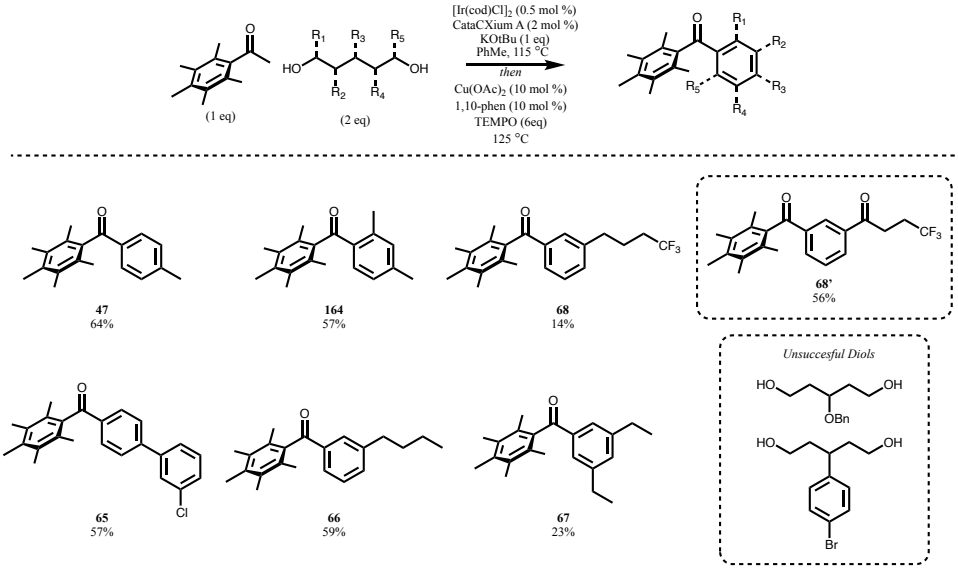

Figure 31: Substrates tested under one pot-cyclization-aromatization conditions.

Compound **68** has a significantly lower yield than all other substrates (14%) pointing to a key limitation in this methodology. The major product in the annulation and aromatization of **68** was the benzyl ketone, **68'** (see Supporting Information) in 56% yield, likely the result of the formation of a stable benzyl radical which captured oxygen and the peroxy radical ultimately decomposes to the carbonyl.[63] Furthermore, compounds **66** and **67** saw formation of the corresponding styrene and 1,3-butadiene products (<7% for **66** and <15% for **67**), these were inseparable to the desired parent compound. In testing substrates with branched aliphatic chains it becomes possible for

TEMPO to abstract an acyclic proton leading to undesired oxidation. This side reactivity is likely highly substrate dependent, being affected by the steric and electronic environments within the ring and side chains. Nonetheless, the high excess of TEMPO required likely would lead to undesired reactivity even if the aromatization of the cyclohexene is favored. Furthermore, diols bearing a protected (benzyl) alcohol and an aryl bromide were unsuccessful; these substrates have worked previously under a hydrogen borrowing paradigm which suggests these functionalities are incompatible with the aromatization step.

2.5 Ph* Cleavage of diaryl ketone substrates.

To prove the synthetic utility of this method it remained imperative to show that the Ph* group could indeed be removed from the substrates made and reveal the underlying benzoic acid moiety. Pleasingly, the Ph* was found to be readily displaced to afford to corresponding *p*-methyl benzoic acid **69** under mildly acidic conditions in 95% yield as shown in Figure 32. The selectivity of the acid formed (ArCOOH vs Ph*COOH) can be rationalized from the observation that the Ph* ring remains unconjugated to the ketone, thus remaining electron rich and prone to *ipso*-addition with a suitable electrophile to then undergo the desired retro-Friedel-Crafts acylation.[41]

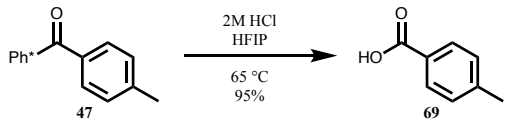

Figure 32: Removal of Ph* to generate benzoic acid.

2.6 Conclusion

A method for the one-pot cyclization and subsequent aromatization of 1,5-pentane diols with **8** was developed as a strategy to access substituted arenes in moderate yields. Our initial hypothesis, exploiting the rich chemistry of palladium to effect both the initial alcohol dehydrogenation and the subsequent dehydrogenations of the cyclized enone were unsuccessful. As suggested by the conversion rates to a cyclized product (Table 1), palladium(II) must effect the initial dehydrogenation of the diol very well, setting the stage for the desired (5+1) cyclization with **8**. However upon formation of the cyclized product, we fail to reliably see the formation of arenes. It remains plausible that under aerobic conditions palladium(II) mediates the disproportionation of the cyclized products to produce a mixture of cyclohexane, cyclohexene, and arene. When shifting from aerobic conditions to utilizing copper(II) salts as oxidant we were indeed able to observe the desired reactivity and aromatize a series of cyclohexenes, however these reaction conditions were orthogonal to the conditions required for the cyclization step making a one-pot protocol not viable.

Shifting to a Copper/TEMPO dehydrogenative system proved key to achieve the desired transformation. We showed that applying the iridium catalyzed acceptorless dehydrogenation conditions developed previously by the Donohoe lab and subsequently adding catalytic Cu(OAc)2/1,10-phen in conjuction with TEMPO to the same pot affords the desired arenes. This method is complementary to known methods for arene construction which traditionally rely on metal-catalyzed [2+2+2] cycloadditions of alkynes[64] or [4+2] cycloadditions (via Diels-Alder/Didehydro-Diels-Alder and subsequent dehydrogenation or tetradehydro-Diels-Alder). [65] This method grants access to Ph* protected benzoic acid substrates, the Ph* can be readily cleaved to afford the corresponding acid.

3 Stereochemical control of alpha-stereocenters in polysubstituted cyclohexanes

3.1 Introduction to stereochemical control in HB (5+1) annulation

3.1.1 General Considerations

As was previously discussed in (section 1.3.3), control of the γ-stereocenter in the synthesis of cyclohexanes was an especially challenging obstacle to overcome. (Figure 33) The basic conditions required under the HB paradigm meant that substituents about the γ-carbon were inherently prone to racemization through the formation of extended enolates. (Figure 33)

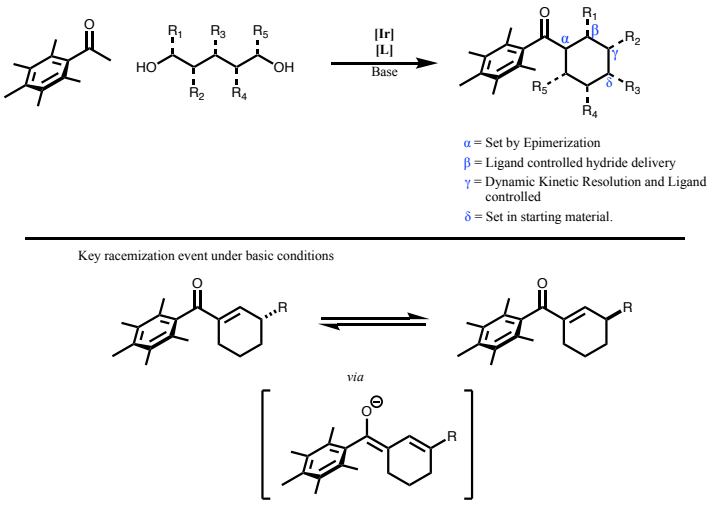

Figure 33: Strategies for stereochemical control of cyclohexane substituents under HB. Key racemization event making control of γ-stereocenter challenging.

3.1.2 Stereocontrol of the gamma-stereocenter

The dynamic nature of this racemization event made this system perfectly poised to be exploited through dynamic kinetic resolution (DKR), as once the enone (**II**; Figure 34) is reduced the γ-protons are no longer acidic enough to be deprotonated, thereby locking the substrate in its final configuration (**III**). This insight was executed by Cheang *et al*. in 2025, reporting a catalytic system that could perform an effective HB-cyclization transformation to yield enantioenriched 3-substituted cyclohexanes from *racemic* linear precursors (**I**) with the use of ligand [R_P,*S*]-PPF-NH_2 ([L] in Figure).[53] (Figure 34).

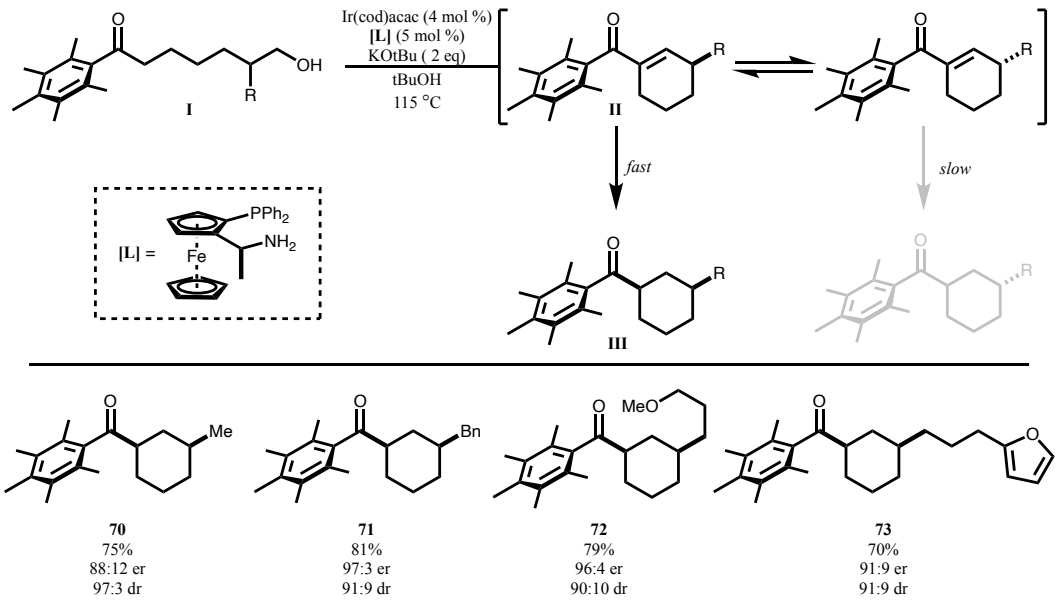

Figure 34: DKR strategy to controlling the γ-stereocenter and selected products.

Shown in Figure 34 are a select sample of cyclohexane products that were synthesized from the *racemic* linear alcohol. The size of substitutent R has a noticeable effect on the enantiomeric ratio of the product, with R = Me (**70**) having the lowest e.r. of the substrates tested, however larger

groups have excellent e.r. as exemplified by R = Bu (**71**). Furthermore, the yields obtained were excellent, ranging between 70-90% and functional groups such as methoxy ethers (**72**) and THF rings (**73**) are well tolerated.

3.1.3 Issues with diol cyclization

In improving this new methodology to make cyclohexanes from 1,5-diols directly (rather than from the linear precursor shown above), a new challenge arises. Extending this methodology to 1,5-diols is highly desirable, partly due to the greater elegance of the transformation, but also because the linear precursors **I** (Figure 34) can be very laborious to make and are not commercially available (in contrast to 1,5-diol starting materials). The γ-carbon in the cyclohexane ring constructed corresponds to the 2-position in a 1,5-diol (**I**; Figure 35). As a result, there isn't enough steric bulk close enough to either alcohol to favor the selective oxidation of one alcohol over the other and this results in two different aldehydes (**II and II'**) which can then undergo the traditional aldol condensation-[1,5] hydride shift-aldol condensation cyclization sequence to yield two distinct regioisomers **III** and **III'**. Note that it has also been postulated that the two aldehydes may interconvert via a [1,5]-hydride shift.

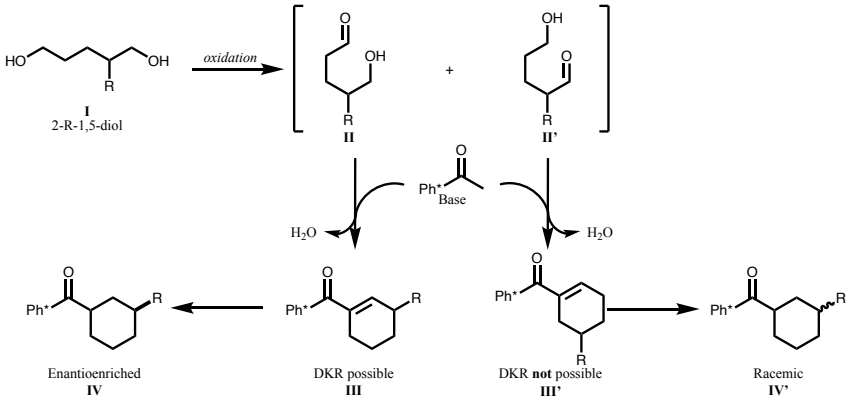

Figure 35: Challenge in applying DKR method to acces enantioenriched 3-substituted cyclohexanes from 1,5-diols.

Once enones **III** and **III'** are reduced to the corresponding hexane, the resulting γ-substituted cyclohexane is the same: however at the enone stage only **III** can form an extended enolate that will racemize R, whereas **III'** cannot. The consequence of this regioselectivity problem is that while **III** is capable of undergoing DKR and yield enantioenriched IV, enone **B** cannot, and will inevitably yield a racemic product **IV'**. Initial attempts at circumventing these issues were fairly successful: by increasing the concentration of the reaction mixture to (0.6M to 3M) to promote the intermolecular hydrogen borrowing, and employing excess Ph* methyl ketone (2 equivalents) to ensure the aldol condensation would outcompete the aldehyde interconversion via [1,5]-hydride shift, it was possible to effect the desired transformation with diols in good yields and e.r. (see Figure 36). Indeed the 3-butyl and 3-benzyl substrates were synthesized in 83% and 70% yield respectively with good e.r. (86:14 and 90:10, respectively).[66] However, the e.r. of these were notably less than for the linear precursors and could be improved upon.

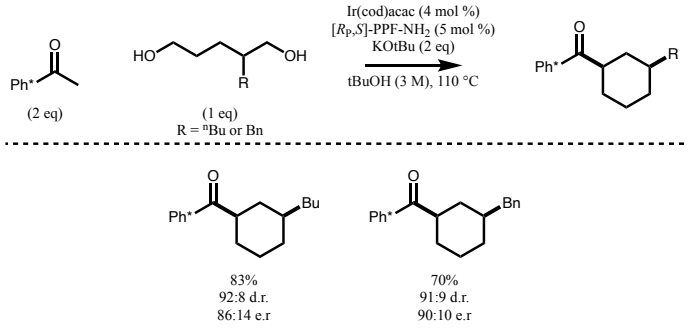

Figure 36: Intermolecular alkylation, cyclization and preparation of enantioenriched, 3-substituted, cyclohexanes via DKR methodology.

As another strategy to address this problem (which at its heart stems from a lack of steric differentiation of a 1,5-diol substrate), the Donohoe group postulated that introducing a 4-R-substituted-1,5-hexanediol could solve this problem. Unlike a 2-R-substituted-1,5-pentanediol, a 4-R-substituted-1,5-hexanediol would have a single primary alcohol (with the 5-OH being secondary) and therefore the first oxidation event would be expected to highly favor the formation of the aldehyde and this should solve the regioselectivity problems identified above. (Figure 37)

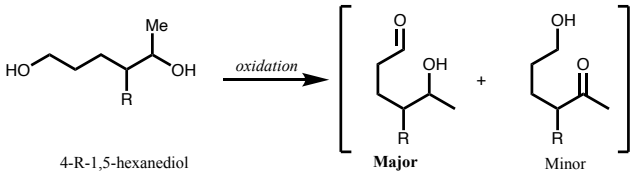

Figure 37: Potential solution to regiochemical challenge in oxidation of asymmetric diols.

To this end, 4-Me-1,5-hexanediol (**74**) was prepared (Figure 38A). Mono-alkylation of δ-valerolactone was achieved in 36% yield in a 55 mmol scale, the resulting methyl lactone was then reduced to the lactol with DIBAL and concomitant addition of MeMgBr yielded **74** in 23% yield over three steps. We then submitted the diol to the reaction conditions reported by Cheang *et al*. (2025), but substituting the ferrocene ligand ([L]; Figure 34) for the commercially available (*R*)-DTBM-SEGPHOS. (Figure 38B). Early work using an extensive ligand screen, showed that[R_P,*S*]-PPF-NH_2 was optimal due to the excellent e.r. of the hydrogen borrowing/DKR cyclizations of the linear substrates discussed above. On the other hand (*R*)-DTBM-SEGPHOS was also known to effect the desired DKR transformation with slightly better yields (albeit at the cost of lower e.r.). Synthetically, the key difference between these two is that the absolute stereochemistry of the product is reversed, where using [R_P,*S*]-PPF-NH_2 favors the formation of the (*S*) enantiomer and (*R*)-DTBM-SEGPHOS favors the formation of the (*R*) enantiomer. Importantly however, (*R*)-

DTBM-SEGPHOS is readily available in stark contrast to [R_P,*S*]-PPF-NH_2, and so it was chosen as the ligand of choice to proceed with our study. Three distinct diastereomers were produced (**75**, **76**, and **76b**, Figure 38); diastereomer **75** was readily isolated however **76** and **76b** could not be separated (this mixture is 82% **76** and 18% **76b**), in a collective yield of 74%. The relative stereochemistry of each isomer was assigned through nOe correlations *J*-coupling constants, and furthermore the data for these diastereomers was known and had been previously published.[67] Pleasantly, the stereochemistry about the dimethyl substituents was good, with the major product **75** being produced with good enantioselectivity 91:9 e.r. and **76** having an e.r. of 93:7. This is a significant improvement in enantioselectivity of the reaction relative to the exclusively 3-substituted substrates in Figure 36 above. This suggest that indeed issues with the regiochemistry of the first oxidation may have been a contributing factor in the loss of e.r. (Figure 35) and greater differentiation of the two ends of the diol is a viable solution.

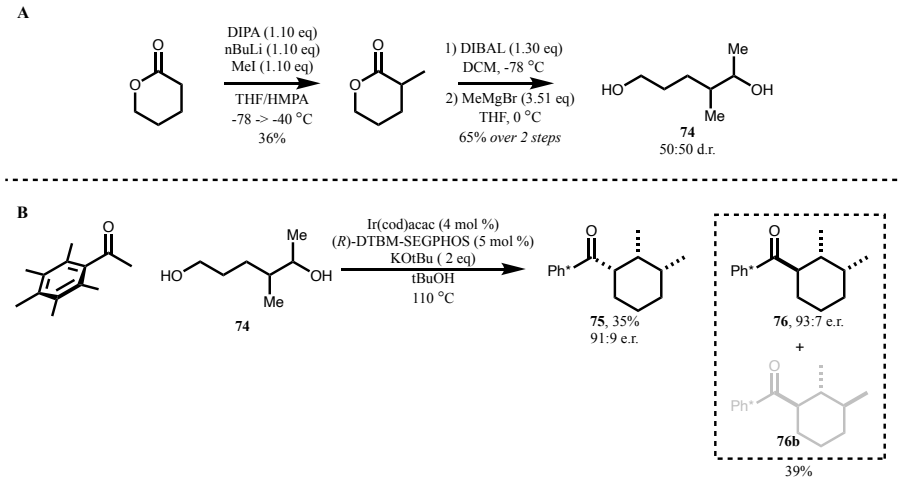

Figure 38: A) Preparation of 4-Me-1,5-hexanediol. B) Using 4-Me-1,5-hexanediol under DKR method to access enantioenriched 2,3-substituted cyclohexanes from 1,5-diols.

As discussed before, the α-stereocenter is prone to epimerization under the reaction conditions and consequently will be driven to thermodynamic equilibrium. In this instance the thermodynamic equilibrium at the α-stereocenter yields a roughly equal distribution of *cis*- (**75**) and *trans*- (**76**) products relative to the *cis*-dimethyl (35% **75** and 32% of **76**). Substrates with no β-substituents (i.e. only γ-substituent) traditionally display excellent diastereoselectivity in these reactions in favor of the *cis* product. This can be rationalized by favoring substituents at C-α and C-γ taking an equatorial position to minimize steric clashes and afford the lowest energy product. However the addition of a β-substituent, more importantly a *cis*-substituent (relative to the γ-substituent) as with **75** and **76**, can have a significant impact. As a result of both methyl groups being *cis*- to each other, there must always be one axial and one equatorial methyl group, consequently the chair conformations that would ultimately re-protonate to form **75** and **76** are likely of very similar energy and ring flipping among these would be facile. This results in the approximately equal mixture at the α-stereocenter that we observe.

3.2 Control of the alpha-stereocenter in **75** and **76**

Due to the synthetic value of the enantioenriched dimethyl scaffold, we were driven to establish a reliable method to interconvert the inseparable mixture of **75** and **76** and so gain access to a single enantiomer and diastereomer. Although the thermodynamic equilibrium of the α-stereocenter doesn't distinguish between **75** or **76** under the reaction conditions (110 °C), we postulated that two approaches may be fruitful in changing the ratio: exploiting the thermodynamic equilibrium at lower temperatures and deprotonation/protonating under kinetic conditions (Figure 39). These approaches aim at exploiting the very subtle differences between the chair conformations of **75** and **76**. Though the chairs of **75** and **76** are likely of very similar energy, there is indeed an

asymmetry (not 50:50 mixture); this is likely a reflection of the different steric constraints observed in **75** where the equatorial carbonyl is syn to the axial methyl, whereas **76** poses the axial methyl anti to the carbonyl (Figure 39). At high temperatures these effects aren't sufficient to drive the equilibrium in one direction but at lower temperatures we can possibly drive the thermodynamic equilibrium to the more stable diastereomer. Furthermore, this difference in the steric environment around the proximity of the α-stereocenter may impose a rate difference in the protonation face of these substrates which can be exploited as well in a separate kinetic approach.

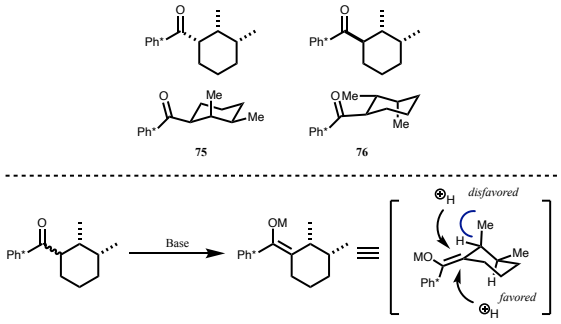

Figure 39: Structures of **75** and **76**.

3.2.1 Thermodynamic Control

It was hypothesized that the thermodynamic equilibrium between **75** and **76** could be driven to favor one or the other by lowering the reaction temperature, to favor the configuration that is least sterically frustrated and thereby lower in energy. Initial studies submitting **75** to the standard reaction conditions: potassium tert-butoxide (2 eq) in *tert*-butanol, at a lower temperatures (Figure 40). Indeed, lowering the temperature to 85 °C showed a measurable difference in the ratio of **75** and **76**. When submitting **75** to these basic conditions with a protic solvent at 85 °C, the thermodynamic equilibrium shifts from 1.0:0.91 of **75**:**76** to 1:0.75 (Figure 40, entry b). When

submitting **75** to the same conditions we similarly observe the ratio of **75**:**76** be 1:0.77 which suggest we indeed have reached equilibrium.

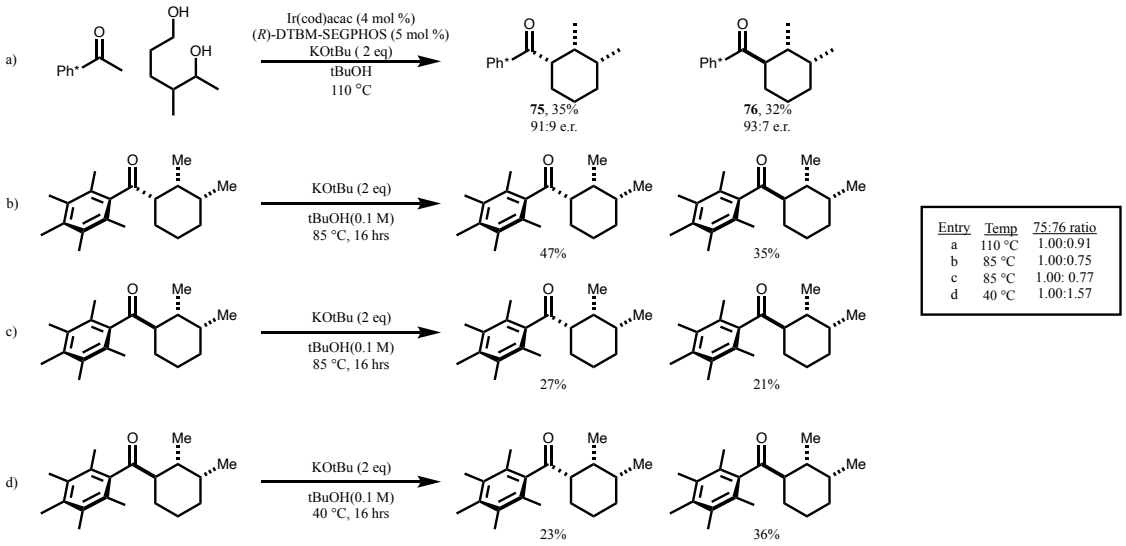

Figure 40: Effect of temperature on thermodynamic equilibrium between **75**:**76**.

When lowering the temperature further to 40 °C, 16 hours was likely not sufficient time for the system to achieve thermodynamic equilibrium (entry d), as the ratio of **75**:**76** is seen to be flipped when starting from B, suggesting it's likely deprotonation of the cyclohexane is very slow at this temperature. Extending the reaction time to 66 hrs to ideally reach equilibrium led to a complex mixture of products and was not viable. Continuing to lower the reaction temperature in order to shift equilibrium made deprotonation increasingly slower and as such the interconversion of products less accessible. Furthermore, due to the inherent energy similarity between **75** and **76**, the temperature required for the thermodynamic equilibrium to favor **75** over **76** would be too low to achieve the desired effect. We can perform a rudimentary calculation using the two temperature data points we observe, namely that **75**:**76** = 1.0:0.91 at 110°C and **75**:**76** = 1.0:0.76 at 85°C, to calculate:

$$\Delta\Delta G = -RTln\left(\frac{k_{76}}{k_{75}}\right);\ \Delta\Delta G\ (T = 383\ K) = -R(383)ln(0.91)\ ,\Delta\Delta G\ (T = 358\ K) = -R(358)ln(0.87)$$

$$\Delta\Delta G\ (T = 383\ K) = 0.30\frac{\text{kJ}}{\text{mol}}\ ,\Delta\Delta G\ (T = 358\ K) = 0.82\frac{\text{kJ}}{\text{mol}}$$

These relative difference in Gibbs free energy for **75** and **76** at these temperatures allow us to calculate relative ΔH and ΔS.

$$\Delta\Delta G = \Delta\Delta H - T\Delta\Delta S:\ 0.30 = \Delta\Delta H - (383)\Delta\Delta S\ ,\qquad 0.82 = \Delta\Delta H - (358)\Delta\Delta S$$

$$\Delta\Delta H = 8.3\frac{\text{kJ}}{\text{mol}}, \Delta\Delta S = 0.0208\frac{\text{kJ}}{\text{mol}}$$

Equipped with these values (and assuming these are constant, though they likely would not be) we can predict the approximate necessary temperature for a given ratio of **75**:**76**, in example: a ratio **75**:**76** of 10:1, which would be more synthetically useful:

$$\Delta\Delta G = -RTln\left(\frac{k_{76}}{k_{75}}\right);\ \Delta\Delta G = \Delta\Delta H - T\Delta\Delta S$$

$$-RTln\left(\frac{1}{10}\right) = 8.3 - T(0.0208)$$

$$0.03995T = 8.3$$

$$T = 208\ \text{K}$$

Based solely on these calculations, which is an oversimplification and would need further experimental data to back up, it suggests that on a purely thermodynamic basis the equilibration of **75** and **76** would need to be done at around 208K (-65.15 °C). This value is not to be taken as an unchangeable figure, as small changes to the empirically obtained ratios are compounded throughout the equation. For instance, it is not uncommon to see an error variability of approximately 10% in NMR yields, inputting a plus or minus 10% range of error to the above equation provides a temperature range of -117 °C to -18 °C. This is a very large range of possible temperature points when considering only a possible 10% error, however the key take away is the temperatures required to achieve the desired ratio of **75** to **76** would be too cold to achieve

thermodynamic equilibrium. For these reasons we decided to pursue a different approach as will be shown below.

3.2.2 Kinetic Control and silyl enol ethers as enolate precursor

As it was deemed unlikely that the thermodynamic equilibrium approach would be viable under standard operating temperatures it was decided to pursue kinetic (re)protonation of the enolate. Using a strong lithium base under cryogenic temperatures we aimed to create the conditions necessary for carbon protonation of the enolate which paired with a bulky proton source could exploit the less sterically hindered face of the enolate (Figure 39). At -78 °C n-butyl lithium was not able to effect the desired deprotonation of **75** to yield the enolate to great extent. Methyl lithium could effectively deprotonate the cyclohexane substrate as measured by deuteration of the enolate, however attempts to protonate the resulting enolate with bulky proton sources (i.e. BHT) were unreliable and yielded poor recovery of the material (64%). As a result, it was decided to prepare the stable silyl enol ether analogues. (Figure 41) Standard methods employing an amine and TMSOTf proved to be unsuccessful; similarly treatment with strong bases (NaH and MeLi) and TMSCl did not lead to desirable silyl enol ethers. Ultimtately $B(C_6F_5)$ and Me_2PhSiH (frustrated LA and silane Lewis base pair) were necessary to form the corresponding bulky silyl enol ethers.

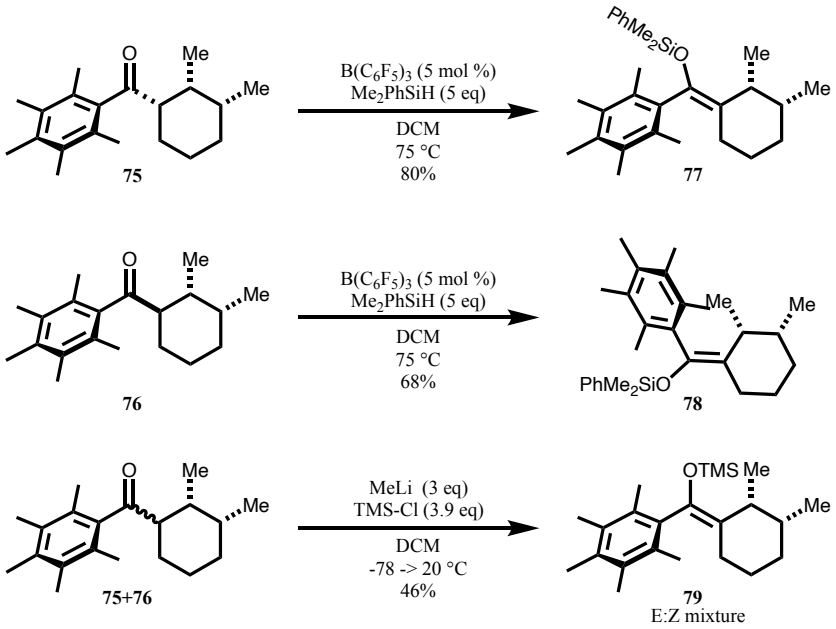

Figure 41: Synthesis of silyl enol ethers of **75** and **76**

Employing the silyl enol ether instead of preparing the enolate *in situ* brings about a series of benefits, namely: can readily ensure C- over O-protonation and there is significant literature precedent to the asymmetric protonation of silyl enol ethers.[68] To that end, **75** was used to prepare silyl enol ether **77** and **76** yielded silyl enol ether **78** using the method described by Blackwell *et al*.,[69] in good yields (80% and 68% respectively). This method relies on generating the frustrated Lewis acid-base pair between tris(pentafluorophenyl)borane (BCF) and dimethyl phenylsilane to activate the silane for O-attack from the carbonyl, and subsequent deprotonation with the boron-bound hydride to afford the desired silyl enol ether. Interestingly it was observed that **75** and **76** afforded different isomers, 2D NOESY experiments revealed **75** produced the *Z*-isomer exclusively while **76** formed the *E* isomer. This is understandable as **75** and **76** differ in the stereochemistry at the α-proton which undergoes deprotonation, thereby directly affecting the geometry of the resulting enolate. The TMS silyl enol ether **79** was prepared in 46% yield by standard methods, using methyl lithium and TMS-Cl.

A series of enantioselective protonation reactions of silyl enol ether were tested on compound **79**. Previously the Levacher lab had reported an organocatalytic enatioselective protonation protocol using cinchona alkaloids and carboxylic acids,[70] however this method proved unsuccessful in our system, returning only starting material. (Figure 42) Warming up this reaction to room temperature (20 C) and stirring for 72 hours similarly did not lead to any reaction. Similarly, the Yanagisawa group had reported an excellent AgF-(*R*)BINAP system which can protonate silyl enol ethers with > 99% ee;[71] however this system also was unreactive in our system when tested with **77**, only returning 5% of the desired ketone, with 72% of starting material being recovered.

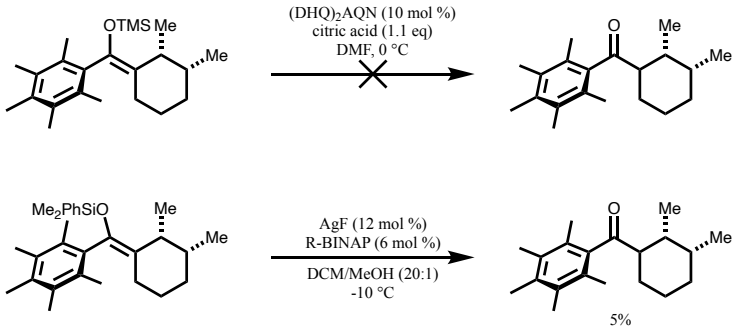

Figure 42: Methods for the enantioselective protonation of silyl enol ethers.

Taking advantage of the access these silyl enol ethers to the corresponding enolates, we could once again test the kinetic protonation of the enolate now under more readily controlled conditions. We postulated that transmetalation of the silyl enol ether with methyl lithium would reliably afford the lithium enolate, we could then once more attempt to protonate the resulting enolate under kinetic control conditions. To our dismay, at this point it became clear that the face of the enolate which accepts the proton delivery is primarily controlled by the geometry of the starting enolate, as opposed to the dimethyl substituents. This was evidence by submitting the *Z* and *E* enolates **77** and

78 independently to a bulky proton source. As seen in Figure 43, *Z*-silyl enol ether **77** upon formation of the lithium enolate and subsequent treatment with a bulky proton source at -78 °C yields almost exclusively **75**, which was the isomer used to prepare *Z*-silyl enol ether **77** in the first place. The protonation of the *E*-enolate, prepared from *E*-silyl enol ether **78** is less selective for **76** than its *Z*-counterpart, as **75** side product is formed to a greater extent, but still **76** is the major product observed. The diastereomeric enolates (E vs Z) are locked in conformation and impose a large constraint on the face from which protonation is most accessible. The face of the enolate which is ultimately protonated likely is dictated by the overall geometry of the alkene and the way in which the Ph* moiety is therein directed, as well as the cyclohexane conformation in which the olefin is locked in; likely the steric environment collectively generated by the two methyl groups and orientation of the Ph* ultimately control the face of protonation.

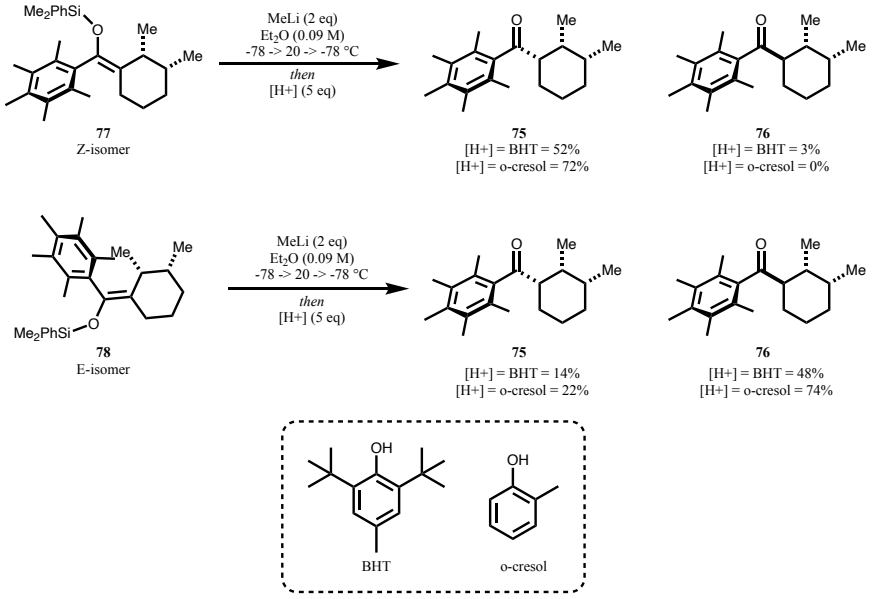

Figure 43: Transmetalation and enolate protonation under kinetic control.

3.2.3 Ph* removal

One last attempt at controlling the stereochemistry about the alpha-stereocenter was conducted using the esters in Figure 44. The Ph* was cleaved from **75** and **76** to generate butyl esters **80** and **81** correspondingly, these esters were then utilized to perform the kinetic controlled protonation experiment attempted earlier with the ketone precursors. We hypothesized that the protonation behavior observed with the Ph* enolates, where the enolate geometry played a greater role in determining the preferred face of protonation, may be largely controlled by the steric bulk established by the Ph* ring. If so, removal of the Ph* ring may then allow for dimethyl substituents to have a more robust effect on the protonation of the enolate. Unfortunately this was not observed, deprotonation of the butyl esters with LDA followed by protonation with BHT at -78 °C lead to epimerization of the esters without a significant preference for either isomer. (Figure 44)

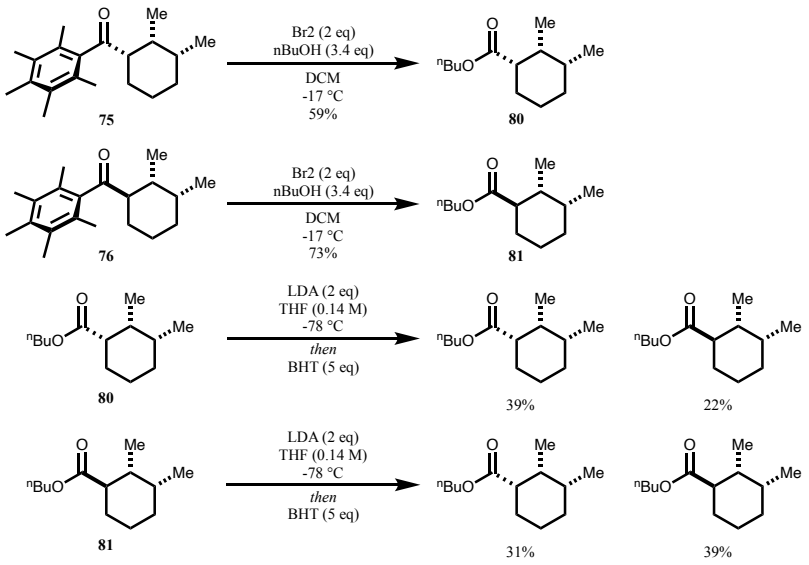

Figure 44: Cleavage of Ph* and epimerization of esters.

3.2.4 Formation of ketene and interception

As a last attempt at controlling chirality at the α-stereocenter, we attempted to take advantage of the intermediate acyl bromide formed during Ph* cleavage. Treatment of acyl halides (**I**, Figure 45A) with an acidic α-stereocenter can be deprotonated with a non-nucleophilic (i.e. DIPEA) base to generate the corresponding ketene *in situ* (**II**).[72] The ketene can subsequently be intercepted by a chiral alkaloid ligand (i.e. quinine) (**III**) and allow for the asymmetric C-protonation of the resulting enolate (**IV**). The ligand can subsequently be displaced by a nucleophile (**V**). Unfortunately attempts at intercepting the ketene in this fashion proved unsuccessful (Figure 45B), in fact quenching of the reaction with deuterated methanol after treatment with DIPEA showed no deuteration at the α-position. This is evidence that in fact no ketene formation occurs under reaction conditions as we would expect D incorporation if the ketene was indeed formed.

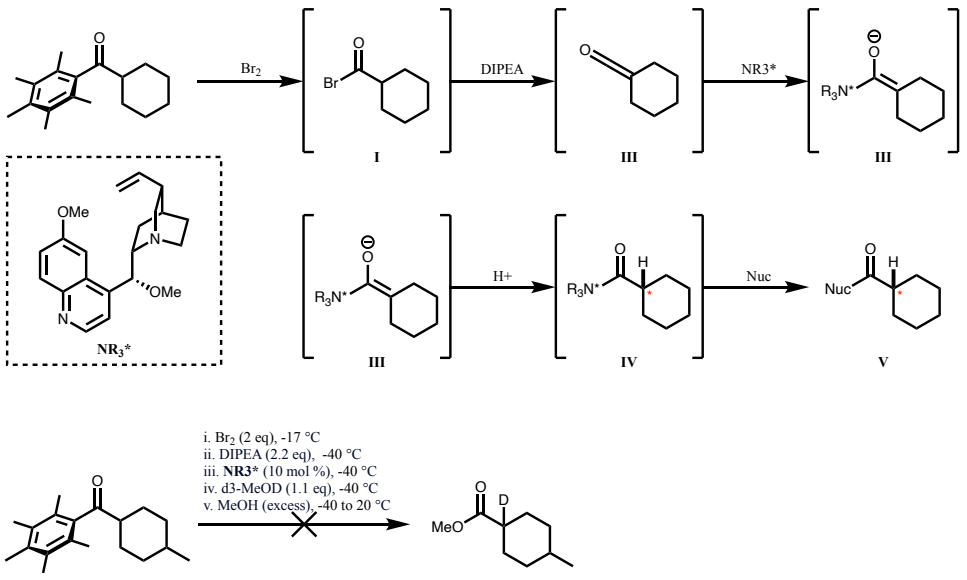

Figure 45: Proposed reaction pathway for ketene formation and interception.

3.3 Substrates beyond 2,3-dimethyl-cyclohexane

The inability to reliably control the α-stereocenter, in addition to the lack of enantioselectivity and efficiency observed when synthesizing 2,3-disubstituted cyclohexanes with substituents larger than methyl groups (Figure 46) with this methodology, ultimately led us to abandon this effort. To test the applicability of this chemistry to substrates with larger substituents, diols **82** and **83** were prepared. Both diols were prepared analogously to **74**, though now alkylating δ-valerolactone with benzyl bromide in place of methyl iodide, this reaction is more efficient than the methyl counterpart (62% yield instead of 36%). Subsequent reduction of the lactone with DIBAL followed by treatment with MeMgBr produced **82** in 77% over two steps, and treatment with PhMgBr produced **83** in 48% yield over two steps. Attempts to perform the same cyclization with diol **82**, which substitutes the 4-Me in diol **74** for a bulkier 4-Bn substituent, led to a mixture of multiple diastereomers (**84A**, **84B**, and **84C**) in low yields. Similarly, introducing another bulky substituent, replacing the 5-Me of diol **82** for a phenyl group gives diol **83**. Submitting **83** to our HB-cyclization conditions leads to a steric environment too congested to yield any meaningful amount of product, and instead resulted only in a low yield (27%) of the unreduced enone product **85**.

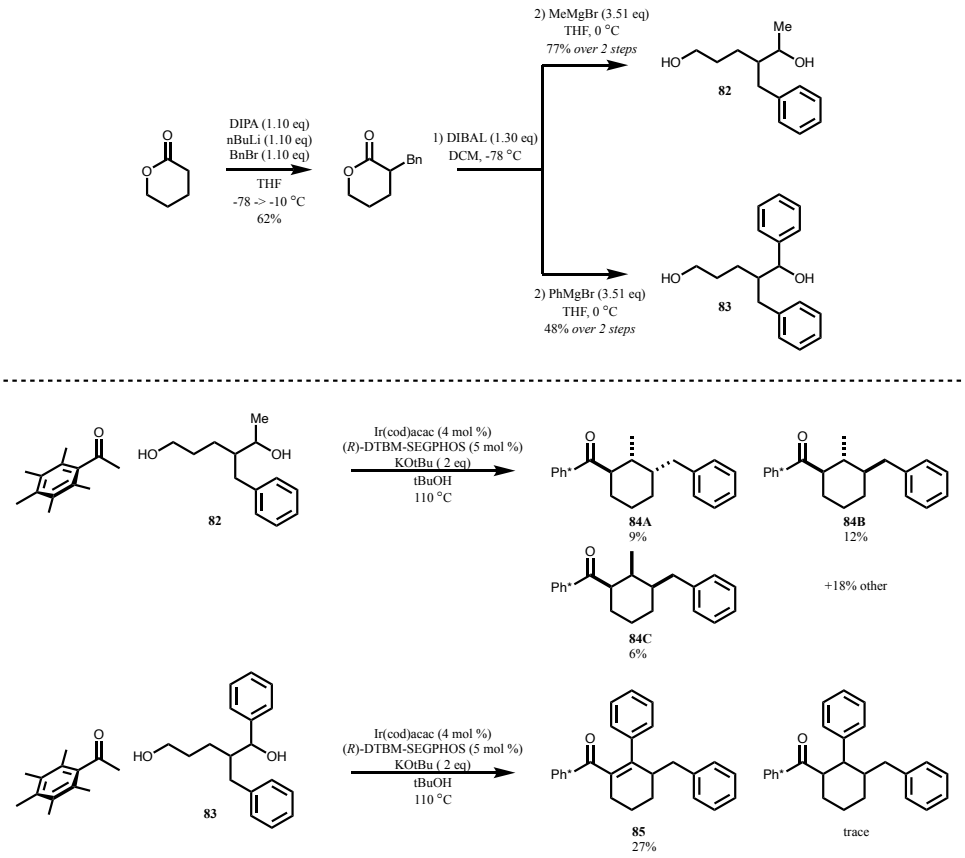

Figure 46: Attempts at employing DKR HB conditions on 3,4-substituted diols with bulkier substituents.

3.4 Conclusions

All efforts at controlling the stereochemistry about the alpha stereocenter of **75/76** were unfortunately unsuccessful. The alpha stereocenter has been shown to epimerize to its most stable configuration under the reaction conditions.[50] For cyclohexanes bearing a single β- or δ-substituent, this conformation is usually *trans*, alternatively for γ-substituted cyclohexanes the acyl-Ph* substituent is traditionally takes a *cis* conformation relative to the substituent. With a 2,3-

disubstituted system, as is the case with **75**/**76**, the thermodynamic equilibrium between *cis* and *trans* conformations does not significantly favor **75** or **76**. Attempts at driving this equilibrium in a single direction by employing lower temperatures was a viable strategy, as the ratio of **75**:**76** could indeed be shifted (1:0.91 at 110 °C vs 1:0.75 at 85 °C), however the ratio remained too low. Lower temperatures are likely to further shift the thermodynamic equilibrium in favor of **76**, however the rate of deprotonation at those temperatures would likely be too slow to effectively achieve thermodynamic equilibrium; this was observed when submitting **76** to basic conditions at 40 °C.

Subsequent studies to ensure kinetically protonating the less hindered face of **75** and **76** enolates also proved unfortunately ineffective. It is likely that indeed under the conditions tested we achieve C- protonation over O- protonation, as protonation of the enolate leads to regeneration of the parent isomer with little epimerization. In contrast to the kinetic protonation studies of **75**/**76**, when conducting the same tests with esters **80**/**81** we observed racemization of the α-stereocenter. It is possible that protonation of the ester enolate goes through O-protonation initially, which upon tautomerization yields the product. Conversely, if indeed reaction goes through C-protonation, the steric hindrance generated by the dimethyl substituents may not be sufficient to favorably drive protonation from the less hindered side of the enolate. These results point at the fact that, for the enolates of **75** and **76**, it is the geometry of the enolate and specifically the role played by Ph* which drives the face of protonation.

Lastly, it had been posited that we could take advantage of the intermediate acyl bromide generated during Ph* cleavage to *in situ* generate a ketene which could be intercepted by a nucleophile asymmetrically. Unfortunately, this approach did not work and no sign of the desired ketene forming was observed.

4 Introduction: DAT and DAT Inhibitors

4.1 Introduction to DAT and DAT inhibitors

4.1.1 Introduction to Dopamine

Dopamine (DA; see Figure 47) is perhaps among the most colloquially popular molecules, often thought of as the "feel good" or "pleasure" molecule in the brain. In fact, DA, or rather 3-hydroxytyramine, is responsible for a myriad of functions, and its discovery as a neurotransmitter is regarded as one of the seminal discoveries in neuroscience.[73] Originally believed to be just a precursor to noradrenaline[74], DA was first found to be a neurotransmitter within the brain in a series of papers published in 1957-1958.[75–77] Along with their discovery of DA in the brains of various mammals, Carlsson et al. also conclusively showed DA was essential to facilitating movement and locomotor activity through their studies with reserpinized mice.[77] Since its discovery in the brain, this neurotransmitter has been found to play a crucial role not just in motor function, but learning, reward, motivation, and most importantly for the current volume: addiction.[73]

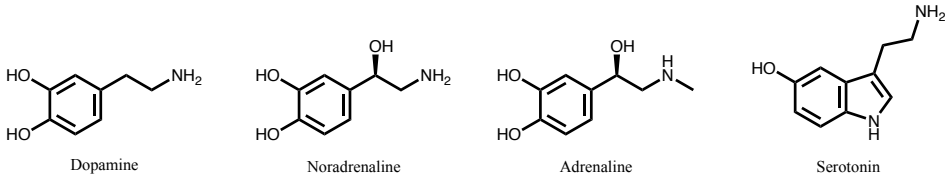

Figure 47: Common monoamine neurotransmitters.

DA would remain associated primarily as a mediator of motor function and as a key intermediator in relevant pathologies (i.e. Parkinson's Disease)[78] until the 1970's. By the early 1970's evidence that chlorpromazine, the first marketed neuroleptic, and other antipsychotics such as haloperidol,

were likely acting on the dopaminergic system was mounting,[79] putting DA at the forefront of psychopharmacological research. By the late 1970's and into the 1980's, it was becoming increasingly clear that the rewarding, and consequently addicting, effects of substances of abuse must also be mediated through DA.[79–84] Of note, this early work focused on psychostimulants such as cocaine and the amphetamines, which act directly on the dopaminergic system (as will be expanded on below). However, by 1987 evidence that likely all abused drugs effect their rewarding and reinforcing effects through dopaminergic activation was becoming accepted dogma in the field of addiction medicine.[85]

4.1.2 DA and Drug Abuse

The role of DA in drug abuse and addiction cannot be understated. In a seminal 1988 paper, Gaetano Di Chiara and Assunta Imperato showed that amphetamine, cocaine, opiates (morphine), ethanol, and nicotine all increased the concentration of extracellular DA in the nucleus accumbens and the dorsal caudate nucleus (both terminal dopaminergic areas, the former of the mesolimbic system and the latter of subcortical motor system) in rat brains; this increase was most significant in the nucleus accumbens.[81] Importantly, drugs that are not abused did not show an analogous increase in DA concentration in the limbic system. These findings consolidated work done over the previous decade showing definitive role of DA and the dopaminergic system in the pharmacology of drugs of abuse. Koob and Bloom summarize the generalizability of this concept poignantly: "Despite the diversity in their primary sites and mechanisms of action, all three classes of drugs [psychostimulants, opiates, ethanol] may elicit their initial arousing-reinforcing effects via neurons that are components of the VTA-nucleus accumbens-ventral pallidal extrapyramidal

motor regulator system [mesolimbic region]."[86] In simpler terms, regardless of the independent mechanism of action that each drug of abuse may have (i.e. cocaine is a DAT inhibitor, morphine is an agonist at mu-opioid receptor), downstream effects result in an increased concentration of extracellular DA in the mesolimbic region, the dopaminergic region of the limbic region (brain structure associated with emotions and motivation, among others).[87]

The above experiments, while relevant, were conducted in rodents. Subsequent studies with PET imaging conducted throughout the 1990's and early 2000's further validated them in humans. Early studies using Carbon-11 labeled cocaine and methylphenidate (commonly known as Ritalin, also a DAT inhibitor) showed that indeed, in humans, they both bind primarily to the DAT in the striatum;[88,89] the brain structure where the nucleus accumbens resides and densely populated by dopaminergic neurons. Of interest to the reader, though outside the scope of the current thesis, this striatal increase in DA (and concomitant activation of DA receptors) is believed to result in both the rewarding effects of these drugs while also encoding motivation and reinforcement.[90,91] A similar increase in striatal DA was similarly reported for a wide range of drugs of abuse which act on different targets, such as amphetamine,[92,93] nicotine,[94] alcohol,[95] ketamine,[96] and THC,[97] when tested by PET imaging in humans, to cite a few. Subsequent studies have also shown measurable synaptic alterations within the mesolimbic region as a result of chronic drug use and addiction.[98] This effect is most notable in psychostimulant (i.e. cocaine and methamphetamine) users[99–101] though has also been shown in individuals who are alcohol-dependent[102–104] and to a lesser extent opiate users,[105,106] where expression of DA receptors is markedly decreased relative to non-user controls. In addition to decreased receptor availability, users with dependence on these drugs also experience blunted DA release in the striatum. This effect was originally measured in cocaine

dependent participants[107] but has since also been observed in opiate and alcohol-dependent individuals.[104,106] By hijacking the dopaminergic system, natures-given circuitry to enable reinforcement and learning, drugs effectively "reinforce their own acquisition."[108]

4.1.3 DA and DAT

There is substantial evidence pointing to DA as the key modulator of psychostimulant use disorder (PSUD). Being able to regulate dopaminergic signaling in a dysfunctional system therefore is a vital element in the strategy for the treatment of PSUD. DA is produced by presynaptic cells, stored in vesicles, and subsequently released into a synaptic cleft upon excitation.[109] Upon release into the synaptic cleft, DA can bind to DA receptors post-synaptically to effect downstream signaling in the target neuron or it can bind to presynaptic autoreceptors to reduce the release of DA.[110] DAT is the only cellular machinery designed to remove DA from the synapse to re-enter the presynaptic cell and be recycled, ending signaling. As a result, DAT plays a pivotal role in healthy dopaminergic signaling. Visual representation of the above process is provided below in Figure 48.

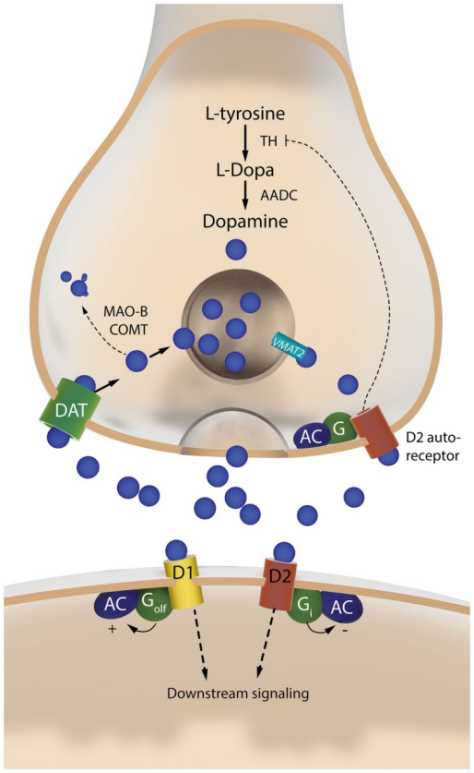

Figure 48: General representation of DA in synaptic cleft from Cenci *et al*.[111]

The DAT is a Na^+/Cl^- coupled transporter embedded within the plasma membrane of dopaminergic cells exclusively[112] (Figure 49). Comprised of 12 transmembrane helices, DAT alternates between an outward and inward facing conformations[113,114] wherein it captures DA from the synapse in its outward facing conformation, it consequently undergoes a conformational shift to an intermediate stable phase termed "Occluded" before transitioning to the inward-facing conformation and subsequent release of DA into the cytosol. Within the structure of DAT are two known binding sites, S1 and S2. S1 is the binding site well within the transporter cavity where DA (or other substrates) bind to engage the transporter. The S2 site conversely lies in an extracellular vestibule and can enable allosteric modulation of the transporter.[115] Inhibition of DAT consequently leads to the buildup of extracellular DA, leading to subjective experience of "high."[116]

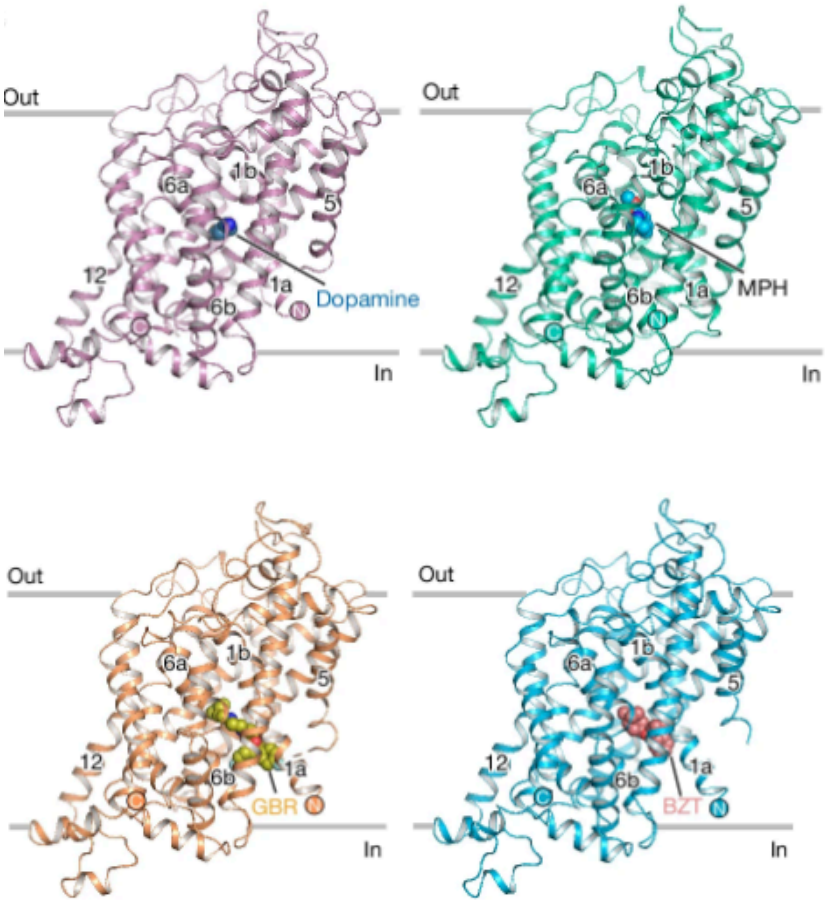

Figure 49: Structures of human DAT bound to DA (purple), methylphenidate (green), GBR12909 (orange), and benztropine (blue). Image shows methylpheniate binds S1, binding site for DA. GBR12909 and benztropine share similar binding poses distinct from DA and methylphenidate. Image obtained from Li *et al*.[117]

4.1.4 Drugs of Abuse as DAT inhibitors

Psychostimulants are drugs of abuse which directly target DAT. Amphetamines (i.e. methamphetamine, though over 200 different chemical entities are known[118]) function as DAT substrates[119] (also act as VMAT substrates[120]and MAO inhibitors,[121] all of which affect DA

transmission). The Vesicular Monoamine Transporter (VMAT) is responsible for the recruitment of monoamines (including DA) into vesicles to for synaptic release, their disruption leads to increased DA concentration in the cytosol and increased DA reverse transport. Similarly, disruption of monoamine oxidase (MAO) enzymes, responsible for the degradation of monoamines, leads to increased concentration of monoamines such as DA and concominant increased reverse transport. DAT substrates are classically understood as replacing DA in the transport mechanism of DAT, getting transported into the cell, increasing the number of DATs that are inward facing and decreasing the amount of DA undergoing DAT reuptake while simultaneously increasing probability that intracellular DA will bind to the inward-facing DAT and undergo reverse transport.[122] Significant evidence suggests that perhaps the key driving force to DA efflux by amphetamines is the increased intracellular concentration of Na^+ generated through transport (DAT imports 2 Na^+ ions with every substrate transported).[123] Also of note, amphetamines have been reported to actively interfere with DAT expression in the membrane, stimulating the internalization of DAT and thereby lowering extracellular DA reuptake.[124,125] The process by which amphetamines increase synaptic DA is complex, relies on multiple mechanisms both DAT-dependent and -independent, remains vastly contested, and is ultimately outside the scope of the current study. Of importance, the effect of amphetamines can often be blocked by cocaine. Unlike amphetamines, which as substrates compete with DA and are transported through DAT, cocaine actively inhibits DAT function.[126] Cocaine binds to the S1 region of DAT, overlapping with the site that would be occupied by DA (see Figure 49), thereby precluding regular function of the transporter.[127] Unlike amphetamines and DA however cocaine is not transported by DAT but rather stabilizes DAT in its outward-facing conformation and will block any DA reuptake until it passively dissociates from the transporter.

Cocaine is known to effect an increase in extracellular DA by inhibiting DAT, however there are various DAT-inhibitors that do not induce a cocaine-like increase in DA levels nor result in cocaine-like behavior. Inspired by the work of Chen and Justice, who showed cocaine primarily stabilizes the norepinephrine transporter (NET) in an outward conformation,[128] Chen *et al*. hypothesized in 2001 that cocaine likely bound to DAT in its outward facing conformation as well, pointing to a sharp decrease in cocaine's affinity for DAT mutants stabilized in an inward facing conformation.[129] This methodology would prove a valuable tool in predicting which DAT conformation (i.e. outward facing vs inward facing/occluded) was preferred by different DAT ligands.

4.2 Atypical DAT inhibitors

4.2.1 Rise of Atypical DAT Inhibitors

In the mid to late 1990's interest in the benztropine scaffold as a medicinally relevant chemical backbone was rising. In 1994, Newman *et al*.[130] reported a series of benztropine (**86**) analogues that they claimed were a structural hybrid of cocaine (**87**) (bearing the classical tropane ring) and GBR12909 (**88**) (See Figure 50) which had been reported in 1980 to have good affinity for the monoamine transporter and showed a different behavioral profile to that of cocaine.[131] Their lead compound, Compound 7a (**89**), showed comparable affinity to cocaine in their radioligand binding assay (though reduced potency), though interestingly did not affect the same increase in locomotor activity: one of the behavioral hallmarks of cocaine. Furthermore, rats trained to discriminate cocaine from saline did not recognize **89** as being cocaine-like. Further SAR campaigns with this

scaffold would yield high affinity and selective DAT inhibitors with behavioral profiles which deviated significantly from cocaine, the lead of which was found to be JHW007 (**90**) (Figure 50).[132,133]

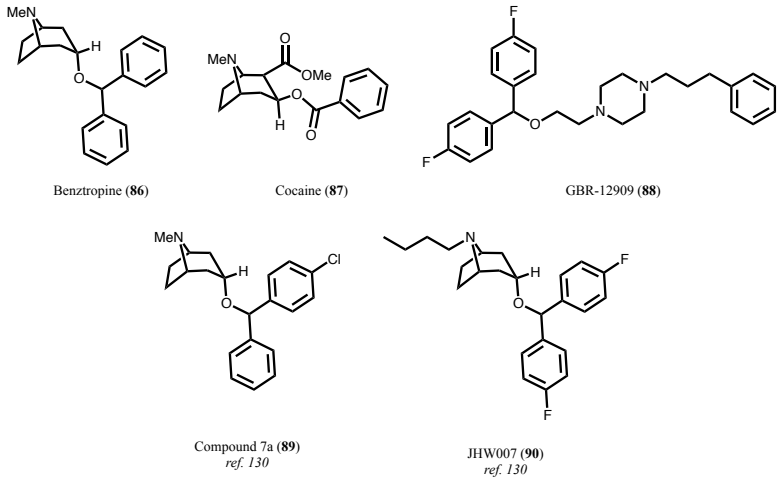

Figure 50: First wave of DAT inhibitors without cocaine-like profile.

This new series of ligands based on the benztropine scaffold was uncovering an interesting pharmacology that had been noted decades prior with the commercially available modafinil (**91**) (brand name Provigil). In 1974, Roger Gambert and Emile Assous at Lafon Labs developed Adrafinil (**92**) (Figure 51) as a pill to treat daytime sleepiness and fatigue. Though two years later it was discovered that **92** serves as a prodrug, metabolized to the active species, **91** (Figure 51).[134] Modafinil, a drug that promotes wakefulness, treats narcolepsy, and most importantly a DAT inhibitor, showed no increase in locomotion in rodents and no amphetamine-like side effects. Modafinil would ultimately become commercially available in France (1994) and the USA (1998).[134] As was the case with the benztropine analogues, interest in this molecule grew, as it

seemed to bind selectively to DAT over other monoamine transporters,[135,136] yet had a markedly different behavioral profile to cocaine. By the early 2000's the addiction science community had begun to notice the potential this molecule may have as treatment for PSUD.[137,138]

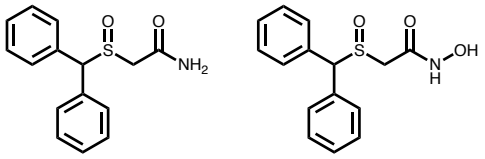

Modafinil (**91**) Adrafinil (**92**)

Figure 51: Structures of Adrafinil and Modafinil.

4.2.2 What makes a DAT inhibitor atypical?

By the mid-2000's it was becoming abundantly clear that there were various DAT inhibitors that despite inhibiting the transporter, categorically did not possess a traditional cocaine-like pharmacology,[139] notably GBR12909, JHW007, and modafinil. This new class of DAT inhibitors, which fail to display cocaine-like behavior, came to be termed "Atypical".[140] The key insight to explain the chasm between the behavioral outcomes of cocaine-like and atypical DAT inhibitors came down to the conformational state of DAT stabilized by the different ligands. Cocaine had been shown to stabilize DAT in an outward-facing conformation (Figure 52), whereas evidence continued to mount showing atypical ligands (i.e. GBR12909, JHW007) consistently showing greater stabilization of DAT in its occluded or inward-facing conformation (Figure 52). This trend was shown for the GBR12909 and benztropine analogues[141] as well as for modafinil[142] in studies employing mutant DATs to stabilize the different conformational states and measure the affinity of ligands at each state. These inferences were finally cemented when in 2024, Li and coworkers

published the cryoEM structures of DAT bound to cocaine, GBR12909, and benztropine, unambiguously showing that indeed cocaine binds the outward-facing conformation of the transporter and the atypical ligands bind the inward-facing counterpart.[117] The stabilization of different DAT conformational states as the key differentiator between cocaine-like and atypical remains largely as the leading explanation for the differing behavioral effects elicited by the corresponding ligands.

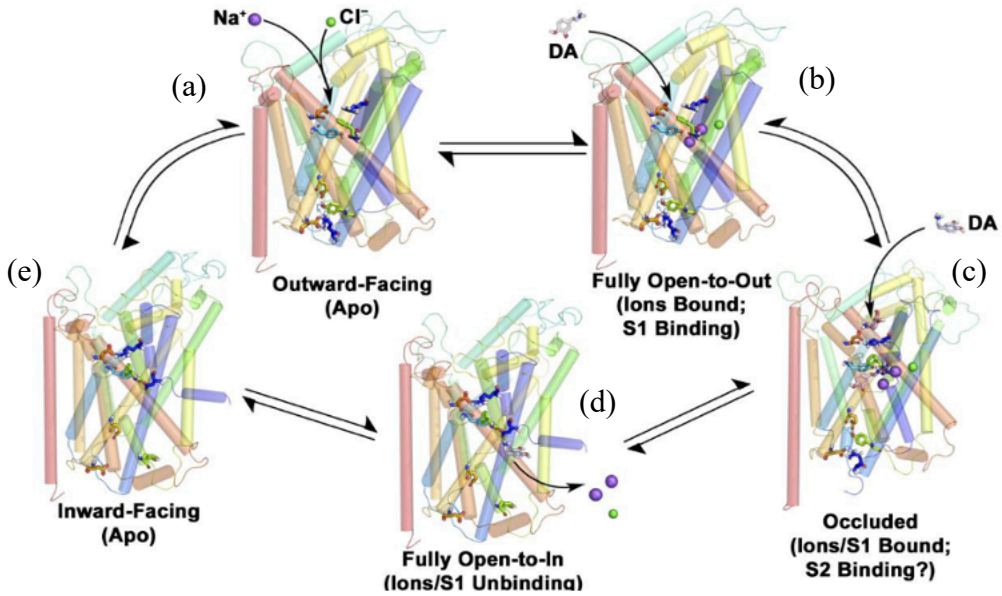

Figure 52: Illustration of the different conformational poses of DAT during DA translocation. Image obtained from Schmitt *et al.*[140] DAT poses cycle through the following conformations: (a) outward-facing Apo conformation, where the transporter is open towards the synaptic cleft and unbound to any ligands or ions. Recruitment of a sodium ion will lead to a conformational shift in DAT to be fully open (b), and capable of binding DA. Once DA binds the S1 site of DAT, the transporter shifts to an occluded (c) conformation where it no longer is open to the synaptic cleft. Binding of a second DA molecule induces a conformational shift to fully open the transporter

towards the cytosol releasing the DA and bound ions into the cell (d). Upon release of DA and ions into the cell the transporter undergoes a further conformational change to an inward-facing apo state (e) which requires phosphorylation to return to the outward-facing apo (a) state and is the rate limiting step in the cycle.

It remains noteworthy that other elements may also play an important role in defining the behavioral effects of these drugs. There is evidence, for example, that the binding kinetics of the drug-to-transporter may be important. Niello *et al*. showed that the residence time of the drug within the transporter, measured by its off rate, is directly correlated to the intensity of its behavioral effects in vivo, and play a definitive factor in cocaine-like effects observed.[143] In a study analyzing the cocaine-like effects of a series of pyrovalerone analogues with varying rates of dissociation, they found that slower rates of dissociation (and longer residence times of the drug within DAT) had a direct effect on psychostimulant effect and duration of the drug; they suggest that faster dissociation rates may lead to the dampened psychostimulant effects of atypical inhibitors. Furthermore, it has been suggested that indeed slower rates of association with the transporter, leading to lower levels of DAT occupancy by the ligand, may be responsible for the mitigation of cocaine-like behavioral effects in some benztropine analogues, such as JHW007.[144–146] It is known that in vivo the level of occupancy of psychostimulants in DAT has a direct effect on the subjective experience of "high", adding credence to this hypothesis.[147] It remains possible that these kinetic effects are in fact a direct result of the structural constraints imposed by the preferred DAT conformations stabilized by cocaine-like and atypical ligands.[117]

4.2.3 Atypical DAT inhibitors as treatment for PSUD

In the USA, deaths as a result of psychostimulant drug overdoses have increased steadily since 2014, rising from 5716 deaths in 2015 to 34855 in 2023 according to the CDC. Despite this growing problem, currently there is no FDA-approved medical treatment for PSUD. Patients must rely on cognitive behavioral therapy or case-by-case treatment provided by the individual medical provider (in fact, no country has an approved therapeutic treatment for PSUD).[148] Since the systematic development of atypical DAT inhibitors by the Newman lab in the mid to late 1990's and early 2000's, largely focused on benztropine analogues, it was postulated that atypical DAT inhibitors could bear great therapeutic potential for the treatment of PSUD. Significant effort has been dedicated to assessing the therapeutic potential of various leads (i.e. GBR12909 and JHW007) however for the purposes of the current volume I will focus on modafinil and relevant analogues thereof.

Among the benefits of using modafinil as a treatment for PSUD is that it is an FDA-approved drug with known safety profiles and can be administered by a medical professional. Modafinil has little, if any at all, abuse liability and studies have shown it does not share the same subjective effects as cocaine[149] or other similar DAT-mediated drugs (i.e. methylphenidate). [Some studies have shown that modafinil may have some subjective stimulant-like effects as reported by non-dependent participants,[150] however there are no reports of dependence or intoxication[151]] As such, human studies to assess the effectiveness of modafinil for the treatment of cocaine dependence were done as early as 2003, where Dackis *et al*. concluded in a double-blind, placebo-controlled study that indeed co-administration of modafinil and cocaine resulted in no medical risks and effectively blunted the subjective cocaine "euphoria".[137] Later in 2005 Dackis et al. showed in a group of

treatment seeking cocaine-dependent individuals that modafinil significantly increased the proportion of negative urinary benzoylecgonine (BE) levels samples (measure used to detect cocaine metabolites in urine), they claim modafinil could indeed help in establishing protracted cocaine abstinence.[152] A subsequent study by Anderson *et al*. found that modafinil effectively increased the amount of cocaine non-use in cocaine-dependent patients that did not have also have alcohol-dependence and also significantly reduced cocaine craving.[153] A meta-analysis of 57 studies, including 11 double-blind randomized control trials, all with at least 20 patients, treating cocaine-dependence with modafinil showed that while modafinil treatment did not improve rates of patient drop-out from the study, cocaine-abstinence levels were significantly greater for modafinil-treated subjects relative to placebo.[148] Furthermore, in a double-blind placebo-controlled trial conducted with methamphetamine-dependent individuals also showed a significant reduction in methamphetamine consumption by patients taking modafinil relative to placebo over a 10 week period.[154]

Despite its potential, modafinil is not designed as a PSUD treatment and is not FDA-approved for the treatment of PSUD, nor has it been broadly adopted as an off-label treatment of such. We hypothesized that improvement of its pharmacological profile may result in better therapeutic potential for the treatment of PSUD. Most notably, the affinity of modafinil for DAT is surprisingly low, with *R*-Modafinil (the eutomer) having an affinity of 3.05 μM for DAT,[155] racemic modafinil has been measured to have an affinity of 4.8 μM, compared to cocaine which has an affinity of 187 nM (25-fold higher affinity) and similar to that of methamphetamine (4.6 μM).[136,184] Furthermore, the reported subjective stimulant effects of modafinil may present a problem in-so-far as subsequent abuse (though analysis of clinical use and post-marketing surveillance have not shown this to be a problem).[151]

4.3 SAR of Modafinil Analogues

4.3.1 First Generation of Modafinil Analogues

For these reasons, significant medicinal chemistry efforts have been dedicated to modafinil and modafinil analogues. There were some early structure activity relationship (SAR) campaigns that utilized the modafinil scaffold for a series of targets,[156–158] but the systematic study of the modafinil scaffold as a potential atypical DAT inhibitor was pioneered by the Newman lab at the National Institute on Drug Abuse in the 2010's. Of note, the DAT, SERT, and NET affinity data for the following series of modafinil analogues published by the Newman lab shown within this introduction correspond to the transporter of Sprague-Dawley rats (i.e. rDAT, rSERT, rNET). Introduced later in the chapter is the work on modafinil analogues synthesized by the Lubec lab which report their binding affinity to the human transporter isoforms (i.e. hDAT, hSERT, hNET). Despite the species differences, binding affinities of various drugs of addiction have been tested in transporters of rodent and non-human primates relative to human isoforms and have proven to be good models, showing within 4-fold similarity in affinity.[185,186] All binding affinities reported as part as the work done for this thesis corresponds to the affinity to the human transporter isoforms (i.e. hDAT and hSERT). In their first paper they describe a series of modafinil analogues where they introduce symmetric substitutions at the 4,4' positions of the bisphenyl backbone and, furthermore they explore the change in affinity in exchanging the sulfoxide for the reduced sulfide, and lastly introduce a series of changes about modafinil's primary amide, introducing both alkyl substituents to the amide as well as a tertiary amine in its place.[159] Some of the analogues prepared showed an improved affinity for DAT relative to modafinil, most notably **93**, **94**, and **95** had submicromolar affinity for DAT (Figure 53), with **95** having the best measured affinity for DAT

(194 ± 16.8 nM) being comparable to that of cocaine. Of note, they noticed that trends in the effect of substitutions about the bisphenyl backbone differed from the trends observed for benztropine analogues (which have an analogous bisphenyl backbone). They also showed that basic tertiary amines could replace the primary amide of modafinil and result in an improved affinity for DAT while still remaining inactive at other monoamine transporters. Notably, their lead in the study, **93**, showed modest increases in locomotor activity, in mice, relative to both cocaine and modafinil, which is indicative of retaining the desired atypical pharmacology.

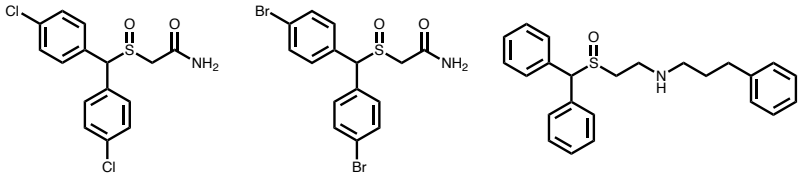

93
Compound 5c
ref. 159
DAT Ki ± SEM (nM)
919 ± 52.8

94
Compound 5d
ref. 159
DAT Ki ± SEM (nM)
600 ± 47.3

95
Compound 9a
ref. 159
DAT Ki ± SEM (nM)
194 ± 16.8

Figure 53: First set of modafinil analogues identified as leads in Cao *et al*.[159]

The Newman lab continued to expand the SAR of their modafinil analogues by now analyzing a series of 3,3'-disubstituted backbones and a greater extent of amines in place of the primary amide as well as a series of secondary (as opposed to tertiary) amides.[160] They showed that substitution of the amide for amines, though improving affinity for DAT, often decreased the selectivity of the analogues for DAT over the other monoamine transporters, particularly the serotonin transporter (SERT). Nonetheless, lead compounds **96**, **97**, and **98** bearing secondary amines, still showed excellent affinities for DAT and selectivity over SERT (Figure 54). Interestingly, retaining the recognizable modafinil core, they report a lead compound (**99**) with a DAT affinity comparable to

that of cocaine (275 nM) but 29000-fold selective for DAT over SERT. SERT and NET, the norepinephrine transporter, are the most common off-targets for DAT inhibitors due to their homology with DAT, and as such selectivity over them is of paramount importance, as they are complicit in various undesired side effects.[184] Most important for the work in this volume: compound **100**, which corresponds to the 3-Br-modafinil, showed a near 5-fold improved affinity from 2.6 uM for modafinil (as reported in this study) to 550 nM (Figure 54). Interestingly, the molecular docking and mutagenesis studies herein reported highlight a key protein interaction with TM10 facing the S1 binding site that appears to be unique to this class of atypical inhibitors and is not present when cocaine binds in S1.[161] It is also important to note this study showed sulfide analogues on average had better affinities for DAT than their corresponding sulfoxides.

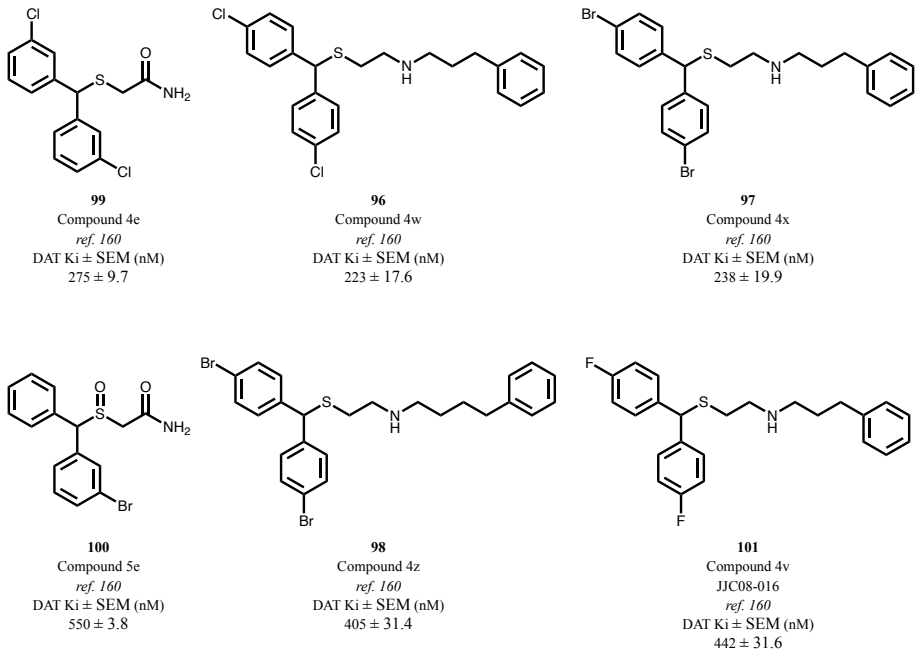

Figure 54: Modafinil analogues identified as leads in Okunola-Bakare *et al*.[160]

Compound 4v, **101**, called JJC08-016 in the literature (Figure 54), would ultimately be picked as the lead compound for testing in *in vivo* studies.[155,162] In these studies, JJC08-016 showed no classical cocaine-like behavior, and instead was shown to dose-dependently inhibit cocaine-induced locomotion and cocaine-self administration. It also validated the potential of these drugs as treatment for PSUD as JJC08-016 also reduced cocaine-induced reinstatement of drug seeking behavior. Measures of extracellular DA release also showed no increase, in sharp contrast to cocaine.[155] When tested in rodents self-administering methamphetamine, JJC08-016 decreased self-administration of methamphetamine in both short (1 h) and long (6 h) drug access sessions.[162] Furthermore, brain microdialysis and fast scan cyclic voltammetry studies showed that indeed JJC08-016 did not produce a significant increase in extracellular DA levels at the doses used in the above studies nor did it increase the electrically evoked DA peak, despite reducing DA clearance rates.[163] This study also showed no effect in locomotion effected by JJC08-016, a standard measure of cocaine-like DAT inhibition. Collectively these results highlight the atypical profile of JJC08-016. It is important to note that JJC08-016 showed good metabolic stability (77% remaining after 60 minutes incubation with mouse liver microsomes in presence of NADPH) and has excellent brain penetrability through both oral and intravenous administration,[162] suggesting that these effects are indeed likely attributable to the atypical pharmacology of JJC08-016.

4.3.2 Second Generation of Modafinil Analogues and JJC-compounds

The next breakthrough in their SAR of modafinil analogues came in introducing the N-2 hydroxy propyl piperazine moiety to these compounds (see **102** (JJC08-089), **103** (JJC08-091), and **104** (JJC08-088) in Figure 55).[164] Deviating more significantly from the original modafinil template, these compounds introduce the piperazine moiety of GBR-12909, and showed excellent affinities for DAT with exceptional selectivity over SERT and NET (i.e. JJC08-088 DAT: K_i=2.53 ± 0.25 nM; SERT/DAT: 1822, NET/DAT: 5929). JJC08-088 was chosen as a lead for further investigation as it showed promise in its affinity for the Y156F DAT mutant, showing a preferred affinity for the inward facing DAT conformation (a predictor of atypical activity). Furthermore, JJC08-088 initially showed significantly reduced locomotor activity relative to cocaine. Nevertheless, further *in vivo* studies revealed JJC08-088 to be cocaine-like,[163] increasing extracellular DA in rodent models[165,166] and showing cocaine-like activity in monkeys.[167] On the other hand, JJC08-091 showed promise in *in vivo* models, showing no self-administration in rodents,[166] and no cocaine-like effects.[163] Moreover, JJC08-091 effectively reduced the self-administration of cocaine and methamphetamine.[162] Computational studies were conducted to ascertain the interactions of JJC08-088 and JJC08-091 in DAT which could be responsible for this drastic difference in behavioral profiles despite their structural similarity. These predicted, in accordance with the inward vs outward facing DAT conformation hypothesis presented earlier, that JJC08-088 would bind an outward facing conformation whereas JJC08-091 would stabilize an occluded conformation.[166]

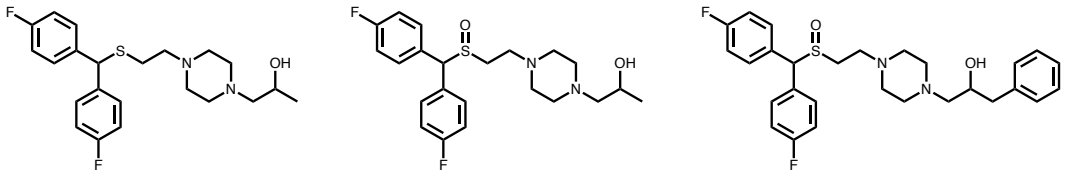

102
Compound 8d
JJC08-089
ref. 164
DAT Ki ± SEM (nM)
16.7 ± 1.22
SERT/DAT: 106
NET/DAT: 1066

103
Compound 9d
JJC08-091
ref. 164
DAT Ki ± SEM (nM)
289 ± 43.0
SERT/DAT: 174
NET/DAT: >346

104
Compound 11b
JJC08-088
ref. 164
DAT Ki ± SEM (nM)
2.53 ± 0.25
SERT/DAT: 1822
NET/DAT: 5929

Figure 55: Lead compounds JJC08-089, JJC08-091, JJC08-088.

Two issues remained with JJC08-091 and compounds in this study, their metabolic stability and considerable affinity for hERG. The hERG (human ether-a-go-go-related gene) channel protein is a common off-target and plays an important role in regulating electrical activity in heart tissue, inhibition of this protein may lead to cardiotoxicity and as such is screened for in all leads.[168] This would inspire the Newman lab to continue their SAR work, identifying the metabolically labile region of this piperazine-bearing class of analogues and redirect medicinal chemistry efforts to improving the metabolic profile of these compounds.[169] Furthermore, they postulated that the piperazine moiety may be responsible for the observed hERG activity,[170] and as such sought to explore SAR in this region. Substitution of the JJC08-091 piperazine for a 2,6-dimethylpiperazine (**105**, Figure 56) proved advantageous in this regard, endowing these analogues with improved metabolic stability. Substitution of the piperazine moiety for the diazaspiro units as exemplified by **106** (Figure 56) was met with a loss of affinity for DAT and improved affinity for SERT relative to its piperazine counterpart. **107** was ultimately identified as the lead compound for showing the desired atypical binding profile, improved metabolic stability (half-life over 40 minutes in human liver microsomes) and having an acceptable DAT vs hERG affinity ratio (approximately 30-fold selectivity for target over hERG is believed to be sufficient to avoid hERG mediated cardiotoxic effects[171]). Further SAR was conducted in the piperazine ring region, as the metabolic stability of

these analogues remained a significant challenge to overcome,[172,173] though no major improvements were observed.

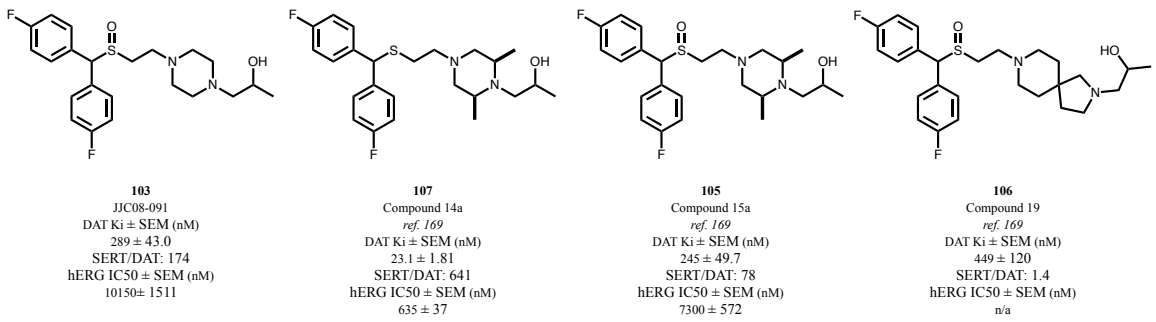

Figure 56: Lead compounds reported by Slack *et al*.[169]

4.3.3 New Approach at Modafinil Analogues

At this juncture our drug design was inspired by a series of papers from Lubec and co-workers. Similarly interested in modafinil's atypical pharmacology, the Lubec group set out to repurpose the modafinil scaffold into a more efficient DAT atypical inhibitor. Their approach was complementary to the studies by Newman lab, deciding to exchange the modafinil primary amide for an extensive series of aromatic heterocycles (as opposed to aliphatic amines). Figure 57A below shows a select group of examples to exemplify the diversity of substrates tested in their first paper by Kalaba *et al*. (2017)[183] It is important to note in all the following reported compounds, affinity is reported as IC_{50} (half maximal inhibitory concentration) in contrast to K_i (inhibition constant) as was the case up to this point. IC_{50} and K_i are related by the Cheng-Prusoff equation:

$$K_i = \frac{IC_{50}}{1 + \frac{[S]}{K_M}}$$

Where [S] denotes the concentration of the competing substrate, in this case DA, used in the assay and K_M the Michaelis constant for DA to DAT. Unlike K_i, IC_{50} is not a constant as it is affected

by assay conditions. Nonetheless it can be readily used to compare relative data under the same assay conditions. Their reuptake assay is reported to use [DA] of 0.2 μM, there are conflicting values for the K_M of DA to DAT, with early reports supporting a K_M of 2.4 μM[174] though this value has recently been disputed and measured to be closer to 0.55[175] μM. Therefore, we can compare the IC_{50} values shown to previously provided K_i values, as they should be approximately equivalent to between 1.08 K_i and 1.36 K_i, meaning $IC_{50} \approx K_i$.

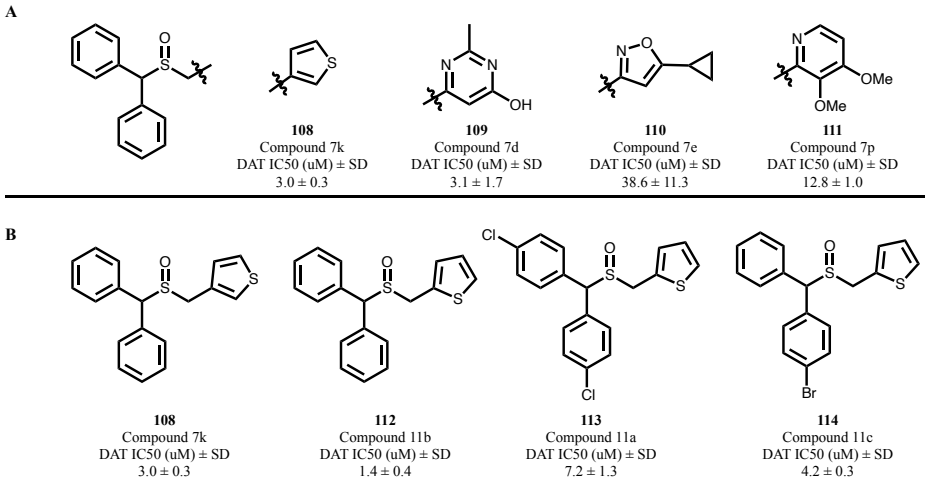

Figure 57: A) Select examples of heterocycles tested by Kalaba *et al*. (2017)[183] on modafinil backbone. B) Select examples of optimization with thiophene-bearing analogue. All binding data corresponds to a minimum of three independent experiments performed in triplicate.

The initial heterocycle screen revealed thiophene, and Cl-substituted thiophenes to have the best affinity for DAT, with **108** having the best IC_{50} = 3.0 μM. Analogues bearing pyrimidines (**109**) had promise, while the corresponding oxazoles (**110**), and pyridines (**111**) were largely inactive. This led the Lubec group to test a variety of thiophene-bearing analogues, shifting from 3-substituted thiophene to 2-substituted thiophene (**112**) and noting an improvement in affinity (from

3.0 μM to 1.4 μM). Subsequent modifications of the backbone as seen **113** and **114** proved deleterious to DAT affinity in this series. However, they would continue to expand their SAR on the current lead, compound 11b. In a series of papers Lubec and co-workers identified replacing the thiophene for a thiazole led to a series of analogues with excellent potential.[176–178] This led to an extensive medicinal chemistry campaign to study thiazole bearing analogues, see Figure 58 for select examples by Kalaba *et al*. (2019).

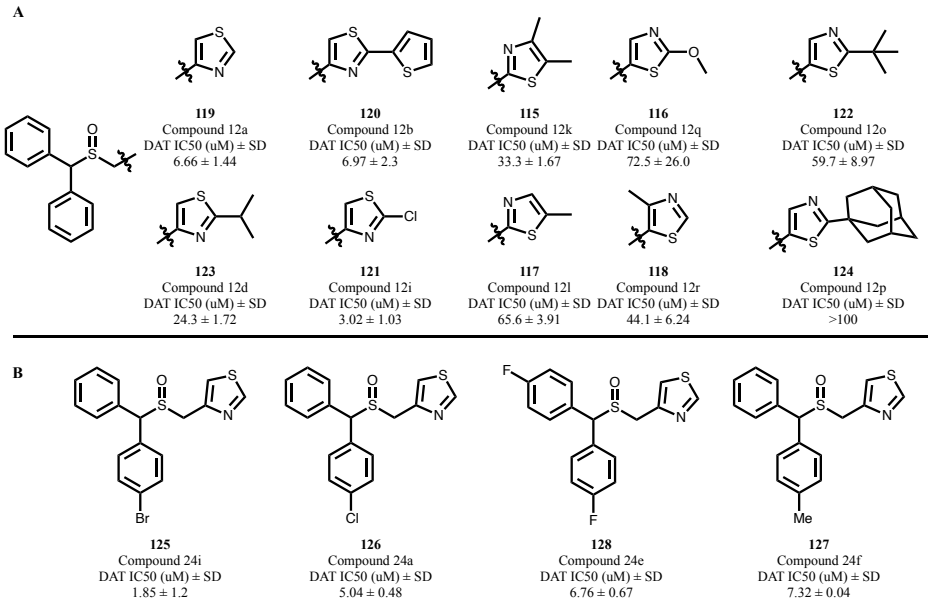

Figure 58: A) Select examples of thiazoles tested. B) Select examples of optimization of bisphenyl backbone. All binding data corresponds to a minimum of three independent experiments performed in triplicate.

As seen in Figure 58A, the campaign to optimize the thiazole bearing modafinil analogues yielded compounds with a wide range of affinities. Appending the thiazole to the modafinil backbone in the 2 or 5 position was deleterious to affinity (compounds **115**, **116**, **117**, and **118**); substitution at the 4 position was best tolerated (**119**, **120**, **121**). Introduction of bulky substituents was also

deleterious (Compounds **122**, **123**, and **124**). It was ultimately decided to continue with an unsubstituted thiazole appended to the modafinil backbone at C4. Kalaba *et al*. (2019) subsequently proceeded to introduce a series of substitutions about the bisphenyl backbone (Figure 58B). Of the analogues synthesized, the 4-Br substituted analogue **125** had the best affinity for DAT (1.85 μM; Figure 58B). The Cl- (**126**) and Me- (**127**) analogues had a 2.7- and 4-fold drop in affinity, and symmetric 4,4'-diF substitution (**128**) which had been useful in analogues reported by the Newman group, was ineffective in improving DAT affinity. Separation of all the stereoisomers of **125** subsequently revealed that the (S_S, S_C) stereoisomer of **125** was the most active (0.65 ± 0.07 μM) while the (R_S, S_C) stereoisomer was the least active (63.7 ± 6.77 μM).

This SAR campaign would ultimately yield their lead compound (*S*, *S*)-CE-158, **129**, reported by Lubec *et al*. to have a K_i =13 nM for DAT.[179] In our in-house radioligand binding assay we repeated the Lubec synthesis of all four stereoisomers of CE-158 and found (*S*, *S*)-CE-158 to be the most active one with a K_i =56 nM. (*R*, *R*)-CE-158 had a K_i =564 nM and the other two stereoisomer binding in the micromolar range. (Figure 59).

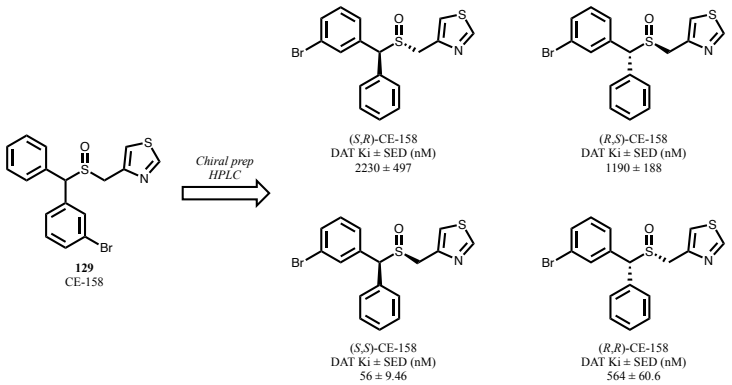

Figure 59: Lead modafinil analogue developed by the Lubec Lab, CE-158. Binding data from the Newman lab (unpublished)

5 Synthesis of Modafinil Analogues as DAT Inhibitors

5.1 Initial Drug Design

As discussed earlier, the modafinil scaffold has long been known to effect an atypical (in contrast to cocaine) pharmacology at DAT. As a result, extensive effort has been focused on utilizing the modafinil scaffold to develop ligands that inhibit DAT selectively and atypically (see section 4.3). The initial drug design was inspired from a series of compounds originally reported by the Lubec lab, in particular **129** (Figure 60)[179] which was reported to possess an atypical pharmacological profile at DAT. Lubec et al. showed that a single meta bromine in the bisphenyl backbone and replacement of the primary amide of modafinil with a thiazole resulted in a large improvement in affinity for DAT (Of note, Okunola-Bakare *et al*. (2014) had similarly shown this substitution would improve the affinity of modafinil five-fold, see **100**) and selectivity for SERT. Previous SAR campaigns from the Newman lab based on modafinil revealed that extending a chain further from the position of the amide nitrogen was well tolerated, and in fact beneficial (i.e. N-2-propanol-piperazine in **103**, similarly **104** (JJC08-088).) Inspired by these collective findings, we hypothesized that replacement of the thiazole in **129** with a triazole would retain the geometry of **129** but provide a functional handle which could be used to append variable side chains which might improve binding affinity at DAT. Furthermore, we postulated that the increased polarity of the triazole relative to the thiazole would be more consistent with currently available SAR using tertiary amines in that position, a motif present in atypical inhibitors such as GBR12909 and benztropine, and be better at mimicking the H-bonding ability of these. Lastly, the improved metabolic stability of triazoles relative to thiazoles made these an interesting alternative.

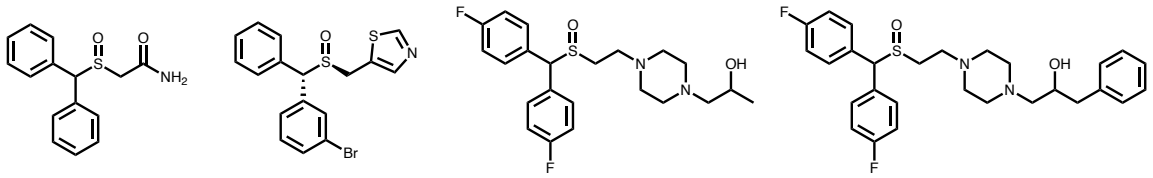

Figure 60: Key leads upon which current SAR was inspired.

Synthesis of the triazole-containing analogues was originally envisioned to be conducted in modular fashion (Figure 61), where a series of bisphenyl backbones could be readily installed from the corresponding benzyhydrols (**I**) and various triazole substituents could be accessed from commercially available azides (**III**). Crucial to this synthetic pathway was access to propargylthiol (**II**), both as a source of the sulfur in the desired position and the alkyne necessary to construct the triazole through conventional click chemistry.

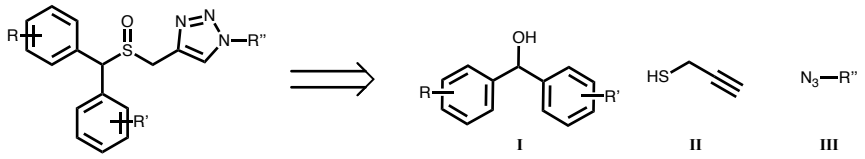

Figure 61: Proposed retrosynthetic deconstruction of triazole-containing modafinil analogues.

5.2 First Synthetic Approach for making Modafinil analogues

5.2.1 Propargyl thiol as a building block and first series of analogues

Despite its relative similarity to the widely used propargyl alcohol, propargylthiol is an inherently difficult chemical to prepare and handle. In addition to its high volatility and repulsive smell, propargylthiol is highly unstable and undergoes rapid polymerization.[180] As such, attempts to have a reliable source of propargylthiol proved ultimately unsuccessful. Attempts at following the protocol described by Castro *et al*.[180] proved unreliable. Accurate yields of the reaction mixture could not be measured and required immediate use of the unprotected thiol. Attempts to store the thiol as a dilute solution in diethyl ether showed fast decomposition of the material. An attempt to use the desired propargyl thiol in situ to react with the model systems in accordance with the protocol published by Castro et al. proved largely inefficient (Figure 62). The acetate protected thiol (**132**) could be readily prepared (Figure 62, entry a) from propargyl bromide in high yield (93%) and proved stable if stored in the freezer. However following acetate deprotection with LAH the free thiol (**133**), in ether solution, was incapable of alkylating a series of key benhydryl mesylates (Figure 62, entries b-d). Mesylates **134**, **136**, and **138** which were all prepared from the corresponding benzhydrol and used *in* situ without purification, however, they all failed to yield the corresponding sulfide (i.e. **135**, **137**, and **139** respectively). The only substrate that was successfully displaced with the propargyl thiol was the 4,4'-difluoro benzhydryl bromide **140** (entry e), albeit using an excess (2 eq.) of **133**, to afford sulfide **141** in 42% yield. It was observed that the mesylate starting material was not consumed over the course of the reaction and mild heating (35 °C) was applied but the reactions remained unsuccessful.

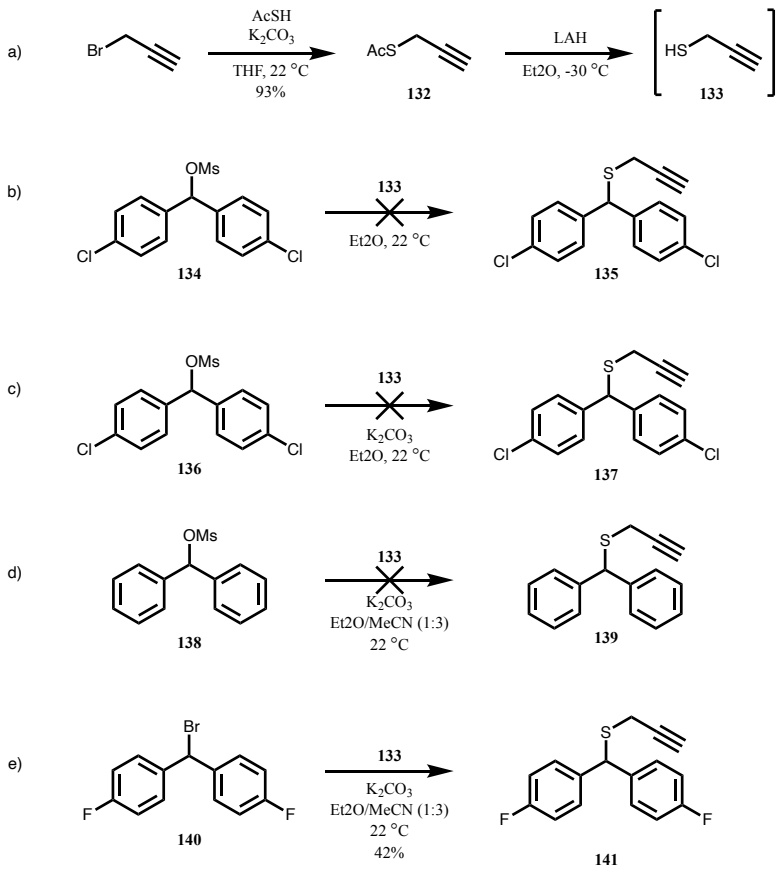

Figure 62: Initial attempts at using propargyl thiol to alkylate commercially available benzhydrols.

Compound **141** was used to continue to assess the feasibility of the proposed retrosynthetic pathway in Figure 61. With the sulfide and alkyne installed in the desired position, we could now access the necessary sulfoxide and triazole moieties. Oxidation of sulfide **141** to sulfoxide **142** (Figure 63, entry a) under standard conditions proceeded with modest yield (41%). Copper(I)-catalyzed azide-alkyne cycloaddition (CuAAC) of **141** (Figure 63, entry b) and **142** (Figure 63, entry c) proceeded with modest yields (35% and 60% respectively) to provide the methylene-TMS triazoles **143** and **144**. The TMS group is readily removed with TBAF to afford the N-methyl triazoles **145** and **146** (entries b and c).

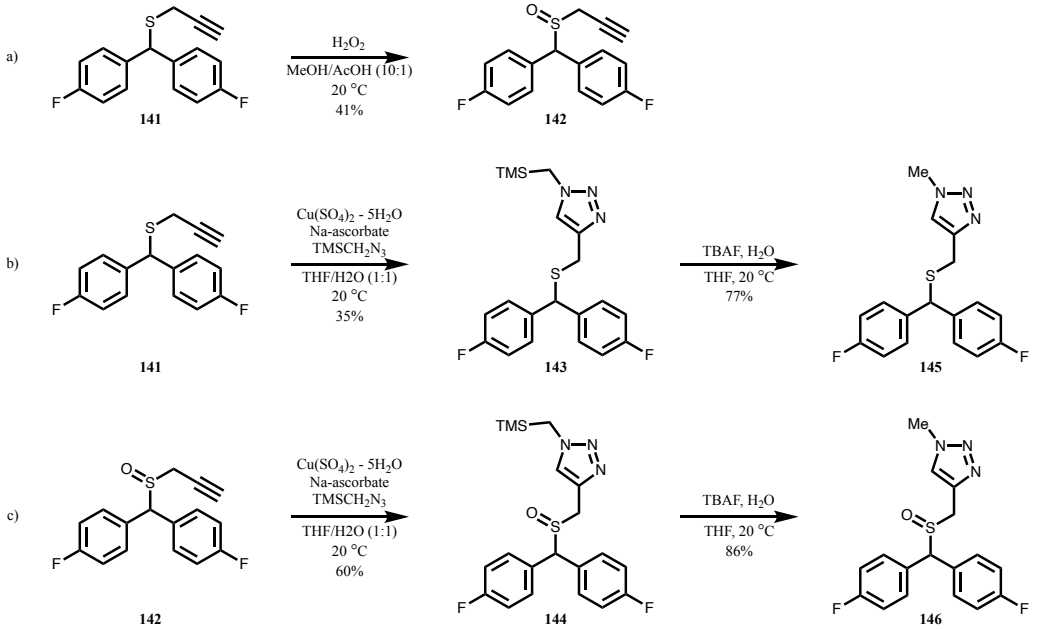

Figure 63: Synthesis of N-methyl triazole analogues through modular approach.

We posited that **146** would be a useful starting point to test the effect of the new triazole moiety in these modafinil analogues. The 4,4'-difluorophenyl backbone had been shown to improve DAT affinity in both previous modafinil analogues as well as in the benztropine series (i.e. JJC08-91, see introduction) and we hypothesized that a small substituent on the triazole would mimic the steric space occupied by the thiazole in **129** (Figure 60), making the N-methyl analogue a reasonable place to start. To test the affinity of the compounds prepared, they were all submitted to our in house radioligand binding assay, where we test their affinity in HEK293 cells transfected with hDAT and hSERT in competition with [^{3}H]-WIN-35428 for DAT and [^{3}H]-Citalopram from SERT. Despite the structural similarity between **129** and **146**, compound **146** lost considerable affinity for DAT relative to **129** (51.9 μM; nearly 1000-fold lower affinity relative to (*S*,*S*)-**129**). To our surprise, intermediate **144**, with the much bulkier CH2-TMS substituent at the triazole demonstrated a five-fold improvement in affinity for DAT (9.69 uM) relative to **146**. These results

were counterintuitive when compared to **129**, though not completely surprising given that many modafinil analogues with high DAT affinities have large side chains extending from the basic nitrogen we mimic with the triazole. Furthermore, SAR from the Lubec lab (section 4.3.3) had previously shown most small heterocycles employed in place of the thiazole of **44** result in DAT inhibitors with affinities in the micromolar range.

5.2.2 Changing propargyl thiol for alkenyl-TIPS propargyl thiol

At this point however working with propargyl thiol became increasingly unreliable and preparation was essentially irreproducible. In an attempt to retain the modular approach detailed in Figure 61, which would allow for a common alkyne-bearing backbone which could then be functionalized with a wide variety of azides (i.e. **141** and **142**), we decided to proceed with the TIPS-protected analogue **149** (Figure 64A). Starting once again from propargyl bromide, this material could be TIPS protected in good yield (69%) and the bromide subsequently displaced with AcSK to afford the acetate protected thiol **148**. We hypothesized that by adding a triisopropylsilyl (TIPS) group to the terminal alkyne the resulting **149** might be less volatile relative to the propargyl thiol, facilitating purification and accurate yield measurements, and increasing its stability. Unfortunately, **149** proved to also be air sensitive and had to be prepared similarly in strict oxygen-free conditions and used rapidly upon preparation.

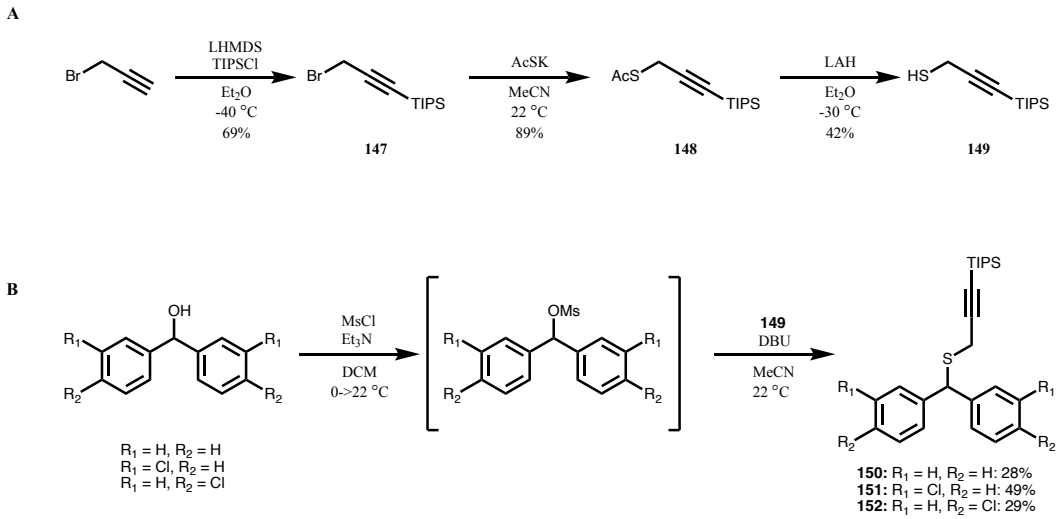

Figure 64: A) Synthesis of TIPS protected alkyne. B) Use of thiol bearing alkenyl-TIPS to displace mesylates.

Despite not showing improved stability relative to the propargyl thiol, **149** was ultimately preferred due to more practical handling. To test if compound **149** was compatible with the desired synthetic route, it was used to prepare a series of sulfides (**150**, **151**, **152**; Figure 64B). Starting from commercially available benzhydrols, these were mesylated and subsequently reacted with **149** to afford the desired TIPS protected sulfides. In contrast to propargyl thiol, **149** showed greater consistency of results when reacted with desired mesylates, albeit with low yields.

Removal of the TIPS group at this stage proved challenging and unreliable. Initial attempts using standard deprotection methods using tetrabutylammonium fluoride (TBAF) at 0 °C for 1 h returned only starting material. Allowing the reaction to stir overnight at room temperature resulted in the removal of the TIPS group but yielded inseparable mixtures of the desired alkyne and the corresponding allene (**153**, **154**, **155**; Figure 65). All attempts to improve selectivity for the alkyne product resulted in mixtures of products; as a result, removal of the TIPS group at this stage was abandoned.

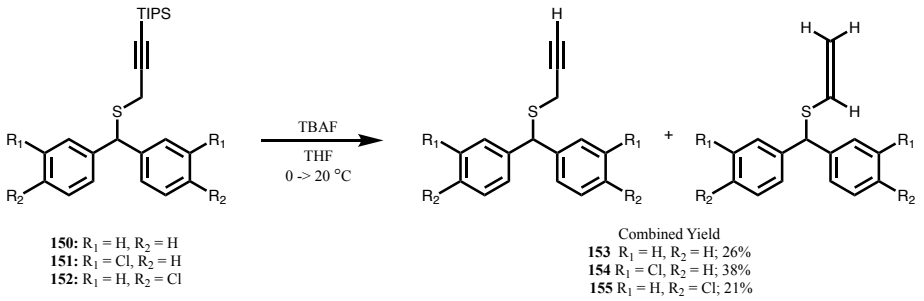

Figure 65: Removal of TIPS from alkenyl-TIPS sulfide substrates.

We then proceeded to test the oxidation of the sulfides to form the desired sulfoxides. Treating sulfides with an excess of hydrogen peroxide in MeOH/AcOH, as had been previously reported,[159] was unsuccessful (Figure 66A) and returned exclusively starting material. This is more likely due to solubility issues of the starting material in an H_2O/MeOH/AcOH solvent system than a lack of reactivity. We decided to use *m*-chloroperbenzoic acid (mCPBA) in dichloromethane (DCM) instead, as the sulfides showed excellent solubility in DCM as well as employing a more reactive oxidizing reagent. Using **150** as a model system, it was determined that optimum conditions for oxidation to the sulfoxide **156** would require low temperatures (-10 °C) and rapid quenching of the mCPBA (15 minutes); higher temperatures and longer reaction times lead to complete consumption of the starting material but also a complex mixture of side products, most notably overoxdidation to the sulfone which could be largely mitigated by cold temperatures and short reaction times (Figure 66B).

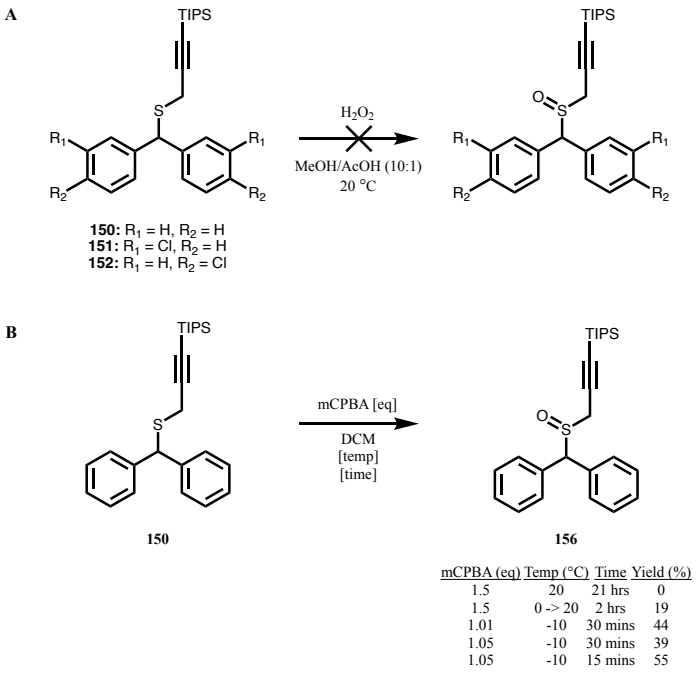

Figure 66: A) Standard oxidation conditions used in modafinil analogues. B) Optimization of sulfide oxidation to sulfoxide.

With the sulfoxides in hand, the next step necessitated the removal of the TIPS group to unmask the alkyne and enable the final azide-alkyne cycloaddition. Unsurprisingly, even very mild TBAF conditions (1 eq TBAF, 0 °C, 0.1 M) resulted in very complex mixtures. Furthermore, it was evident that a mixture of allene and alkyne were formed, which is not surprising as we anticipated the sulfoxide to favor allene isomerization relative to the sulfide analogues due to increased acidity at the propargyl position.

At this point it had become increasingly clear that this synthetic approach was too unreliable and impractical. We decided to change our current approach (as shown in Figure 61) which was chosen because it would allow for diversification of a common alkyne intermediate, for a method that would be more synthetically reliable. The new method will be expanded upon in section 5.3 below, and relies on constructing the triazole prior to the formation of the thiol, resulting in more stable thiols to be used throughout the synthesis.

5.2.3 Computational Predictions and shift to N-Benzyl Triazoles

The results observed for compounds **143** and **146** encouraged us to consider reaching out to our intramural collaborators Dr. Kuo Hao Lee and Dr. Lei Shi from the Computational Chemistry and Molecular Biophysics Section at NIDA. Their group has a QSAR model, trained with the ChEMBL34 dataset and our in-house radioligand binding data of **129** and its constitutive enantiomers, capable of predicting novel ligands' affinities (inhibitory constants, K_i) at DAT and hERG.[181] A series of modafinil analogues were submitted for testing with these models to predict their affinities to DAT and further validate this series of triazole containing modafinil analogues as a viable scaffold worth synthesizing.

A total of 180 different analogues were submitted for prediction, including an array of sulfoxides and sulfides, a range of different bisphenyl backbones, and a series of different substituents on the triazole (ranging from small (i.e. methyl) to large (i.e. pyrene)) based on commercially available building blocks. The predictive power of the model suffers with poorly binding substrates (i.e. low affinity) as it will overestimate the affinity. For example, compounds **143** and **146** were both tested in the computational model, the model predicted affinity values of 1.41 μM for **143** and 1.99 μM for **146**, where we measured 9.69 μM and 51.9 μM respectively. However, we postulated the relative values predicted by the model could provide important insights insofar as SAR trends to consider. To this end, Graph 1 below shows a select group of 96 compounds submitted for prediction. These represent 24 distinct bisphenyl backbones, all of which were tested with 4 distinct moieties: Sulfide+N-Benzyl triazole (orange), Sulfide+N-Methyl triazole (green), Sulfoxide+N-Benzyl triazole (dark blue), Sulfoxide+N-Methyl triazole (light blue).

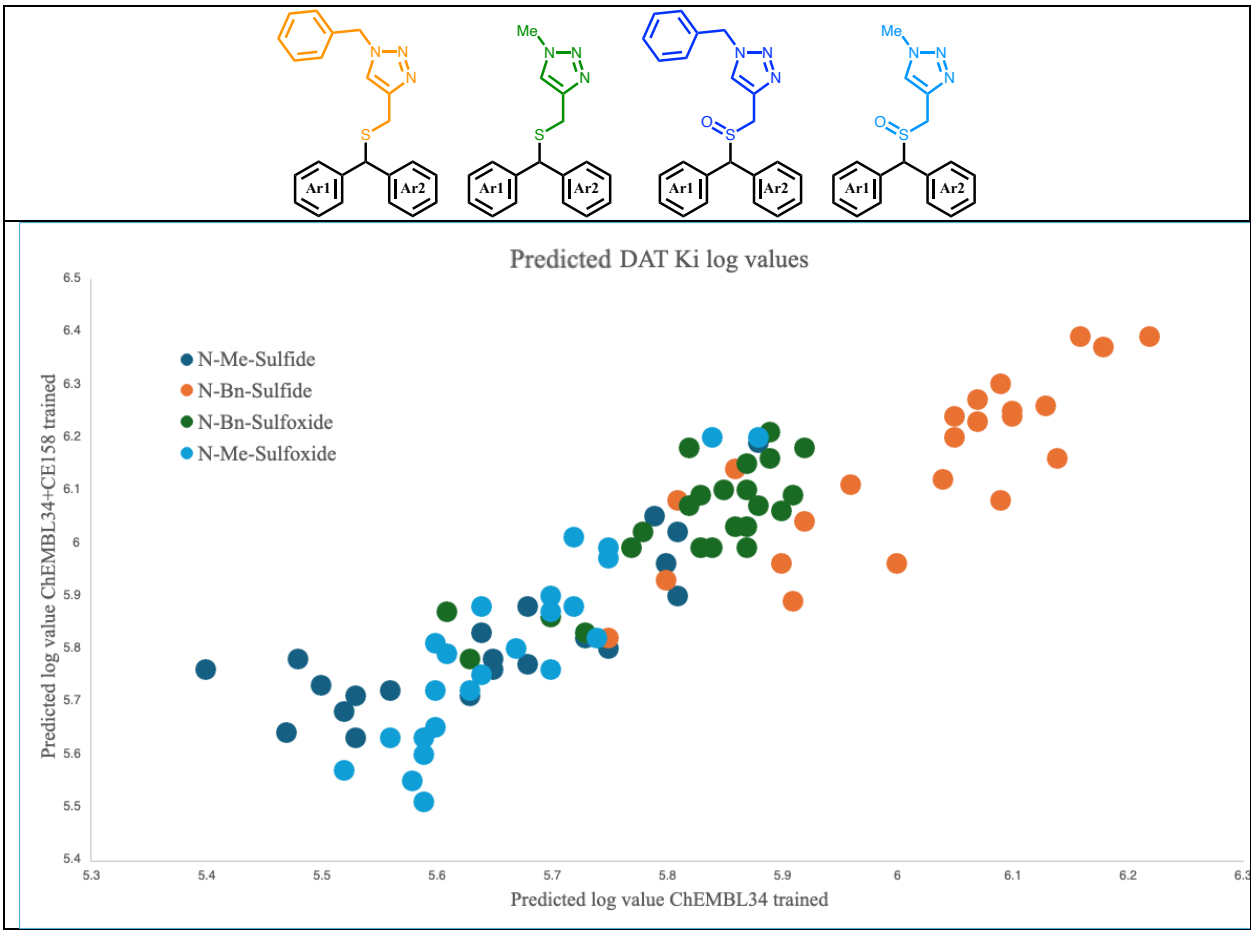

Graph 1: General plot showing predicted log K_i affinity for DAT of 24 different bisphenyl backbones to observe trend of the effect of sulfide vs sulfoxide and N-methyl vs N-benzyl triazole. The affinity of 24 different bisphenyl backbones was calculated in conjuction with: sulfide + N-Bn triazole (orange), sulfide + N-Me triazole (green), sulfoxide + N-Bn triazole (dark blue), and sulfoxide + N-Me triazole (light blue), to assess the general impact of oxidation state of the sulfur and substituents on the triazole on modafinil analogues. Computational predictions performed by Dr. Kuo Hao Lee of the Computational Chemistry and Molecular Biophysics Section in NIDA.

The 96 compounds submitted to our predictive model were subsequently assigned two predicted affinity values, one based on the model trained exclusively on the ChEMBL34 dataset, and the other based on a second iteration of the model that has been refined by being trained with data

from **129**. The two axes of Graph 1 correspond to the two output values obtained from these two models; therefore, a linear relationship is indeed expected. The predicted affinity outputs from this model are shown as the negative logarithm of the K_i in Graph 1, as such the higher the logarithmic value shown the better the compound affinity (the lower the K_i). With this in mind, the trend shown in Graph 1 indicates that the general scaffold with best predicted binding affinities contains a sulfide and a large (Benzyl) substituent in the triazole (orange). Conversely, the worst affinities were predicted for sulfoxides and sulfides with a small (methyl) substituent at the triazole (dark and light blue). Sulfoxides with a large (benzyl) triazole substituent were predicted to have better affinities than analogues with a methyl-triazole however slightly lower affinities than their sulfide counterparts. This trend was consistent throughout all compounds submitted for prediction (full list in Appendix Table A4).

5.3 First Generation of Modafinil analogues

5.3.1 New proposed synthetic route

Encouraged by the predictions unveiled through our collaboration with the Computational Chemistry and Molecular Biophysics Section, we proceeded to synthesize a series of compounds focused on introducing larger substituents on the triazole terminal. A new synthetic route was designed wherein the triazole is formed first from the stable and commercially available compound **132**. Deprotection of the resulting acetate-protected thiol would afford thiols that can be readily alkylated with benzhydryl bromides or mesylates (Figure 67). The key drawback to this approach is by constructing the two sides of the desired compound separately, there is no common

intermediate among analogues from which a series of analogues can be diversified. However, the triazole performs a similar role to the TIPS group before, adding stability and reducing the volatility of the thiol used.

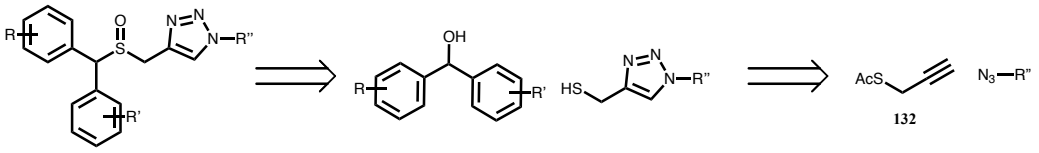

Figure 67: Revised synthetic approach to modafinil analogues.

With the QSAR predictions obtained through our collaboration with the Computational Chemistry and Molecular Biophysics Section, there was a clear starting point as to which bisphenyl backbones, and which triazoles, were most likely to bind well. Predictions had shown the best backbones to be relatively simple (despite the diverse array of backbones submitted for submission), revealing simple 3-, and 4-halogen substitutions or 4-Me substitution about the backbone to be best. Furthermore, triazoles with large N-substituents were predicted to be best (i.e. Ph, Bn, and 4-substituted Bn). With this knowledge in hand, a series of triazole starting materials were prepared (Figure 68). The N-benzyl triazole was prepared from the commercially available alcohol **157**, which was converted to the alkyl bromide (**159**) through standard Appel conditions in good yield (77%) and later reacted with potassium thioacetate to yield the acetate protected thiol **160**. Similarly, the N-phenyl analogue of **160** could also be prepared from the commercially available alcohol **158**, in this case the sequence of two reactions was done without isolation or purification of the bromo intermediate **161** and after alkylation with potassium thioacetate afforded protected thiol **162** in 18% yield over two steps. To construct triazoles with

slightly more complicated substitution patterns it was necessary to build the triazole from its constituent azide and alkyne **132**. Azides **163** and **164** were prepared from alkylation of their corresponding benzyl bromides with sodium azide in excellent yield (90% and 93% correspondingly) and subsequent CuAAC with **132** to afford the acetate protected thiols **165** and **166** in 69% and 67% yield accordingly.

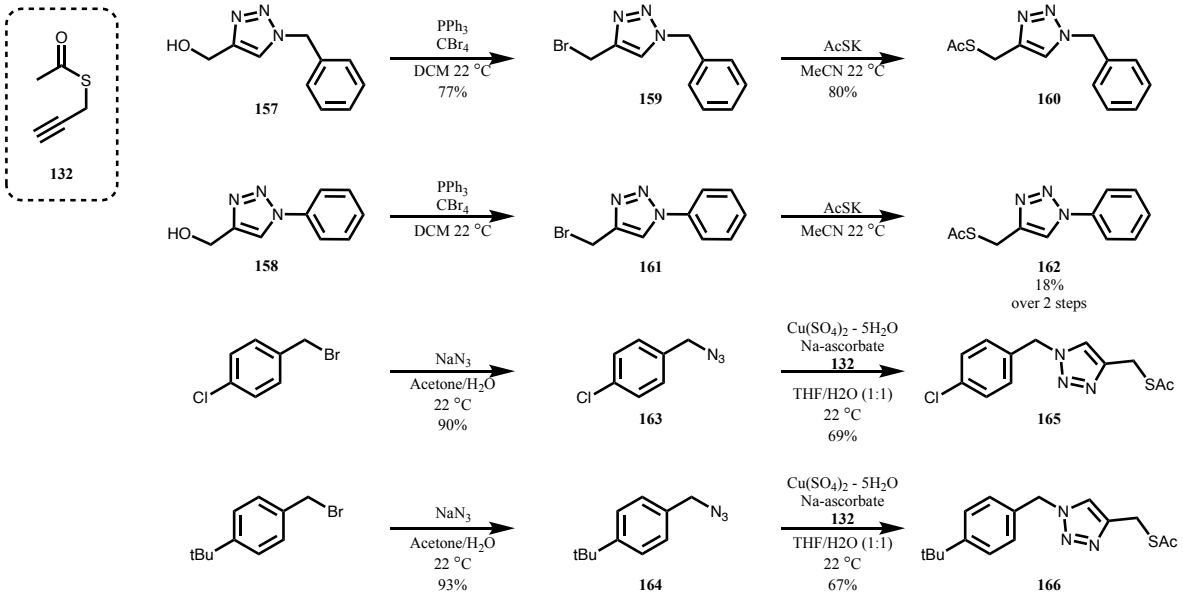

Figure 68: Synthesis of acetate protected thiols.

With the above protected thiols in hand a series of sulfide modafinil analogues were readily prepared (Figure 69). Compounds **169** and **170** both contain a 4-Cl backbone and were prepared from the commercially available benzhydryl chloride (Conditions A). Hydrolysis of **160** and **162** with sodium hydroxide and water released the unprotected thiol, which was used immediately without purification and was reacted with the desired benzhydryl chloride to afford **169** and **170** in 27% and 26% yield accordingly. Similarly, reaction of the deprotected thiols with 4,4'-benzhydryl bromide afforded **167** and **168** in 31% and 32% yields. Compounds **171** through **176**

were prepared from the corresponding benzhydrols, which were mesylated and the mesylate was treated with the corresponding deprotected thiol. Compounds **171** through **174** contain an unsubstituted N-Benzyl triazole and all compounds contain bisphenyl backbones predicted to have the highest affinity for DAT, namely 3-Br (**171**), 4-Br (**172**), 3-Cl (**173**), and 4-Me (**174**). In addition, compounds **175** and **176** exhibited among the highest predicted affinities in our computational models and have a 4-Me bisphenyl backbone and a 4-Cl benzyl substituted triazole (**175**) and 4-tBu benzyl substituted triazole (**176**). Compounds **171** through **176** were synthesized via Conditions B, in situ preparation of the mesylate of the corresponding benzhydrol, followed by alkylation with the necessary thiol.

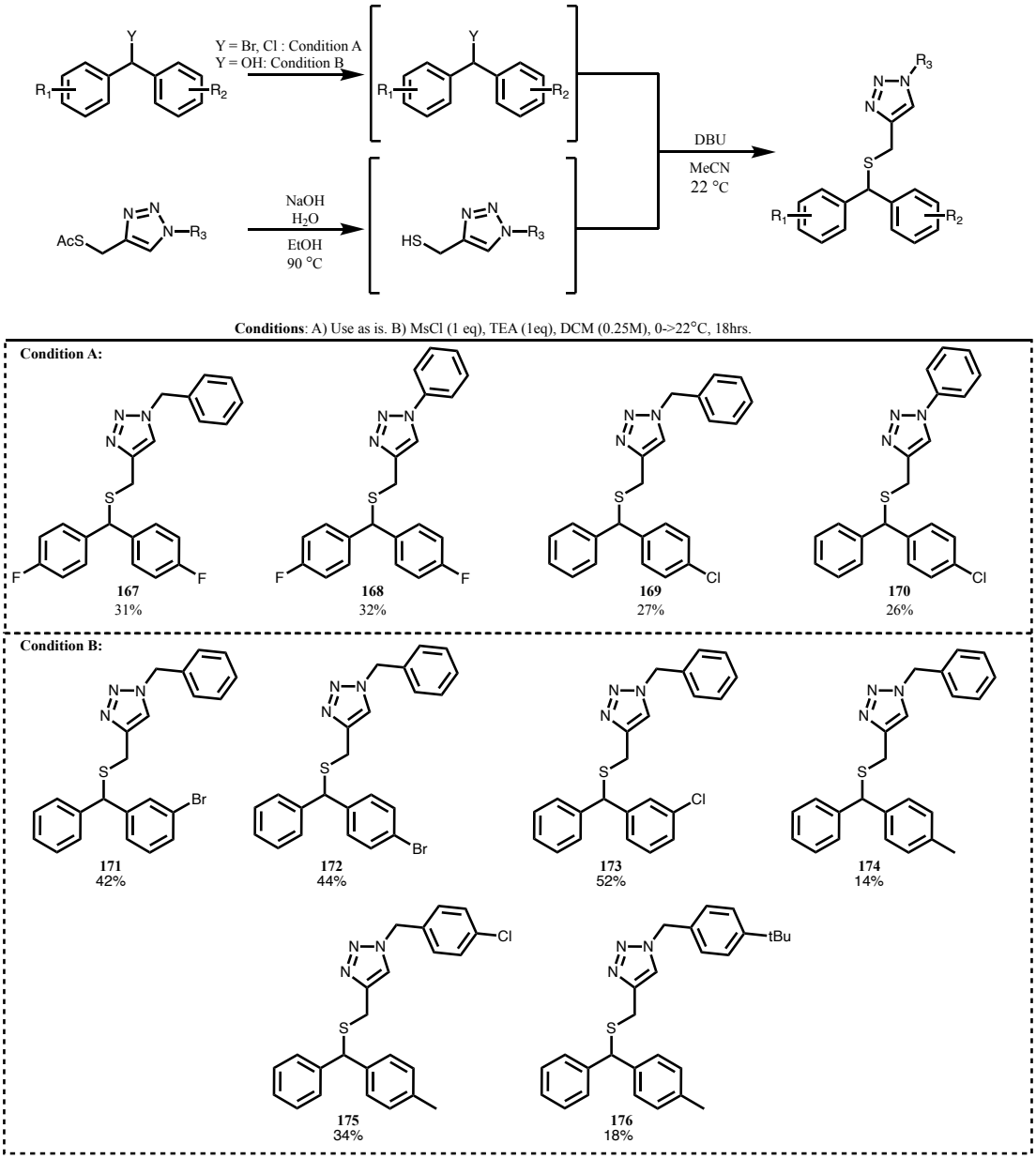

Figure 69: First generation of sulfide analogues.

SAR studies of modafinil analogues in the literature have shown there is a relationship between the affinity observed for sulfides and their corresponding sulfoxides.[160] The results from compounds **167** through **176** informed our synthesis of which sulfoxides held the most promise. We proceeded to synthesize the sulfoxides of selected sulfide analogues which showed the most interesting binding profiles at DAT and SERT. All sulfoxides were synthesized by treating the corresponding sulfide with mCPBA (1.05 eq) at -10 °C (Figure 70). Yields were consistently good,

with the only notable side product observed in all reactions being the over-oxidation of the sulfoxide to the sulfone though this was readily separated by standard column chromatography. Compounds **177**, **178** and **179** all contain bisphenyl backbones that are well established in the literature and are distinctly symmetric in an effort to reduce the number of enantiomers present in testing (2 vs 4). Compounds **180** and **181** possess a single meta halogen substitution in their backbone, which we later demonstrated is key for binding affinity and ensures an optimal binding pose within DAT. Compounds **182** and **183** were synthesized as they had the best affinity score as determined by the computational predictions good training tools to feed back the computational model and thereby increase its predictive power.

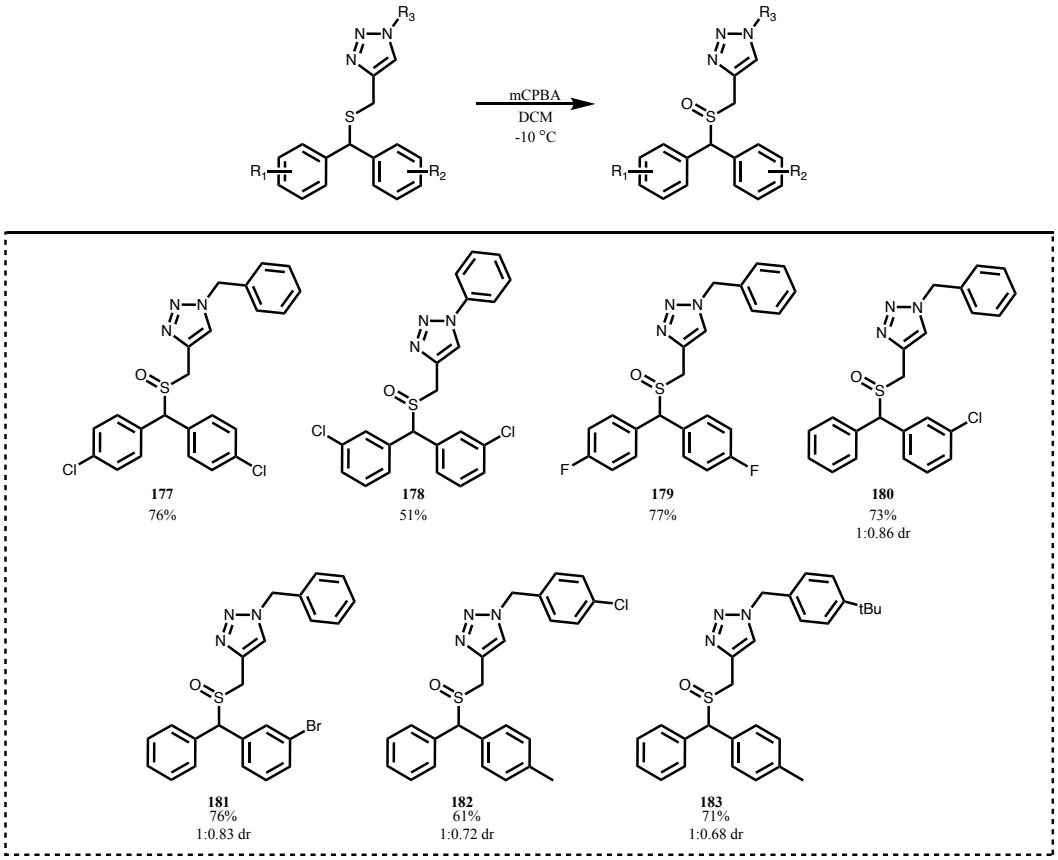

Figure 70: First generation of sulfoxide modafinil analogues.

5.3.2 Radioligand binding studies results for first generation of modafinil analogues

The modafinil analogues were tested in radioligand binding competition assays for DAT and SERT. Radioligand binding assays measure the binding affinity of a ligand to a target protein by means of competing the ligand with a radioligand of known affinity for the target protein. By competing our ligand in increasing concentrations against a known radioligand, we can determine a half-maximal inhibitory concentration (IC_{50}; concentration of ligand required to inhibit 50% of the radioligand from binding). The IC_{50} value can be used, in turn, to calculate an inhibition constant (K_i) through the Cheng-Prusoff equation. The K_i value of any ligand is then in theory a measure of the concentration of ligand required to occupy 50% of available receptors in the absence of competing ligands and should be an inherent property of the ligand relative to its target protein. Since K_i values are a concentration, it is worth noting that lower K_i values correspond to lower concentrations needed to occupy 50% of available target proteins, and therefore a high affinity of the ligand for its target. Likewise, a higher K_i value corresponds to lower affinity of the ligand for the protein. (See introduction for greater detail of K_i to IC_{50} relationship)

The binding affinities of the series of compounds synthesized above were determined for both DAT and SERT, the main off-target in this family of compounds and are shown in Table 4 below. The first effort to synthesize N-methyl triazoles, to retain a similar steric environment to that of **129**, and a privileged 4,4'-difluoro bisphenyl backbone showed a complete loss of affinity for DAT relative to **129**. Compound **145** showed very low affinity for DAT (8.96 ± 0.56 μM), and the sulfoxide **146** was completely inactive with a measured K_i = 51.9 ± 10.2 μM; a drastic loss of affinity relative to our lead compound **129**, yet in line with the predictions by our computational

models. Intriguingly, **144**, with a large TMS group appended to the triazole, had a five-fold higher affinity (9.69 ± 1.6 μM) at DAT than **146**. These results supported the predictions by our computational models as well, suggesting bulky hydrophobic substituents stemming from the triazole were key to improve affinity.

Table 4.

Radioligand Binding Studies of First Generation of Analogues

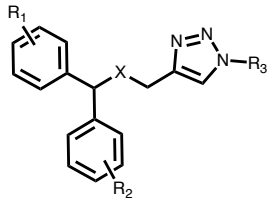

Compound	R_1	R_2	X	R_3	hDAT K_i (μM) ± SEM	hSERT K_i (μM) ± SEM	SERT/DAT
144	4-F	4-F	S=O	CH_2TMS	9.69 ± 1.6	3.61 ± 1.1	0.4
145	4-F	4-F	S	Me	8.96 ± 0.56	I.A.	> 1.1
146	4-F	4-F	S=O	Me	51.9 ± 10	I.A.	N/A
167	4-F	4-F	S	Bn	2.25 ± 0.4	I.A.	1.9
168	4-F	4-F	S	Ph	I.A.	I.A.	N/A
169	4-Cl	-	S	Bn	3.49 ± 0.2	I.A.	> 2.9
170	4-Cl	-	S	Ph	I.A.	I.A.	N/A
171	3-Br	-	S	Bn	8.46 ± 1.8	2.79 ± 0.51	0.35
172	4-Br	-	S	Bn	2.18 ± 0.2	I.A.	4.6
173	3-Cl	-	S	Bn	2.63 ± 0.1	3.55± 0.7	1.6
174	4-Me	-	S	Bn	I.A.	I.A.	N/A
175	4-Me	-	S	4-Cl-Bn	I.A.	I.A.	N/A
176	4-Me	-	S	4-tBu-Bn	I.A.	I.A.	N/A
177	4-Cl	4-Cl	S=O	Bn	2.31 ± 0.3	I.A.	> 4.3

178	3-Cl	3-Cl	S=O	Bn	I.A.	I.A.	N/A
179	4-F	4-F	S=O	Bn	9.98 ± 0.2	17.7 ± 0.6	1.8
180	3-Cl	-	S=O	Bn	5.22 ± 0.9	5.53 ± 1.2	1.1
181	3-Br	-	S=O	Bn	3.20 ± 0.6	0.48 ± 0.06	0.15
182	4-Me	-	S=O	4-Cl-Bn	5.35 ± 0.5	I.A.	> 1.9
183	4-Me	-	S=O	4-tBu-Bn	I.A.	I.A.	N/A

I.A. = Inactive (> 10 μM), unless otherwise noted.
Each K_i value derived from at least three independent experiments conducted in triplicate.

Shifting attention to N-benzyl analogues, a series of sulfides were made bearing different bisphenyl backbones known in the literature to convey improved affinity in modafinil analogues. The 4,4'-difluoro analogues, **167**, indeed showed an improved affinity (K_i = 2.25 ± 0.4 μM) relative to the N-methyl analogue, the same was true for its sulfoxide **179** which had an K_i = 9.98 ± 0.2 μM, a 5-fold improvement from **146**. Interestingly, the affinity of **179** was almost identical to **144**, which is to be expected considering the similar steric space they occupy. Work from the Lubec lab, who developed **129**, had shown a single halogen substitution (chloro or bromo) at the 3 or 4 position on the bisphenyl backbone had been pivotal to their drug discovery efforts with modafinil analogues.[176,179] Sulfide analogues bearing these substitution patterns and an N-benzyl triazole were promptly prepared but proved to have only modest (low μM) affinity for DAT. Compounds **169** and **172** (4-Cl and 4-Br bisphenyl backbones respectively) were found to have a K_i = 3.49 ± 0.2 μM and 2.18 ± 0.2 μM correspondingly for DAT, and to be inactive at SERT. The 3-Cl and 3-Br analogues, **173** and **171**, have similar affinities at DAT of 2.63 ± 0.1 μM and 8.46 ± 1.8 μM correspondingly, but with a rescued affinity for SERT falling within our K_i < 10 μM threshold (K_i = 2.97 μM for **173** and 4.16 μM for **171**). Sulfoxide analogues bearing the 3-Cl and 3-Br-phenyl backbones were of significant interest, as **129** and its chloro analogue are both known to have high (low K_i) affinities for DAT and completely inactive (>10 μM) at SERT. In light of the known SAR

of **129** and its chloro counterpart, the binding affinities for **181** and **180** were very surprising. Compound **181** saw a slight improvement in affinity for DAT relative to the sulfide (3.20 ± 0.6 μM), but notably saw a vast improvement in affinity for SERT (486 ± 59 nM), making this ligand 6.5-fold selective for SERT over DAT. This flip in selectivity for SERT over DAT (and the corresponding high affinity for SERT) is exclusively mediated by the N-benzyl triazole moiety. Of note, this SERT-favoring selectivity is observed exclusively in the 3-Br substrates (i.e. **171** and **181**), as all other substrates are, albeit to a modest extent, DAT selective. Furthermore, this 3-Br SERT-selectivity is mediated by the N-benzyl triazole, as the presence of other heterocycles retains DAT selectivity,[182] and was only observed in one other substrate in the current study (see below).

Compounds **174**, **175**, **176**, **182**, and **183** all bear a 4-methyl bisphenyl backbone. This backbone was predicted to ensure the highest affinity for DAT of all compounds tested in the QSAR model. In addition to the N-benzyl triazole, substrates with increased bulkiness (**176** and **183**) and hydrophobicity (**175**, **176**, **182**, and **183**) were prepared in accordance with the predicted trend. Except for **182**, which had very modest affinity for DAT (5.35 ± 0.5 μM), all compounds proved to be completely inactive at both DAT and SERT. It is possible the lack of observed affinity for DAT and SERT in our assay was due to the poor solubility of these compounds in the solvent system used in our radioligand binding assay (i.e. 30% DMSO in water during drug dilutions, and 3% DMSO in water during testing), all 4-methyl analogues were observed to crash out of solution during the preparation of drug dilutions and may have not engaged in proper binding competition during the assay.

Up to this point, the radioligand binding studies conducted showed all triazole bearing modafinil analogues exhibited very modest affinities for DAT and low selectivity for DAT in favor of SERT. The DAT affinities observed are not however outside the range of affinities observed by the Lubec group in similar analogues, as shown previously. Still, none of the previous analogues show a significant improvement over currently available modafinil-like DAT inhibitors. Of most interest at this stage was the role of the benzyl triazole in flipping the DAT vs. SERT selectivity of modafinil analogues bearing a 3-Br-bisphenyl backbone. This change in selectivity is not due to a dampening of DAT affinity but rather to an improved affinity for SERT.

5.4 Second Generation of Modafinil analogues

5.4.1 Synthesis of extended chain thiols and imidazole thiols

While the modafinil analogues shown thus far provided insightful SAR and served as useful tools to develop an efficient synthetic route to this chemotype, the radioligand binding studies conducted revealed mostly modest DAT affinity and poor selectivity for DAT over SERT. Following close analysis of the binding poses of our lead compounds within DAT, as well as reported binding poses of analogous compounds,[179] prompted two distinct hypotheses. Firstly, a wide range of dopaminergic ligands (modafinil-like and otherwise) show a key salt-bridge interaction with the ASP 79 residue within the S1 site in DAT.[179] Computational analysis of the binding poses of our lead **181** (Figure 71) revealed the triazole moiety was likely too far from ASP79 to engage in this strong interaction, we hypothesized that extending the distance between the sulfoxide and the triazole (i.e. 2,3, or 4 methylene units instead of 1) would enable the triazole to reach ASP79 and

thereby increase the ligand affinity. Secondly, the design underlying the current SAR campaign was directly inspired by **129** (Figure 60). Molecular dynamics and docking simulation studies conducted by the Lubec lab of *S*,*S*-**44** (the most active stereoisomer of **129**) show the thiazole moiety engaging in hydrophobic interactions primarily, interacting with Phe76 and Val328.[179]

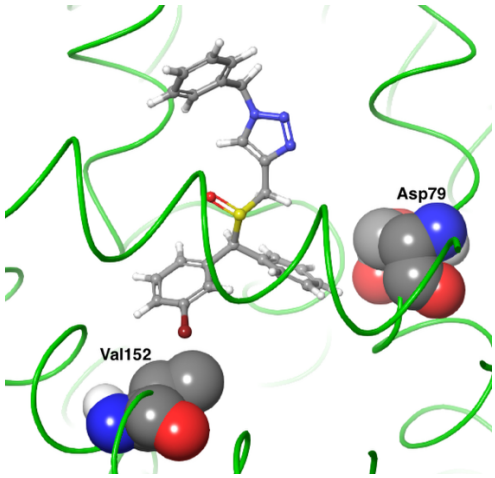

Figure 71: Docking of compound **181** in DAT S1, showing Val152 and Asp79. Docking performed by Dr. Abhishek Thakur of the Computational Chemistry and Molecular Biophysics Section in NIDA.

This insight reveals that the effect on binding by the thiazole ring may be due to electronic, rather than steric, effects. As such, we hypothesized that despite triazoles being geometrically and sterically similar to the thiazole in **129**, the clear electronic differences may underlie the drastic reduction in affinity between the epimers of **129** (56 nM) and **181** (792 nM). We therefore decided to replace the triazole that launched this medicinal chemistry campaign for an imidazole, which maintains the ability to append further substitutions from a nitrogen in the imidazole ring, maintaining a largely similar steric profile to the triazoles, but is a better isoelectronic analogue to the thiazole.

To test the first hypothesis, namely if by extending the chain-length between triazole and sulfoxide, a series of N-methyl and N-benzyl triazoles were constructed analogous to **160** with varying methylene units between triazole and thiol (see boxed general structure in Figure 72). The N-methyl and N-benzyl analogues with four methylene units between the triazole and thiol (n=4) were both made starting from 5-hexyn-1-ol. Copper(I)-catalyzed azide-alkyne cycloaddition with $TMSCH_2N_3$ and benzyl azide yielded triazoles **184** (63%) and **187** (36%) respectively. Subsequent bromination of the alcohols provided the key bromo intermediates **185** (48%) and **188** (31%) which could then be reacted with potassium thioacetate to afford the acetate protected thiols **186** and **189** in 72% and 74% yields respectively.

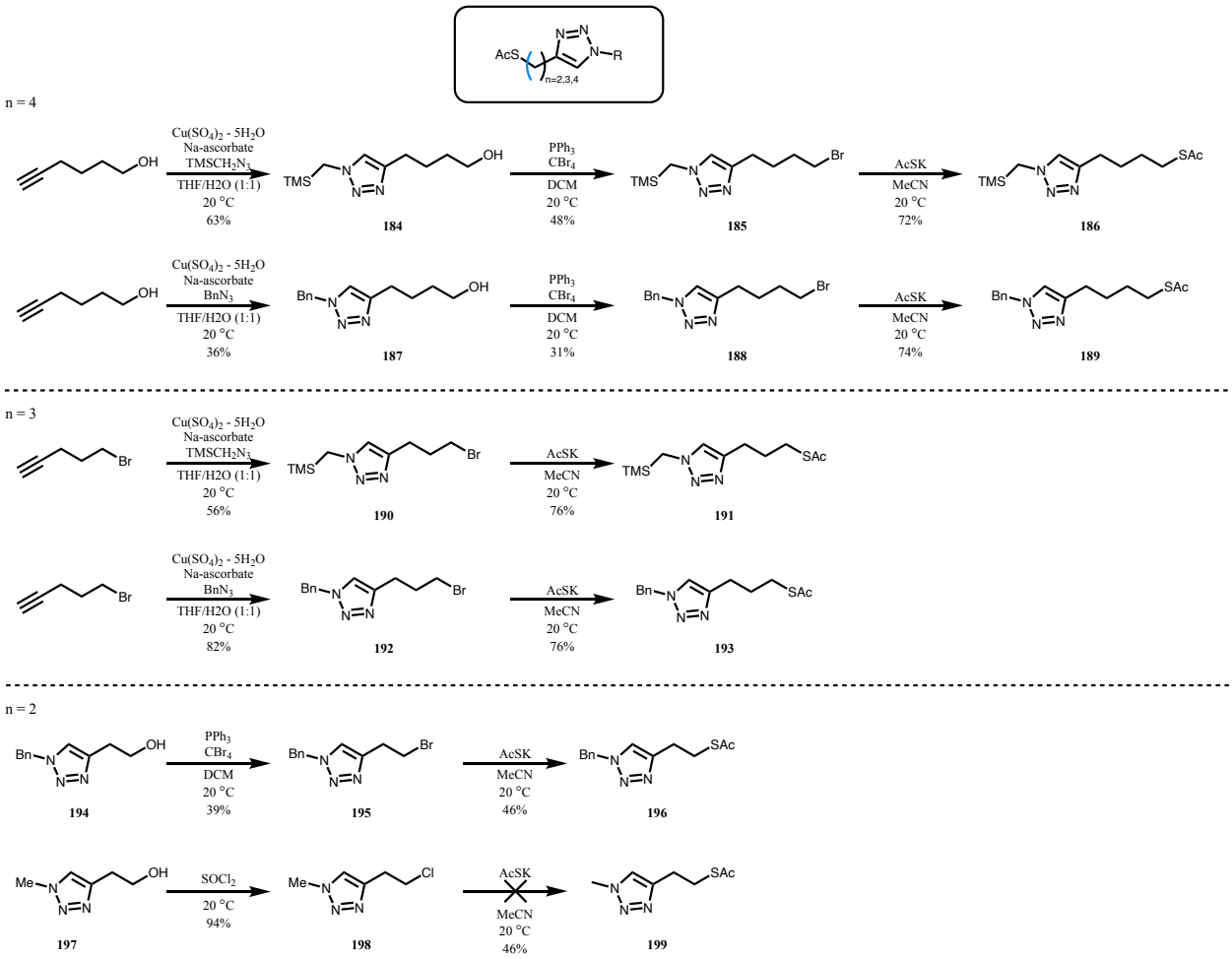

Figure 72: Synthesis of acetate protected thiols with triazoles for second generation of modafinil analogues.

The N-methyl and N-benzyl analogues with three methylene units between the triazole and thiol (n=3) were both made starting from 5-bromo-1-pentene. Analogous to the route described for compounds **186** and **189**, 5-bromo-1-pentene was first treated with copper(II) sulphate pentahydrate, sodium ascorbate and the corresponding azide to afford **190** and **192** in 56% and 82% yields correspondingly via CuAAC. The bromine is subsequently displaced by potassium thioacetate to generate the desired n=3 protected thiols **191** and **193**. Lastly, the N-benzyl thiol with an n=2 carbon chain was prepared starting from commercially available alcohol **194**, this was subject to Appel conditions to afford bromide **195** in 39% yield. Subsequent displacement with

potassium thioacetate yielded the desired **196**. The N-methyl analogue bearing a two methylene unit linker could not be prepared, as following the chlorination of alcohol **197** with thionyl chloride to afford **198**, the displacement with AcSK failed and resulted in a complex mixture and no **199** was obtained. Since the final sulfoxides with n=3 and n=4 had already been synthesized. The N-benzyl analogues had significantly better affinities relative to the N-methyl analogues, thus the pursuit of the n=2 N-methyl analogue was discontinued.

To test our second hypothesis, it was necessary to substitute the triazole moiety in our analogues for imidazoles, thus it was necessary to prepare the analogous imidazole-bearing thiols (see boxed general structure in Figure 73). The most basic imidazole analogue (N-H) to our delight was commercially available as an HCl salt in its free thiol form (**200**, Figure 73). The analogous N-benzyl analogue could be prepared by LAH reduction of acid **201**, chlorination of the resulting alcohol, and subsequent displacement of the chloride with potassium thioacetate to yield **202** in 30% yield over 3 steps. Compound **204** was prepared to incorporate the steric effects of a benzyl group emerging from the imidazole but retaining the N-H of the imidazole which proved to be essential as will be discussed below. It was prepared in a single step from the commercially available HCl salt **203** in 28% yield. Finally, the N-methyl analogue, **206**, could also be synthesized in a single step from the commercially available HCl salt **205**. Both **204** and **206** were prepared by reacting the primary alkyl chloride with potassium thioacetate to afford the acetate protected thiols.

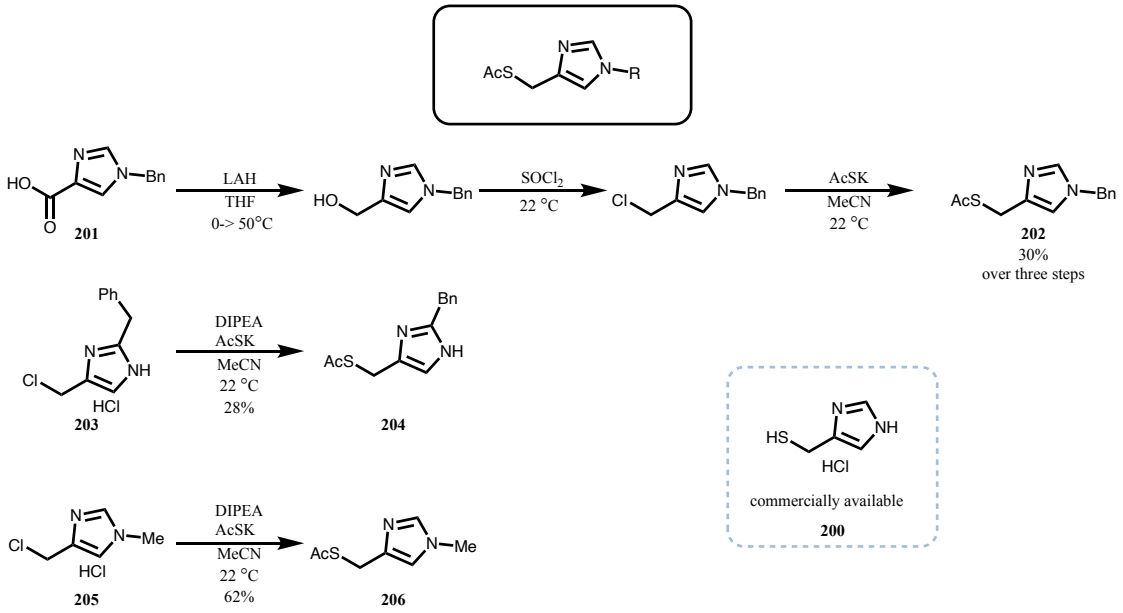

Figure 73: Synthesis of acetate protected thiols with imidazoles for second generation of modafinil analogues.

5.4.2 Synthesis of second generation of analogues

With the necessary thiols to test the two new templates we hypothesized would improve affinity, synthesizing the corresponding sulfides could be achieved in analogous fashion to the first generation of triazoles reported earlier. Except for **207**, all compounds prepared bear the same 3-bromo bisphenyl backbone. Compound **207** was prepared due to the literature relevance of the 4,4'-difluoro bisphenyl backbone. As such, **207** and its corresponding sulfoxide are relevant points of comparison with previously reported modafinil analogues which had this backbone. As shown in Figure 74 below, Compounds **208** and **209** are the N-methyl triazole analogues with n=4 and n=3 chain length correspondingly. The N-benzyl analogues, compounds **210** and **211** were also prepared. Yields for the N-benzyl analogues were typically better (69% for **210** and 73% for **211** v. 39% for **208** and 54% for **209**). The discrepancy in yields likely stems from the N-CH_2-TMS

thiols **186** and **191**; the sodium hydroxide mediated deacetylation of these intermediates simultaneously deacetylates the thiol and removes the TMS group to unveil the desired N-methyl moiety. It is likely that the need for two reactions to proceed (as opposed to a singular deacetylation as is the case for the N-benzyl thiols) results in lower yields for these analogues. The n=2 chain length analogue for the N-benzyl sulfide **214** was prepared in 42% yield. No n=2 analogue was prepared of the N-methyl triazole, as prior attempts had failed and at this point it was clear that N-methyl analogues were inferior to N-benzyl. Furthermore, compounds **212** and **213** bore the desired imidazole in place of the triazole to test our second hypothesis. Alkylation of thiols **204** and **206** both yielded only trace amounts of the desired sulfide and were discarded.

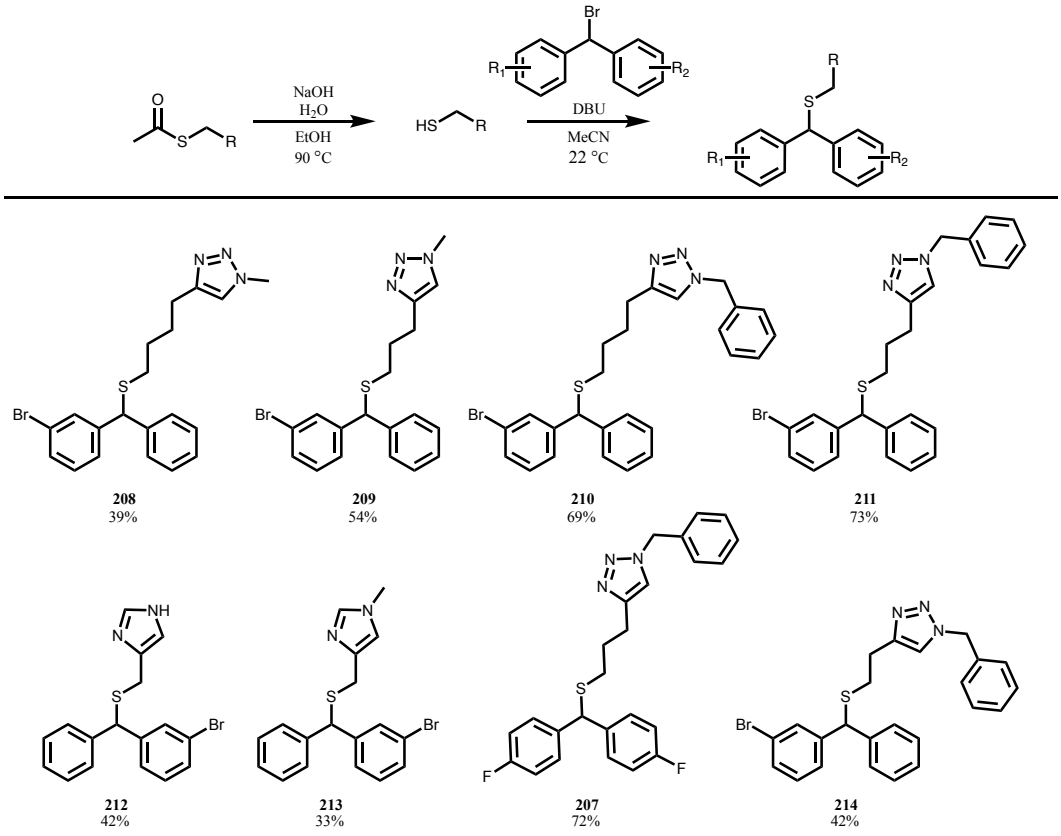

Figure 74: Second generation of sulfide modafinil analogues prepared.

Sulfides in Figure 74 were subsequently oxidized to their corresponding sulfoxides as shown in Figure 75 below. Sulfoxides **215**, **216**, **217**, **220** and **221** were synthesized to test our first hypothesis, placing the triazole further away from the sulfoxide will result in an improved affinity due to its improved proximity to Asp79. These were all prepared by oxidation of the prerequisite sulfide with mCPBA in moderate yields (34-54%) Sulfide **209** was oxidized but its sulfoxide was subsequently lost in purification.

Sulfoxides **218** and **219** were the imidazole analogues designed to test our second hypothesis. The unsubstituted imidazole substrate **218** faired modestly under the reaction conditions. The imidazole moiety was unaffected by the mild oxidative conditions, however the reaction yield was low (32%). In contrast the N-methyl imidazole proved a better substrate under these conditions and reacted to form the desired sulfoxide in 63% yield.

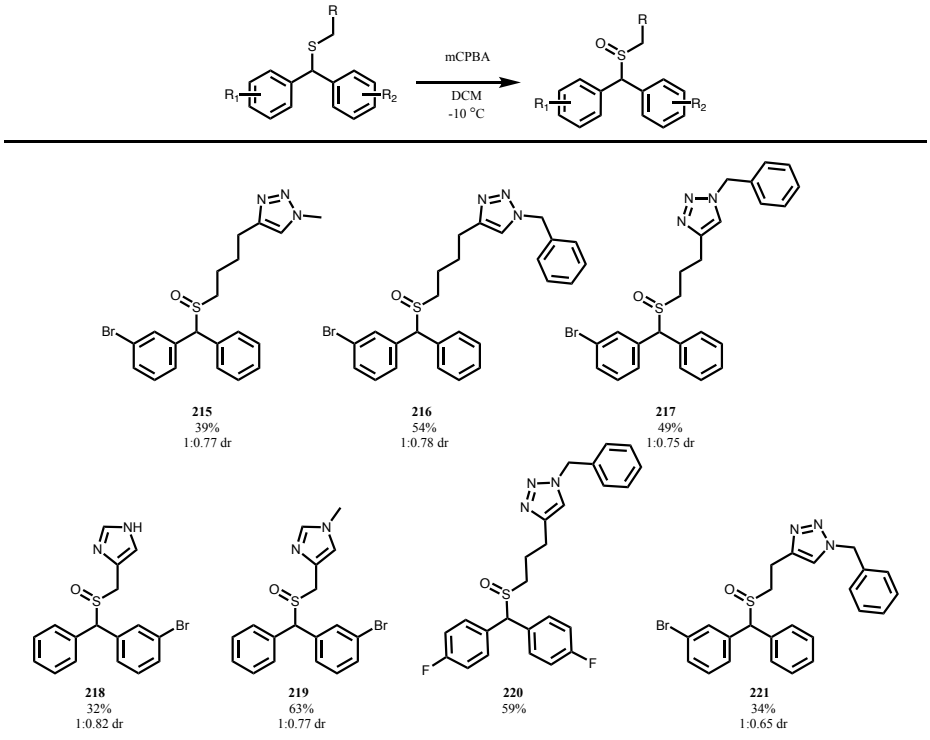

Figure 75: Second generation of sulfoxide modafinil analogues prepared.

5.4.3 Radioligand binding studies on second generation of modafinil analogues

The new set of ligands was subsequently tested in the same radioligand binding assays for DAT and SERT. Generally, the new set of modifications proved to be favorable in both improving affinity for DAT and selectivity over SERT.

Our first hypothesis was that extending the linking carbon chain between the backbone and the triazole moiety may lead to favorable interactions within the binding site of DAT resulting in an improved affinity. To this end compounds **209-211**, **213**, **215-217**, and **221** were prepared. Initial results (Table 5 below) with the sulfide analogues revealed that extending the linking chain from a single methylene unit to 3 or 4 methylene units had a significantly positive effect on all analogues, with the N-benzyl triazole analogues retaining a higher affinity for DAT than the corresponding N-methyl analogues. Compounds **208** and **209** possess a terminal N-methyl triazole separated from the sulfide by 3 and 4 methylene units correspondingly. Compound **208** had an affinity of 2.72 ± 0.2 μM for DAT and 5.63 ± 0.9 μM for SERT, which lies within the range of the analogues discussed in the previous section. Analogue **209** did show a modest improvement in DAT affinity (K_i = 823 ± 61 nM), while affinity at SERT remained poor (K_i = 4.93 ± 0.4 μM) representing a noteworthy shift towards better DAT activity and greater selectivity (approximately 6-fold over SERT). The N-benzyl triazole analogues showed further improvement upon extension of the linking chain. Compounds **210** and **211**, with a terminal N-benzyl triazole, separated from the sulfide by 4 and 3 methylene units respectively. This change led to dramatically improved affinities at DAT and concomitantly eliminated all activity at SERT. Compound **211**, with three methylene units separating the triazole from the sulfide, had a DAT K_i = 170 ± 49 nM and a SERT affinity of 171 ± 25 μM - a 1000-fold selectivity for DAT/SERT. This is a notable (50-fold)

improvement from the parent compound, short chain sulfide **171**, which had a K_i = 8.46 ± 1.8 μM. Adding an additional methylene unit to the linking chain yielded **210**, and results in a slight decrease in affinity for DAT (621 ± 120 nM) and slight improvement in SERT affinity (147 ± 29 μM), yet still remaining functionally inactive at SERT.

Table 5.

Radioligand Binding Studies of Second Generation of Analogues

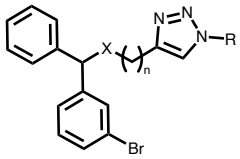

Compound	X	n	R	hDAT K_i (μM) ± SEM	hSERT K_i (μM) ± SEM	SERT/DAT
208	S	4	Me	0.82 ± 0.06	4.93 ± 0.4	6
209	S	3	Me	2.72 ± 0.2	5.63 ± 0.9	2.1
210	S	4	Bn	0.62 ± 0.1	147 ± 29	237
211	S	3	Bn	0.17 ± 0.05	171 ± 25	1000
215	S=O	4	Me	I.A.	I.A.	N/A
216	S=O	4	Bn	0.33 ± 0.03 2	3.18 ± 0.3	9.6
217	S=O	3	Bn	0.08 ± 0.01	7.67 ± 0.4	98
220*	S=O	3	Bn	0.261 ± 0.01	8.93 ± 0.57	34.2
221	S=O	2	Bn	1.04 ± 0.42	I.A.	N/A

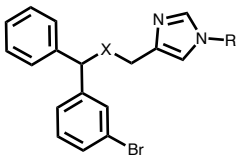

Compound	X	R	hDAT K_i (μM) ± SEM	hSERT K_i (μM) ± SEM	SERT/DAT
212	S	H	16.6 ± 2.5	0.800 ± 0.16	0.05
213	S	Me	0.21 ± 0.02	5.55 ± 0.51	26.4
218	S=O	H	0.23 ± 0.04	219 ± 31	960
219	S=O	Me	I.A.	I.A.	N/A

I.A. = Inactive (> 10 μM), unless otherwise noted.
Each K_i value derived from at least three independent experiments conducted in triplicate.
*: bisphenyl is 4,4'-difluoro substituted in place of 3-Br.

Compounds **213** and **212** were synthesized to address hypothesis two, namely, that replacing the triazole for a heterocycle isoelectronic to a thiazole would be beneficial. Naturally an oxazole would be the key candidate for an isoelectronic heterocycle to a thiazole however we were interested in adding substituents to the heterocycle to better exploit the binding site at DAT, as such the imidazole was the best next option. Compounds **213** and **212** provided very interesting results, the sole difference between these is **212** contains an N-H, whereas the imidazole in **213** is substituted with N-methyl. Despite this slight difference they have contrasting properties with respect to their affinity at both DAT and SERT. Notably, **213** shows good affinity at DAT (K_i = 211 ± 21 nM) and only modest affinity at SERT (K_i = 6.29 ± 0.8 μM), leading to approximately 30-fold selective for DAT over SERT. In stark contrast, the nor analogue, **212** proved to be SERT selective, with a SERT K_i = 587 ± 218 nM and 16.6 ± 2.5 μM affinity for DAT, being approximately 28-fold selective for SERT. It is plausible that within the binding pocket of SERT the imidazole N-H serves as an analogue to the indole N-H of serotonin. Interestingly however we did not see this behavior with the corresponding sulfoxide.

Radioligand binding data for the sulfoxides were just as interesting as for the sulfides. **208** and **209** when oxidized to their corresponding sulfoxides (**219** and **215**) saw complete loss of affinity at both DAT and SERT. Most interestingly, the sulfoxide of **212**, **218**, saw a complete reversal of affinity. Where sulfide **212** proved to be SERT selective, the corresponding sulfoxide **218** had excellent affinity at DAT (228 ± 41 nM) and was completely inactive at SERT (219 ± 32 μM) providing the most DAT selective (racemic) sulfoxide in this series (960-fold selective for DAT over SERT). Compounds **216**, **217** and **221** revealed a similar trend to the sulfides, where the optimal distance between triazole and sulfoxide appears to be three methylene units. Compound **216** has a promising affinity for DAT (326 ± 27 nM) and low affinity for SERT (3.18 ± 0.3 μM), making it approximately 10-fold selective. Pleasingly, compound **217** showed the highest affinity for DAT of all analogues prepared, with an affinity of 78.3 ± 14 nM. Furthermore, it was largely inactive at SERT with an affinity of 7.67 ± 0.45 μM, making it nearly 100-fold selective for DAT over SERT. After separating the stereoisomers of **217** and testing them individually, we observed that indeed this affinity for DAT is largely driven by a single stereoisomer (see next section) and as such this would become our lead compound moving forward. Compound **220** is interesting, as we decided to employ the canonical 4,4'-difluoro backbone with this newly optimized aliphatic chain length. The 4,4'-difluoro backbone had been successfully employed by the Newman group in numerous occasions with various modafinil analogues, however showed no promise in any of the analogues tested previously (**145**, **167**, **144**, **146**, **168**, **179**). Pleasingly, when coupled with the three methylene linker and N-benzyl triazole, compound **220** showed very good affinity for DAT (K_i = 260.9 ± 7.8 nM) and only very modest affinity for SERT (K_i = 8.93 ± 0.57 μM). This is particularly interesting from a synthetic standpoint as the symmetric substitution of bisphenyl backbone means only 2 enantiomers are formed as opposed to 4 stereoisomers, making the

asymmetric synthesis simpler. Lastly compound **221** revealed two methylene units to be too short, with a significant loss in DAT affinity (1039 ± 417 nM) though still completely inactive at SERT (> 10 μM).

5.5 Stereoisomers of **217**

Compound **217** showed the highest affinity for DAT and good selectivity over SERT (100-fold) as a mixture of stereoisomers. Inspired by CE-158, which has one dominant stereoisomer (*S*, *S*) and the other stereoisomers are comparatively inactive, we were driven to separate the constituent stereoisomers of **217** and test them individually. The four stereoisomers of **217** can be readily separated by preparative HPLC (see below).

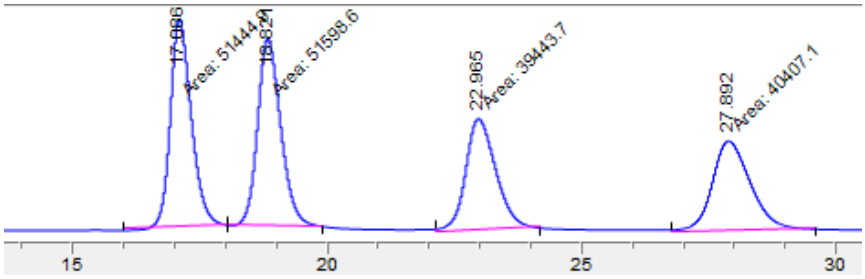

The four stereoisomers of **217** were isolated and tested individually and revealed that indeed a single stereoisomer of **217** is largely responsible for driving affinity for DAT, as was observed for CE-158. Shown in Table 6 below are the binding affinities of the independent stereoisomers of **217**. Excitingly, the most active stereoisomer of **217 (217C**) is largely responsible for the affinity of **217** for DAT, with an affinity of K_i = 22.3 ± 3.1 nM. Noticeably two of the stereoisomers have affinities in the micromolar range and **217D** has an affinity 10 times lower than **217C**.

Table 6.

Radioligand Binding Studies of the stereoisomers of **217**

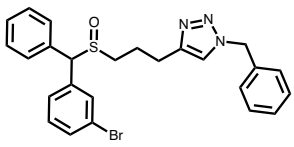

Compound	hDAT K_i (nM) ± SEM	hSERT K_i (nM) ± SEM	SERT/DAT
rac-217	78.3 ± 14	7674 ± 452	98
217A	3139 ± 332	I.A.	> 3.2
217B	2373 ± 162	I.A.	> 4.2
217C	22.3 ± 3.1	23170 ± 2850	1039
217D	230 ± 31	3757 ± 275	16.3

I.A. = Inactive (> 10 μM), unless otherwise noted.
Each K_i value derived from at least three independent experiments conducted in triplicate.

Pleasingly, **217C** also has the best selectivity for DAT over SERT (i.e. over 1000-fold). These results make **217C** an excellent lead moving forward. At this juncture efforts at identifying the absolute configurations of all stereoisomers, and most importantly **217C**, are underway however remain unclear at present. Unfortunately, due to the benzhydryl cation that can form in the formation of these substrates, issues with epimerization have complicated characterization of that chiral center. Efforts at crystallizing the individual stereoisomer are ongoing.

5.6 Computational Studies of **217**

In an effort to understand the DAT binding affinities observed in **217** and its constituent stereoisomers, we performed docking of the four stereoisomers predict how they may be posed

within the DAT binding site. Shown in Figure 76 below is a representative binding pose of (*S*,*S*)-CE-158 in DAT which was acquired from a 120 ns molecular dynamics simulation of (*S*,*S*)-CE-158 docked in the cryo-EM structure of human DAT in complex with benztropine. Comparisons with (*S*,*S*)-CE-158 is important in part due to the structural similarity of **217** to (*S*,*S*)-CE-158, therefore likely engaging in similar interactions, but also since (*S*,*S*)-CE-158 has consistently shown atypical DAT inhibition. As atypical DAT inhibition has been closely linked to the pose in which the inhibitor stabilizes the transporter, mirroring the pose of (*S*,*S*)-CE-158 is desirable.

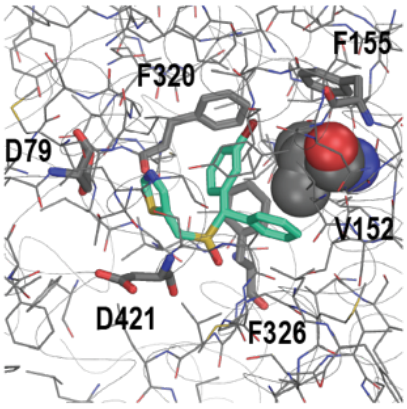

Figure 76: Representative docking pose of (*S*,*S*)-CE-158 within DAT. Docking performed by Dr. Kuo Hao Lee of the Computational Chemistry and Molecular Biophysics Section in NIDA.

The key interaction observed in this simulation was the benzhydryl backbone with Val152. This interaction was stable throughout the entire 120 ns simulation and was also observed in previous studies.[179] Using this framework with (*S*,*S*)-CE-158 in DAT, we proceeded to perform induced fit docking (IDF) of the four stereoisomers of **217** to assess the most stable binding poses of each stereoisomer. Shown in Figure 75 below, are the three poses with best IDF scores for each of the stereoisomers of **217**, representing the likely most stable binding poses within DAT.

A

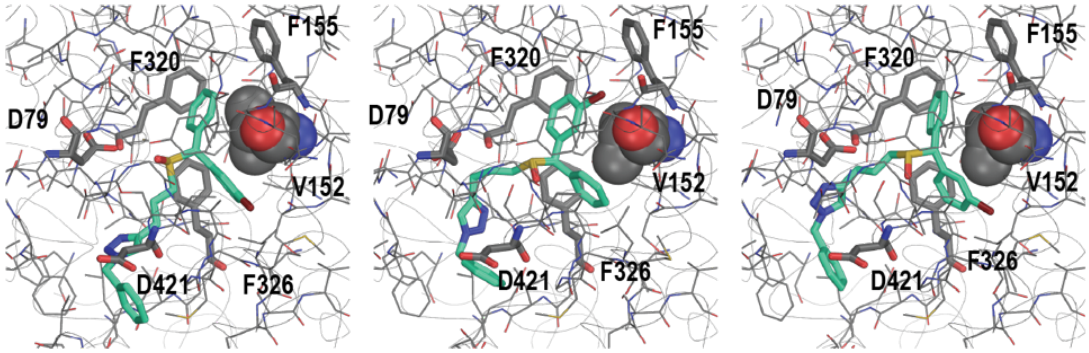
F155
F320
D79
V152
D421
F326
F155
F320
D79
V152
D421
F326
F155
F320
D79
V152
F326
D421

B

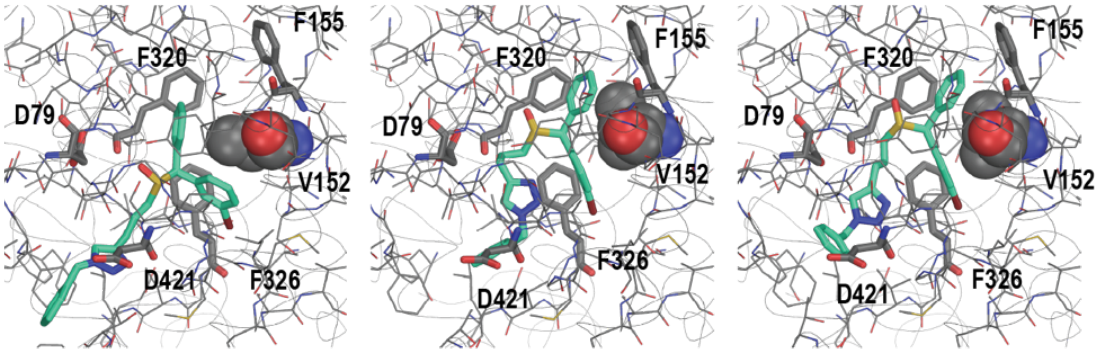
F155
F320
D79
V152
D421
F326
F155
F320
D79
V152
F326
D421
F155
F320
D79
V152
F326
D421

C

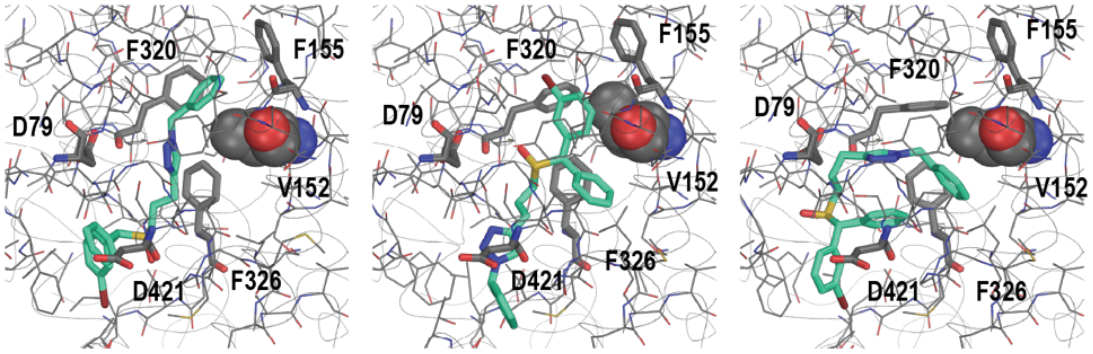
F320
F155
D79
V152
D421
F326
F155
F320
D79
V152
F326
D421
F155
F320
D79
V152
D421
F326

D

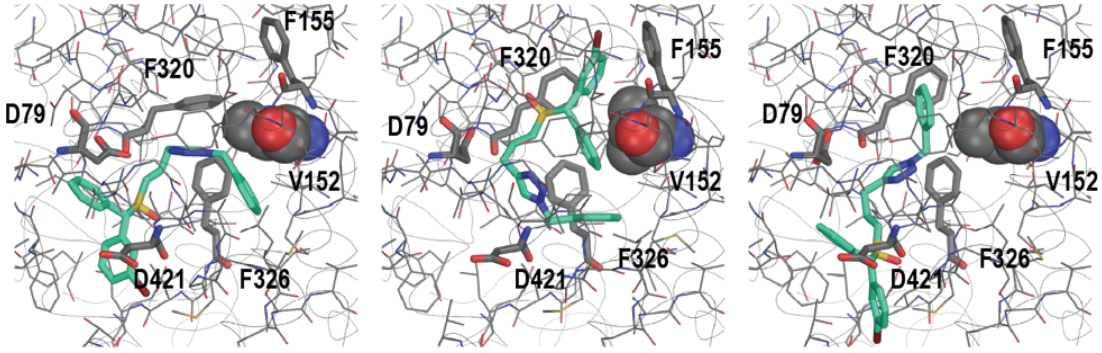
F155
F320
D79
V152
D421
F326
F155
F320
D79
V152
F326
D421
F155
F320
D79
V152
F326
D421

Figure 77: Representative docking poses of **217** in DAT. Shown in green is **217**, in grey are DAT side chains, highlighted is Val152. A) Top three binding poses for (*R*,*R*)-**217**, B) Top three binding poses for (*S*,*S*)-**217**, C) Top three binding poses for (*R*,*S*)-**217**, D) Top three binding poses for (*S*,*R*)-**217.** Docking performed by Dr. Kuo Hao Lee of the Computational Chemistry and Molecular Biophysics Section in NIDA.

Figure 77A shows the docking of (*R*,*R*)-**217** and Figure 77B shows the docking of (*S*,*S*)-**217**, interestingly both of these stereoisomers show the same interaction between the benhydryl backbone and Val152 that was observed for (*S*,*S*)-CE-158. These results are encouraging and suggest it's likely one of these stereoisomers corresponds to **217C**. On the other hand both (*R*,*S*)-**217** and (*S*,*R*)-**217** (Shown in Figure 77C and 77D respectively) do not show a particularly stable pose. For both of these stereoisomers, the top three poses show no converging binding pose, where the orientation of **217** changes drastically from one pose to the other and we don't observe the desired interaction with Val152. It is possible these stereoisomers correspond to **217A** and **217B** which show very poor affinity for DAT.

Interestingly, a key difference between (*R*,*R*)-**217** and (*S*,*S*)-**217** appears to be the position of the benzyl triazole moiety. As seen in the three poses of (*R*,*R*)-**217** (Figure 77A), the aromatic N-Benzyl ring forms an interaction with D421. On the other hand, the most stable poses for (*S*,*S*)-**217** (Figure 77B) do not converge to a common pose for the N-Benzyl moiety, taking different positions in all docking poses and not forming a stable interaction. Considering the binding affinities of **216** (326 nM), **217** (78 nM), and **221** (1039 nM), which are differentiated exclusively by a single methylene unit linking the bisphenyl backbone to the triazole, it is clear the role and

positioning of the triazole is essential to the binding of these analogues. We expect a significant interaction between the protein and the benzyl triazole must be present and the results from this docking suggest it is likely it is engaging with D421. Further experiments and mutagenesis studies will be necessary to validate this hypothesis.

It remains imperative to characterize the identity of **217A-D** to further validate these docking results and to derive meaningful relationships between the radioligand binding results obtained and the insights obtained from the computational studies. Though pending further confirmation, these docking results are encouraging, and suggest that (*R*,*R*)-**217** and (*S*,*S*)-**217** have binding poses which mirror that of known atypical inhibitor (*S*,*S*)-CE-158. Though not certain, these results suggest our lead may induce a similar behavioral profile to (*S*,*S*)-CE-158 (i.e. atypical inhibitor).

5.7 Conclusions

A series of modafinil analogues were synthesized and their affinity at DAT and its most common off-target (SERT) were assessed. Our drug design relied on employing a triazole moiety in place of the thiazole in **129**. We identified the 3-bromo bisphenyl backbone to be a privileged structure, conducive to improved affinity for DAT. Analogues with a single methylene unit separating the sulfoxide from the triazole were largely inactive at DAT, yielding affinities in the micromolar range (comparable to modafinil) and not providing an improvement from known modafinil analogues. Furthermore, insofar as employing a triazole moiety as a bioisostere for the modafinil primary amide, the size of the modafinil substituent (N-R) has a significant effect on DAT affinity.

Small substituents (i.e. N-Me) result in inactive compounds, this was shown with compound **146** and further substantiated with our computational model.

The second generation of modafinil analogues employed two untested motifs: an extended carbon chain separating the sulfoxide from the triazole moiety, and an imidazole in place of the thiazole in **129**. Both of these chemical manipulations were fruitful, resulting in two leads: **217** and **218**. Compound **217** retained the triazole which inspired this study but separated from the sulfoxide by the optimal three methylene units. Compound **218** replaced the thiazole in compound **129** with an unsubstituted imidazole. Both compounds, when tested as the mixture of stereoisomers, revealed excellent affinities for DAT comparable (or better) than cocaine. Importantly, both compounds have multi-parameter optimization (MPO; a metric used to predict the potential drugability of a certain compound based on a series of parameters of the molecule like molecular mass, lipophilicity, number of H-donors/acceptors, among others. Notably, for CNS drugs, a score greater than 3-4 signifies good potential blood brain barrier (BBB) permeability) scores above 3 (**217**: 3.6, **218**: 5.1), suggesting they are likely to penetrate the BBB and supporting them as candidates to carry on to *in vivo* studies. Ultimately compound **217** was identified as the lead to carry forward in our studies, primarily due to the chemical flexibility afforded by its scaffold. Despite the good affinity measured for compound **218**, a slight change (i.e. methylation of the imidazole to form **219**) was dramatically detrimental to DAT binding. This result suggest that it is plausible the N-H bond in **218** is essential to its binding; this imposes a strict limitation of the extent of modifications that can be applied to **218**. On the other hand, **217** enjoys a linker which can be functionalized and a N-benzyl triazole which can be further optimized. For example, the binding poses shown in Figure 77A and 77B show the benzyl ring attached to the triazole is

oriented close to Asp421, substituents on the phenyl ring which fortify this interaction (i.e. H-bond donors) may further improve affinity for DAT. Consequently, we pursued **217** further, separating the individual stereoisomers of **217** to find the most active stereoisomer, **217C**, which showed excellent affinity for DAT (K_i = 22.3 ± 3.1 nM) and excellent selectivity over SERT. Current work to determine the precise identity of **217C** remains underway.

6 Conclusion and Future Work

This thesis reported elements of two lines of work. Discussed in Chapters 2 and 3 is work in relation to HB and related methodologies. Chapter 4 focuses on the development of novel modafinil analogues developed as potential atypical DAT inhibitors.

Chapter 2 described the development of a one-pot procedure for the synthesis of arenes in a single step from linear 1,5-diols and Ph* methyl ketone **8**. Initial attempts at using palladium salts to mediate the aromatization reaction were not fruitful, as the conditions necessary to effect the aromatization of the intermediate cyclohexene were orthogonal to the conditions necessary for the initial cyclization step. Pleasantly, a one pot procedure was achieved by coupling the method previously derived for acceptorless dehydrogenations with a tandem Cu/1,10-phen/TEMPO dehydrogenation, which is capable of affording substituted 1-acyl arenes in moderate yields. This strategy for arene formation is unique in its disconnection: (5+1) cyclization and complementary to previous methodologies developed by the Donohoe lab which generate cyclohexanes and cyclohexenes.

Chapter 3 describes efforts to control the stereochemistry about (2*R*,3*R*)-dimethyl cyclohexanes **75** and **76**. The cis dimethyl presented a synthetically useful motif and as such it was deemed valuable to selectively interconvert between **75** and **76** which otherwise are generated in approximately a 1:1 ratio under reaction conditions. Attempts at driving the thermodynamic equilibrium of these two isomers in favor of one isomer over the other were unsuccessful.

Furthermore, attempts at selectively accessing a single enantiomer by interconverting these **75** and **76** under kinetic control also proved unsuccessful, this is true for **75**/**76** as well as their corresponding silyl enol ethers and corresponding esters.

Chapter 4 detailed the synthesis of novel modafinil analogues as DAT inhibitors. A series of analogues are described with a wide range of affinities, the first generation of analogues is the most akin to analogues already known in the literature and had the lowest measured affinities for DAT. The second generation of analogues introduces two novel motifs, namely: an extended linker with a triazole moiety, and an imidazole. This led to two potential leads: compounds **217** and **218**. Both lead compounds had good DAT affinities (K_i < 250 nM) and MPO scores (i.e. 3.6 and 5.1 respectively) however chemically **217** provides a better scaffold for future medicinal chemistry efforts, allowing for further chemical manipulations and development of more analogues, as such **217** was chosen as the lead to proceed with. Computational studies to analyze the binding dynamics of **217** were conducted in collaboration with the Computational Chemistry and Molecular Biophysics Section in NIDA.. Furthermore, a method for the separation of the most active stereoisomer of **217** was developed.

Future studies to assess the pharmacology of **217** remain to be conducted and to confirm the atypical pharmacological profile of **217**. Despite the substantial efforts directed at identifying atypical vs cocaine-like DAT inhibitors *a priori,* to determine atypical pharmacology requires *in vivo* studies to assess the behavioral effects of a drug as well as the extent of extracellular DA release generated by treatment with the drug. For these reasons, it remains necessary to conduct studies in rodent models to assess its viability as a medication for the treatment of PSUD.

7 References

(1) Corma, A.; Navas, J.; Sabater, M. J. Advances in One-Pot Synthesis through Borrowing Hydrogen Catalysis. *Chem. Rev.* **2018**, *118* (4), 1410–1459. https://doi.org/10.1021/acs.chemrev.7b00340.

(2) Podyacheva, E.; Afanasyev, O. I.; Vasilyev, D. V.; Chusov, D. Borrowing Hydrogen Amination Reactions: A Complex Analysis of Trends and Correlations of the Various Reaction Parameters. *ACS Catal.* **2022**, *12* (12), 7142–7198. https://doi.org/10.1021/acscatal.2c01133.

(3) Black, P. J.; Harris, W.; Williams, J. M. J. Catalytic Electronic Activation: Indirect Addition of Nucleophiles to an Allylic Alcohol This Work Was Supported by the University of Bath and Roche Discovery (P.J.B.). *Angew. Chem. Int. Ed.* **2001**, *40* (23), 4475. https://doi.org/10.1002/1521-3773(20011203)40:23%253C4475::AID-ANIE4475%253E3.0.CO;2-P.

(4) Whitney, S.; Grigg, R.; Derrick, A.; Keep, A. $[Cp^*IrCl_2]_2$ -Catalyzed Indirect Functionalization of Alcohols: Novel Strategies for the Synthesis of Substituted Indoles. *Org. Lett.* **2007**, *9* (17), 3299–3302. https://doi.org/10.1021/ol071274v.

(5) Yang, G.; Pan, J.; Ke, Y.; Liu, Y.; Zhao, Y. Tandem Catalytic Indolization/Enantioconvergent Substitution of Alcohols by Borrowing Hydrogen to Access Tricyclic Indoles. *Angew. Chem. Int. Ed.* **2021**, *60* (38), 20689–20694. https://doi.org/10.1002/anie.202106514.

(6) Black, P. J.; Edwards, M. G.; Williams, J. M. J. Borrowing Hydrogen: Indirect “Wittig” Olefination for the Formation of C–C Bonds from Alcohols. *Eur. J. Org. Chem.* **2006**, *2006* (19), 4367–4378. https://doi.org/10.1002/ejoc.200600070.

(7) Edwards, M. G.; Williams, J. M. J. Catalytic Electronic Activation: Indirect “Wittig” Reaction of Alcohols. *Angew. Chem. Int. Ed.* **2002**, *41* (24), 4740–4743. https://doi.org/10.1002/anie.200290034.

(8) Shermer, D. J.; Slatford, P. A.; Edney, D. D.; Williams, J. M. J. Borrowing Hydrogen in an Indirect Asymmetric Wittig Reaction. *Tetrahedron Asymmetry* **2007**, *18* (24), 2845–2848. https://doi.org/10.1016/j.tetasy.2007.11.019.

(9) Reed-Berendt, B. G.; Latham, D. E.; Dambatta, M. B.; Morrill, L. C. Borrowing Hydrogen for Organic Synthesis. *ACS Cent. Sci.* **2021**, *7* (4), 570–585. https://doi.org/10.1021/acscentsci.1c00125.

(10) Anastas, P.; Eghbali, N. Green Chemistry: Principles and Practice. *Chem Soc Rev* **2010**, *39* (1), 301–312. https://doi.org/10.1039/B918763B.

(11) Guerbet, M. *Acad Sci Paris* **1899**, *128*, 1002.

(12) Grigg, R.; Mitchell, T. R. B.; Sutthivaiyakit, S.; Tongpenyai, N. Transition Metal-Catalysed N-Alkylation of Amines by Alcohols. *J. Chem. Soc. Chem. Commun.* **1981**, No. 12, 611. https://doi.org/10.1039/c39810000611.

(13) Murahashi, S.-I.; Kondo, K.; Hakata, T. Ruthenium Catalyzed Synthesis of Secondary or Tertiary Amines from Amines and Alcohols. *Tetrahedron Lett.* **1982**, *23* (2), 229–232. https://doi.org/10.1016/S0040-4039(00)86792-1.

(14) Arcelli, A.; Bui-The-Khai; Porzi, G. Selective Conversion of Primary Amines into N,N-Dimethylalkyl- or N,N-Dialkylmethyl-Amines with Methanol and RuCl2(Ph3P)3. *J. Organomet. Chem.* **1982**, *235* (1), 93–96. https://doi.org/10.1016/S0022-328X(00)85724-1.

(15) Watanabe, Y.; Tsuji, Y.; Ohsugi, Y. The Ruthenium Catalyzed N-Alkylation and N-Heterocyclization of Aniline Using Alcohols and Aldehydes. *Tetrahedron Lett.* **1981**, *22* (28), 2667–2670. https://doi.org/10.1016/S0040-4039(01)92965-X.

(16) Watanabe, Y.; Tsuji, Y.; Ige, H.; Ohsugi, Y.; Ohta, T. Ruthenium-Catalyzed N-Alkylation and N-Benzylation of Aminoarenes with Alcohols. *J. Org. Chem.* **1984**, *49* (18), 3359–3363. https://doi.org/10.1021/jo00192a021.

(17) Tsuji, Y.; Huh, K. T.; Ohsugi, Y.; Watanabe, Y. Ruthenium Complex Catalyzed N-Heterocyclization. Syntheses of N-Substituted Piperidines, Morpholines, and Piperazines from Amines and 1,5-Diols. *J. Org. Chem.* **1985**, *50* (9), 1365–1370. https://doi.org/10.1021/jo00209a004.

(18) Watanabe, Y.; Morisaki, Y.; Kondo, T.; Mitsudo, T. Ruthenium Complex-Controlled Catalytic *N* -Mono- or *N,N* -Dialkylation of Heteroaromatic Amines with Alcohols. *J. Org. Chem.* **1996**, *61* (13), 4214–4218. https://doi.org/10.1021/jo9516289.

(19) Grigg, R.; Mitchell, T. R. B.; Sutthivaiyakit, S.; Tongpenyai, N. Oxidation of Alcohols by Transition Metal Complexes Part V. Selective Catalytic Monoalkylation of Arylacetonitriles by Alcohols. *Tetrahedron Lett.* **1981**, *22* (41), 4107–4110. https://doi.org/10.1016/S0040-4039(01)82078-5.

(20) Edwards, M. G.; Jazzar, R. F. R.; Paine, B. M.; Shermer, D. J.; Whittlesey, M. K.; Williams, J. M. J.; Edney, D. D. Borrowing Hydrogen: A Catalytic Route to C–C Bond

Formation from Alcohols. *Chem Commun* **2004**, No. 1, 90–91. https://doi.org/10.1039/B312162C.

(21) Cho, C. S.; Kim, B. T.; Kim, T.-J.; Shim, S. C. An Unusual Type of Ruthenium-Catalyzed Transfer Hydrogenation of Ketones with Alcohols Accompanied by C−C Coupling. *J. Org. Chem.* **2001**, *66* (26), 9020–9022. https://doi.org/10.1021/jo0108459.

(22) Cho, C. S.; Kim, B. T.; Kim, T.-J.; Chul Shim, S. Ruthenium-Catalyzed Regioselective α-Alkylation of Ketones with Primary Alcohols. *Tetrahedron Lett.* **2002**, *43* (44), 7987–7989. https://doi.org/10.1016/S0040-4039(02)01625-8.

(23) Taguchi, K.; Nakagawa, H.; Hirabayashi, T.; Sakaguchi, S.; Ishii, Y. An Efficient Direct α-Alkylation of Ketones with Primary Alcohols Catalyzed by $[Ir(Cod)Cl]_2$ /PPh_3 /KOH System without Solvent. *J. Am. Chem. Soc.* **2004**, *126* (1), 72–73. https://doi.org/10.1021/ja037552c.

(24) Sakaguchi, S.; Yamaga, T.; Ishii, Y. Iridium-Catalyzed Transfer Hydrogenation of α,β-Unsaturated and Saturated Carbonyl Compounds with 2-Propanol. *J. Org. Chem.* **2001**, *66* (13), 4710–4712. https://doi.org/10.1021/jo0156722.

(25) Martínez, R.; Ramón, D. J.; Yus, M. RuCl2(DMSO)4 Catalyzes the β-Alkylation of Secondary Alcohols with Primary Alcohols through a Hydrogen Autotransfer Process. *Tetrahedron* **2006**, *62* (38), 8982–8987. https://doi.org/10.1016/j.tet.2006.07.012.

(26) Martínez, R.; Brand, G. J.; Ramón, D. J.; Yus, M. [Ru(DMSO)4]Cl2 Catalyzes the α-Alkylation of Ketones by Alcohols. *Tetrahedron Lett.* **2005**, *46* (21), 3683–3686. https://doi.org/10.1016/j.tetlet.2005.03.158.

(27) Martínez, R.; Ramón, D. J.; Yus, M. Easy α-Alkylation of Ketones with Alcohols through a Hydrogen Autotransfer Process Catalyzed by RuCl2(DMSO)4. *Tetrahedron* **2006**, *62* (38), 8988–9001. https://doi.org/10.1016/j.tet.2006.07.013.

(28) Kwon, M. S.; Kim, N.; Seo, S. H.; Park, I. S.; Cheedrala, R. K.; Park, J. Recyclable Palladium Catalyst for Highly Selective Alpha Alkylation of Ketones with Alcohols. *Angew. Chem. Int. Ed Engl.* **2005**, *44* (42), 6913–6915. https://doi.org/10.1002/anie.200502422.

(29) Cho, C. A Palladium-Catalyzed Route for α-Alkylation of Ketones by Primary Alcohols. *J. Mol. Catal. Chem.* **2005**, S1381116905004498. https://doi.org/10.1016/j.molcata.2005.06.043.

(30) Elangovan, S.; Sortais, J.; Beller, M.; Darcel, C. Iron-Catalyzed α-Alkylation of Ketones with Alcohols. *Angew. Chem. Int. Ed.* **2015**, *54* (48), 14483–14486. https://doi.org/10.1002/anie.201506698.

(31) Alonso, F.; Riente, P.; Yus, M. The α-Alkylation of Methyl Ketones with Primary Alcohols Promoted by Nickel Nanoparticles under Mild and Ligandless Conditions. *Synlett* **2007**, *2007* (12), 1877–1880. https://doi.org/10.1055/s-2007-984522.

(32) Alonso, F.; Riente, P.; Yus, M. Alcohols for the α-Alkylation of Methyl Ketones and Indirect Aza-Wittig Reaction Promoted by Nickel Nanoparticles. *Eur. J. Org. Chem.* **2008**, *2008* (29), 4908–4914. https://doi.org/10.1002/ejoc.200800729.

(33) Peña-López, M.; Piehl, P.; Elangovan, S.; Neumann, H.; Beller, M. Manganese-Catalyzed Hydrogen-Autotransfer C−C Bond Formation: α-Alkylation of Ketones with Primary Alcohols. *Angew. Chem. Int. Ed.* **2016**, *55* (48), 14967–14971. https://doi.org/10.1002/anie.201607072.

(34) Zhang, G.; Wu, J.; Zeng, H.; Zhang, S.; Yin, Z.; Zheng, S. Cobalt-Catalyzed α-Alkylation of Ketones with Primary Alcohols. *Org. Lett.* **2017**, *19* (5), 1080–1083. https://doi.org/10.1021/acs.orglett.7b00106.

(35) Ogawa, S.; Obora, Y. Iridium-Catalyzed Selective α-Methylation of Ketones with Methanol. *Chem Commun* **2014**, *50* (19), 2491–2493. https://doi.org/10.1039/C3CC49626K.

(36) Quan, X.; Kerdphon, S.; Andersson, P. G. C□C Coupling of Ketones with Methanol Catalyzed by a N-Heterocyclic Carbene–Phosphine Iridium Complex. *Chem. – Eur. J.* **2015**, *21* (9), 3576–3579. https://doi.org/10.1002/chem.201405990.

(37) Li, F.; Ma, J.; Wang, N. α-Alkylation of Ketones with Primary Alcohols Catalyzed by a Cp*Ir Complex Bearing a Functional Bipyridonate Ligand. *J. Org. Chem.* **2014**, *79* (21), 10447–10455. https://doi.org/10.1021/jo502051d.

(38) Shen, D.; Poole, D. L.; Shotton, C. C.; Kornahrens, A. F.; Healy, M. P.; Donohoe, T. J. Hydrogen-Borrowing and Interrupted-Hydrogen-Borrowing Reactions of Ketones and Methanol Catalyzed by Iridium. *Angew. Chem. Int. Ed.* **2015**, *54* (5), 1642–1645. https://doi.org/10.1002/anie.201410391.

(39) Chan, L. K. M.; Poole, D. L.; Shen, D.; Healy, M. P.; Donohoe, T. J. Rhodium-Catalyzed Ketone Methylation Using Methanol Under Mild Conditions: Formation of α-Branched Products. *Angew. Chem. Int. Ed.* **2014**, *53* (3), 761–765. https://doi.org/10.1002/anie.201307950.

(40) Frost, J. R.; Cheong, C. B.; Akhtar, W. M.; Caputo, D. F. J.; Stevenson, N. G.; Donohoe, T. J. Strategic Application and Transformation of *Ortho* -Disubstituted Phenyl and Cyclopropyl Ketones To Expand the Scope of Hydrogen Borrowing Catalysis. *J. Am. Chem. Soc.* **2015**, *137* (50), 15664–15667. https://doi.org/10.1021/jacs.5b11196.

(41) Armstrong, R. J.; Donohoe, T. J. Pentamethylphenyl (Ph*) Ketones: Unique Building Blocks for Organic Synthesis. *Tetrahedron Lett.* **2021**, *74*, 153151. https://doi.org/10.1016/j.tetlet.2021.153151.

(42) Akhtar, W. M.; Cheong, C. B.; Frost, J. R.; Christensen, K. E.; Stevenson, N. G.; Donohoe, T. J. Hydrogen Borrowing Catalysis with Secondary Alcohols: A New Route for the

Generation of β-Branched Carbonyl Compounds. *J. Am. Chem. Soc.* **2017**, *139* (7), 2577–2580. https://doi.org/10.1021/jacs.6b12840.

(43) Lee, D.-H.; Kwon, K.-H.; Yi, C. S. Dehydrative C–H Alkylation and Alkenylation of Phenols with Alcohols: Expedient Synthesis for Substituted Phenols and Benzofurans. *J. Am. Chem. Soc.* **2012**, *134* (17), 7325–7328. https://doi.org/10.1021/ja302710v.

(44) Anxionnat, B.; Gomez Pardo, D.; Ricci, G.; Cossy, J. First Intramolecular Alkylation of Nitriles with Primary and Secondary Alcohols Catalyzed by Iridium Complexes. *Eur. J. Org. Chem.* **2012**, *2012* (24), 4453–4456. https://doi.org/10.1002/ejoc.201200850.

(45) Peña-López, M.; Neumann, H.; Beller, M. Ruthenium Pincer-Catalyzed Synthesis of Substituted γ-Butyrolactones Using Hydrogen Autotransfer Methodology. *Chem. Commun.* **2015**, *51* (66), 13082–13085. https://doi.org/10.1039/C5CC01708D.

(46) Cheang, D. M. J.; Armstrong, R. J.; Akhtar, W. M.; Donohoe, T. J. Enantioconvergent Alkylation of Ketones with Racemic Secondary Alcohols *via* Hydrogen Borrowing Catalysis. *Chem. Commun.* **2020**, *56* (24), 3543–3546. https://doi.org/10.1039/D0CC00767F.

(47) Waiba, S.; Jana, S. K.; Jati, A.; Jana, A.; Maji, B. Manganese Complex-Catalysed α-Alkylation of Ketones with Secondary Alcohols Enables the Synthesis of β-Branched Carbonyl Compounds. *Chem. Commun.* **2020**, *56* (60), 8376–8379. https://doi.org/10.1039/D0CC01460E.

(48) Bettoni, L.; Gaillard, S.; Renaud, J.-L. Iron-Catalyzed α-Alkylation of Ketones with Secondary Alcohols: Access to β-Disubstituted Carbonyl Compounds. *Org. Lett.* **2020**, *22* (5), 2064–2069. https://doi.org/10.1021/acs.orglett.0c00549.

(49) Chakraborty, P.; Gangwar, M. K.; Emayavaramban, B.; Manoury, E.; Poli, R.; Sundararaju, B. α-Alkylation of Ketones with Secondary Alcohols Catalyzed by Well-Defined

Cp*Co^{III} -Complexes. *ChemSusChem* **2019**, *12* (15), 3463–3467. https://doi.org/10.1002/cssc.201900990.

(50) Akhtar, W. M.; Armstrong, R. J.; Frost, J. R.; Stevenson, N. G.; Donohoe, T. J. Stereoselective Synthesis of Cyclohexanes via an Iridium Catalyzed (5 + 1) Annulation Strategy. *J. Am. Chem. Soc.* **2018**, *140* (38), 11916–11920. https://doi.org/10.1021/jacs.8b07776.

(51) Hollmann, D. Advances in Asymmetric Borrowing Hydrogen Catalysis. *ChemSusChem* **2014**, *7* (9), 2411–2413. https://doi.org/10.1002/cssc.201402320.

(52) Armstrong, R. J.; Akhtar, W. M.; Young, T. A.; Duarte, F.; Donohoe, T. J. Catalytic Asymmetric Synthesis of Cyclohexanes by Hydrogen Borrowing Annulations. *Angew. Chem. Int. Ed.* **2019**, *58* (36), 12558–12562. https://doi.org/10.1002/anie.201907514.

(53) Cheang, D. M. J.; Crompton, J. L.; Amer, M. M.; Battiti, F.; Skjelstad, B. B.; Christensen, K. E.; Barton, P.; Duarte, F.; Donohoe, T. J. Dynamic Kinetic Resolution Allows Control of Remote Stereochemistry in Asymmetric Hydrogen Borrowing Alkylation. *Angew. Chem. Int. Ed.* **2025**, *64* (13), e202424959. https://doi.org/10.1002/anie.202424959.

(54) Smith, L. B.; Armstrong, R. J.; Matheau-Raven, D.; Donohoe, T. J. Chemo- and Regioselective Synthesis of Acyl-Cyclohexenes by a Tandem Acceptorless Dehydrogenation-[1,5]-Hydride Shift Cascade. *J. Am. Chem. Soc.* **2020**, *142* (5), 2514–2523. https://doi.org/10.1021/jacs.9b12296.

(55) Nishimura, T.; Onoue, T.; Ohe, K.; Uemura, S. Palladium(II)-Catalyzed Oxidation of Alcohols to Aldehydes and Ketones by Molecular Oxygen. *J. Org. Chem.* **1999**, *64* (18), 6750–6755. https://doi.org/10.1021/jo9906734.

(56) Iosub, A. V.; Stahl, S. S. Palladium-Catalyzed Aerobic Dehydrogenation of Cyclic Hydrocarbons for the Synthesis of Substituted Aromatics and Other Unsaturated Products. *ACS Catal.* **2016**, *6* (12), 8201–8213. https://doi.org/10.1021/acscatal.6b02406.

(57) Iosub, A. V.; Stahl, S. S. Palladium-Catalyzed Aerobic Oxidative Dehydrogenation of Cyclohexenes to Substituted Arene Derivatives. *J. Am. Chem. Soc.* **2015**, *137* (10), 3454–3457. https://doi.org/10.1021/ja512770u.

(58) Wang, D.; Weinstein, A. B.; White, P. B.; Stahl, S. S. Ligand-Promoted Palladium-Catalyzed Aerobic Oxidation Reactions. *Chem. Rev.* **2018**, *118* (5), 2636–2679. https://doi.org/10.1021/acs.chemrev.7b00334.

(59) Kandukuri, S. R.; Oestreich, M. Aerobic Palladium(II)-Catalyzed Dehydrogenation of Cyclohexene-1-Carbonyl Indole Amides: An Indole-Directed Aromatization. *J. Org. Chem.* **2012**, *77* (19), 8750–8755. https://doi.org/10.1021/jo301088f.

(60) Shang, Y.; Jie, X.; Jonnada, K.; Zafar, S. N.; Su, W. Dehydrogenative Desaturation-Relay via Formation of Multicenter-Stabilized Radical Intermediates. *Nat. Commun.* **2017**, *8* (1), 2273. https://doi.org/10.1038/s41467-017-02381-8.

(61) Jie, X.; Shang, Y.; Zhang, X.; Su, W. Cu-Catalyzed Sequential Dehydrogenation–Conjugate Addition for β-Functionalization of Saturated Ketones: Scope and Mechanism. *J. Am. Chem. Soc.* **2016**, *138* (17), 5623–5633. https://doi.org/10.1021/jacs.6b01337.

(62) Bowry, V. W.; Ingold, K. U. Kinetics of Nitroxide Radical Trapping. 2. Structural Effects. *J. Am. Chem. Soc.* **1992**, *114* (13), 4992–4996. https://doi.org/10.1021/ja00039a006.

(63) Da Silva, G.; Bozzelli, J. W. Benzoxyl Radical Decomposition Kinetics: Formation of Benzaldehyde + H, Phenyl + CH_2O, and Benzene + HCO. *J. Phys. Chem. A* **2009**, *113* (25), 6979–6986. https://doi.org/10.1021/jp902458d.

(64) Kotha, S.; Brahmachary, E.; Lahiri, K. Transition Metal Catalyzed [2+2+2] Cycloaddition and Application in Organic Synthesis. *Eur. J. Org. Chem*. **2005**, *2005* (22), 4741–4767. https://doi.org/10.1002/ejoc.200500411.

(65) Hoye, T. R.; Baire, B.; Niu, D.; Willoughby, P. H.; Woods, B. P. The Hexadehydro-Diels–Alder Reaction. *Nature* **2012**, *490* (7419), 208–212. https://doi.org/10.1038/nature11518.

(66) Cheang, D. M. J. Controlling Absolute Stereochemistry in Hydrogen Borrowing Catalyzed Alkylation, University of Oxford, Oxford, 2023.

(67) Armstrong, R. J.; Akhtar, W. M.; Frost, J. R.; Christensen, K. E.; Stevenson, N. G.; Donohoe, T. J. Stereoselective Synthesis of Alicyclic Ketones: A Hydrogen Borrowing Approach. *Tetrahedron* **2019**, *75* (48), 130680. https://doi.org/10.1016/j.tet.2019.130680.

(68) Mohr, J. T.; Hong, A. Y.; Stoltz, B. M. Enantioselective Protonation. *Nat. Chem.* **2009**, *1* (5), 359–369. https://doi.org/10.1038/nchem.297.

(69) Blackwell, J. M.; Morrison, D. J.; Piers, W. E. B(C 6 F 5) 3 Catalyzed Hydrosilation of Enones and Silyl Enol Ethers. *Tetrahedron* **2002**, *58* (41), 8247–8254. https://doi.org/10.1016/S0040-4020(02)00974-2.

(70) Poisson, T.; Oudeyer, S.; Dalla, V.; Marsais, F.; Levacher, V. Straightforward OrganocatalyticEnantioselective Protonation of Silyl Enolates by Meansof Cinchona Alkaloids and Carboxylic Acids. *Synlett* **2008**, *2008* (16), 2447–2450. https://doi.org/10.1055/s-2008-1078260.

(71) Yanagisawa, A.; Touge, T.; Arai, T. Enantioselective Protonation of Silyl Enolates Catalyzed by a Binap·AgF Complex. *Angew. Chem. Int. Ed.* **2005**, *44* (10), 1546–1548. https://doi.org/10.1002/anie.200462325.

(72) Orr, R. K.; Calter, M. A. Asymmetric Synthesis Using Ketenes. *Tetrahedron* **2003**, *59* (20), 3545–3565. https://doi.org/10.1016/S0040-4020(03)00491-5.

(73) Björklund, A.; Dunnett, S. B. Fifty Years of Dopamine Research. *Trends Neurosci.* **2007**, *30* (5), 185–187. https://doi.org/10.1016/j.tins.2007.03.004.

(74) Yeragani, V.; Tancer, M.; Chokka, P.; Baker, G. Arvid Carlsson, and the Story of Dopamine. *Indian J. Psychiatry* **2010**, *52* (1), 87. https://doi.org/10.4103/0019-5545.58907.

(75) Carlsson, A.; Lindqvist, M.; Magnusson, T. 3,4-Dihydroxyphenylalanine and 5-Hydroxytryptophan as Reserpine Antagonists. *Nature* **1957**, *180* (4596), 1200–1200. https://doi.org/10.1038/1801200a0.

(76) Montagu, K. A. Catechol Compounds in Rat Tissues and in Brains of Different Animals. *Nature* **1957**, *180* (4579), 244–245. https://doi.org/10.1038/180244a0.

(77) Carlsson, A.; Lindqvist, M.; Magnusson, T.; Waldeck, B. On the Presence of 3-Hydroxytyramine in Brain. *Science* **1958**, *127* (3296), 471. https://doi.org/10.1126/science.127.3296.471.

(78) Ehringer, H.; Hornykiewicz, O. Verteilung Von Noradrenalin Und Dopamin (3-Hydroxytyramin) Im Gehirn Des Menschen Und Ihr Verhalten Bei Erkrankungen Des Extrapyramidalen Systems. *Klin. Wochenschr.* **1960**, *38* (24), 1236–1239. https://doi.org/10.1007/BF01485901.

(79) Iversen, S. D.; Iversen, L. L. Dopamine: 50 Years in Perspective. *Trends Neurosci.* **2007**, *30* (5), 188–193. https://doi.org/10.1016/j.tins.2007.03.002.

(80) Roberts, D. C.; Corcoran, M. E.; Fibiger, H. C. On the Role of Ascending Catecholaminergic Systems in Intravenous Self-Administration of Cocaine. *Pharmacol. Biochem. Behav.* **1977**, *6* (6), 615–620. https://doi.org/10.1016/0091-3057(77)90084-3.

(81) Di Chiara, G.; Imperato, A. Drugs Abused by Humans Preferentially Increase Synaptic Dopamine Concentrations in the Mesolimbic System of Freely Moving Rats. *Proc. Natl. Acad. Sci. U. S. A.* **1988**, *85* (14), 5274–5278. https://doi.org/10.1073/pnas.85.14.5274.

(82) Goeders, N. E.; Smith, J. E. Cortical Dopaminergic Involvement in Cocaine Reinforcement. *Science* **1983**, *221* (4612), 773–775. https://doi.org/10.1126/science.6879176.

(83) Heikkila, R. E.; Orlansky, H.; Mytilineou, C.; Cohen, G. Amphetamine: Evaluation of d- and l-Isomers as Releasing Agents and Uptake Inhibitors for 3H-Dopamine and 3H-Norepinephrine in Slices of Rat Neostriatum and Cerebral Cortex. *J. Pharmacol. Exp. Ther.* **1975**, *194* (1), 47–56.

(84) Roberts, D. C. S.; Koob, G. F. Disruption of Cocaine Self-Administration Following 6-Hydroxydopamine Lesions of the Ventral Tegmental Area in Rats. *Pharmacol. Biochem. Behav.* **1982**, *17* (5), 901–904. https://doi.org/10.1016/0091-3057(82)90469-5.

(85) Wise, R. A.; Bozarth, M. A. A Psychomotor Stimulant Theory of Addiction. *Psychol. Rev.* **1987**, *94* (4), 469–492. https://doi.org/10.1037/0033-295X.94.4.469.

(86) Koob, G. F.; Bloom, F. E. Cellular and Molecular Mechanisms of Drug Dependence. *Science* **1988**, *242* (4879), 715–723. https://doi.org/10.1126/science.2903550.

(87) Wyss, J. M.; Van Groen, T.; Canning, K. J. The Limbic System. In *Neuroscience in Medicine*; Conn, P. M., Ed.; Humana Press: Totowa, NJ, 2003; pp 369–387. https://doi.org/10.1007/978-1-59259-371-2_17.

(88) Volkow, N. D. Is Methylphenidate Like Cocaine?: Studies on Their Pharmacokinetics and Distribution in the Human Brain. *Arch. Gen. Psychiatry* **1995**, *52* (6), 456. https://doi.org/10.1001/archpsyc.1995.03950180042006.

(89) Fowler, J. S.; Volkow, N. D.; Wolf, A. P.; Dewey, S. L.; Schlyer, D. J.; Macgregor, R. R.; Hitzemann, R.; Logan, J.; Bendriem, B.; Gatley, S. J. Mapping Cocaine Binding Sites in Human and Baboon Brain in Vivo. *Synap. N. Y. N* **1989**, *4* (4), 371–377. https://doi.org/10.1002/syn.890040412.

(90) Volkow, N. D.; Wang, G.-J.; Fowler, J. S.; Logan, J.; Gatley, S. J.; Wong, C.; Hitzemann, R.; Pappas, N. R. Reinforcing Effects of Psychostimulants in Humans Are Associated with Increases in Brain Dopamine and Occupancy of D2Receptors. *J. Pharmacol. Exp. Ther.* **1999**, *291* (1), 409–415. https://doi.org/10.1016/S0022-3565(24)35115-8.

(91) Volkow, N. D.; Fowler, J. S.; Wang, G.-J.; Swanson, J. M. Dopamine in Drug Abuse and Addiction: Results from Imaging Studies and Treatment Implications. *Mol. Psychiatry* **2004**, *9* (6), 557–569. https://doi.org/10.1038/sj.mp.4001507.

(92) Drevets, W. C.; Gautier, C.; Price, J. C.; Kupfer, D. J.; Kinahan, P. E.; Grace, A. A.; Price, J. L.; Mathis, C. A. Amphetamine-Induced Dopamine Release in Human Ventral Striatum Correlates with Euphoria. *Biol. Psychiatry* **2001**, *49* (2), 81–96. https://doi.org/10.1016/s0006-3223(00)01038-6.

(93) Oswald, L. M.; Wong, D. F.; McCaul, M.; Zhou, Y.; Kuwabara, H.; Choi, L.; Brasic, J.; Wand, G. S. Relationships among Ventral Striatal Dopamine Release, Cortisol Secretion, and Subjective Responses to Amphetamine. *Neuropsychopharmacol. Off. Publ. Am. Coll. Neuropsychopharmacol.* **2005**, *30* (4), 821–832. https://doi.org/10.1038/sj.npp.1300667.

(94) Brody, A. L.; Olmstead, R. E.; London, E. D.; Farahi, J.; Meyer, J. H.; Grossman, P.; Lee, G. S.; Huang, J.; Hahn, E. L.; Mandelkern, M. A. Smoking-Induced Ventral Striatum Dopamine Release. *Am. J. Psychiatry* **2004**, *161* (7), 1211–1218. https://doi.org/10.1176/appi.ajp.161.7.1211.

(95) Boileau, I.; Assaad, J.-M.; Pihl, R. O.; Benkelfat, C.; Leyton, M.; Diksic, M.; Tremblay, R. E.; Dagher, A. Alcohol Promotes Dopamine Release in the Human Nucleus Accumbens. *Synap. N. Y. N* **2003**, *49* (4), 226–231. https://doi.org/10.1002/syn.10226.

(96) Vollenweider, F. X.; Vontobel, P.; Oye, I.; Hell, D.; Leenders, K. L. Effects of (S)-Ketamine on Striatal Dopamine: A [11C]Raclopride PET Study of a Model Psychosis in Humans. *J. Psychiatr. Res.* **2000**, *34* (1), 35–43. https://doi.org/10.1016/s0022-3956(99)00031-x.

(97) Bossong, M. G.; van Berckel, B. N. M.; Boellaard, R.; Zuurman, L.; Schuit, R. C.; Windhorst, A. D.; van Gerven, J. M. A.; Ramsey, N. F.; Lammertsma, A. A.; Kahn, R. S. Delta 9-Tetrahydrocannabinol Induces Dopamine Release in the Human Striatum. *Neuropsychopharmacol. Off. Publ. Am. Coll. Neuropsychopharmacol.* **2009**, *34* (3), 759–766. https://doi.org/10.1038/npp.2008.138.

(98) Kenny, P. J. Common Cellular and Molecular Mechanisms in Obesity and Drug Addiction. *Nat. Rev. Neurosci.* **2011**, *12* (11), 638–651. https://doi.org/10.1038/nrn3105.

(99) Martinez, D.; Greene, K.; Broft, A.; Kumar, D.; Liu, F.; Narendran, R.; Slifstein, M.; Van Heertum, R.; Kleber, H. D. Lower Level of Endogenous Dopamine in Patients with Cocaine Dependence: Findings from PET Imaging of D(2)/D(3) Receptors Following Acute Dopamine Depletion. *Am. J. Psychiatry* **2009**, *166* (10), 1170–1177. https://doi.org/10.1176/appi.ajp.2009.08121801.

(100) Volkow, N. D.; Wang, G.-J.; Ma, Y.; Fowler, J. S.; Wong, C.; Ding, Y.-S.; Hitzemann, R.; Swanson, J. M.; Kalivas, P. Activation of Orbital and Medial Prefrontal Cortex by Methylphenidate in Cocaine-Addicted Subjects but Not in Controls: Relevance to Addiction. *J. Neurosci. Off. J. Soc. Neurosci.* **2005**, *25* (15), 3932–3939. https://doi.org/10.1523/JNEUROSCI.0433-05.2005.

(101) Volkow, N. D.; Fowler, J. S.; Wang, G. J.; Hitzemann, R.; Logan, J.; Schlyer, D. J.; Dewey, S. L.; Wolf, A. P. Decreased Dopamine D2 Receptor Availability Is Associated with Reduced Frontal Metabolism in Cocaine Abusers. *Synap. N. Y. N* **1993**, *14* (2), 169–177. https://doi.org/10.1002/syn.890140210.

(102) Volkow, N. D.; Wang, G.-J.; Maynard, L.; Fowler, J. S.; Jayne, B.; Telang, F.; Logan, J.; Ding, Y.-S.; Gatley, S. J.; Hitzemann, R.; Wong, C.; Pappas, N. Effects of Alcohol Detoxification on Dopamine D2 Receptors in Alcoholics: A Preliminary Study. *Psychiatry Res.* **2002**, *116* (3), 163–172. https://doi.org/10.1016/s0925-4927(02)00087-2.

(103) Volkow, N. D.; Wang, G. J.; Fowler, J. S.; Logan, J.; Hitzemann, R.; Ding, Y. S.; Pappas, N.; Shea, C.; Piscani, K. Decreases in Dopamine Receptors but Not in Dopamine Transporters in Alcoholics. *Alcohol. Clin. Exp. Res.* **1996**, *20* (9), 1594–1598. https://doi.org/10.1111/j.1530-0277.1996.tb05936.x.

(104) Martinez, D.; Gil, R.; Slifstein, M.; Hwang, D.-R.; Huang, Y.; Perez, A.; Kegeles, L.; Talbot, P.; Evans, S.; Krystal, J.; Laruelle, M.; Abi-Dargham, A. Alcohol Dependence Is Associated with Blunted Dopamine Transmission in the Ventral Striatum. *Biol. Psychiatry* **2005**, *58* (10), 779–786. https://doi.org/10.1016/j.biopsych.2005.04.044.

(105) Wang, G. J.; Volkow, N. D.; Fowler, J. S.; Logan, J.; Abumrad, N. N.; Hitzemann, R. J.; Pappas, N. S.; Pascani, K. Dopamine D2 Receptor Availability in Opiate-Dependent Subjects before and after Naloxone-Precipitated Withdrawal. *Neuropsychopharmacol. Off. Publ. Am. Coll. Neuropsychopharmacol.* **1997**, *16* (2), 174–182. https://doi.org/10.1016/S0893-133X(96)00184-4.

(106) Martinez, D.; Saccone, P. A.; Liu, F.; Slifstein, M.; Orlowska, D.; Grassetti, A.; Cook, S.; Broft, A.; Van Heertum, R.; Comer, S. D. Deficits in Dopamine D(2) Receptors and Presynaptic

Dopamine in Heroin Dependence: Commonalities and Differences with Other Types of Addiction. *Biol. Psychiatry* **2012**, *71* (3), 192–198. https://doi.org/10.1016/j.biopsych.2011.08.024.

(107) Volkow, N. D.; Wang, G. J.; Fowler, J. S.; Logan, J.; Gatley, S. J.; Hitzemann, R.; Chen, A. D.; Dewey, S. L.; Pappas, N. Decreased Striatal Dopaminergic Responsiveness in Detoxified Cocaine-Dependent Subjects. *Nature* **1997**, *386* (6627), 830–833. https://doi.org/10.1038/386830a0.

(108) Sulzer, D. How Addictive Drugs Disrupt Presynaptic Dopamine Neurotransmission. *Neuron* **2011**, *69* (4), 628–649. https://doi.org/10.1016/j.neuron.2011.02.010.

(109) Kanner, B. I.; Schuldiner, S. Mechanism of Transport and Storage of Neurotransmitters. *CRC Crit. Rev. Biochem.* **1987**, *22* (1), 1–38. https://doi.org/10.3109/10409238709082546.

(110) Floresco, S. B.; West, A. R.; Ash, B.; Moore, H.; Grace, A. A. Afferent Modulation of Dopamine Neuron Firing Differentially Regulates Tonic and Phasic Dopamine Transmission. *Nat. Neurosci.* **2003**, *6* (9), 968–973. https://doi.org/10.1038/nn1103.

(111) Cenci, M. A. Presynaptic Mechanisms of L-DOPA-Induced Dyskinesia: The Findings, the Debate, and the Therapeutic Implications. *Front. Neurol.* **2014**, *5*, 242. https://doi.org/10.3389/fneur.2014.00242.

(112) Miller, G. W.; Gainetdinov, R. R.; Levey, A. I.; Caron, M. G. Dopamine Transporters and Neuronal Injury. *Trends Pharmacol. Sci.* **1999**, *20* (10), 424–429. https://doi.org/10.1016/S0165-6147(99)01379-6.

(113) Yamashita, A.; Singh, S. K.; Kawate, T.; Jin, Y.; Gouaux, E. Crystal Structure of a Bacterial Homologue of Na+/Cl--Dependent Neurotransmitter Transporters. *Nature* **2005**, *437* (7056), 215–223. https://doi.org/10.1038/nature03978.

(114) Pramod, A. B.; Foster, J.; Carvelli, L.; Henry, L. K. SLC6 Transporters: Structure, Function, Regulation, Disease Association and Therapeutics. *Mol. Aspects Med.* **2013**, *34* (2–3), 197–219. https://doi.org/10.1016/j.mam.2012.07.002.

(115) Dehnes, Y.; Shan, J.; Beuming, T.; Shi, L.; Weinstein, H.; Javitch, J. A. Conformational Changes in Dopamine Transporter Intracellular Regions upon Cocaine Binding and Dopamine Translocation. *Neurochem. Int.* **2014**, *73*, 4–15. https://doi.org/10.1016/j.neuint.2014.02.003.

(116) Volkow, N. D.; Wang, G.-J.; Fischman, M. W.; Foltin, R. W.; Fowler, J. S.; Abumrad, N. N.; Vitkun, S.; Logan, J.; Gatley, S. J.; Pappas, N.; Hitzemann, R.; Shea, C. E. Relationship between Subjective Effects of Cocaine and Dopamine Transporter Occupancy. *Nature* **1997**, *386* (6627), 827–830. https://doi.org/10.1038/386827a0.

(117) Li, Y.; Wang, X.; Meng, Y.; Hu, T.; Zhao, J.; Li, R.; Bai, Q.; Yuan, P.; Han, J.; Hao, K.; Wei, Y.; Qiu, Y.; Li, N.; Zhao, Y. Dopamine Reuptake and Inhibitory Mechanisms in Human Dopamine Transporter. *Nature* **2024**, *632* (8025), 686–694. https://doi.org/10.1038/s41586-024-07796-0.

(118) Giros, B.; Jaber, M.; Jones, S. R.; Wightman, R. M.; Caron, M. G. Hyperlocomotion and Indifference to Cocaine and Amphetamine in Mice Lacking the Dopamine Transporter. *Nature* **1996**, *379* (6566), 606–612. https://doi.org/10.1038/379606a0.

(119) Nichols, D. E. Chemistry and Structure-Activity Relationships of Psychedelics. *Curr. Top. Behav. Neurosci.* **2018**, *36*, 1–43. https://doi.org/10.1007/7854_2017_475.

(120) Pifl, C.; Drobny, H.; Reither, H.; Hornykiewicz, O.; Singer, E. A. Mechanism of the Dopamine-Releasing Actions of Amphetamine and Cocaine: Plasmalemmal Dopamine Transporter versus Vesicular Monoamine Transporter. *Mol. Pharmacol.* **1995**, *47* (2), 368–373. https://doi.org/10.1016/S0026-895X(25)08549-9.

(121) Miller, H. H.; Shore, P. A.; Clarke, D. E. In Vivo Monoamine Oxidase Inhibition by D-Amphetamine. *Biochem. Pharmacol.* **1980**, *29* (10), 1347–1354. https://doi.org/10.1016/0006-2952(80)90429-3.

(122) Robertson, S. D.; Matthies, H. J. G.; Galli, A. A Closer Look at Amphetamine-Induced Reverse Transport and Trafficking of the Dopamine and Norepinephrine Transporters. *Mol. Neurobiol.* **2009**, *39* (2), 73–80. https://doi.org/10.1007/s12035-009-8053-4.

(123) Khoshbouei, H.; Wang, H.; Lechleiter, J. D.; Javitch, J. A.; Galli, A. Amphetamine-Induced Dopamine Efflux. *J. Biol. Chem.* **2003**, *278* (14), 12070–12077. https://doi.org/10.1074/jbc.M212815200.

(124) Kahlig, K. M.; Galli, A. Regulation of Dopamine Transporter Function and Plasma Membrane Expression by Dopamine, Amphetamine, and Cocaine. *Eur. J. Pharmacol.* **2003**, *479* (1–3), 153–158. https://doi.org/10.1016/j.ejphar.2003.08.065.

(125) Saunders, C.; Ferrer, J. V.; Shi, L.; Chen, J.; Merrill, G.; Lamb, M. E.; Leeb-Lundberg, L. M. F.; Carvelli, L.; Javitch, J. A.; Galli, A. Amphetamine-Induced Loss of Human Dopamine Transporter Activity: An Internalization-Dependent and Cocaine-Sensitive Mechanism. *Proc. Natl. Acad. Sci.* **2000**, *97* (12), 6850–6855. https://doi.org/10.1073/pnas.110035297.

(126) Cheng, M. H.; Block, E.; Hu, F.; Cobanoglu, M. C.; Sorkin, A.; Bahar, I. Insights into the Modulation of Dopamine Transporter Function by Amphetamine, Orphenadrine, and Cocaine Binding. *Front. Neurol.* **2015**, *6*, 134. https://doi.org/10.3389/fneur.2015.00134.

(127) Beuming, T.; Kniazeff, J.; Bergmann, M. L.; Shi, L.; Gracia, L.; Raniszewska, K.; Newman, A. H.; Javitch, J. A.; Weinstein, H.; Gether, U.; Loland, C. J. The Binding Sites for Cocaine and Dopamine in the Dopamine Transporter Overlap. *Nat. Neurosci.* **2008**, *11* (7), 780–789. https://doi.org/10.1038/nn.2146.

(128) Chen, N.; Justice, J. B. Cocaine Acts as an Apparent Competitive Inhibitor at the Outward-Facing Conformation of the Human Norepinephrine Transporter: Kinetic Analysis of Inward and Outward Transport. *J. Neurosci.* **1998**, *18* (24), 10257–10268. https://doi.org/10.1523/JNEUROSCI.18-24-10257.1998.

(129) Chen, N.; Vaughan, R. A.; Reith, M. E. A. The Role of Conserved Tryptophan and Acidic Residues in the Human Dopamine Transporter as Characterized by Site-directed Mutagenesis. *J. Neurochem.* **2001**, *77* (4), 1116–1127. https://doi.org/10.1046/j.1471-4159.2001.00312.x.

(130) Newman, A. H.; Allen, A. C.; Izenwasser, S.; Katz, J. L. Novel 3.Alpha.-(Diphenylmethoxy)Tropane Analogs: Potent Dopamine Uptake Inhibitors without Cocaine-like Behavioral Profiles. *J. Med. Chem.* **1994**, *37* (15), 2258–2261. https://doi.org/10.1021/jm00041a002.

(131) VAN DER ZEE, P.; KOGER, H.; GOOTJES, J.; HESPE, W. ARYL 1,4-DIALK(EN)YLPIPERAZINES AS SELECTIVE AND VERY POTENT INHIBITORS OF DOPAMINE UPTAKE. *Eur. J Med. CHEM* **1980**, *15* (4), 363–370.

(132) Newman, A. H.; Kline, R. H.; Allen, A. C.; Izenwasser, S.; George, C.; Katz, J. L. Novel 4'-Substituted and 4',4''-Disubstituted 3.Alpha.-(Diphenylmethoxy)Tropane Analogs as Potent and Selective Dopamine Uptake Inhibitors. *J. Med. Chem.* **1995**, *38* (20), 3933–3940. https://doi.org/10.1021/jm00020a006.

(133) Agoston, G. E.; Wu, J. H.; Izenwasser, S.; George, C.; Katz, J.; Kline, R. H.; Newman, A. H. Novel N-Substituted 3α-[Bis(4'-Fluorophenyl)Methoxy]Tropane Analogues: Selective Ligands for the Dopamine Transporter. *J. Med. Chem.* **1997**, *40* (26), 4329–4339. https://doi.org/10.1021/jm970525a.

(134) Guglietta, A. *Drug Treatment of Sleep Disorders*; Milestones in Drug Therapy; Springer International Publishing Imprint: Springer: Cham s.l, 2015. https://doi.org/10.1007/978-3-319-11514-6.

(135) Mignot, E.; Nishino, S.; Guilleminault, C.; Dement, W. C. Modafinil Binds to the Dopamine Uptake Carrier Site with Low Affinity. *Sleep* **1994**, *17* (5), 436–437. https://doi.org/10.1093/sleep/17.5.436.

(136) Zolkowska, D.; Jain, R.; Rothman, R. B.; Partilla, J. S.; Roth, B. L.; Setola, V.; Prisinzano, T. E.; Baumann, M. H. Evidence for the Involvement of Dopamine Transporters in Behavioral Stimulant Effects of Modafinil. *J. Pharmacol. Exp. Ther.* **2009**, *329* (2), 738–746. https://doi.org/10.1124/jpet.108.146142.

(137) Dackis, C. A.; Lynch, K. G.; Yu, E.; Samaha, F. F.; Kampman, K. M.; Cornish, J. W.; Rowan, A.; Poole, S.; White, L.; O'Brien, C. P. Modafinil and Cocaine: A Double-Blind, Placebo-Controlled Drug Interaction Study. *Drug Alcohol Depend.* **2003**, *70* (1), 29–37. https://doi.org/10.1016/s0376-8716(02)00335-6.

(138) Malcolm, R.; Book, S. W.; Moak, D.; DeVane, L.; Czepowicz, V. Clinical Applications of Modafinil in Stimulant Abusers: Low Abuse Potential. *Am. J. Addict.* **2002**, *11* (3), 247–249. https://doi.org/10.1080/10550490290088027.

(139) Rothman, R. B.; Baumann, M. H.; Prisinzano, T. E.; Newman, A. H. Dopamine Transport Inhibitors Based on GBR12909 and Benztropine as Potential Medications to Treat Cocaine Addiction. *Biochem. Pharmacol.* **2008**, *75* (1), 2–16. https://doi.org/10.1016/j.bcp.2007.08.007.

(140) Schmitt, K. C.; Rothman, R. B.; Reith, M. E. A. Nonclassical Pharmacology of the Dopamine Transporter: Atypical Inhibitors, Allosteric Modulators, and Partial Substrates. *J. Pharmacol. Exp. Ther.* **2013**, *346* (1), 2–10. https://doi.org/10.1124/jpet.111.191056.

(141) Loland, C. J.; Desai, R. I.; Zou, M.-F.; Cao, J.; Grundt, P.; Gerstbrein, K.; Sitte, H. H.; Newman, A. H.; Katz, J. L.; Gether, U. Relationship between Conformational Changes in the Dopamine Transporter and Cocaine-like Subjective Effects of Uptake Inhibitors. *Mol. Pharmacol.* **2008**, *73* (3), 813–823. https://doi.org/10.1124/mol.107.039800.

(142) Schmitt, K. C.; Reith, M. E. A. The Atypical Stimulant and Nootropic Modafinil Interacts with the Dopamine Transporter in a Different Manner than Classical Cocaine-Like Inhibitors. *PLoS ONE* **2011**, *6* (10), e25790. https://doi.org/10.1371/journal.pone.0025790.

(143) Niello, M.; Sideromenos, S.; Gradisch, R.; O´Shea, R.; Schwazer, J.; Maier, J.; Kastner, N.; Sandtner, W.; Jäntsch, K.; Lupica, C. R.; Hoffman, A. F.; Lubec, G.; Loland, C. J.; Stockner, T.; Pollak, D. D.; Baumann, M. H.; Sitte, H. H. Persistent Binding at Dopamine Transporters Determines Sustained Psychostimulant Effects. *Proc. Natl. Acad. Sci.* **2023**, *120* (6), e2114204120. https://doi.org/10.1073/pnas.2114204120.

(144) Desai, R. I.; Kopajtic, T. A.; Koffarnus, M.; Newman, A. H.; Katz, J. L. Identification of a Dopamine Transporter Ligand That Blocks the Stimulant Effects of Cocaine. *J. Neurosci.* **2005**, *25* (8), 1889–1893. https://doi.org/10.1523/JNEUROSCI.4778-04.2005.

(145) Hiranita, T.; Soto, P. L.; Newman, A. H.; Katz, J. L. Assessment of Reinforcing Effects of Benztropine Analogs and Their Effects on Cocaine Self-Administration in Rats: Comparisons with Monoamine Uptake Inhibitors. *J. Pharmacol. Exp. Ther.* **2009**, *329* (2), 677–686. https://doi.org/10.1124/jpet.108.145813.

(146) Desai, R. I.; Kopajtic, T. A.; French, D.; Newman, A. H.; Katz, J. L. Relationship between in Vivo Occupancy at the Dopamine Transporter and Behavioral Effects of Cocaine, GBR 12909 [1-{2-[Bis-(4-Fluorophenyl)Methoxy]Ethyl}-4-(3-Phenylpropyl)Piperazine], and Benztropine Analogs. *J. Pharmacol. Exp. Ther.* **2005**, *315* (1), 397–404. https://doi.org/10.1124/jpet.105.091231.

(147) Volkow, N. D.; Fowler, J. S.; Wang, G.-J. Role of Dopamine in Drug Reinforcement and Addiction in Humans: Results from Imaging Studies. *Behav. Pharmacol.* **2002**, *13* (5–6), 355–366. https://doi.org/10.1097/00008877-200209000-00008.

(148) Sangroula, D.; Motiwala, F.; Wagle, B.; Shah, V. C.; Hagi, K.; Lippmann, S. Modafinil Treatment of Cocaine Dependence: A Systematic Review and Meta-Analysis. *Subst. Use Misuse* **2017**, *52* (10), 1292–1306. https://doi.org/10.1080/10826084.2016.1276597.

(149) Rush, C. R.; Kelly, T. H.; Hays, L. R.; Wooten, A. F. Discriminative-Stimulus Effects of Modafinil in Cocaine-Trained Humans. *Drug Alcohol Depend.* **2002**, *67* (3), 311–322. https://doi.org/10.1016/s0376-8716(02)00082-0.

(150) Stoops, W. W.; Lile, J. A.; Fillmore, M. T.; Glaser, P. E. A.; Rush, C. R. Reinforcing Effects of Modafinil: Influence of Dose and Behavioral Demands Following Drug Administration. *Psychopharmacology (Berl.)* **2005**, *182* (1), 186–193. https://doi.org/10.1007/s00213-005-0044-1.

(151) Myrick, H.; Malcolm, R.; Taylor, B.; LaRowe, S. Modafinil: Preclinical, Clinical, and Post-Marketing Surveillance--a Review of Abuse Liability Issues. *Ann. Clin. Psychiatry Off. J. Am. Acad. Clin. Psychiatr.* **2004**, *16* (2), 101–109. https://doi.org/10.1080/10401230490453743.

(152) Dackis, C. A.; Kampman, K. M.; Lynch, K. G.; Pettinati, H. M.; O'Brien, C. P. A Double-Blind, Placebo-Controlled Trial of Modafinil for Cocaine Dependence. *Neuropsychopharmacology* **2005**, *30* (1), 205–211. https://doi.org/10.1038/sj.npp.1300600.

(153) Anderson, A. L.; Reid, M. S.; Li, S.-H.; Holmes, T.; Shemanski, L.; Slee, A.; Smith, E. V.; Kahn, R.; Chiang, N.; Vocci, F.; Ciraulo, D.; Dackis, C.; Roache, J. D.; Salloum, I. M.; Somoza, E.; Urschel, H. C.; Elkashef, A. M. Modafinil for the Treatment of Cocaine Dependence. *Drug Alcohol Depend.* **2009**, *104* (1–2), 133–139. https://doi.org/10.1016/j.drugalcdep.2009.04.015.

(154) Shearer, J.; Darke, S.; Rodgers, C.; Slade, T.; van Beek, I.; Lewis, J.; Brady, D.; McKetin, R.; Mattick, R. P.; Wodak, A. A Double-Blind, Placebo-Controlled Trial of Modafinil (200 Mg/Day) for Methamphetamine Dependence. *Addict. Abingdon Engl.* **2009**, *104* (2), 224–233. https://doi.org/10.1111/j.1360-0443.2008.02437.x.

(155) Zhang, H.-Y.; Bi, G.-H.; Yang, H.-J.; He, Y.; Xue, G.; Cao, J.; Tanda, G.; Gardner, E. L.; Newman, A. H.; Xi, Z.-X. The Novel Modafinil Analog, JJC8-016, as a Potential Cocaine Abuse Pharmacotherapeutic. *Neuropsychopharmacology* **2017**, *42* (9), 1871–1883. https://doi.org/10.1038/npp.2017.41.

(156) Jung, J.-C.; Lee, Y.; Son, J.-Y.; Lim, E.; Jung, M.; Oh, S. Simple Synthesis of Modafinil Derivatives and Their Anti-Inflammatory Activity. *Mol. Basel Switz.* **2012**, *17* (9), 10446–10458. https://doi.org/10.3390/molecules170910446.

(157) De Risi, C.; Ferraro, L.; Pollini, G. P.; Tanganelli, S.; Valente, F.; Veronese, A. C. Efficient Synthesis and Biological Evaluation of Two Modafinil Analogues. *Bioorg. Med. Chem.* **2008**, *16* (23), 9904–9910. https://doi.org/10.1016/j.bmc.2008.10.027.

(158) Zhang, J.; Zhang, P.; Liu, X.; Fang, K.; Lin, G. Synthesis and Biological Evaluation of (R)-N-(Diarylmethylthio/Sulfinyl)Ethyl/Propyl-Piperidine-3-Carboxylic Acid Hydrochlorides as Novel GABA Uptake Inhibitors. *Bioorg. Med. Chem. Lett.* **2007**, *17* (13), 3769–3773. https://doi.org/10.1016/j.bmcl.2007.04.010.

(159) Cao, J.; Prisinzano, T. E.; Okunola, O. M.; Kopajtic, T.; Shook, M.; Katz, J. L.; Newman, A. H. Structure-Activity Relationships at the Monoamine Transporters for a Novel Series of Modafinil (2-[(Diphenylmethyl)Sulfinyl]Acetamide) Analogues. *ACS Med. Chem. Lett.* **2010**, *2* (1), 48–52. https://doi.org/10.1021/ml1002025.

(160) Okunola-Bakare, O. M.; Cao, J.; Kopajtic, T.; Katz, J. L.; Loland, C. J.; Shi, L.; Newman, A. H. Elucidation of Structural Elements for Selectivity across Monoamine Transporters: Novel 2-[(Diphenylmethyl)Sulfinyl]Acetamide (Modafinil) Analogues. *J. Med. Chem.* **2014**, *57* (3), 1000–1013. https://doi.org/10.1021/jm401754x.

(161) Bisgaard, H.; Larsen, M. A. B.; Mazier, S.; Beuming, T.; Newman, A. H.; Weinstein, H.; Shi, L.; Loland, C. J.; Gether, U. The Binding Sites for Benztropines and Dopamine in the Dopamine Transporter Overlap. *Neuropharmacology* **2011**, *60* (1), 182–190. https://doi.org/10.1016/j.neuropharm.2010.08.021.

(162) Tunstall, B. J.; Ho, C. P.; Cao, J.; Vendruscolo, J. C. M.; Schmeichel, B. E.; Slack, R. D.; Tanda, G.; Gadiano, A. J.; Rais, R.; Slusher, B. S.; Koob, G. F.; Newman, A. H.; Vendruscolo, L. F. Atypical Dopamine Transporter Inhibitors Attenuate Compulsive-like Methamphetamine Self-Administration in Rats. *Neuropharmacology* **2018**, *131*, 96–103. https://doi.org/10.1016/j.neuropharm.2017.12.006.

(163) Keighron, J. D.; Quarterman, J. C.; Cao, J.; DeMarco, E. M.; Coggiano, M. A.; Gleaves, A.; Slack, R. D.; Zanettini, C.; Newman, A. H.; Tanda, G. Effects of (R)-Modafinil and

Modafinil Analogues on Dopamine Dynamics Assessed by Voltammetry and Microdialysis in the Mouse Nucleus Accumbens Shell. *ACS Chem. Neurosci.* **2019**, *10* (4), 2012–2021. https://doi.org/10.1021/acschemneuro.8b00340.

(164) Cao, J.; Slack, R. D.; Bakare, O. M.; Burzynski, C.; Rais, R.; Slusher, B. S.; Kopajtic, T.; Bonifazi, A.; Ellenberger, M. P.; Yano, H.; He, Y.; Bi, G.-H.; Xi, Z.-X.; Loland, C. J.; Newman, A. H. Novel and High Affinity 2-[(Diphenylmethyl)Sulfinyl]Acetamide (Modafinil) Analogues as Atypical Dopamine Transporter Inhibitors. *J. Med. Chem.* **2016**, *59* (23), 10676–10691. https://doi.org/10.1021/acs.jmedchem.6b01373.

(165) Hersey, M.; Chen, A. Y.; Bartole, M. K.; Anand, J.; Newman, A. H.; Tanda, G. An FSCV Study on the Effects of Targeted Typical and Atypical DAT Inhibition on Dopamine Dynamics in the Nucleus Accumbens Shell of Male and Female Mice. *ACS Chem. Neurosci.* **2023**, *14* (15), 2802–2810. https://doi.org/10.1021/acschemneuro.3c00354.

(166) Newman, A. H.; Cao, J.; Keighron, J. D.; Jordan, C. J.; Bi, G.-H.; Liang, Y.; Abramyan, A. M.; Avelar, A. J.; Tschumi, C. W.; Beckstead, M. J.; Shi, L.; Tanda, G.; Xi, Z.-X. Translating the Atypical Dopamine Uptake Inhibitor Hypothesis toward Therapeutics for Treatment of Psychostimulant Use Disorders. *Neuropsychopharmacol. Off. Publ. Am. Coll. Neuropsychopharmacol.* **2019**, *44* (8), 1435–1444. https://doi.org/10.1038/s41386-019-0366-z.

(167) Allen, M. I.; Rahimi, O.; Johnson, B. N.; Cao, J.; Newman, A. H.; Nader, M. A. Contrasting the Reinforcing Effects of the Novel Dopamine Transport Inhibitors JJC8-088 and JJC8-091 in Monkeys: Potential Translation to Medication Assisted Treatment. *J. Pharmacol. Exp. Ther.* **2025**, *392* (1), 100033. https://doi.org/10.1124/jpet.124.002356.

(168) Johannesen, L.; Vicente, J.; Mason, J. W.; Erato, C.; Sanabria, C.; Waite-Labott, K.; Hong, M.; Lin, J.; Guo, P.; Mutlib, A.; Wang, J.; Crumb, W. J.; Blinova, K.; Chan, D.;

Stohlman, J.; Florian, J.; Ugander, M.; Stockbridge, N.; Strauss, D. G. Late Sodium Current Block for Drug-Induced Long QT Syndrome: Results from a Prospective Clinical Trial. *Clin. Pharmacol. Ther.* **2016**, *99* (2), 214–223. https://doi.org/10.1002/cpt.205.

(169) Slack, R. D.; Ku, T. C.; Cao, J.; Giancola, J. B.; Bonifazi, A.; Loland, C. J.; Gadiano, A.; Lam, J.; Rais, R.; Slusher, B. S.; Coggiano, M.; Tanda, G.; Newman, A. H. Structure–Activity Relationships for a Series of (Bis(4-Fluorophenyl)Methyl)Sulfinyl Alkyl Alicyclic Amines at the Dopamine Transporter: Functionalizing the Terminal Nitrogen Affects Affinity, Selectivity, and Metabolic Stability. *J. Med. Chem.* **2020**, *63* (5), 2343–2357. https://doi.org/10.1021/acs.jmedchem.9b01188.

(170) Bolleddula, J.; DeMent, K.; Driscoll, J. P.; Worboys, P.; Brassil, P. J.; Bourdet, D. L. Biotransformation and Bioactivation Reactions of Alicyclic Amines in Drug Molecules. *Drug Metab. Rev.* **2014**, *46* (3), 379–419. https://doi.org/10.3109/03602532.2014.924962.

(171) Redfern, W. S.; Carlsson, L.; Davis, A. S.; Lynch, W. G.; MacKenzie, I.; Palethorpe, S.; Siegl, P. K. S.; Strang, I.; Sullivan, A. T.; Wallis, R.; Camm, A. J.; Hammond, T. G. Relationships between Preclinical Cardiac Electrophysiology, Clinical QT Interval Prolongation and Torsade de Pointes for a Broad Range of Drugs: Evidence for a Provisional Safety Margin in Drug Development. *Cardiovasc. Res.* **2003**, *58* (1), 32–45. https://doi.org/10.1016/s0008-6363(02)00846-5.

(172) Okorom, A. V.; Camacho-Hernandez, G. A.; Salomon, K.; Lee, K. H.; Ku, T. C.; Cao, J.; Won, S. J.; Friedman, J.; Lam, J.; Paule, J.; Rais, R.; Klein, B.; Xi, Z.-X.; Shi, L.; Loland, C. J.; Newman, A. H. Modifications to 1-(4-(2-Bis(4-Fluorophenyl)Methyl)Sulfinyl)Alkyl Alicyclic Amines That Improve Metabolic Stability and Retain an Atypical DAT Inhibitor Profile. *J. Med. Chem.* **2024**, *67* (1), 709–727. https://doi.org/10.1021/acs.jmedchem.3c02037.

(173) Giancola, J. B.; Bonifazi, A.; Cao, J.; Ku, T.; Haraczy, A. J.; Lam, J.; Rais, R.; Coggiano, M. A.; Tanda, G.; Newman, A. H. Structure-Activity Relationships for a Series of (Bis(4-Fluorophenyl)Methyl)Sulfinylethyl-Aminopiperidines and -Piperidine Amines at the Dopamine Transporter: Bioisosteric Replacement of the Piperazine Improves Metabolic Stability. *Eur. J. Med. Chem.* **2020**, *208*, 112674. https://doi.org/10.1016/j.ejmech.2020.112674.

(174) Wu, X.; Gu, H. H. Molecular Cloning of the Mouse Dopamine Transporter and Pharmacological Comparison with the Human Homologue. *Gene* **1999**, *233* (1–2), 163–170. https://doi.org/10.1016/s0378-1119(99)00143-2.

(175) Srivastava, D. K.; Navratna, V.; Tosh, D. K.; Chinn, A.; Sk, M. F.; Tajkhorshid, E.; Jacobson, K. A.; Gouaux, E. Structure of the Human Dopamine Transporter and Mechanisms of Inhibition. *Nature* **2024**, *632* (8025), 672–677. https://doi.org/10.1038/s41586-024-07739-9.

(176) Kristofova, M.; Aher, Y. D.; Ilic, M.; Radoman, B.; Kalaba, P.; Dragacevic, V.; Aher, N. Y.; Leban, J.; Korz, V.; Zanon, L.; Neuhaus, W.; Wieder, M.; Langer, T.; Urban, E.; Sitte, H. H.; Hoeger, H.; Lubec, G.; Aradska, J. A Daily Single Dose of a Novel Modafinil Analogue CE-123 Improves Memory Acquisition and Memory Retrieval. *Behav. Brain Res.* **2018**, *343*, 83–94. https://doi.org/10.1016/j.bbr.2018.01.032.

(177) Hussein, A. M.; Aher, Y. D.; Kalaba, P.; Aher, N. Y.; Dragačević, V.; Radoman, B.; Ilić, M.; Leban, J.; Beryozkina, T.; Ahmed, A. B. M. A.; Urban, E.; Langer, T.; Lubec, G. A Novel Heterocyclic Compound Improves Working Memory in the Radial Arm Maze and Modulates the Dopamine Receptor D1R in Frontal Cortex of the Sprague-Dawley Rat. *Behav. Brain Res.* **2017**, *332*, 308–315. https://doi.org/10.1016/j.bbr.2017.06.023.

(178) Saroja, S. R.; Aher, Y. D.; Kalaba, P.; Aher, N. Y.; Zehl, M.; Korz, V.; Subramaniyan, S.; Miklosi, A. G.; Zanon, L.; Neuhaus, W.; Höger, H.; Langer, T.; Urban, E.; Leban, J.; Lubec,

G. A Novel Heterocyclic Compound Targeting the Dopamine Transporter Improves Performance in the Radial Arm Maze and Modulates Dopamine Receptors D1-D3. *Behav. Brain Res.* **2016**, *312*, 127–137. https://doi.org/10.1016/j.bbr.2016.06.011.

(179) Lubec, J.; Kalaba, P.; Hussein, A. M.; Feyissa, D. D.; Kotob, M. H.; Mahmmoud, R. R.; Wieder, O.; Garon, A.; Sagheddu, C.; Ilic, M.; Dragačević, V.; Cybulska-Klosowicz, A.; Zehl, M.; Wackerlig, J.; Sartori, S. B.; Ebner, K.; Kouhnavardi, S.; Roller, A.; Gajic, N.; Pistis, M.; Singewald, N.; Leban, J. J.; Korz, V.; Malikovic, J.; Plasenzotti, R.; Sitte, H. H.; Monje, F. J.; Langer, T.; Urban, E.; Pifl, C.; Lubec, G. Reinstatement of Synaptic Plasticity in the Aging Brain through Specific Dopamine Transporter Inhibition. *Mol. Psychiatry* **2021**, *26* (12), 7076–7090. https://doi.org/10.1038/s41380-021-01214-x.

(180) Castro, J.; Moyano, A.; Pericàs, M. A.; Riera, A. A Convenient Laboratory Preparation of Propargylthiol and Its Derivatives. *Synthesis* **1997**, *1997* (05), 518–520. https://doi.org/10.1055/s-1997-1220.

(181) Lee, K. H.; Fant, A. D.; Guo, J.; Guan, A.; Jung, J.; Kudaibergenova, M.; Miranda, W. E.; Ku, T.; Cao, J.; Wacker, S.; Duff, H. J.; Newman, A. H.; Noskov, S. Y.; Shi, L. Toward Reducing hERG Affinities for DAT Inhibitors with a Combined Machine Learning and Molecular Modeling Approach. *J. Chem. Inf. Model*. **2021**, *61* (9), 4266–4279. https://doi.org/10.1021/acs.jcim.1c00856.

(182) Kalaba, P.; Ilić, M.; Aher, N. Y.; Dragačević, V.; Wieder, M.; Zehl, M.; Wackerlig, J.; Beyl, S.; Sartori, S. B.; Ebner, K.; Roller, A.; Lukic, N.; Beryozkina, T.; Gonzalez, E. R. P.; Neill, P.; Khan, J. A.; Bakulev, V.; Leban, J. J.; Hering, S.; Pifl, C.; Singewald, N.; Lubec, J.; Urban, E.; Sitte, H. H.; Langer, T.; Lubec, G. Structure–Activity Relationships of Novel

Thiazole-Based Modafinil Analogues Acting at Monoamine Transporters. *J. Med. Chem.* **2020**, *63* (1), 391–417. https://doi.org/10.1021/acs.jmedchem.9b01938.

(183) Kalaba, P.; Aher, N. Y.; Ilić, M.; Dragačević, V.; Wieder, M.; Miklosi, A. G.; Zehl, M.; Wackerlig, J.; Roller, A.; Beryozkina, T.; Radoman, B.; Saroja, S. R.; Lindner, W.; Gonzalez, E. R. P.; Bakulev, V.; Leban, J. J.; Sitte, H. H.; Urban, E.; Langer, T.; Lubec, G. Structure–Activity Relationships of Novel Thiazole-Based Modafinil Analogues Acting at Monoamine Transporters. *J. Med. Chem.* **2017**, *60* (22), 9330–9348. https://doi.org/10.1021/acs.jmedchem.7b01313.

(184) Esheleman, A. J.; Wolfrum, K. M.; Reed, J. F.; Kim, S. O.; Swnason, T.; Johnson, R. A.; Janowsky. Structure-Activity Relationships of Substituted Cathionones, with Transporter Binding, Uptake, and Release. *J. Pharmacol. Exp. Ther.* **2017**, *360* (1), 33-47. htts://doi.org/10.1124/jpet.116.236349

(185) Gu, H. H.; Wall, S. C.; Rudnick, G. Stable expression of biogenic amine transporters reveals differences in inhibitor sensitivity kineticsm and ion dependence. *J. Biol. Chem.* **1994**, *269* (10), 7124-7130. htts://doi.org/10.1016/S0021-9258(17)37256-3

(186) Han, D. D.; Gu, H. H. Comparison of the moamine transporters from human and mouse in their sensitivities to psychostimulant drugs. *BMC Pharmacol.* **2006**, 6:6. hhts://doi.org/10.1186/1471-2210-6-6

8 Experimental Procedures and Methods

8.1 General Considerations

Reactions and Reagents

All reactions were held under an inert atmosphere using oven-dried glassware unless otherwise stated. All reagents were obtained from commercial sources and used without further purification. Solvents were also obtained from commercial sources unless specified as anhydrous. For procedures detailed in chapters 2 and 3, anhydrous solvents were obtained from Grubbs canisters passing through activated alumina column, provided by the University of Oxford's internal supplies.

Chromatography:

Thin layer chromatography (TLC) was used to monitor reaction progression using Merck aluminium backed DC60 F_{254} plates (particle size 0.25 mm). Spots in TLC plates were visualized by UV light (254 nm) and stained with potassium permanganate as appropriate.

For procedures corresponding to chapters 2 and 3: FCC was conducted using Merck silica gel 60 (particle size 43 – 60 μm), column eluent solvent systems are specified individually in procedures below.

For procedures corresponding to chapter 4: FCC conducted using Teledyne ISCO, RediSep Rf Gold 20-40 microns and RediSep Rf Flash columns 40 to 60 microns silica gel cartridges in a combiFlash RF or combiFlash EZ prep, Teledyne ISCO instrument.

Spectroscopy:

^{1}HNMR and carbon ^{13}CNMR spectra were obtained on a Bruker AVG400 (400/101 MHz) or a JOEL 400YH instrument. All spectra were obtained at ambient temperature. Spectra were referenced to the residual solvent peak ($CDCl_3$: H 7.26, C 77.16 ppm). Peak assignment was determined based on chemical shifts, integrations, coupling constants, as well as COSY, and HSQC.

Infrared (IR) spectra were obtained a Bruker Tensor 27 FT-IR spectrometer. Peak absorption maxima are reported in wavenumbers (cm^{-1}).

For data corresponding to chapters 2 and 3: High resolution mass (HRMS) spectra were recorded by Chemistry Research Laboratory staff through the submission service using a Bruker Daltronics MicroTOF spectrometer (ESI). Mass to charge ratios (m/z) are reported in Daltons.

For data corresponding to chapter 5: High resolution mass (HRMS) spectra was recorded using Matrix-Assisted Laser Desorption/Ionization Mass Spectrometry (MALDI-MS): Mass analysis was conducted using a LTQ-XL-Orbitrap with a MALDI ion source (Thermo Fisher Scientific, San Jose, CA) in positive ion mode. Electrospray Ionization Mass Spectrometry (ESI-MS): Samples were analyzed by direct injection (10 μL) using a Vanquish UHPLC system (ThermoFisher, Waltham, MA) with tandem Orbitrap Exploris 120 mass spectrometer (ThermoFisher). In MS mode, the mass resolution was set at 120,000 while in MS/MS mode the mass resolution was set at 15,000.

8.2 Experimental Methods

8.2.1 Radioligand Binding Studies

Followed the procedure described for hDAT and hSERT in Reference 1, please see Appendix for greater detail.

8.2.2 General Procedures

General Procedure A: Acceptorless dehydrogenation synthesis of cyclohexenes

Procedure for cyclohexene formation follows protocol reported in reference 3. To a 2–5 mL Biotage® microwave vial is added $[Ir(cod)Cl]_2$ (0.5 mol%), CataCXium® A (2 mol%), 1-(2,3,4,5,6-Pentamethylphenyl)ethan-1-one (1 eq.), KOH (4 eq.) and the diol (2 eq.). The reaction vessel was sealed with a microwave vial cap (containing a Reseal™ septum) and toluene (0.25M) is added via syringe. The vial is then placed in a preheated oil bath at 115 °C for 24 hours. After cooling to RT, HCl (3M, 5 mL) was added to the reaction mixture and the organic phase separated. The aqueous phase is then extracted with diethyl ether (4 x 10 mL). The combined organic phases were dried over MgSO4, filtered and concentrated in vacuo and purified by FCC.

General Procedure B: Pd(TFA)2 and Copper(II) Aromatization

To an oven dried 2–5 mL Biotage® microwave vial equipped with a stir bar was added cyclohexene (1.0 eq), $Pd(TFA)_2$ (5 mol%), and $CuCl_2$ (2.0 eq) sequentially. The vial was subsequently sealed and the air removed by vacuum and refilled with argon three times. Following addition of DMF (0.5 M) via syringe, the reaction mixture was placed in a preheated oil bath at

115 °C to stir for 18 h. The reaction mixture was then allowed to return to room temperature and the reaction solvent removed under a flow of N_2. The crude mixture was then purified via FCC.

General Procedure C: Acceptorless Deyhydrogenation Cyclization and TEMPO-aromatization

To a 0.5-2.0 mL Biotage® vial were added a diol (1.50 eq.), followed sequentially by 1-(2,3,4,5,6-pentamethylphenyl)ethan-1-one (57.0 mg, 0.30 mmol, 1.00 eq.), $Ir(cod)Cl_2$ (1.0 mg, 0.0015 mmol, 0.5 mol %), cataCXium® A (2.1 mg, 0.006 mmol, 2 mol %), and potassium tert-butoxide (32.0 mg, 0.30 mmol, 1.00 eq.). The vial was then immediately sealed and the atmosphere made inert by vacuum and refilling with N_2 three times, and toluene (1.20 mL, 0.25 M) was added via syringe to the reaction mixture; the vial was then placed in a preheated oil bath at 115 °C. After 18 h, the vial is removed from the oil bath, cooled to room temperature, opened, and copper acetate (5.4 mg, 0.03 mmol, 10 mol %), 1,10-phenanthroline (5.4 mg, 0.03 mmol, 10 mol %), and TEMPO (182.0 mg, 1.80 mmol, 6.00 eq.) are added sequentially to the reaction mixture. The vial is resealed, placed in a preheated oil bath at 125 °C and the reaction stirred for 48 h. Upon completion of the 48 h, the vial is removed from the oil bath and cooled to room temperature. The reaction mixture is diluted with diethyl ether (2.00 mL) and an aqueous solution of 3M HCl (1.50 mL) and saturated sodium thiosulphate (1.50 mL) is added to the vial. The biphasic reaction mixture is allowed to stir at room temperature for 30-45 minutes (Note: this work up removes a significant amount of the excess TEMPO, removal of TEMPO prior to purification was found to be crucial for ease isolating product through FCC). The organic and aqueous layers are then separated, the aqueous layer washed three times with diethyl ether (3 x 3.0 mL). The combined organic layers are then dried

with sodium sulphate, filtered, and concentrated. The crude mixture is then purified by FCC (gradient 100:0 to 98:2 pentane:diethyl ether).

General procedure D: Synthesis of Sulfide Using benzhydryl chloride/bromide:

In a 2-5mL Biotage vial, thioacetate (1.0 eq) and sodium hydroxide (NaOH; 2.0 eq) are added, the vial is sealed and purged with argon. Degassed ethanol (0.5 M) is added to the vial and water (11 eq) is added via syringe. The vial is then placed in a hot bath at 90 °C and stirred for two hours. The ethanol is then removed, the concentrated is suspended with 1M HCl until pH about 5-6, and then the aqeous layer is extract with ethyl acetate three times. The combined organic layers are dried with Na_2SO_4 and concentrated under reduced pressure. The resulting thiol is then redissolved in degassed acetonitrile (MeCN; 0.5M) and added to a round bottom flask under nitrogen. To the solution of thiol is then added corresponding benzyl chloride/bromide (1.0 eq) and DBU (1.0 eq). The solution is then stirred at 20 °C for 18 hours. The solvent is then removed under reduced pressure and the crude is purified by FCC 0->30% Ethyl Acetate in Hexanes.

General Procedure E: Synthesis of Sulfide Condition B Using mesylate:

In a round bottom flask, benzyhydrol (1.0 eq) is dissolved in DCM (0.5 M) and cooled to 0 °C under argon. To this solution is added dropwise triethyl amine (TEA; 1.0 eq) followed by mesyl chloride (MsCl; 1.1 eq). This reaction is stirred for 20 hours under argon, allowing it to achieve room temperature. After 20 hours, the reaction mixture is quenched with a solution of 5% sodium bicarbonate (1:1 to DCM used in reaction), the organic layer is then washed once with water, and subsequently dried with Na2SO4 and concentrated under reduced pressure in cold temperature (<

10 °C; removing solvent with heat (i.e. 40 °C) often leads to decomposition of the mesylate). The mesylate is used in its crude form moving forward (must be used immediately).

In a 2-5mL Biotage vial, thioacetate (1.0 eq) and sodium hydroxide (NaOH; 2.0 eq) are added, the vial is sealed and purged with argon. Degassed ethanol (0.5 M) is added to the vial and water (11 eq) is added via syringe. The vial is then placed in a hot bath at 90 °C and stirred for two hours. The ethanol is then removed, the concentrated is suspended with 1M HCl until pH about 5-6, and then the aqeous layer is extract with ethyl acetate three times. The combined organic layers are dried with Na2SO4 and concentrated under reduced pressure. The resulting thiol is then redissolved in degassed acetonitrile (1M) and added to a round bottom flask under nitrogen. In a separate round bottom flask, the mesylate is dissolved with degassed MeCN (1M). To the solution of the mesylate, the solution of the thiol is added via syringe, subsequently added DBU (1.0 eq). The solution is then stirred at 20 °C for 18 hours. The solvent is then removed under reduced pressure and the crude is purified by FCC 0->30% Ethyl Acetate in Hexanes.

General Procedure F: Synthesis of Sulfide Condition C Using *in situ* benzhydryl bromide:

In a round bottom flask, 3-Br-benzyhydrol (1.0 eq) is dissolved in hydrobromic acid (33% in acetic acid) (0.4M) at 0 °C under argon and the reaction is warmed to room temperature. Once at room temperature the reaction mixture is stired for 30 minutes. The reaction mixture is diluted with ice water and neutralized with a solution of 15% sodium bicarbonate to pH 7-8. The aqueous layer is then extracted three times with ethyl acetate, and subsequently dried with Na2SO4 and concentrated under reduced. The benzhydryl bromide is used in its crude form moving forward. (must be used the immediately as it is unstable)

In a 2-5mL Biotage vial, thioacetate (1.0 eq) and sodium hydroxide (NaOH; 2.0 eq) are added, the vial is sealed and purged with argon. Degassed ethanol (0.5 M) is added to the vial and water (11 eq) is added via syringe. The vial is then placed in a hot bath at 90 °C and stirred for two hours. The ethanol is then removed, the concentrated is suspended with 1M HCl until pH about 5-6, and then the aqeous layer is extract with ethyl acetate three times. The combined organic layers are dried with Na2SO4 and concentrated under reduced pressure. The resulting thiol is then redissolved in degassed acetonitrile (1M) and added to a round bottom flask under nitrogen. In a separate round bottom flask, the benzyhydryl bromide is dissolved with degassed MeCN (1M). To the solution of the benzhydryl bromide, the solution of the thiol is added via syringe, subsequently added DBU (1.0 eq). The solution is then stirred at 20 °C for 18 hours. The solvent is then removed under reduced pressure and the crude is purified by FCC 0->30% Ethyl Acetate in Hexanes.

Follows procedure from patent: Patent Number US20220033393

General procedure G: Oxidation of sulfide to sulfoxide

In a round bottom flash under argon, Sulfide (1.0 eq) is dissolved in DCM (0.1M) and cooled to -15 °C. Separately, *m*-chloroperbenzoic acid (mCPBA; 1.05 eq) is dissolved in DCM (0.25M) and cooled to -15 °C. The solution of mCPBA is then added dropwise over 30 seconds to the solution of the sulfide. The reaction is stirred at -15 °C for 15 minutes and then quenched with the addition of 10% aqueous sodium thiosulphate solution (1:1 to DCM used in reaction). The reaction mixture is allowed to warm to room temperature and aqeous and organic layers were separated. The organic layer is washed once with 10% sodium bicarbonate solution. The orgnic layer is then dried with Na2SO4 and concentrated under reduced pressure. The sulfoxide is then purified by FCC 0->50% Ethyl Acetate in Hexanes.

General procedure H: Copper(I)-catalyzed azide-alkyne cycloaddition

To a round bottom flask at room temperature is added alkyne (1.0 eq), copper(II) sulfate pentahydrate (0.10 eq), and sodium ascorbate (0.30 eq). These reagents are then suspended dissolved in a THF:Water (1:1; 0.2 M) biphasic system. Subsequently add the corresponding azide (1.05 eq) and stir at room temperature for 20 hours. Then transfer reaction into a separatory funnel, organic layer is removed and the aqueous layer is extracted three times with ethyl acetate. The combined organic layers are washed with brine and then dried with Na2SO4 and concentrated under reduced pressure. The resulting triazoles are purified by FCC 0->25% Ethyl Acetate in Hexanes.

8.2.3 Data for Chapter 2

1-(2,3,4,5,6-Pentamethylphenyl)ethan-1-one (8)

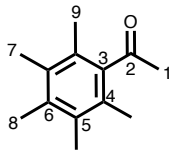

Compound **52** was prepared in accordance to procedure reported in the literature.[6] Pentamethylbenzene (5.00 g, 33.7 mmol, 1.0 eq.) and acetyl bromide (2.60 mL, 37.1 mmol, 1.1 eq.) were dissolved in dichloromethane (DCM; 500 mL) and cooled to 0 °C in an ice/water bath, then, aluminum trichloride ($AlCl_3$; 5.62 g, 42.2 mmol, 1.25 eq.) was added portionwise to the reaction mixture. The reaction was stirred for 1 h, and then was poured into ice-cold water. The organic layer was separated and the aqueous layer extracted with DCM (3 x 100 mL) and the

combined organic layers were dried with $MgSO_4$ and concentrated. The crude product was then purified by FCC (SiO_2, pentane:Et_2O, 90:10) to give the desired compound as a white solid (5.82 g, 91%).

^{1}HNMR (400 MHz, $CDCl_3$) δ 2.46 (s, 3H, H_3C(1)), 2.24 (s, 3H, H_3C(8)), 2.19 (s, 6H, 2 x H_3C(7)), 2.13 (s, 6H, 2 x H_3C(9)).

^{13}CNMR(101 MHz, $CDCl_3$) δ 210.22 *C*(2), 141.08 C_{AR}, 135.50 C_{AR}, 133.23 C_{AR}, 127.14 C_{AR}, 33.25 *C*(1), 17.21 *C*(8), 16.80 *C*(7), 16.08 *C*(9).

All data matches that previously reported in the literature.[2]

(4-Methylcyclohex-1-en-1-yl)(2,3,4,5,6-pentamethylphenyl)methanone (46)

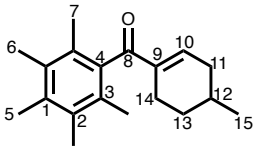

Compound was prepared by following General Procedure A, using [Ir(cod)Cl]2 (3.5 mg, 0.5 mol%), CataCXium® A (7.5 mg, 2 mol%), **8** (200 mg, 1.05 mmol,1 eq.), KOH (230 mg, 1.05 mmol, 4 eq.) and the 3-methyl-1,5-pentane diol (125 mg, 2.10 mmol, 2 eq.) in 2.5 mL of toluene. Purification was accomplished by FCC (SiO_2, n-pentane:Et_2O, 95:5) and gave the desired compound (190 mg, 67 %) as a white solid.

^{1}HNMR (400 MHz, $CDCl_3$) δ 6.50 – 6.43 (m, 1H, *H*C(10)), 2.70 – 2.59 (m, 1H, H_aC(14)), 2.36 – 2.25 (m, 2H, H_bC(14) + H_aC(11)), 2.24 (s, 3H, H_3C(5)), 2.18 (s, 6H, 2 × H_3C(6)), 2.01 (s, 6H, 2

× H_3C(7)), 1.91 – 1. H_aC(11)65 (m, 3H, H_aC(11) + HC(12) + H_bC(13)), 1.27 (dtd, J = 13.1, 10.5, 5.5 Hz, 1H, H_bC(13)), 0.99 (d, J = 6.4 Hz, 3H, H_3C(15)).

^{13}CNMR(101 MHz, $CDCl_3$) δ 203.53 (C(8)), 145.18 (C(10)), 140.51 (C(10)), 138.42 (C_{AR}), 135.04 (C_{AR}), 132.67 (C_{AR}), 129.20 (C_{AR}), 34.77 (C(12)), 30.37 (C(13)), 27.97 (C(11)), 22.52 (C(14)), 21.54 (C(15)), 17.56 (C(7)), 16.80 (C(6)), 16.07 (C(5)).

IR ν_{max} (film)/cm^{-1}: 2949, 2869, 2360, 2341, 1653, 1193, 1003, 862.

HRMS (ESI^+): Found $[M+H]^+$ = 271.2056; $C_{19}H_{26}O$ requires 271.2056, Δ -0.05 ppm. All data matches that previously reported in the literature.[3]

(2,3,4,5,6-Pentamethylphenyl)(*p*-tolyl)methanone (47)

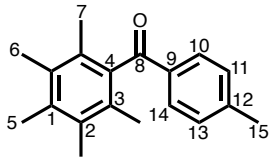

Prepared using General Procedure B, using **46** (33.1 mg, 0.12 mmol, 1 eq.), $Pd(TFA)_2$ (2.0 mg, 5 mol%), and $CuCl_2$ (32.9 mg, 0.25 mmol, 2.0 eq) in DMF (2M). The product was purified by FCC (SiO_2, toluene:pentane, 90:10) gave the desired compound (20.5 mg, 63 %) as a white solid.

^{1}HNMR (400 MHz, $CDCl_3$) δ 7.73 (d, J = 7.9 Hz, 1H, HC(10) + HC(14)), 7.23 (d, J = 7.6 Hz, 1H, HC(11) + HC(13)), 2.41 (s, 3H, H_3C(15)), 2.29 (s, 3H, H_3C(5)), 2.22 (s, 6H, 2 x H_3C(6)), 2.02 (s, 6H, 2 x H_3C(7)).

^{13}CNMR(101 MHz, $CDCl_3$) δ 201.75 *C*(8), 144.46 C_{AR}, 138.03 C_{AR}, 135.52 C_{AR}, 135.46 C_{AR}, 132.96 C_{AR}, 129.83 C_{AR}, 129.57 C_{AR}, 129.13 C_{AR}, 21.87 *C*(15), 17.64 *C*(5), 16.87 *C*(6), 16.09 *C*(7).

IR ν_{max} (film)/cm^{-1}: 2981, 2360, 1668, 1604, 1314, 1272, 1173, 892.

HRMS (ESI^+): Found $[M+H]^+$ = 267.1743; $C_{19}H_{22}O$ requires 267.1743, Δ 0.14 ppm.

M.P.: 130 - 132 °C.

((1R,4R)-4-methylcyclohexyl)(2,3,4,5,6-pentamethylphenyl)methanone

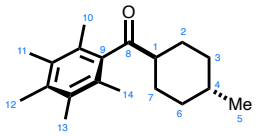

To a 2-5 mL Biotage® vial was added 3-methylpentane-1,5-diol (130.0 mg, 1.10 mmol, 1.10 eq.), by **8** (190.0 mg, 1.00 mmol, 1.00 eq.), pentamethylcyclopentadienyliridium(III) chloride dimer (8.0 mg, 0.01 mmol, 1 mol %), and potassium tert-butoxide (56.1 mg, 0.50 mmol, 0.50 eq.) sequentially. The vial was then immediately sealed and the atmosphere made inert by vacuum and refilling with N_2 three times. Lastly, tert-amyl alcohol (1.00 mL, 1.00 M) which had been bubbled through a stream of Argon gas for a minimum of 20 minutes was added via syringe to the reaction mixture and the vial placed in a preheated oil bath at 115 °C. The reaction mixture was stirred for 18 h, and then the reaction was removed from the oil bath, cooled to room temperature, diluted

with diethyl ether (2.00 mL) and run through a silica pad, eluting with 30.0 mL of diethyl ether. The crude eluate evaporated and the mixture then purified by FCC (gradient 100:0 to 98:2 pentane:diethyl ether) to afford 190.2 mg (70%) of the product as a white solid.

^{1}HNMR (400 MHz, CDCl3) δ 2.56 (tt, J = 12.1, 3.3 Hz, 1H; C1-H), 2.23 (s, 3H; C12-H_3), 2.18 (s, 6H; C10-H_3 + C14-H_3), 2.09 (s, 6H; C11-H_3 + C13-H_3), 1.99 – 1.88 (m, 2H; C7-H_{ax} +C2-H_{ax}), 1.85 – 1.71 (m, 2H; C3-H_{eq} + C6-$H_{eq.}$), 1.54 – 1.42 (m, 2H; C2-H_{eq} + C7-$H_{eq.}$), 1.41 – 1.33 (m, 1H; C4-H), 0.99 – 0.91 (m, 2H; C3-H_{ax} + C6-H_{ax}), 0.88 (d, J = 6.6 Hz, 3H; C5-H_3).

^{13}CNMR(101 MHz, CDCl3) δ 215.24 (C8), 140.29 (C9), 135.36 (C_{AR}), 133.05 (C_{AR}), 128.13 (C_{AR}), 52.92 (C1), 34.61 (C4), 32.23 (C3/6), 28.21 (C2/7), 22.52 (C5), 17.94 (C12), 16.73 (C10/14), 16.03 (C11/13).

All spectroscopic data is consistent with the literature.[2]

(3,4-Dimethylphenyl)(2,3,4,5,6-pentamethylphenyl)methanone (48)

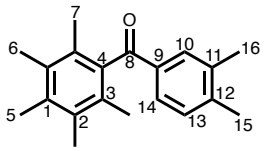

Prepared using General Procedure B, using (3,4-dimethylcyclohex-1-en-1-yl)(2,3,4,5,6-pentamethylphenyl)methanone (35.3 mg, 0.12 mmol, 1 eq.), $Pd(TFA)_2$ (2.0 mg, 5 mol%), and $CuCl_2$ (33.3 mg, 0.25 mmol, 2.0 eq) in DMF (2M). The product was purified by FCC (SiO_2, toluene:pentane, 90:10) gave the desired compound (21.7 mg, 62 %) as a white solid.

^{1}HNMR (400 MHz, $CDCl_3$) δ 7.69 (d, *J* = 1.9 Hz, 1H, *H*C(14)), 7.49 (dd, *J* = 7.8, 2.0 Hz, 1H, *H*C(10)), 7.17 (d, *J* = 7.8 Hz, 1H, *H*C(13)), 2.32 (s, 3H, H_3C(15)), 2.30 (s, 3H, H_3C(16)), 2.29 (s, 3H, H_3C(5)), 2.22 (s, 6H, 2 x H_3C(6)), 2.02 (s, 6H, 2 x H_3C(7)).

^{13}CNMR (101 MHz, $CDCl_3$) δ 202.05 *C*(8), 143.28 C_{AR}, 138.15 C_{AR}, 137.30 C_{AR}, 135.85 C_{AR}, 135.44 C_{AR}, 132.91 C_{AR}, 130.32 C_{AR}, 130.10 C_{AR}, 129.13 C_{AR}, 127.86 C_{AR}, 20.25 *C*(16), 19.86 *C*(15), 17.66 *C*(5), 16.87 *C*(6), 16.10 *C*(7).

IR ν_{max} (film)/cm^{-1}: 2921, 2856, 2360, 2343, 1667, 1604, 1449, 1269, 1235, 855.

HRMS (ESI^+): Found $[M+H]^+$ = 281.1900; $C_{20}H_{24}O$ requires 281.1900, Δ 0.15 ppm.

M.P.: 136-138 °C.

(2,3,4,5,6-Pentamethylphenyl)(*m*-tolyl)methanone (49)

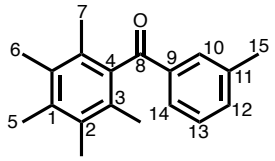

Prepared using General Procedure B, using (3-methylcyclohex-1-en-1-yl)(2,3,4,5,6-pentamethylphenyl)methanone (23.9 mg, 0.09 mmol, 1 eq.), $Pd(TFA)_2$ (1.8 mg, 5 mol%), and $CuCl_2$ (23.7 mg, 0.18 mmol, 2.0 eq) in DMF (2M). The product was purified by FCC (SiO_2, toluene:pentane, 90:10) gave the desired compound (13.0 mg, 55 %) as a white solid.

^{1}HNMR (400 MHz, $CDCl_3$) δ 7.73 – 7.68 (m, 1H, *H*C(14)), 7.57 (dd, *J* = 7.7, 1.7 Hz, 1H, *H*C(10)), 7.41 – 7.36 (m, 1H, *H*C(13)), 7.30 (t, *J* = 7.6 Hz, 1H, *H*C(12)), 2.39 (s, 3H, H_3C(15)), 2.29 (s, 3H, H_3C(5)), 2.22 (s, 6H, 2 x H_3C(6)), 2.02 (s, 6H, 2 x H_3C(7)).

^{13}CNMR(101 MHz, $CDCl_3$) δ 202.35 *C*(8), 138.72 C_{AR}, 138.01 C_{AR}, 137.86 C_{AR}, 135.59 C_{AR}, 134.41 C_{AR}, 132.98 C_{AR}, 129.74 C_{AR}, 129.16 C_{AR}, 128.73 C_{AR}, 127.28 C_{AR}, 21.46 *C*(15), 17.68 *C*(5), 16.90 *C*(6), 16.11 *C*(7).

IR ν_{max} (film)/cm^{-1}: 2922, 2348, 1667, 1600, 1311, 1273, 1161, 794.

HRMS (ESI^+): Found $[M+H]^+$ = 267.1744; $C_{19}H_{22}O$ requires 267.1743, Δ 0.25 ppm.

M.P.: 102-105 °C.

(3-Methyl-[1,1'-biphenyl]-4-yl)(2,3,4,5,6-pentamethylphenyl)methanone (50)

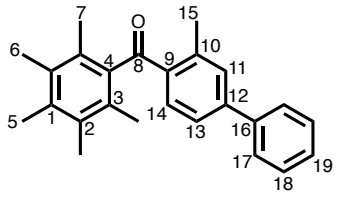

Prepared using General Procedure B, using (5-methyl-1,2,3,6-tetrahydro-[1,1'-biphenyl]-4-yl)(2,3,4,5,6-pentamethylphenyl)methanone (52.8 mg, 0.15 mmol, 1 eq.), $Pd(TFA)_2$ (2.5 mg, 5 mol%), and $CuCl_2$ (61.3 mg, 0.30 mmol, 2.0 eq) in DMF (2M). The product was purified by FCC (SiO_2, toluene:pentane, 80:20) gave the desired compound (15.5 mg, 30 %) as a white solid.

^{1}HNMR (400 MHz, $CDCl_3$) δ 7.64 – 7.59 (m, 2H, *H*C(14) + *H*C(11)), 7.57 – 7.52 (m, 1H, *H*C(13)), 7.49 – 7.43 (m, 3H, 2 x *H*C(17) + *H*C(19)), 7.42 – 7.33 (m, 2H, 2 x *H*C(18)), 2.84 (s, 3H, H_3C(15)), 2.30 (s, 3H, H_3C(5)), 2.23 (s, 6H, 2 x H_3C(6)), 2.07 (s, 6H, 2 x H_3C(7)).

^{13}CNMR(101 MHz, $CDCl_3$) δ 203.68 *C*(8), 144.96 C_{AR}, 141.08 C_{AR}, 140.11 C_{AR}, 139.67 C_{AR}, 135.54 C_{AR}, 135.50 C_{AR}, 133.68 C_{AR}, 133.03 C_{AR}, 131.21 C_{AR}, 129.14 C_{AR}, 129.08 C_{AR}, 129.02 C_{AR}, 128.24 C_{AR}, 127.42 C_{AR}, 124.57 C_{AR}, 22.67 *C*(15), 17.57 *C*(5), 16.94 *C*(6), 16.15 *C*(7).

IR ν_{max} (film)/cm^{-1}: 2924, 2360, 2341, 1668, 1437, 1309, 1212, 907.

HRMS (ESI^+): Found $[M+H]^+$ = 343.2058; $C_{25}H_{26}O$ requires 343.2056, Δ 0.40 ppm.

M.P.: 156-157 °C.

(3-Benzylphenyl)(2,3,4,5,6-pentamethylphenyl)methanone (51)

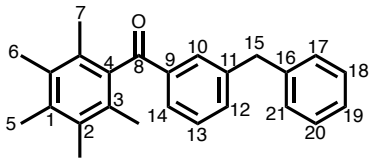

Prepared using the General Procedure B, using (3-benzylcyclohex-1-en-1-yl)(2,3,4,5,6-pentamethylphenyl)methanone (25.3 mg, 0.07 mmol, 1 eq.), $Pd(TFA)_2$ (1.2 mg, 5 mol%), and $CuCl_2$ (19.5 mg, 0.15 mmol, 2.0 eq) in DMF (2M). The product was purified by FCC (SiO_2, toluene:pentane, 85:15) gave the desired compound (10.5 mg, 42 %) as a white solid.

^{1}HNMR (400 MHz, $CDCl_3$) δ 7.78 (d, *J* = 1.9 Hz, 1H, *H*C(14)), 7.58 (dt, *J* = 7.5, 1.6 Hz, 1H, *H*C(10)), 7.40 – 7.26 (m, 4H, 4 x *H*C_{AR}), 7.24 – 7.11 (m, 3H, 3 x *H*C_{AR}), 4.02 (s, 2H, H_2C(15)), 2.28 (s, 3H, H_3C(5)), 2.21 (s, 6H, 2 x H_3C(6)), 2.00 (s, 6H, 2 x H_3C(7)).

^{13}CNMR(101 MHz, $CDCl_3$) δ 202.16 *C*(8), 142.03 C_{AR}, 140.57 C_{AR}, 137.98 C_{AR}, 137.87 C_{AR}, 135.64 C_{AR}, 134.16 C_{AR}, 133.00 C_{AR}, 129.64 C_{AR}, 129.17 C_{AR}, 129.04 C_{AR}, 129.00 C_{AR}, 128.71 C_{AR}, 128.08 C_{AR}, 126.43 C_{AR}, 41.83 *C*(15), 17.72 *C*(7), 16.90 *C*(6), 16.11 *C*(5).

IR ν_{max} (film)/cm^{-1}: 2917, 2360, 1669, 1310, 1271, 804.

HRMS (ESI$^+$): Found $[M+H]^+$ = 343.2057; $C_{25}H_{26}O$ requires 343.2057, Δ 0.14 ppm.

M.P.: 125-126 °C.

(3,5-Dimethylphenyl)(2,3,4,5,6-pentamethylphenyl)methanone (52)

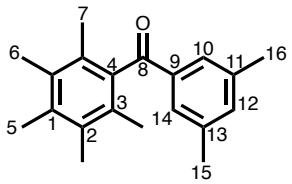

Prepared using General Procedure B, using (3,5-dimethylcyclohex-1-en-1-yl)(2,3,4,5,6-pentamethylphenyl)methanone (34.6 mg, 0.12 mmol, 1 eq.), $Pd(TFA)_2$ (2.0 mg, 5 mol%), and $CuCl_2$ (32.6 mg, 0.24 mmol, 2.0 eq) in DMF (2M). The product was purified by FCC (SiO_2, toluene:pentane, 85:15) gave the desired compound (9.0 mg, 26 %) as a white solid.

^{1}HNMR (400 MHz, $CDCl_3$) δ 7.28 (d, *J* = 8.0 Hz, 1H, *H*C(10)), 7.12 (s, 1H, *H*C(14)), 6.93 (d, *J* = 7.8 Hz, 1H, *H*C(12)), 2.73 (s, 3H, H_3C(16)), 2.35 (s, 3H, H_3C(15)), 2.27 (s, 3H, H_3C(5)), 2.20 (s, 6H, 2 x H_3C(6)), 2.02 (s, 6H, 2 x H_3C(7)).

^{13}CNMR(101 MHz, $CDCl_3$) δ 203.62 *C*(8), 143.13 C_{AR}, 140.64 C_{AR}, 139.83 C_{AR}, 135.31 C_{AR}, 134.31 C_{AR}, 133.36 C_{AR}, 133.33 C_{AR}, 132.93 C_{AR}, 129.09 C_{AR}, 126.61 C_{AR}, 22.42 *C*(16), 21.63 *C*(15), 17.48 *C*(5), 16.90 *C*(6), 16.12 *C*(7).

IR ν_{max} (film)/cm^{-1}: 2922, 2359, 2341, 1662, 1456, 1311, 1206, 814.

HRMS (ESI$^+$): Found $[M+H]^+$ = 281.1898; $C_{20}H_{24}O$ requires 281.1900, Δ -0.83 ppm.

M.P.: 131-133 °C.

[1,1'-Biphenyl]-3-yl(2,3,4,5,6-pentamethylphenyl)methanone (53)

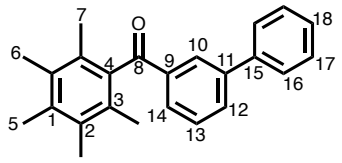

Prepared using General Procedure B, using (2,3,4,5,6-pentamethylphenyl)(1,4,5,6-tetrahydro-[1,1'-biphenyl]-3-yl)methanone (10.2 mg, 0.03 mmol, 1 eq.), $Pd(TFA)_2$ (0.5 mg, 5 mol%), and $CuCl_2$ (12.3 mg, 0.06 mmol, 2.0 eq) in DMF (2M). The product was purified by FCC (SiO_2, toluene:pentane, 85:15) gave the desired compound (4.9 mg, 49 %) as a white solid.

^{1}HNMR (400 MHz, $CDCl_3$) δ 8.14 (t, *J* = 1.8 Hz, 1H, *H*C(10)), 7.79 (ddd, *J* = 7.7, 1.9, 1.2 Hz, 1H, *H*C(14)), 7.74 – 7.69 (m, 1H, *H*C(13)), 7.61 – 7.56 (m, 2H, 2 x *H*C(16)), 7.52 – 7.42 (m, 3H, 2 x *H*C(17) + *H*C(12)), 7.40 – 7.34 (m, 1H, *H*C(18)), 2.29 (s, 3H, H_3C(5)), 2.22 (s, 6H, 2 x H_3C(6)), 2.05 (s, 6H, 2 x H_3C(7)).

^{13}CNMR(151 MHz, $CDCl_3$) δ 202.20 *C*(8), 142.05 C_{AR}, 140.34 C_{AR}, 138.39 C_{AR}, 137.79 C_{AR}, 135.78 C_{AR}, 133.08 C_{AR}, 132.25 C_{AR}, 129.33 C_{AR}, 129.18 C_{AR}, 129.02 C_{AR}, 127.91 C_{AR}, 127.40 C_{AR}, 17.75 *C*(5), 16.92 *C*(6), 16.14 *C*(7).

IR ν_{max} (film)/cm^{-1}: 2923, 2851, 2359, 1670, 1452, 1313, 1193, 805.

HRMS (ESI^+): Found $[M+H]^+$ = 329.1898; $C_{24}H_{24}O$ requires 329.1900, Δ -0.52 ppm.

M.P.: 113-117 °C.

(2-Isobutylphenyl)(2,3,4,5,6-pentamethylphenyl)methanone (54)

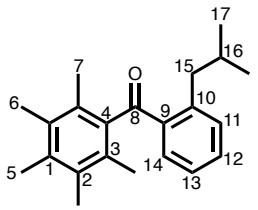

Prepared using General Procedure B, using(2-isobutylcyclohex-1-en-1-yl)(2,3,4,5,6-pentamethylphenyl)methanone (31.9 mg, 0.10 mmol, 1 eq.), $Pd(TFA)_2$ (1.7 mg, 5 mol%), and $CuCl_2$ (27.4 mg, 0.20 mmol, 2.0 eq) in DMF (2M). The product was purified by FCC (SiO_2, toluene:pentane, 85:15) gave the desired compound (9.2 mg, 29 %) as a white solid.

^{1}HNMR (400 MHz, $CDCl_3$) δ 7.45 – 7.34 (m, 2H, *H*C(14) + *H*C(12)), 7.28 (dd, *J* = 8.0, 1.4 Hz, 1H, *H*C(13)), 7.18 – 7.09 (m, 1H, *H*C(11)), 3.03 (d, *J* = 7.0 Hz, 2H, H_2C(15)), 2.27 (s, 3H, H_3C(5)), 2.20 (s, 6H, 2 x H_3C(6)), 2.10 (hept, *J* = 6.7 Hz, 1H, *H*C(16)), 2.01 (s, 6H, 2 x H_3C(7)), 0.99 (d, *J* = 6.6 Hz, 6H, 2 x H_3C(17)).

^{13}CNMR(101 MHz, $CDCl_3$) δ 203.80 *C*(8), 144.29 C_{AR}, 139.78 C_{AR}, 136.42 C_{AR}, 135.36 C_{AR}, 133.71 C_{AR}, 132.92 C_{AR}, 132.76 C_{AR}, 132.10 C_{AR}, 129.19 C_{AR}, 126.07 C_{AR}, 43.91 *C*(15), 29.85 *C*(16), 22.86 *C*(17), 17.52 *C*(5), 16.92 *C*(6), 16.12 *C*(7).

IR ν_{max} (film)/cm^{-1}: 2981, 2359, 2341, 1669, 1457, 668.

HRMS (ESI^+): Found $[M+H]^+$ = 309.221; $C_{22}H_{28}O$ requires 309.2213, Δ -0.62 ppm.

M.P.: 76-78 °C.

(2-Butylphenyl)(2,3,4,5,6-pentamethylphenyl)methanone (55)

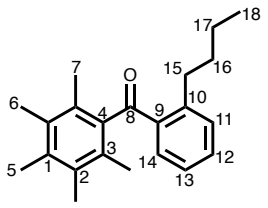

Prepared using General Procedure B, using (2-butylcyclohex-1-en-1-yl)(2,3,4,5,6-pentamethylphenyl)methanone (29.7 mg, 0.11 mmol, 1 eq.), $Pd(TFA)_2$ (1.8 mg, 5 mol%), and $CuCl_2$ (29.5 mg, 0.22 mmol, 2.0 eq) in DMF (2M). The product was purified by FCC (SiO_2, toluene:pentane, 85:15) gave the desired compound (8.1 mg, 49 %) as a yellow solid.

^{1}HNMR (400 MHz, $CDCl_3$) δ 7.44 – 7.35 (m, 2H, *H*C(14) + *H*C(12)), 7.33 (dd, *J* = 7.6, 1.4 Hz, 1H, *H*C(11)), 7.12 (ddd, *J* = 8.0, 7.3, 1.4 Hz, 1H, *H*C(13)), 3.18 – 3.09 (m, 2H, H_2C(15)), 2.27 (s, 3H, H_3C(5)), 2.20 (s, 6H, 2 x H_3C(6)), 2.03 (s, 6H, 2 x H_3C(7)), 1.77 – 1.64 (m, 2H, H_2C(16)), 1.48 (hept, *J* = 7.2 Hz, 2H, H_2C(17)), 0.98 (t, *J* = 7.3 Hz, 3H, H_3C(18)).

^{13}CNMR(101 MHz, $CDCl_3$) δ 203.81 *C*(8), 145.42 C_{AR}, 139.78 C_{AR}, 136.47 C_{AR}, 135.42 C_{AR}, 133.33 C_{AR}, 132.94, C_{AR} 132.39 C_{AR}, 131.71 C_{AR}, 129.21 C_{AR}, 125.89 C_{AR}, 34.48 *C*(15), 33.58 *C*(16), 23.14 *C*(17), 17.54 *C*(5), 16.92 *C*(6), 16.12 *C*(7), 14.18 *C*(18).

IR ν_{max} (film)/cm^{-1}: 2925, 2361, 1669, 1309, 1202, 1021, 891.

HRMS (ESI^+): Found $[M+H]^+$ = 309.2213; $C_{22}H_{28}O$ requires 309.2213, Δ -0.03 ppm.

M.P.: 69-70 °C.

(2,3,4,5,6-Pentamethylphenyl)(*o*-tolyl)methanone (56)

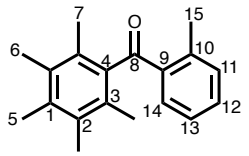

Prepared using General Procedure B, using (2-methylcyclohex-1-en-1-yl)(2,3,4,5,6-pentamethylphenyl)methanone (29.7 mg, 0.11 mmol, 1 eq.), $Pd(TFA)_2$ (1.8 mg, 5 mol%), and $CuCl_2$ (29.5 mg, 0.22 mmol, 2.0 eq) in DMF (2M). The product was purified by FCC (SiO_2, toluene:pentane, 90:10) gave the desired compound (7.2 mg, 25 %) as a white solid.

^{1}HNMR (400 MHz, $CDCl_3$) δ 7.42 – 7.37 (m, 2H, *H*C(14) + *H*C(13)), 7.33 – 7.29 (m, 1H, *H*C(12)), 7.14 (tt, *J* = 7.0, 0.9 Hz, 1H, *H*C(11)), 2.75 (s, 3H, H_3C(15)), 2.28 (s, 3H, H_3C(5)), 2.21 (s, 6H, 2 x H_3C(6)), 2.03 (s, 6H, 2 x H_3C(7)).

^{13}CNMR(101 MHz, $CDCl_3$) δ 204.08 *C*(6), 140.45 C_{AR}, 139.62 C_{AR}, 136.88 C_{AR}, 135.51 C_{AR}, 132.91 C_{AR}, 132.38 C_{AR}, 129.15 C_{AR}, 125.98 C_{AR}, 22.36 *C*(15), 17.49 *C*(7), 16.93 *C*(6), 16.12 *C*(5).

IR ν_{max} (film)/cm^{-1}: 2923, 2360, 2341, 1664, 1311, 1209, 893, 736.

HRMS (ESI^+): Found $[M+H]^+$ = 267.1743; $C_{19}H_{22}O$ requires 267.1743, Δ 0.02 ppm.

M.P.: 143-145 °C.

(2,3,4,5,6-Pentamethylphenyl)(phenyl)methanone (57)

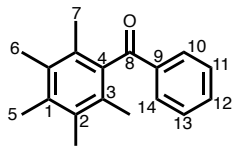

Prepared using General Procedure B, using cyclohex-1-en-1-yl(2,3,4,5,6-pentamethylphenyl)methanone (37.0 mg, 0.14 mmol, 1 eq.), $Pd(TFA)_2$ (2.4 mg, 5 mol%), and $CuCl_2$ (37.5 mg, 0.28 mmol, 2.0 eq) in DMF (2M). The product was purified by FCC (SiO_2, toluene:pentane, 90:10) gave the desired compound (8.1 mg, 25 %) as a white solid.

^{1}HNMR (400 MHz, $CDCl_3$) δ 7.86 – 7.79 (m, 2H, *H*C(10) + *H*C(14)), 7.61 – 7.50 (m, 1H, *H*C(12)), 7.43 (dd, *J* = 8.2, 7.1 Hz, 2H, *H*C(11) + *H*C(13)), 2.28 (s, 3H, H_3C(5)), 2.22 (s, 6H, 2 x H_3C(6)), 2.02 (s, 6H, 2 x H_3C(7)).

^{13}CNMR(101 MHz, $CDCl_3$) δ 202.18 *C*(8), 137.86 C_{AR}, 135.73 C_{AR}, 133.59 C_{AR}, 133.07 C_{AR}, 129.72 C_{AR}, 129.22 C_{AR}, 128.90 C_{AR}, 17.71 *C*(7), 16.94 *C*(6), 16.15 *C*(5).

IR ν_{max} (film)/cm^{-1}: 2918, 2360, 2342, 1671, 1448, 1317, 1209, 891.

HRMS (ESI^+): Found $[M+H]^+$ = 253.1588; $C_{18}H_{20}O$ requires 253.1587, Δ 0.48 ppm.

M.P.: 118-120 °C.

4-Methylcyclohex-1-ene-1-carboxylic acid (58)

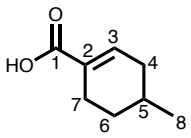

Added **46** (90.0 mg, 0.33 mg, 1 eq..) to a 2–5 mL Biotage® microwave vial and subsequently dissolved 0.88 mL of hexafluoroisopropanol (HFIP, 1.75 mL) and then added 37% HCl (0.25 mL) dropwise to the reaction mixture. The vial was then sealed and placed to stir in a preheated oil bath at 65 °C. The reaction was stirred for 20 hrs and then returned to room temperature, diluted with water (10 mL) and the aqueous layer extracted with DCM (3 x 10 mL). The combined organic layers were dried with MgSO4, filtered, and concentrated. The crude mixture was purified by FCC (SiO2, DCM:MeOH, 95:5) to yield the product (42.2 mg, 92%) as a white solid.

^{1}HNMR (400 MHz, $CDCl_3$) δ 10.82 (br s, 1H, COO*H*), 7.09 (dtd, *J* = 5.2, 2.6, 1.2 Hz, 1H, *H*C(3)), 2.46 – 2.26 (m, 2H, H_aC(7) + H_aC(4)), 2.25 – 2.12 (m, 1H, H_bC(7)), 1.88 – 1.73 (m, 2H, H_aC(6) + H_bC(4)), 1.72 – 1.60 (m, 1H, *H*C(5)), 1.23 (dtd, *J* = 13.0, 10.8, 5.4 Hz, 1H, H_bC(6)), 0.98 (d, *J* = 6.6 Hz, 3H, H_3C(8)).

^{13}CNMR(101 MHz, $CDCl_3$) δ 173.25 *C*(1), 142.22 *C*(3), 129.63 *C*(2), 34.46 *C*(4), 30.34 *C*(6), 27.59 *C*(5), 23.88 *C*(7), 21.52 *C*(8).

IR ν_{max} (film)/cm^{-1}: 3040, 2950, 2360, 2342, 1684, 1604, 1425, 1258, 1024, 804.

HRMS (ESI^+): Found $[M+H]^+$ = 139.0756; $C_8H_{12}O_2$ requires 139.0754, Δ 0.62 ppm.

M.P.: 103-104 °C.

In accordance with literature.[3]

***N*-Methoxy-*N*,4-dimethylcyclohex-1-ene-1-carboxamide (59)**

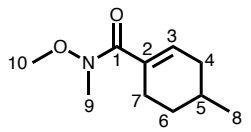

Compound **58 (acid from above)** (230 mg, 1.60 mmol, 1 eq.) was added to a 25 mL round bottom flask and dissolved in DCM (5 mL). The solution was cooled to 0 °C in an ice/water bath and oxalyl chloride (0.15 mL, 0.18 mmol, 1.1 eq) was added dropwise to the reaction mixture followed by 3 drops of DMF. The reaction mixture was stirred for 30 mins at 0 °C and then allowed to warm to room temperature over 1 h. The reaction was then cooled back to 0 °C and *N,O*-dimethylhydroxylamine hydrochloride (MeNHOMe-HCl, 176 mg, 0.18 mmol, 1.1 eq.) was added to the reaction mixture followed by triethylamine (TEA, 0.92 mL, 6.4 mmol, 4 eq.), the reaction mixture was allowed to stir at 0 °C for 20 minutes and then allowed to warm to room temperature over 10 minutes. The reaction was then quenched with saturated sodium bicarbonate (5 mL), and the organic layer then washed with water (5 mL). The organic layer was dried with $MgSO_4$, concentrated, and purified by FCC (SiO_2, pentane:EtOAc, 80:20) to yield the product (60.1 mg, 20%) as a colorless oil.

^{1}HNMR (400 MHz, $CDCl_3$) δ 6.17 – 6.09 (m, 1H), 3.64 (dd, *J* = 2.4, 0.8 Hz, 3H), 3.22 (dd, *J* = 2.5, 0.9 Hz, 3H), 2.36 – 2.27 (m, 2H), 1.81 – 1.65 (m, 3H), 1.26 (ddtd, *J* = 12.8, 10.3, 7.9, 2.5 Hz, 1H), 0.99 – 0.95 (m, 3H).

^{13}CNMR(101 MHz, $CDCl_3$) δ 172.11, 133.62, 130.79, 61.16, 33.88, 33.66, 30.55, 27.86, 25.74, 21.73.

IR ν_{max} (film)/cm^{-1}: 2950, 2360, 2341, 1652, 1635, 1457, 1376, 1022, 972.

HRMS (ESI$^+$): Found $[M+H]^+$ = 184.1333; $C_{10}H_{17}NO_2$ requires 184.1332, Δ 0.52 ppm.

(4-Methoxyphenyl)(4-methylcyclohex-1-en-1-yl)methanone (60)

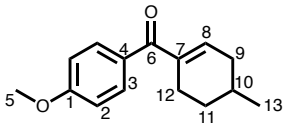

Magnesium turnings (Mg; 29.0 mg, 1.2 mmol, 1.1 eq.) were added to a flame dried round bottom flask and the flask was purged with argon. To the flask was added anhydrous THF (1.5 mL) then added 4-bromoanisole (0.15 mL, 1.2 mmol, 1.1 eq) and 2 drops of bromoethane and stirred vigorously for 3 h. Then added a solution of N-Methoxy-N,4-dimethylcyclohex-1-ene-1-carboxamide (200 mg, 1.1 mmol, 1.0 eq.) in THF (2.5 mL) to the reaction mixture and stirred at room temperature for 2.5 h. The reaction was then quenched with sat. NH_4Cl (5 mL), the organic layer was separated and the aqueous layer extracted with diethyl ether (3 x 5 mL). Combined organic layers were dried with $MgSO_4$, concentrated, and purified by FCC (SiO2, pentane:EtOAc, 95:5) to yield the product (36.7 mg, 15%) as a crystalline solid.

^{1}HNMR (400 MHz, $CDCl_3$) δ 7.73 – 7.63 (m, 2H, 2 x *H*C(3)), 6.96 – 6.86 (m, 2H, 2 x *H*C(2)), 6.46 (ddt, *J* = 4.9, 3.6, 2.0 Hz, 1H, *H*C(8)), 3.85 (d, *J* = 1.0 Hz, 3H, H_3C(5)), 2.62 – 2.50 (m, 1H, H_aC(12)), 2.42 – 2.26 (m, 2H, H_2C(11)), 1.94 – 1.81 (m, 1H, H_aC(9)), 1.79 – 1.67 (m, 1H, *H*C(10)), 1.30 (dtd, *J* = 13.0, 10.9, 5.4 Hz, 1H, H_bC(12)), 1.09 – 0.97 (m, 4H, H_3C(13) + H_bC(9)).

^{13}CNMR(101 MHz, $CDCl_3$) δ 197.18 *C*(6), 162.57 *C*(1), 141.26 *C*(8), 138.50 *C*(7), 131.71 C_{AR}, 131.68 C_{AR}, 131.17 C_{AR}, 113.41 C_{AR}, 55.52 *C*(5), 34.48 *C*(9), 30.49 *C*(12), 27.97 *C*(10), 24.55 *C*(11), 21.68 *C*(13).

IR ν_{max} (film)/cm^{-1}: 2924, 2870, 2360, 2341, 1637, 1600, 1253, 1171, 1028.

HRMS (ESI$^+$): Found $[M+H]^+$ = 231.1381; $C_{15}H_{18}O_2$ requires 231.1380, Δ 0.72 ppm.

(4-Methylcyclohex-1-en-1-yl)(4-(trifluoromethyl)phenyl)methanone (61)

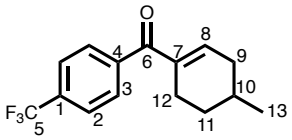

Followed the same procedure as for compound **103**, using N-Methoxy-N,4-dimethylcyclohex-1-ene-1-carboxamide (100 mg, 0.55 mmol, 1.0 eq.), 4-bromotrifluorobenzene (0.09 mL, 0.64 mmol, 1.1 eq), and Mg (14.7 mg, 0.64 mmol, 1.1 eq.). Product was purified by FCC (SiO2, pentane:EtOAc, 95:5) to yield the product (23.2 mg, 16%) as a crystalline solid.

^{1}HNMR (400 MHz, $CDCl_3$) δ 7.68 (m, 4H, 4 x HC_{AR}), 6.55 (h, J = 2.0 Hz, 1H, HC(8)), 2.67 – 2.55 (m, 1H, H_aC(9)), 2.47 – 2.26 (m, 2H, H_bC(9) + H_aC(12)), 1.89 (dtt, J = 16.2, 6.2, 3.0 Hz, 2H, H_bC(12) + H_aC(11)), 1.75 (dtdd, J = 11.4, 6.7, 4.9, 2.9 Hz, 1H, HC(10)), 1.30 (dtd, J = 12.5, 10.5, 5.0 Hz, 1H, H_bC(11)), 1.02 (d, J = 6.6 Hz, 3H, H_3C(13)).

^{13}CNMR(101 MHz, $CDCl_3$) δ 196.93 C(6), 145.44 C(8), 142.26 C(7), 138.63 C_{AR}, 129.34 C_{AR}, 125.27 C_{AR}, 125.24 C_{AR}, 125.16 C(5), 34.79 C(9), 30.28 C(12), 27.89 C(10), 23.89 C(11), 21.61 C(13).

^{19}F NMR (377 MHz, $CDCl_3$) δ -62.92.

IR ν_{max} (film)/cm^{-1}: 2927, 2872, 2348, 1650, 1325, 1129, 1017, 915, 878.

HRMS (ESI$^+$): Found $[M+H]^+$ = 269.1147; $C_{15}H_{15}F_3O$ requires 269.1148, Δ -0.34 ppm.

M.P.: 85-87 °C.

(4-Methoxyphenyl)(*p*-tolyl)methanone (62)

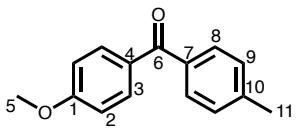

Prepared using General Procedure B, using **103** (32.5 mg, 0.14 mmol, 1 eq.), $Pd(TFA)_2$ (2.3 mg, 5 mol%), and $CuCl_2$ (37.7 mg, 0.28 mmol, 2.0 eq) in DMF (0.25M). The product was purified by FCC (SiO_2, toluene:pentane, 85:15) gave the product (17.3 mg, 54 %) as a white solid.

^{1}HNMR (400 MHz, $CDCl_3$) δ 7.81 (dt, *J* = 4.9, 2.8 Hz, 2H, 2 x *H*C(3)), 7.68 (dt, *J* = 4.6, 2.5 Hz, 2H, 2 x *H*C(8)), 7.27 (d, *J* = 8.2 Hz, 2H, 2 x *H*C(9)), 6.96 (dt, *J* = 4.9, 2.9 Hz, 2H, 2 x *H*C(2)), 3.89 (s, 3H, H_3C(5)), 2.44 (s, 3H, H_3C(11)).

^{13}CNMR(101 MHz, $CDCl_3$) δ 195.49 *C*(6), 163.17 C_{AR}, 142.74 C_{AR}, 135.66 C_{AR}, 132.56 C_{AR}, 130.14 C_{AR}, 129.01 C_{AR}, 113.62 C_{AR}, 55.62 *C*(5), 21.75 *C*(11).

IR ν_{max} (film)/cm^{-1}: 2952, 1649, 1601, 1257, 1171, 1029, 928.

HRMS (ESI^+): Found $[M+H]^+$ = 227.1068; $C_{15}H_{14}O_2$ requires 227.1067, Δ 0.62 ppm.

M.P.: 79-81 °C.

(2,4-Dimethylphenyl)(2,3,4,5,6-pentamethylphenyl)methanone (64)

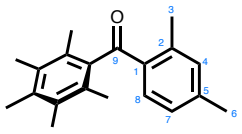

The parent compound was prepared by submitting 3-methylhexane-1,5-diol

(59.0 mg, 0.45 mmol, 1.50 eq.) to **General Procedure C**. Purification by FCC (gradient 100:0 to 98:2 pentane:diethyl ether) afforded 47.7 mg (57%) of the product as a white solid.

^{1}HNMR (400 MHz, $CDCl_3$) δ 7.27 (d, *J* = 7.7 Hz, 1H; H8), 7.12 (s, 1H; H4), 6.93 (d, *J* = 7.6 Hz, 1H; H7), 2.72 (s, 3H; C(6)H_3), 2.35 (s, 3H; C(3)H_3), 2.27 (s, 3H; $C_{AR}CH_3$), 2.20 (s, 6H; 2 x $C_{AR}CH_3$), 2.02 (s, 6H; 2 x $C_{AR}CH_3$).

^{13}CNMR(101 MHz, $CDCl_3$) δ 203.62 (C2), 143.13 (C_{AR}), 140.64 (C1), 139.83 (C2), 135.31 (C5), 134.33 (C_{AR}), 133.36 (C8), 133.33 (C4), 132.93 (C_{AR}), 129.09 (C_{AR}), 126.61 (C7), 22.40 (C6), 21.62 (C3), 17.48 ($C_{AR}CH_3$), 16.90 ($C_{AR}CH_3$), 16.11 ($C_{AR}CH_3$).

IR ν_{max} (film)/cm^{-1}: 2927, 2360, 2341, 1669, 1611, 1450, 1312, 1210, 1145, 872, 724.

HRMS: (ESI^+) m/z calculated. $C_{20}H_{24}ONa$ $[M+Na]^+$ 303.1719; found at 303.1727, Δ 2.51 ppm.

M.P.: 125 - 127 °C.

(3'-Chloro-[1,1'-biphenyl]-4-yl)(2,3,4,5,6-pentamethylphenyl)methanone (65)

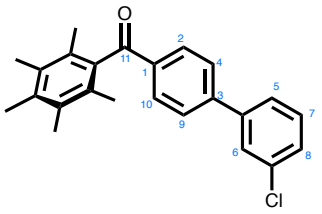

The parent compound was prepared by submitting 3-(3-chlorophenyl)pentane-1,5-diol

(96.8 mg, 0.45 mmol, 1.50 eq.) to **General Procedure C**. Purification by FCC (gradient 100:0 to 98:2 pentane:diethyl ether) afforded 62.4 mg (57%) of the product as a white solid.

^{1}HNMR (400 MHz, $CDCl_3$) δ 7.94 – 7.86 (m, 2H; C2H + C10H), 7.66 – 7.57 (m, 3H; C4H + C9H + C6H), 7.49 (dt, *J* = 7.1, 1.8 Hz, 1H; C5H), 7.44 – 7.33 (m, 2H; C7H + C8H), 2.30 (s, 3H; $C_{AR}CH_3$), 2.23 (s, 6H; 2 x $C_{AR}CH_3$), 2.05 (s, 6H; 2 x $C_{AR}CH_3$).

^{13}CNMR(101 MHz, $CDCl_3$) δ 201.62 (C11), 144.73 (C3), 141.96 (C3'), 137.72 (C_{AR}), 137.04 (C-Cl), 135.82 (C_{AR}), 135.02 (C_{AR}), 133.12 (C_{AR}), 130.34 (C2/10), 129.18 (C8), 128.36 (C7), 127.60 (C4/9), 125.62 (C5), 17.74 ($C_{AR}CH_3$), 16.93 ($C_{AR}CH_3$), 16.14 ($C_{AR}CH_3$).

IR ν_{max} (film)/cm^{-1}: 2926, 2360, 2342, 1671, 1604, 1463, 1272, 1215, 1179, 893, 735.

HRMS: (ESI^+) m/z calculated. $C_{24}H_{27}ClON$ $[M+NH_4]^+$ 380.1776; found at 380.1777, Δ 0.34 ppm.

M.P.: 120 - 123 °C.

(3-Butylphenyl)(2,3,4,5,6-pentamethylphenyl)methanone (66)

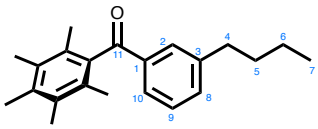

The parent compound was prepared by submitting 2-butylpentane-1,5-diol

(72.0 mg, 0.45 mmol, 1.50 eq.) to **General Procedure C**. Purification by FCC (gradient 100:0 to 98:2 pentane:diethyl ether) afforded 61.3 mg (66%) of the product as a white solid; by NMR it can be observed that the product elutes with minor amounts (< 7%) of the styryl side product due to over oxidation extending into the side chain.

^{1}HNMR (400 MHz, $CDCl_3$) δ 7.74 (s, 1H; C10-H), 7.54 (dt, *J* = 7.7, 1.6 Hz, 1H; C2-H), 7.39 (dt, *J* = 7.6, 1.6 Hz, 1H; C9-H), 7.33 (t, *J* = 7.5 Hz, 1H; C8-H), 2.70 – 2.60 (t, *J* = 7.3 Hz, 2H; C4-H_2), 2.29 (s, 3H; C_{AR}-CH_3), 2.22 (s, 6H; 2 x C_{AR}-CH_3), 2.02 (s, 6H; 2 x C_{AR}-CH_3), 1.60 (tt, *J* = 9.2, 7.6 Hz, 2H; C5-H_2), 1.41 – 1.30 (m, 2H; C6-H_2), 0.92 (t, *J* = 7.3 Hz, 3H; C7-H_3).
^{13}CNMR(101 MHz, $CDCl_3$) δ 202.41 (C11), 143.76 (C_{AR}), 138.03 (C1), 137.82 (C3), 135.57 (C_{AR}), 133.79 (C9), 132.98 (C_{AR}), 129.18 (C_{AR}), 129.03 (C10), 128.70 (C8), 127.67 (C2), 35.57 (C4), 33.66 (C5), 22.44 (C6), 17.70 (2 x C_{AR}-Me), 16.90 (C_{AR}-Me), 16.11 (2 x C_{AR}-Me), 14.05 (C7).

HRMS: (ESI^+) m/z calculated. $C_{22}H_{29}O$ $[M+H]^+$ 309.2213; found at 309.2225, Δ 3.90 ppm.

IR ν_{max} (film)/cm^{-1}: 2929, 2860, 2360, 2341, 1672, 1599, 1582, 1439, 1273, 1163, 1069, 998, 916, 829.

M.P.: 78 - 80 °C.

(3,5-Diethylphenyl)(2,3,4,5,6-pentamethylphenyl)methanone (67)

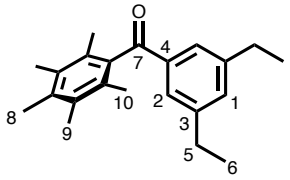

The parent compound was prepared by submitting 2,4-diethylpentane-1,5-diol (96.2 mg, 0.60 mmol, 2.0 eq.) to **General Procedure C**. Purification by FCC (gradient 100:0 to 98:2 pentane:diethyl ether) afforded 20.9 mg (23%) of the product as a white solid.

^{1}HNMR (400 MHz, $CDCl_3$) δ 7.51 – 7.46 (m, 2H, 2 x C2-H), 7.36 (br s, 1H, C1-H), 2.68 – 2.61 (m, 4H; 2 x C5-H_2), 2.28 (s, 3H; C_{AR}-CH_3), 2.22 (s, 6H; 2 x C_{AR}-CH_3), 2.02 (s, 6H; 2 x C_{AR}-CH_3), 1.22 (t, J = 7.9 Hz, 6H; 2 x C6-H_3).

^{13}CNMR(101 MHz, $CDCl_3$) δ 202.62 (C7), 145.32 (C3),145.00 (C_{AR}), 138.43 (C1), 137.82 (C4), 135.57 (C_{AR}), 132.98 (C_{AR}), 129.18 (C_{AR}), 126.63 (C2), 28.79 (C5), 17.76 (2 x C_{AR}-Me), 16.91 (C_{AR}-Me), 16.13 (2 x C_{AR}-Me), 15.76 (C6).

HRMS: (ESI^+) m/z calculated. $C_{22}H_{29}O$ $[M+H]^+$ 309.2140; found at 309.2138, Δ -0.65 ppm.

IR ν_{max} (film)/cm^{-1}: 2933, 2340, 1670, 1591, 1442, 1275, 1071, 805.

M.P.: 108-110 °C.

(2,3,4,5,6-Pentamethylphenyl)(2-(4,4,4-trifluorobutyl)phenyl)methanone (68)

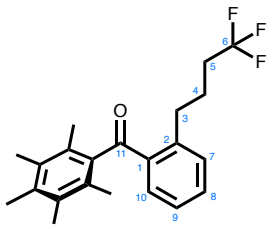

The parent compound was prepared by submitting 9,9,9-trifluorononane-1,5-diol (96.4 mg, 0.45 mmol, 1.5 eq.) to **General Procedure C**. Purification by FCC (gradient 100:0 to 98:2 pentane:diethyl ether) afforded 15.3 mg (14%) of the product as an off-white solid, as well as 63.4 mg (56%) of a yellow solid (see below) as the main product.

^{1}HNMR (400 MHz, $CDCl_3$) δ 7.49 – 7.38 (m, 2H; H10, H8), 7.38 – 7.28 (m, 1H; H7), 7.17 (dt, *J* = 7.6, 1.0 Hz, 1H; H9), 3.20 (t, *J* = 7.7 Hz, 2H; $C3H_2$), 2.28 (s, 3H), 2.26 – 2.16 (m, 8H; $C5H_2$ + 2 x $C_{AR}CH_3$), 2.07 – 1.96 (m, 8H; $C4H_2$ + 2 x $C_{AR}CH_3$).

^{13}CNMR(101 MHz, $CDCl_3$) δ 203.87 (C11), 143.30 (C_{AR}), 136.38 (C2), 135.62 (C1), 133.73 (C10), 133.04 (C8), 132.75 (C_{AR}), 131.76 (C7), 129.13 (C_{AR}), 127.61 (C9), 126.70 (C_{AR}), 39.89 (C6), 33.98 (C5), 33.68 (C3), 23.58 (C4), 17.52 ($C_{AR}CH_3$), 16.93 ($C_{AR}CH_3$), 16.12 ($C_{AR}CH_3$).

^{19}F NMR (377 MHz, $CDCl_3$) δ -66.16.

IR ν_{max} (film)/cm^{-1}: 2928, 2361, 2341, 1668, 1571, 1311, 1211, 1141, 1007, 844, 743.

HRMS: (ESI^+) m/z calculated. $C22H25F3O$ $[M+H]^+$ 363.1930; found at 363.1939, Δ 2.40 ppm.

M.P.: 71-73 °C.

4,4,4-Trifluoro-1-(2-(2,3,4,5,6-pentamethylbenzoyl)phenyl)butan-1-one (68')

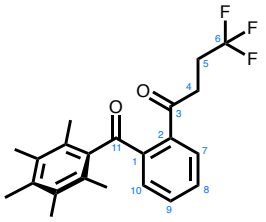

^{1}HNMR (400 MHz, $CDCl_3$) δ 7.62 (ddd, *J* = 7.5, 5.1, 3.6 Hz, 1H; C9H), 7.45 – 7.36 (m, 2H; C10H + C8H), 7.32 (d, *J* = 7.5 Hz, 1H; C7H), 3.06 – 2.98 (m, 2H; $C4H_2$), 2.87 – 2.70 (m, 2H; $C5H_2$), 2.29 (s, 3H; $C_{AR}CH_3$), 2.22 (s, 6H; 2 x $C_{AR}CH_3$), 2.03 (s, 6H; 2 x $C_{AR}CH_3$).

^{13}CNMR(101 MHz, $CDCl_3$) δ 204.25 (C11), 201.96 (C3), 143.32 (C_{AR}), 136.41 (C2), 136.33 (C1), 135.40 (C_{AR}), 133.67 (C9), 133.26 (C_{AR}), 132.32 (C10), 129.97 (C8), 129.46 (C_{AR}), 126.23 (C7), 36.16 (C5), 36.14 (C4), 29.05 (C6), 17.61 ($C_{AR}CH_3$), 16.95 ($C_{AR}CH_3$), 16.08 ($C_{AR}CH_3$).

^{19}F NMR (377 MHz, $CDCl_3$) δ -66.50.

IR ν_{max} (film)/cm^{-1}: (ESI^+) m/z calculated. $C_{22}H_{23}F_3O_2Na$ $[M+Na]^+$ 399.1542; found at 399.1538, Δ -1.10 ppm.

FTIR: 2940, 1710, 1666, 1444, 1330, 1217, 973, 896.

M.P.: 108 - 110 °C.

4-Methylbenzoic acid(69)

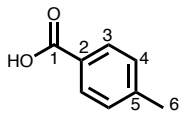

Added **92** (50.0 mg, 0.19 mmol, 1 eq.) to a 2–5 mL Biotage® microwave vial and subsequently dissolved 0.88 mL of hexafluoroisopropanol (HFIP, 1.75 mL) and then added 37% HCl (0.25 mL) dropwise to the reaction mixture. The vial was then sealed and placed to stir in a preheated oil bath at 65 °C. The reaction was stirred for 20 h and then returned to room temperature, diluted with water (10 mL) and the aqueous layer extracted with DCM (3 x 10 mL). The combined organic layers were dried with $MgSO_4$, filtered, and concentrated. The crude mixture was purified by FCC (SiO_2, DCM:MeOH, 95:5) to yield the product (24.1 mg, 96%) as a white crystalline solid.

^{1}HNMR (400 MHz, $CDCl_3$) δ 8.02 (d, *J* = 8.2 Hz, 2H, 2 x *H*C(3)), 7.28 (dt, *J* = 8.0, 0.7 Hz, 2H, 2 x *H*C(4)), 2.44 (s, 3H, H_3C(6)).

^{13}CNMR(101 MHz, $CDCl_3$) δ 172.46 *C*(1), 144.74 C_{AR}, 130.42 C_{AR}, 129.35 C_{AR}, 126.83 C_{AR}, 21.90 *C*(6).

IR ν_{max} (film)/cm^{-1}: 3397, 2360, 2341, 1657, 1418, 1285, 753.

HRMS (ESI^+): Found $[M+H]^+$ = 135.0444; $C_8H_7O_2$ requires 135.0452, Δ -5.47 ppm.

M.P.: 178-180 °C

8.2.4 Data for Chapter 3

3-Methyltetrahydro-2H-pyran-2-one

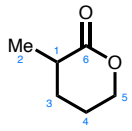

The procedure was adapted from the protocol published by Kuehne *et al*. To an oven-dried round bottom flask equipped with a stir bar, under a N_2 atmosphere, was added diisopropylamine (DIPA; 7.75 mL, 55.0 mmol, 1.10 eq.) and was then diluted with anhydrous tetrahydrofuran (THF; 25.0 mL). The solution was subsequently cooled to 0 °C using an ice/water cold bath. To the solution of DIPA was added n-butyl lithium (nBuLi; 22.0 mL, 55.0 mmol, 1.10 eq, 2.5M in hexanes) dropwise over 1 h using a syringe pump, upon complete addition the reaction mixture was cooled down to -78 °C. A solution of δ-valerolactone (5.00 g, 50.0 mmol, 1.00 eq.) was prepared in THF (8.50 mL) and added dropwise to the reaction mixture over 30 minutes using a syringe pump (note: an ice bag was placed over the syringe containing δ-valerolactone throughout the addition process in order to minimize potential polymerization.) A solution of methyl iodide (MeI; 3.10 mL, 50.0 mmol, 1.10 eq.) in hexamethylphosphoramide (HMPA; 8.70 mL) was prepared and then added to the reaction mixture dropwise over 40 minutes using a syringe pump. Upon complete addition of the methyl iodide, the reaction is warmed to -40 °C and stirred for an additional 3 h. The reaction was then quenched by slow addition of saturated aqueous ammonium chloride (120 mL). The organic layer was separated and the aqueous layer extracted with dichloromethane (CH_2Cl_2; 3 x 40 mL). The combined organic layers were then washed with water (3 x 160 mL), brine (1 x 120 mL), and subsequently dried with magnesium sulphate, filtered, and concentrated. The crude

mixture was subsequently purified by FCC (5:5:1 pentane:CH_2Cl_2:diethyl ether) to afford 2.05 g (36%) of a colorless oil.

^{1}HNMR (400 MHz, CDCl3) δ 4.28 (ttd, J = 5.9, 4.1, 3.0 Hz, 2H; C5-H_2), 2.62 – 2.47 (m, 1H; C1-H), 2.06 (dq, J = 13.4, 6.7 Hz, 1H; C3-H_aH_b), 1.95 – 1.79 (m, 2H; C4-H_2), 1.58 – 1.43 (m, 1H; C3-H_aH_b), 1.22 (d, J = 6.9 Hz, 3H; C2-H_3).

^{13}CNMR(101 MHz, CDCl3) δ 175.36 (C6), 68.59 (C5), 34.65 (C1), 27.12 (C3), 22.05 (C4), 16.71 (C2).

All spectroscopic data is consistent with the literature.[4]

4-Methylhexane-1,5-diol (74)

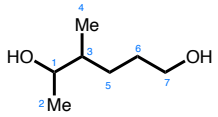

To a round bottom flask, 3-methyltetrahydro-2H-pyran-2-one (2.00 g, 17.5 mmol, 1.00 eq.) was added and the atmosphere made inert by vacuum and refilling with N_2 three times. The lactone was subsequently dissolved in anhydrous dichloromethane (CH_2Cl_2; 35.0 mL, 0.500 M) and the solution cooled to -78 °C with a dry ice/acetone cold bath. Once at -78 °C, diisobutylaluminum hydride (22.8 mL, 22.8 mmol, 1.30 eq, 1M in hexanes) was added dropwise over approximately 10 minutes and the reaction was stirred for 1.5 h. The reaction was then quenched by addition of

a saturated solution of Rochelle's salt (35.0 mL) and the reaction removed from the dry ice/acetone cold bath to allow to reach room temperature. The quenched reaction mixture was allowed to stir vigorously 18 h to ensure separation of organic and aqueous layers. The organic layer was then separated and the aqueous layer extract with diethyl ether (3 x 25 mL). The combined organic layers were dried with sodium sulphate, filtered, and concentrated. The dry crude was oil was subsequently dissolved in tetrahydrofuran (THF; 70 mL, 0.25 M) and added dropwise to a solution of methylmagnesium bromide (MeMgBr; 3.10 mL, 9.30 mmol, 3.51 eq, 3M in diethyl ether) at 0 °C. Upon complete addition of the lactol, the reaction mixture was then allowed to reach room temperature and stirred for 2.5 h. The reaction was subsequently quenched by slow addition at 0 °C of saturated aqueous ammonium chloride (75 mL), the organic layer was separated and the aqueous layer was extracted with diethyl ether (3 x 50 mL). The combined organic layers were dried with sodium sulphate, filtered, and concentrated. The crude mixture was then purified by FCC (40:60 pentane:EtOAc) to afford 1.501 g (65%) of the racemic parent compound as a colorless oil.

^{1}HNMR (400 MHz, CDCl3) δ 3.73 (qd, J = 6.4, 3.9 Hz, 1H; C_a1-H), 3.65 – 3.53 (m, 3H; C_b1-H + C7-H_2), 2.90 (s, 2H; 2 x O-H). 1.69 – 1.40 (m, 4H; C5-H_2 + C6-H_2), 1.23 – 1.05 (m, 4H; C3-H + C_{ab}4-H_3), 0.85 (dd, J – 6.8, 4.8, 3H; C_{ab}4-H_3).

^{13}CNMR(101 MHz, CDCl3) δ 71.15 (C_b1), 71.01 (C_a1), 62.83 (C_b7), 62.79 (C_a7), 39.90 (C_b6), 39.32 (C_a6), 30.38 (C_b5), 29.96 (C_a5), 28.70 (C_b3), 28.38 (C_a3), 19.95 (C_b2), 19.73 (C_a2), 15.07 (C_b4), 14.48 (C_a4).

All spectroscopic data is consistent with the literature.[2]

(2,3-Dimethylcyclohexyl)(2,3,4,5,6-pentamethylphenyl)Methanone (75,76,76b)

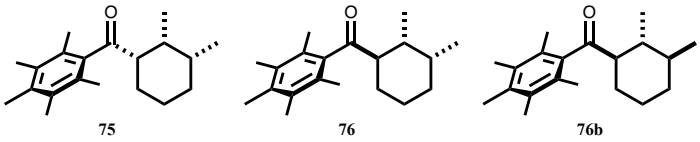

75 76 76b

To a 0.5-2.0mL Biotage® vial were added 4-methylhexane-1,5-diol (79.0 mg, 0.60 mmol, 2.00 eq.), followed sequentially by 1-(2,3,4,5,6-pentamethylphenyl)ethan-1-one (57.0 mg, 0.30 mmol, 1.00 eq.), Ir(cod)acac (4.8 mg, 0.012 mmol, 4 mol %), (*R*)-DTBM-SEGPHOS (18.0 mg, 0.015 mmol, 5 mol %), and potassium tert-butoxide (135.0 mg, 1.20 mmol, 4.00 eq.). The vial was then immediately sealed and the atmosphere made inert by vacuum and refilling with N_2 three times. Lastly tert-butanol (0.10 mL, 3.00 M) which had been bubbled through a stream of Argon gas for a minimum of 20 minutes was added via syringe to the reaction mixture and the vial placed in a preheated oil bath at 110 °C. After 18 h, the reaction was removed from the oil bath, cooled to room temperature, diluted with diethyl ether (2.00 mL) and run through a silica pad, eluting with 30 mL of diethyl ether. The crude eluate evaporated and the mixture then purified by FCC (gradient 100:0 to 99:1 pentane:diethyl ether) using fine silica to afford a yield of 63.7 mg (74%) of combined A+B+C. Isomer A was isolated cleanly with a yield of 29.8 mg (35%). Isomers B and C are insperable and isolated in a yield of 33.9 mg (39%) as an inseparable mixture in 81:19 ratio.

*Data **75***

((1S,2R,3R)-2,3-dimethylcyclohexyl)(2,3,4,5,6-pentamethylphenyl)methanone

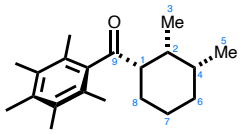

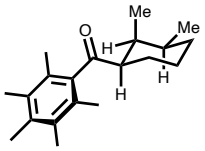

^{1}HNMR (400 MHz, $CDCl_3$) δ 2.74 (dt, *J* = 12.3, 3.2 Hz, 1H; C1-H), 2.23 (s, 3H; C_{AR}-CH_3), 2.18 (s, 6H; 2 x C_{AR}-CH_3), 2.10 (s, 6H; 2 x C_{AR}-CH_3), 182– 1.51 (m, 4H; C4-H + C8-H_2 + C7-$H_{eq.}$), 1.38 – 1.16 (m, 3H; C6-H2 + C7-H_{ax}), 0.90 (d, *J* = 6.9 Hz, 3H; C3-H_3), 0.86 (d, *J* = 6.8 Hz, 3H; C5-H_3).

^{13}CNMR(101 MHz, $CDCl_3$) δ 214.64 (C9), 140.72 (C_{AR}), 135.34 (C_{AR}), 133.14 (C_{AR}), 58.55 (C1), 36.80 (C4), 33.74 (C2), 27.91 (C6), 26.22 (C7), 21.50 (C8), 20.02 (C5), 16.87 (C_{AR}-CH3), 16.17 (C_{AR}-CH3), 7.50 (C3).

IR ν_{max} (film)/cm^{-1}: 2952, 2363, 2340, 1692, 1460, 1383, 1274, 1089.

HRMS: (ESI^+) m/z calculated. $C_{20}H_{30}Na$ $[M+Na]^+$ 309.2189; found at 309.2187, Δ -0.62 ppm.

Chiral HPLC: Chiralpak IG with guard, 0.8% IPA, 99.2% hexane, 1 mL/min, 25 °C, , λ = 214 nm, 10 μL injection; τ_R (major) = 23.6 min, 90.9%, τ_R (minor) = 32.5 min, 9.00%.

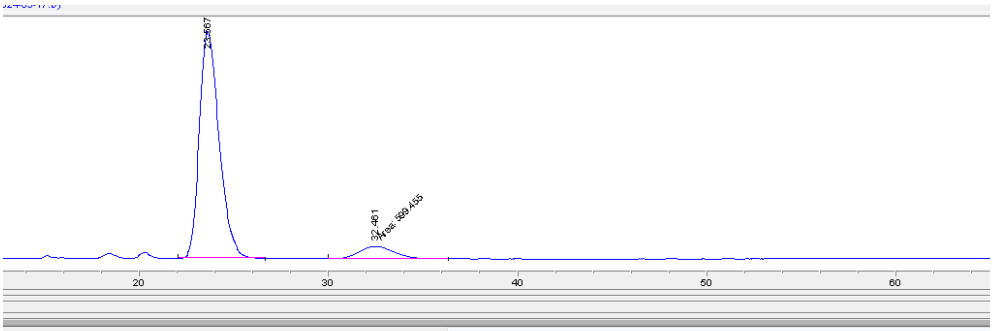

#	Time	Type	Area	Height	Width	Area%	Symmetry
1	23.567	BB	6058.3	83.3	1.1069	90.996	0.689
2	32.461	MM	599.5	4.6	2.1585	9.004	0.776

*Data for mixture **76***

((1R,2R,3R)-2,3-dimethylcyclohexyl)(2,3,4,5,6-pentamethylphenyl)methanone

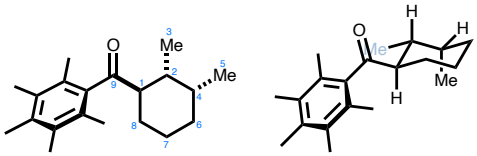

Note: Inseparable from the anti-product (76b)

^{1}HNMR (400 MHz, CDCl3) δ 2.77 (td, *J* = 8.4, 4.2 Hz, 1H; C1-H), 2.24 (s, 3H; C_{AR}-CH_3), 2.19 (s, 3H, 2 x C_{AR}-CH_3), 2.17 – 2.12 (m, 7H; 2 x C_{AR}-CH_3 + C2-H), 2.01 – 1.93 (m, 1H; C4-H), 1.79 – 1.68 (m, 1H; C8-$H_{eq.}$), 1.58 – 1.51 (m, 1H; C7-$H_{eq.}$), 1.51 – 1.31 (m, 4H; C6-H_2 + C8-H_{ax} + C7-H_{ax}), 1.03 (d, *J* = 7.2 Hz, 3H; C3-H_3), 0.87 (d, *J* = 7.1 Hz, 3H; C5-H_3).

^{13}CNMR(101 MHz, $CDCl_3$) δ 213.78 (C9), 140.08 (C_{AR}), 135.44 (C_{AR}), 133.06 (C_{AR}), 127.31 (C_{AR}), 53.71 (C1), 34.47 (C2), 32.57 (C4), 31.51 (C6), 27.40 (C8), 21.24 (C7), 17.91 (C_{AR}-CH3), 17.02 (C_{AR}-CH3), 16.78 (C3), 16.08 (C_{AR}-CH3), 15.12 (C5).

IR ν_{max} (film)/cm^{-1}: 2963, 1693, 1458, 1263, 1104, 866.

HRMS: (ESI$^+$) m/z calculated. $C_{20}H_{30}Na$ $[M+Na]^+$ 309.2189; found at 309.2192, Δ 1.00 ppm.

Chiral HPLC: Chiralpak IG with guard, 0.8% IPA, 99.2% hexane, 1 mL/min, 25 °C, , λ = 214 nm, 10 μL injection; ***syn*-19bi**: τ_R (major) = 14.8 min, 92.8%, τ_R (minor) = 19.4 min, 7.2 %; ***anti*-19b**: τ_R (minor) 21.7 min.

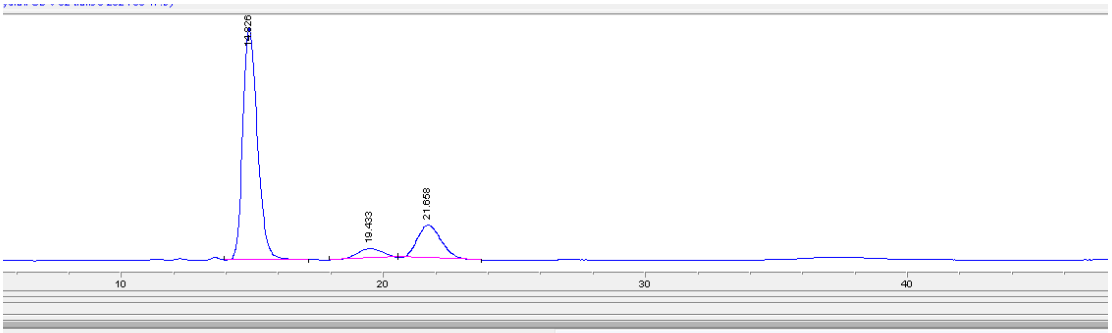

#	Time	Type	Area	Height	Width	Area%	Symmetry
1	14.826	BB	9088.2	235.1	0.5989	76.134	0.707
2	19.433	BB	701.9	10.1	0.8468	5.880	1.038
3	21.658	BB	2146.9	33.5	0.9748	17.986	0.797

((Z)-((2R,3R)-2,3-Dimethylcyclohexylidene)(2,3,4,5,6-pentamethylphenyl)methoxy)dimethyl(phenyl)silane (77)

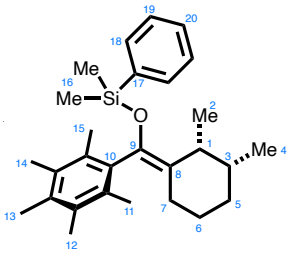

To a 2-5 mL Biotage® vial was added compound **75** (25.1 mg, 0.08 mmol, 1.00 eq) and tris(pentafluorophenyl)borane (1.8 mg, 0.005 mmol, 5 mol %). The vial was sealed and the

atmosphere made inert by vacuum and refilling with N_2 three times. The reagents were then dissolved with anhydrous dichloromethane (CH_2Cl_2; 1.00 mL) and subsequently added dimethylphenylsilane (56.0 uL, 0.50 mml, 5.00 eq.) dropwise to the reaction mixture. Addition of the silane to the reaction mixture led to evolution of hydrogen gas as well as the reaction color turning yellow. The reaction mixture was stirred at room temperature for 6 h and then placed in a preheated oil bath at 75 °C to stir for 13 h. The reaction was then cooled to room temperature, diluted with diethyl ether (3.00 mL), stirred for five minutes, and then filtered through a silica plug, eluting with diethyl ether (25.0 mL). The eluate was then concentrated and the crude mixture purified by FCC (100% pentane) to afford 33.0 mg (80%) of a colorless oil.

^{1}HNMR (600 MHz, CDCl3) δ 7.39 – 7.29 (m, 3H; C18-2H + C20-H), 7.24 (t, J = 7.2 Hz, 2H; C19-2H), 3.29 – 3.23 (m, 1H; C1-H), 2.20 (s, 3H; C13-H_3), 2.12 – 2.07 (m, 9H; 3 x C_{AR}-H_3), 1.96 (s, 3H; C_{AR}-H_3), 1.77 – 1.66 (m, 2H; C7-H_{ax} + C3-H), 1.61 – 1.56 (m, 1H; C7-$H_{eq.}$), 1.54 – 1.50 (m, 1H; C6-H_{ax}), 1.36 (dt, J = 11.3, 3.6 Hz, 1H; C5-$H_{eq.}$), 1.27 (qd, J = 12.8, 3.6 Hz, 1H; C5-H_{ax}), 1.13 (qt, J = 13.0, 4.1 Hz, 1H; C6-$H_{eq.}$), 0.97 (d, J = 7.2 Hz, 3H; C2-H_3), 0.93 (d, J = 6.9 Hz, 3H; C4-H_3), 0.07 (s, 6H; 2 x C16-H_3).

^{13}CNMR(151 MHz, CDCl3) δ 139.98 (C9), 138.90 (C19), 135.21 (C10), 133.97 (C_{AR}), 133.43 (C_{AR}), 132.51 (C_{AR}), 132.47 (C_{AR}), 132.11 (C_{AR}), 131.95 (C_{AR}), 129.39 (C_{AR}), 127.38 (C_{AR}), 127.36 (C_{AR}), 123.98 (C8), 35.79 (C3), 33.23 (C1), 28.99 (C5), 27.34 (C6), 24.14 (C7), 20.14 (C4), 18.28 (C15), 17.51 (C11), 16.82 (C13), 16.60 (C12), 16.58 (C14), 11.37 (C2), -0.68 (C_a16), -0.70 (C_b16).

IR ν_{max} (film)/cm^{-1}: 2953, 2920, 2870, 2361, 2340, 1728, 1667, 1459, 1251, 1165, 885, 849, 832, 786.

HRMS: (ESI^+) m/z calculated. $C_{28}H_{40}OSiNa$ $[M+Na]^+$ 443.2741; found at 443.2733, Δ -1.73 ppm.

((E)-((2R,3R)-2,3-Dimethylcyclohexylidene)(2,3,4,5,6-pentamethylphenyl)methoxy)dimethyl(phenyl)silane (78)

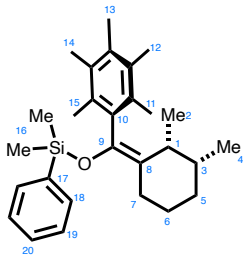

To a 2-5 mL Biotage® vial was added compound **76** (35.5 mg, 0.12 mmol, 1.00 eq) and tris(pentafluorophenyl)borane (2.7 mg, 0.008 mmol, 5 mol %). The vial was sealed and the atmosphere made inert by vacuum and refilling with N_2 three times. The reagents were then dissolved with anhydrous dichloromethane (CH_2Cl_2; 1.00 mL) and subsequently added dimethylphenylsilane (56.0 uL, 0.50 mml, 5.00 eq.) dropwise to the reaction mixture. Addition of the silane to the reaction mixture led to evolution of hydrogen gas as well as the reaction color turning yellow. The reaction mixture was stirred at room temperature for 6 h and then placed in a preheated oil bath at 75 °C to stir for 13 h. The reaction was then cooled to room temperature, diluted with diethyl ether (3.00 mL), stirred for five minutes, and then filtered through a silica plug, eluting with diethyl ether (25.0 mL). The eluate was then concentrated and the crude mixture purified by FCC (100% pentane) to afford 46.7 mg (68%) of a colorless oil.

^{1}HNMR (600 MHz, CDCl3) δ 7.41 – 7.28 (m, 3H; C18-2H + C20-H), 7.27 – 7.21 (m, 2H; C19-2H), 2.99 (d, J = 13.6 Hz, 1H; C7-H_{ax}), 2.21 (s, 3H; C13-H_3), 2.13 – 2.08 (m, 9H; 3 x C_{AR}-H_3),

2.02 (s, 3H; C_{AR}- H_3), 1.96 – 1.90 (m, 1H; C1-H), 1.88 (dd, J = 13.1, 4.5 Hz, 1H; C7-$H_{eq.}$), 1.86 – 1.80 (m, 1H; C6-$H_{eq.}$), 1.65 – 1.57 (m, 1H; C3-H), 1.42 – 1.25 (m, 3H; C5-H_2 + C6-H_{ax}), 0.75 (td, J = 7.0 Hz, 3H; C2-H_3), 0.72 (d, J = 7.0 Hz, 3H; C4-H_3), 0.08 (d, J = 15.4, 6H; C16-2H_3). **^{13}CNMR**(151 MHz, CDCl3) δ 139.97 (C9), 139.15 (C19), 135.09 (C10), 133.97 (C_{AR}), 133.42 (C_{AR}), 132.72 (C_{AR}), 132.27 (C_{AR}), 132.14 (C_{AR}), 131.93 (C_{AR}), 129.39 (C_{AR}), 127.37 (C_{AR}), 123.92 (C8), 36.58 (C1), 35.92 (C3), 29.20 (C5), 27.38 (C6), 21.48 (C7), 19.87 (C4), 18.58 (C15), 18.28 (C11), 16.84 (C13), 16.66 (C14), 16.56 (C12), 11.48 (C2), -0.62 ($C_1$16), -0.84 ($C_2$16).

IR ν_{max} (film)/cm^{-1}: 2918, 2871, 2362, 1728, 1665, 1459, 1252, 1156, 882, 831, 786.

HRMS: (ESI$^+$) m/z calculated. $C_{28}H_{44}OSiN$ $[M+NH_4]^+$ 438.3187; found at 438.3183, Δ -0.85 ppm.

((2R,3R)-2,3-Dimethylcyclohexylidene)(2,3,4,5,6-pentamethylphenyl)methoxy)trimethylsilane (79)

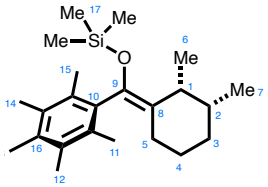

To a 2-5 mL Biotage® vial was added a 1:1 (1*S*,2*R*,3*R*) to (1*R*,2*R*,3*R*) mixture of (2,3-dimethylcyclohexyl)(2,3,4,5,6-pentamethylphenyl)Methanone (23.0 mg, 0.08 mmol, 1.00 eq.), the vial was sealed and the atmosphere vacuumed and back filled with nitrogen three times. Subsequently dissolved A with anhydrous diethyl ether (2.0 mL) and the solution was cooled to -78 °C, and then methyl lithium (0.15 mL, 0.24 mmol, 3.00 eq; 1.6M in ether) was added dropwise to the solution. The reaction was then stirred at to -78 °C for 5 minutes before allowing to it reach room temperature and stirring at 20 °C for 2 h. The reaction was then cooled to 0 °C and trimethylsilyl chloride (0.04 mL, 0.31 mmol, 3.90 eq.) was added dropwise to the reaction. Continued to stir for 30 minutes at 0 °C before adding 2 mL of water to quench the reaction. The organic and aqueous layers were then separated, and the aqueous layer was with diethyl ether (3 x 2 mL). The combined organic layers were dried with sodium sulphate and concentrated. The crude mixture was subsequently purified by FCC (99.5:0.5 pentane:diethyl ether) to afford 13.3 mg (46%) of a colorless glass solid as an inseparable mixture of E/Z isomers.

(Z)-dimethyl((2-methylcyclohexylidene)(2,3,4,5,6-pentamethylphenyl)methoxy)(phenyl)silane (Z-125)

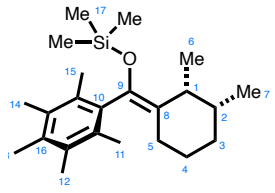

[1]HNMR (400 MHz, CDCl3) δ 3.20 – 3.12 (m, 1H; C1- H*a*H*b*), 2.22 (s, 6H; C15-H_3 + C11-H_3), 2.18 (d, J = 3.7 Hz, 6H; C14-H_3 + C12-H_3), 2.14 (s, 3H; C16-CH_3), 1.81 – 1.63 (m, 2H; C2-H +

C3- *Ha*Hb), 1.59 (dt, J = 15.1, 2.1 Hz, 1H; C3- Ha*Hb*), 1.56 – 1.50 (m, 1H; C5- *Ha*Hb), 1.41 – 1.32 (m, 1H; C4- *Ha*Hb), 1.32 – 1.23 (m, 1H; C4- Ha*Hb*), 1.19 – 1.04 (m, 1H; C5- Ha*Hb*), 0.96 (d, J = 7.2 Hz, 3H; C6- H_3), 0.92 (d, J = 6.9 Hz, 3H; C7-H_3), -0.16 (s, 9H; 3 x C17-H_3).

(E)-Dimethyl((2-methylcyclohexylidene)(2,3,4,5,6-pentamethylphenyl)methoxy)(phenyl)silane (E-125)

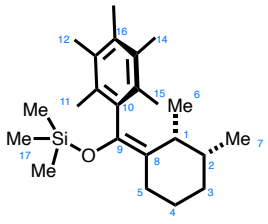

^{1}HNMR (400 MHz, $CDCl_3$) δ 2.91 – 2.82 (m, 1H; C5- *Ha*Hb), 2.24 (s, 6H; C11- H_3 + C15- H_3), 2.19 (d, *J* = 3.4 Hz, 9H; C12- H_3 + C14- H_3 + C16- CH_3), 1.93 (dt, *J* = 11.4, 5.7 Hz, 1H; C1-H), 1.87 – 1.74 (m, 2H; C4-H_2), 1.64 (ddd, *J* = 11.1, 6.9, 4.0 Hz, 1H; C2-H), 1.42 – 1.17 (m, 3H; C5- Ha*Hb* + C3-H_2), 0.74 (dd, *J* = 7.0, 5.3 Hz, 6H; C6-H_3 + C7-H_3), -0.15 (s, 9H; 3 x C17-H_3).

From mixture:

^{13}CNMR(101 MHz, CDCl3) δ 139.31 (C19B), 139.13 (C19A), 135.52 (C_{AR}B), 135.42 (C_{AR}A), 133.85 (C_{AR}A), 132.61 (C_{AR}B), 132.48 (C_{AR}A), 132.28 (C_{AR}B), 132.22 (C_{AR}A), 131.94 (C_{AR}A),131.91 (C_{AR}B), 123.90 (C9B), 123.88 (C9A) , 36.57 (C5B), 35.91 (C4B), 35.78 (C2A), 33.15 (C1A), 30.48 (C2B), 29.21 (C1B), 29.02 (C5A), 27.40 (C4A), 24.15 (C3A), 21.42 (C3B), 20.15 (C7A), 19.92 (C6B), 18.70 (C_{AR}-Me), 18.59 (C_{AR}-Me), 18.40 (C_{AR}-Me), 17.76 (C_{AR}-Me),

16.89 (C_{AR}-Me), 16.77 (C_{AR}-Me), 16.69 (C_{AR}-Me), 16.65 (C_{AR}-Me), 11.51 (C6A), 11.38 (C7B), 0.77 (C17A), 0.72 (C17B).

IR ν_{max} (film)/cm^{-1}: 2957, 2927, 1693, 1460, 1251, 1171, 889, 843.

HRMS: (ESI^{+}) m/z calculated. $C_{23}H_{38}OSiNa$ $[M+Na]^{+}$ 381.2584; found at 381.2580, Δ -1.10 ppm.

Butyl (1S,2R,3R)-2,3-dimethylcyclohexane-1-carboxylate (80)

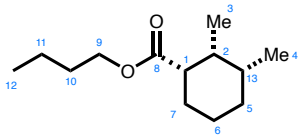

Removal of the Ph* moiety has been developed previously by the Donohoe lab[2] A 2-5 mL Biotage® vial was loaded with ((1*S*,2*R*,3*R*)-2,3-dimethylcyclohexyl)(2,3,4,5,6-pentamethylphenyl)methanone (47.6mg, 0.17 mmol, 1.00 eq.) and sealed, the atmosphere made inert by vacuum and refilling with N_2 three times. Subsequently dissolved with dichloromethane (0.83 mL) and cooled to -17 °C using a cryo-cooler. To the solution was added bromine (0.02 mL, 0.39 mmol, 2.29 eq.) via syringe and the reaction was stirred for 15 minutes and subsequently added n-butanol (nBuOH; 0.05 mL, 0.58 mmol, 3.41 eq.). The reaction was stirred at -17 °C for an additional 5 minutes and then allowed to stir at room temperature for 16 h. The reaction was then diluted with diethyl ether (3.00 mL) and washed with water (1 x 3.0 mL). The organic layer was separated and the aqueous layer extracted with diethyl ether (3 x 2.0 mL). The combined organic layers were then washed with saturated sodium bicarbonate solution (1 x 3.0 mL) and

saturated sodium thiosulphate solution (1 x 3.0 mL). The combined organic layers were then dried with sodium sulphate, filtered, and concentrated. The crude mixture was purified by FCC (gradient 100:0 to 99:1 pentane:diethyl ether) to afford 20.7 mg (59%) of a colorless liquid.

^{1}HNMR (400 MHz, CDCl3) δ 4.14 – 3.99 (m, 2H; C9-H_2), 2.44 (dt, J = 12.5, 3.9 Hz, 1H; C1-H), 2.17 (qt, J = 7.3, 4.0 Hz, 1H; C2-H), 1.79 – 1.70 (m, 1H; C6-H_{ax}), 1.69 – 1.56 (m, 4H; C10-H_2 + C7-H_{eq} + C13-H), 1.56 – 1.46 (m, 1H; C7-H_{ax}), 1.44 – 1.29 (m, 3H; C11-H_2 + C5-$H_{eq.}$), 1.28 – 1.19 (m, 1H; C6-$H_{eq.}$), 1.19 – 1.08 (m, 1H; C5-H_{ax}), 0.93 (t, J = 7.4 Hz, 3H; C12-H_3), 0.88 (d, J = 6.9 Hz, 3H; C4-H_3), 0.71 (d, J = 7.1 Hz, 3H; C3-H_3).

^{13}CNMR(101 MHz, CDCl3) δ 175.51 (C8), 64.02 (C9), 48.26 (C1), 36.10, 35.82 (C2), 30.89 (C10), 27.84 (C5), 25.59 (C6), 21.43 (C7), 20.09 (C4), 19.33 (C11), 13.86 (C12), 7.54 (C3).

IR ν_{max} (film)/cm^{-1}: 2957, 2872, 2361, 1734, 1464, 1223, 1171, 1064.

HRMS: (ESI^{+}) m/z calculated. C13H25O2 $[M+H]^{+}$ 213.1849; found at 213.1853, Δ 1.83 ppm.

Butyl (1R,2R,3R)-2,3-dimethylcyclohexane-1-carboxylate (81)

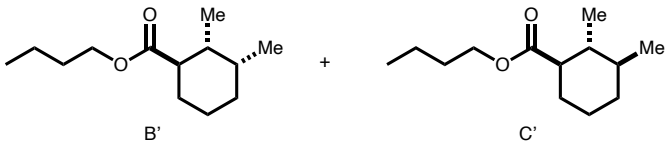

Following the same procedure described for compound **76**, starting from an inseparable mixture of ((1*R*,2*R*,3*R*)-2,3-dimethylcyclohexyl)(2,3,4,5,6-pentamethylphenyl)methanone and C (100.0 mg, 0.29 mmol, 1.00 eq; 75:25 B:C). The crude mixture was purified by FCC (gradient 100:0 to

99:1 pentane:diethyl ether) to afford 44.3 mg (73%) of a colorless liquid, an inseparable mixture of compounds B' and C'.

^{1}HNMR (400 MHz, CDCl3) δ 4.06 (t, J = 6.7 Hz, 2H), 2.23 (td, J = 9.8, 3.7 Hz, 1H), 2.00 (ddd, J = 12.3, 10.8, 3.5 Hz, 0H), 1.94 – 1.85 (m, 1H), 1.85 – 1.71 (m, 1H), 1.68 – 1.54 (m, 3H), 1.54 (s, 0H), 1.39 (dt, J = 15.0, 7.5 Hz, 2H), 1.33 – 1.22 (m, 0H), 1.09 – 0.99 (m, 0H), 0.93 (t, J = 7.3 Hz, 4H), 0.89 – 0.81 (m, 6H).

^{13}CNMR(101 MHz, CDCl3) δ 176.70, 176.59, 64.02, 51.82, 45.57, 40.50, 38.07, 36.52, 35.21, 32.77, 32.25, 30.87, 30.53, 28.81, 25.71, 20.28, 20.07, 19.32, 19.30, 17.79, 17.06, 13.85, 13.63.

IR ν_{max} (film)/cm^{-1}: 1960, 1875, 2359, 2339, 1735, 1460, 1291, 1174, 1140, 1065.

HRMS: (ESI^{+}) m/z calculated. $C_{13}H_{24}O_2Na$ $[M+Na]^{+}$ 235.1669; found at 235.1673, Δ 1.89 ppm.

3-Benzyltetrahydro-2H-pyran-2-one

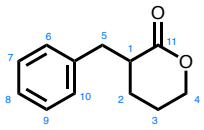

To an oven-dried round bottom flask equipped with a stir bar, under a N_2 atmosphere, was added diisopropylamine (DIPA; 8.11 mL, 57.5 mmol, 1.10 eq.) and was then diluted with anhydrous tetrahydrofuran (THF; 100 mL). The solution was subsequently cooled to -78 °C using a dry

ice/acetone cold bath. To the solution of DIPA was added n-butyl lithium (nBuLi; 23.0 mL, 57.5 mmol, 1.10 eq, 2.5M in hexanes) dropwise over 15 mins using a syringe pump and reaction mixture was allowed to stir at -78 °C for 1 h following complete addition of the nBuLi. A solution of δ-valerolactone (5.00 g, 50.0 mmol, 1.00 eq.) was prepared in THF (50.0 mL) and added dropwise to the reaction mixture over 30 minutes using a syringe pump (note: an ice bag was placed over the syringe containing δ-valerolactone throughout the addition process in order to minimize potential polymerization.) The reaction mixture was then stirred for 1.5 h at -78 °C and then a solution of benzyl bromide (BnBr; 6.00 mL, 50.5 mmol, 1.01 eq.) in THF (25.0 mL) was added to the reaction mixture dropwise over 15 minutes using a syringe pump. Upon complete addition of the benzyl bromide, the reaction continued to stir at -78 °C for 1 h, and then was warmed to -10 °C and stirred for an additional 3 h. The reaction was then quenched by slow addition of saturated aqueous ammonium chloride (100 mL). The organic layer was separated and the aqueous layer extracted with dichloromethane (CH_2Cl_2; 3 x 50 mL). The combined organic layers were dried with sodium sulphate, filtered, and concentrated. The crude mixture was subsequently purified by FCC (gradient 60:40 to 40:60 pentane:CH_2Cl_2) to afford 5.89 g (62%) of a colorless oil.

^{1}HNMR (400 MHz, CDCl3) δ 7.46 – 7.31 (m, 5H; C_{AR}-H_5), 4.48 – 4.32 (m, 2H; C4-H_2), 3.56 – 3.43 (m, 1H; C1-H), 2.92 – 2.77 (m, 2H; C5-H_2), 2.09 – 1.88 (m, 3H; C3-H_2 + C2-*Ha*Hb), 1.70 – 1.60 (m, 1H; C2-Ha*Hb*).

^{13}CNMR(101 MHz, CDCl3) δ 174.25 (C11), 139.10 (C_{AR}), 129.34 (C_{AR}), 128.69 (C_{AR}), 126.66 (C_{AR}), 68.70 (C4), 41.66 (C5), 37.35 (C1), 24.22 (C2), 22.07 (C3).

All spectroscopic data is consistent with the literature.[5]

4-Benzylhexane-1,5-diol (82)

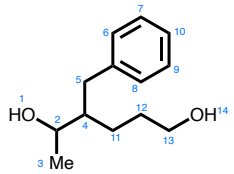

To a round bottom flask, 3-benzyltetrahydro-2H-pyran-2-one (500.0 mg, 2.65 mmol, 1.00 eq.) was added and the atmosphere made inert by vacuum and refilling with N_2 three times. The lactone was subsequently dissolved in anhydrous dichloromethane (CH_2Cl_2; 5.50 mL) and the solution cooled to -78 °C with a dry ice/acetone cold bath. Once at -78 °C, diisobutylaluminum hydride (3.50 mL, 3.45, 1.32 eq, 1M in hexanes) was added dropwise over approximately 2 minutes and the reaction was stirred for 1.5 h. The reaction was then quenched by addition of a saturated solution of Rochelle's salt (5.00 mL) and the reaction removed from the dry ice/acetone cold bath to allow to reach room temperature. The quenched reaction mixture was allowed to stir vigorously for 18 h to ensure separation of organic and aqueous layers. The organic layer was then separated and the aqueous layer extract with diethyl ether (3 x 10 mL). The combined organic layers were dried with sodium sulphate, filtered, and concentrated. The dry crude was oil was placed under a nitrogen atmosphere by vacuum and refilling with N_2 three times, and subsequently dissolved in tetrahydrofuran (THF; 10.0 mL) and cooled to 0 °C. To this solution was added a solution of methylmagnesium bromide (MeMgBr; 3.10 mL, 9.30 mmol, 3.51 eq, 3M in diethyl ether) and the reaction mixture was then allowed to reach room temperature and stirred for 5 h. The reaction was subsequently quenched by slow addition at 0 °C of saturated aqueous ammonium chloride (10.0 mL), the organic layer was separated and the aqueous layer was extracted with diethyl ether (3 x 10 mL). The combined organic layers were dried with sodium sulphate, filtered, and concentrated. The crude mixture was then purified by FCC (gradient 70:30 to 50:50 pentane:EtOAc) to afford 422.7 mg (77%) of the racemic parent compound as a colorless oil.

^{1}HNMR (400 MHz, CDCl3) δ 7.28 (dt, J = 7.1, 4.0 Hz, 2H; C_{AR}-H), 7.18 (dd, J = 8.1, 6.3 Hz, 3H; C_{AR}-H), 3.84 (dqd, J = 12.8, 6.3, 4.1 Hz, 1H; C2-H), 3.63 – 3.53 (m, 2H; C_a13-H_2), 3.49 (q, J = 7.1 Hz, 2H; C_b13-H_2), 2.73 (ddd, J = 45.6, 13.7, 6.5 Hz, 1H; C5-*Ha*Hb), 2.53 (ddd, J = 28.6, 13.7, 7.9 Hz, 1H; C5-Ha*Hb*), 2.32 (s, 2H; H1,O-H), 1.83 – 1.65 (m, 1H; C4-H), 1.62 – 1.50 (m, 2H; C12-H_2), 1.49 – 1.34 (m, 1H; C11-*Ha*Hb), 1.28 – 1.17 (m, 5H; C11-Ha*Hb* + C3-H_3).

^{13}CNMR(101 MHz, CDCl3) δ 141.40 (C_{AR}), 141.32 (C_{AR}), 129.35 (C_{AR}), 129.24 (C_{AR}), 128.53 (C_{AR}), 126.05 (C_{AR}), 68.90 (C2a), 68.81 (C2b), 66.05, 63.06 (C13a), 62.91 (C13b), 46.82 (C4a), 46.47 (C4b), 36.64 (C5a), 36.62 (C5b), 30.43 (C12a), 30.32 (C12b), 25.27 (C11a), 25.09 (C11b), 20.42, 19.43 15.45(C3a).

IR ν_{max} (film)/cm^{-1}: 3365, 3027, 2938, 1496, 1454, 1061, 896, 740, 701.

HRMS: (ESI^{+}) m/z calculated. C13H20O2Na $[M+Na]^{+}$ 231.1356; found at 231.1358, Δ 1.06 ppm.

2-Benzyl-1-phenylpentane-1,5-diol (83)

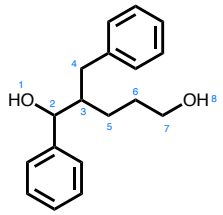

Parent compound was prepared using the protocol described for **82**, starting from 3-benzyltetrahydro-2H-pyran-2-one (500.0 mg, 2.65 mmol, 1.00 eq.), all conditions remain the same for the lactone reduction to the lactol. In the Grignard addition, methylmagnesium bromide was

replaced by phenylmagnesium bromide (PhMgBr; 9.30 mL, 9.30 mmol, 3.51 eq, 1M in THF), all other conditions remain equal. The crude mixture was purified by FCC (gradient 80:20 to 50:50 pentane:EtOAc) to afford 584.9 mg (48%) of the racemic diol as a white solid.

^{1}HNMR (400 MHz, CDCl3) δ 7.50 – 7.32 (m, 7H; C_{AR}-H), 7.31 – 7.19 (m, 3H; C_{AR}-H), 4.86 (d, J = 5.1 Hz, 1H; C_a2-H), 4.71 (d, J = 5.5 Hz, 1H; C_b2-H), 3.64 – 3.48 (m, 2H; C_{ab}7-H_2), 2.87 (dd, J = 13.9, 4.4 Hz, 1H; C_a4-$H_a$$H_b$), 2.75 (dd, J = 13.6, 6.8 Hz, 1H; C_b4-$H_a$$H_b$), 2.67 – 2.54 (m, 2H; C_a4-$H_a$$H_b$ + C_b4-$H_a$$H_b$), 2.39 – 2.33 (s, 2H; O1-H + O8-H), 2.21 – 2.10 (m, 2H; C_a3-H + C_b3-H), 1.71 – 1.47 (m, 5H; C5-$H_a$$H_b$ + C6-$H_a$$H_b$), 1.40 – 1.20 (m, 3H; C5-$H_a$$H_b$ + C6- $H_a$$H_b$).
^{13}CNMR(101 MHz, CDCl3) δ 143.85 (C_{AR}), 143.62 (C_{AR}), 141.20 (C_{AR}), 141.11 (C_{AR}), 129.42 (C_{AR}), 129.27 (C_{AR}), 128.54 (C_{AR}), 128.47 (C_{AR}), 128.44 (C_{AR}), 127.52 (C_{AR}), 126.59 (C_{AR}), 126.49 (C_{AR}), 126.10 (C_{AR}), 125.98 (C_{AR}), 75.36 (C_a2), 75.26 (C_b2), 66.05 (C_a7), 63.03 (C_b7), 47.06 (C_a3), 46.94 (C_b3), 37.14 (C_b4), 35.33 (C_a4), 30.14 (C_a6), 29.92 (C_b6), 25.57 (C_a5), 24.21 (C_b5).

IR ν_{max} (film)/cm^{-1}: 3375, 3027, 2942, 1603, 1495, 1454, 1057, 703.

HRMS: (ESI^{+}) m/z calculated. C18H23O2 $[M+H]^{+}$ 271.1693; found at 271.1703, Δ 3.83 ppm.

M.P.: 62 - 63 °C.

(3-Benzyl-2-methylcyclohexyl)(2,3,4,5,6-pentamethylphenyl)methanone (84)

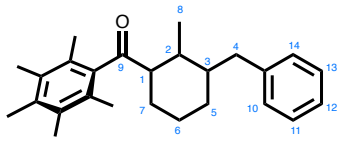

The same procedure for **75**/**76** was conducted starting from diol **82** (44.0 mg, 0.21 mmol, 1.30 eq.), 1-(2,3,4,5,6-pentamethylphenyl)ethan-1-one (32.0 mg, 0.16 mmol, 1.00 eq.), Ir(cod)acac (2.7 mg, 0.006 mmol, 4 mol %), (*R*)-DTBM-SEGPHOS (9.5 mg, 0.008 mmol, 5 mol %), potassium tert-butoxide (37.5 mg, 0.33 mmol, 2.00 eq.), and tert-butanol (0.1 mL, 1.60 M). The resulting crude mixture was purified by FCC (gradient 100:0 to 99:1 pentane:diethyl ether) using fine silica to separate three distinct isomers. Isolated a combined total of 49.7 mg (46%) of the three isomers, with 10.1 mg 84A, 13.0 mg of 84M, and 6.7 mg of 84B (the remainder of the mass isolated as mixtures of diastereomers).

84A

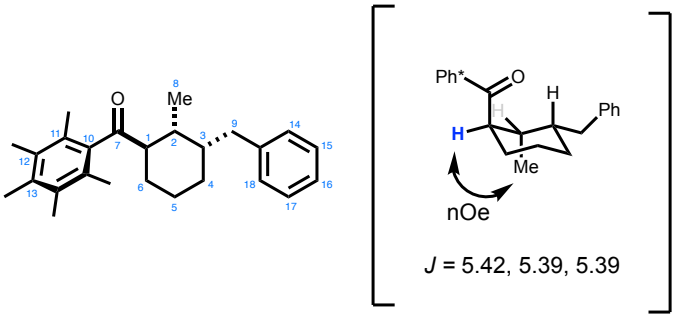

^{1}HNMR (400 MHz, CDCl3) δ 7.31 – 7.22 (m, 3H; C15-H + C16-H + C17-H), 7.21 – 7.09 (m, 2H; C18-H + C14-H), 2.82 (q, J = 5.3 Hz, 1H; C1-H), 2.64 (dd, J = 13.4, 5.6 Hz, 1H; C9-H_aH$_b$), 2.42 (dd, J = 13.4, 9.7 Hz, 1H; C9-H$_a$$H_b$), 2.29 – 2.20 (m, 4H; C13-CH$_3$ + C2-H), 2.20 – 2.11 (m, 8H; 2 x C11-CH$_3$ + C3-H), 2.08 (s, 6H; 2 x C12-CH$_3$), 1.89 – 1.68 (m, 1H; C6- H_aH$_b$), 1.68 – 1.49 (m, 3H; C6-H$_a$$H_b$ + C5-H$_2$), 1.40 – 1.32 (m, 2H; C4-H$_2$), 1.11 (d, J = 7.1 Hz, 3H; C8-H$_3$).

^{13}CNMR(101 MHz, CDCl3) δ 214.22 (C7), 141.52 (C10), 140.24 (C$_{AR}$), 135.54 (C$_{AR}$), 133.19 (C$_{AR}$), 129.46 (C$_{AR}$), 129.20 (C$_{AR}$), 128.32 (C$_{AR}$), 128.25 (C$_{AR}$), 125.76 (C$_{AR}$), 54.76 (C1), 39.59 (C3), 37.31 (C9), 33.29 (C2), 26.60 (C4), 25.08 (C6), 22.10 (C5), 18.03 (C13), 16.90 (C11), 16.21 (C12), 15.59 (C8).

IR ν_{max} (film)/cm^{-1}: 2932, 1691, 1453, 1381, 1103, 911, 736.

HRMS: (ESI^{+}) m/z calculated. C26H35O [M+H]$^{+}$ 363.2682; found 363.2681, Δ -0.40 ppm.

M.P.: 107 - 110 °C.

84B

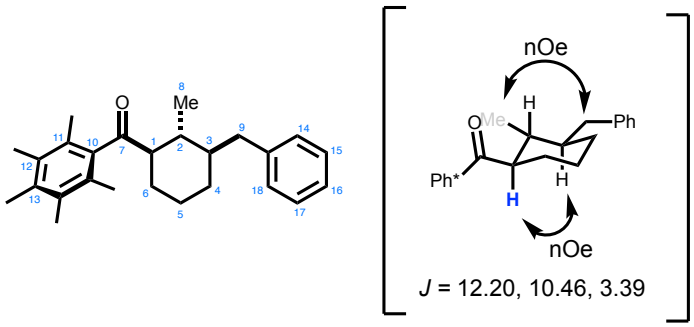

^{1}HNMR (400 MHz, CDCl3) δ 7.32 – 7.24 (m, 2H; C18-H + C14-H), 7.21 – 7.13 (m, 3H; C15-H + C16-H + C17-H), 3.18 (dd, J = 13.4, 3.5 Hz, 1H; C9-H_aH$_b$), 2.60 (ddd, J = 12.2, 10.4, 3.3 Hz,

1H; C1-H), 2.27 – 2.21 (m, 4H; C13-CH_3 + H_aH_b), 2.19 (s, 6H; 2 x C11-CH_3), 2.13 (s, 6H; 2 x C11-CH_3), 1.94 – 1.72 (m, 2H; C2-H + C6-H_aH_b), 1.66 (dt, J = 12.8, 3.2 Hz, 1H; C5-H_aH_b), 1.59 – 1.49 (m, 1H; C4- H_aH_b), 1.40 – 1.31 (m, 1H; C3-H), 1.28 (d, J = 6.2 Hz, 3H; C8-H_3), 1.24 – 0.99 (m, 2H; C5-H_aH_b + C6-H_aH_b), 0.87 (tdd, J = 12.8, 11.6, 3.5 Hz, 1H; C4- H_aH_b).

^{13}CNMR(101 MHz, CDCl3) δ 212.90 (C7), 141.56 (C10), 139.73 (C_{AR}), 135.70 (C_{AR}), 133.22 (C_{AR}), 129.45 (C_{AR}), 128.27 (C_{AR}), 128.25 (C_{AR}), 125.78 (C_{AR}), 125.76 (C_{AR}), 59.52 (C1), 45.12 (C3), 40.38 (C9), 37.10 (C2), 31.41 (C4), 29.99 (C6), 26.32 (C5), 18.39 (C8), 18.08 (C13), 16.93 (C11), 16.21 (C12).

IR ν_{max} (film)/cm^{-1}: 2930, 1691, 1454, 1303, 1151, 1089, 911, 737, 700.

HRMS: (ESI$^+$) m/z calculated. $C_{26}H_{35}O$ $[M+H]^+$ 363.2682; found 363.2685, Δ 0.70 ppm.

M.P.: 96 - 100 °C.

84C

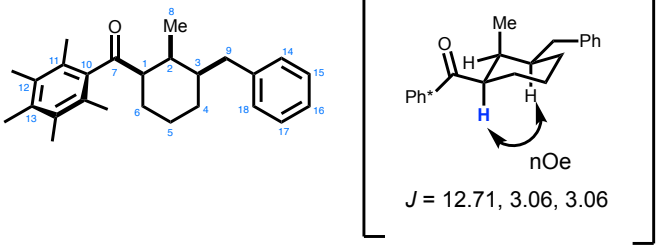

^{1}HNMR (400 MHz, CDCl3) δ 7.29 – 7.21 (m, 2H; C18-H + C14-H), 7.19 – 7.09 (m, 2H; C15-H + C16-H + C17-H), 2.71 (dt, J = 12.4, 3.1 Hz, 1H; C1-H), 2.57 (dd, J = 13.3, 5.9 Hz, 1H; C9-H_aH_b), 2.43 (dd, J = 13.4, 8.9 Hz, 1H; C9-H_aH_b), 2.37 – 2.29 (m, 1H; C9-H), 2.23 (s, 3H; C13-

CH_3), 2.18 (s, 6H; 2 x C11-CH_3), 2.07 (s, 6H; 2 x C12-CH_3), 1.80 – 1.72 (m, 1H; C6-H_aH_b), 1.72 – 1.60 (m, 3H; C3-H + C4-H_2), 1.46 – 1.34 (m, 1H; C5-H_aH_b), 1.33 – 1.07 (m, 2H; C6-H_aH_b + C5-H_aH_b), 1.02 (d, J = 7.0 Hz, 3H; C8-H_3).

^{13}CNMR(101 MHz, CDCl3) δ 214.40 (C7), 141.26 (C10), 140.68 (C_{AR}), 135.34 (C_{AR}), 133.16 (C_{AR}), 129.18 (C_{AR}), 128.32 (C_{AR}), 125.88 (C_{AR}), 58.33 (C1), 44.45 (C3), 41.10 (C9), 32.42 (C2), 26.14 (C6), 25.34 (C5), 22.02 (C4), 16.87 (C13), 16.16 (C11), 15.43 (C12), 8.13 (C8).

IR ν_{max} (film)/cm^{-1}: 2933, 2359, 1691, 1453,1385, 1261, 1092, 739.

HRMS: (ESI$^+$) m/z calculated. $C_{26}H_{35}O$ $[M+H]^+$ 363.2682; found 363.2699, Δ 4.55 ppm.

M.P.: 89 - 91 °C.

(6-Benzyl-2,3,4,5-tetrahydro-[1,1'-biphenyl]-2-yl)(2,3,4,5,6-pentamethylphenyl)methanone (85)

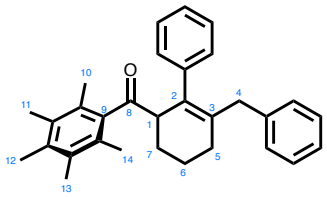

To a 0.5-2.0mL Biotage® vial were added diol **83** (160.0 mg, 0.59 mmol, 2.00 eq.), followed sequentially by 1-(2,3,4,5,6-pentamethylphenyl)ethan-1-one (57.0 mg, 0.30 mmol, 1.00 eq.), Ir(cod)acac (4.8 mg, 0.012 mmol, 4 mol %), (*R*)-DTBM-SEGPHOS (18.0 mg, 0.015 mmol, 5 mol %), and potassium tert-butoxide (134.0 mg, 1.20 mmol, 4.00 eq.). The vial was then immediately sealed and the atmosphere made inert by vacuum and refilling with N_2 three times. Lastly tert-

butanol (0.10 mL, 3.00 M) which had been bubbled through a stream of Argon gas for a minimum of 20 minutes was added via syringe to the reaction mixture and the vial placed in a preheated oil bath at 110 °C. After 18 h, the reaction was removed from the oil bath, cooled to room temperature, diluted with diethyl ether (2.00 mL) and run through a silica pad, eluting with 30.0 mL of diethyl ether. The crude eluate evaporated and the mixture then purified by FCC (gradient 100:0 to 99:1 pentane:diethyl ether) to afford 34.8 mg (27%) of the unreduced enone. Trace of the desired saturated product were observed but could not be isolated.

^{1}HNMR (400 MHz, CDCl3) δ 7.24 – 7.03 (m, 10H; 10 x C_{AR}-H), 3.78 (d, J = 4.8 Hz, 1H; C1-H), 3.22 (dd, J = 26.7, 14.8 Hz, 2H; C4-H), 2.19 – 2.04 (m, 4H; C12-H_3 + C5-H_1H_2), 2.04 – 1.81 (m, 14H; ; C10-H_3 + C11-H_3 + C13-H_3 + C14-H_3 + C5-H_1H_2 + C6-H_1H_2), 1.72 – 1.56 (m, 3H; C7-H_2 + C5-H_1H_2).

^{13}CNMR(101 MHz, CDCl3) δ 210.82 (C8), 142.61, 140.57, 139.49, 136.28, 135.39, 132.90, 132.14, 129.58, 128.73, 128.26, 127.85, 126.30, 125.73, 56.18 (C1), 40.27 (C4), 28.55 (C5), 24.62 (C6), 19.33 (C7), 17.20 (C10 + C14), 16.72 (C12), 15.94 (C11 + C13).

IR ν_{max} (film)/cm^{-1}: 3024, 2938, 2248, 1694, 1493, 1451, 1115, 910, 732, 702.

HRMS: (ESI^{+}) m/z calculated. $C_{31}H_{34}OK$ $[M+K]^{+}$ 461.2241; found at 461.2223, Δ -3.96 ppm.

8.2.5 Data for Chapter 5

(Bis(4-fluorophenyl)methyl)(prop-2-yn-1-yl)sulfane (**141**):

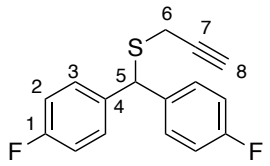

Using General procedure D: Starting with thiol **133** (215.0 mg, 2.99 mmol, 2.0 eq) and 4,4'-(bromomethylene)bis(fluorobenzene) (422.5 mg, 1.49 mmol, 1.00 eq). Instead of DBU, K_2CO_2 was used (515.6 mg, 3.73 mmol, 2.50 eq). The crude was filtered and the solvent removed under reduced pressure. Crude was purified ramping from 0->4% ethyl acetate in hexane to yield 172.7 mg (42.2%) of a colorless oil.

^{1}HNMR (400 MHz, CDCl3) δ 7.41 – 7.35 (m, 4H, 4 x C2-H), 7.06 – 6.97 (m, 4H, 4 x C3-H), 5.39 (s, 1H, C5-H), 3.03 (d, J = 2.6 Hz, 2H, C6-H_2), 2.28 (t, J = 2.6 Hz, 1H, C8-H)

^{13}CNMR(101 MHz, CDCl3) δ 162.15 (d, J = 247.5 Hz), 130.10 (C4), 130.02 (C3), 115.66 (d, J = 21.2 Hz, C2), 79.47 (C7), 71.69 (C8), 51.77 (C5), 19.87 (C6).

^{19}F NMR (376 MHz, CDCL3) δ -114.62.

IR ν_{max} (film)/cm^{-1}: 3301, 2911, 1893, 1602, 1504, 1408, 1222, 1156, 825, 640, 571.

HRMS: (ESI-) m/z calculated. C16H12F2S [M-H]- 273.0555; found at 273.0557, Δ 0.92 ppm.

4,4'-((Prop-2-yn-1-ylsulfinyl)methylene)bis(fluorobenzene) (142)

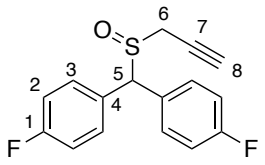

Sulfide **141** (29.7 mg, 0.11 mmol, 1.00 eq) was dissolved in 0.33 mL of (10:1) Methanol:Acetic acid, subsequently added hydrogen peroxide (30% in water, 0.11 mL, 1.08 mmol, 10.0 eq). After 1.5 hours, the solvent was then removed with a steady stream of air flow and the crude was purified by FCC ramping up from 0 -> 30% ethyl acetate in hexanes to yield 12.8 mg (40.7%) of a colorless oil.

^{1}HNMR (400 MHz, CDCl3) δ 7.49 – 7.44 (m, 4H, 4 x C2-H), 7.13 – 7.08 (m, 4H, 4 x C3-H), 5.22 (s, 1H, C5-H), 3.29 (dq, J = 13.1, 3.2 Hz, 2H, C6-H_2), 2.55 (t, J = 2.8 Hz, 1H, C8-H).

^{13}CNMR(101 MHz, CDCl3) δ 163.04 (d, J = 250.1 Hz, C1), 131.59 (d, J = 8.2 Hz, C3), 128.79 (d, J = 3.5 Hz), 116.49 (d, J = 22.2 Hz, C2), 77.18 (C7), 72.65 (C8), 67.08 (C5), 40.30 (C6).

^{19}F NMR (376 MHz, CDCL3) δ -112.59 (d, J = 75.2 Hz)

IR ν_{max} (film)/cm^{-1}: 3301, 2923, 1603, 1507, 1414, 1227, 1160, 1101, 1058, 1015, 861, 835.

HRMS: (ESI+) m/z calculated. C16H12F2OS [M+Na]+ 313.0461; found 313.0465, Δ 1.37 ppm.

4-(((Bis(4-fluorophenyl)methyl)thio)methyl)-1-((trimethylsilyl)methyl)-1H-1,2,3-triazole (143)

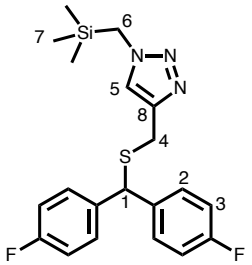

Following General procedure H, using alkyne **141** (49.7 mg, 0.18 mmol, 1.00 eq), copper sulfate pentahydrate (4.5 mg, 0.018 mmol, 0.10 eq), and sodium ascorbate (10.8 mg, 0.054 mmol, 0.30 eq) dissolved in 0.5mL of THF and 0.5mL of Water, then adding (azidomethyl)trimethylsilane (0.13 mL, 0.19 mmol, 1.5 M in tert-butyl methyl ether, 1.05 eq). The crude was purified by FCC ramping up 0->30% ethyl acetate in hexanes, to yield 25.6 mg (35.0%) of a colorless gel.

^{1}HNMR (400 MHz, CDCl3) δ 7.42 – 7.33 (m, 4H, C3-H), 7.24 (s, 1H, C5-H), 7.00 (td, *J* = 8.6, 1.9 Hz, 4H, C2-H), 5.18 (s, 1H, C1-H), 3.87 (s, 2H, C4-H_2), 3.63 (s, 2H, C6-H_2), 0.14 (s, 9H, 3 x C7-H_3).

^{13}CNMR(101 MHz, CDCL3) δ 162.00 (C-F, d, J = 247.5 Hz), 145.05 (C_{AR}), 136.71 (C8), 130.09 (d, J = 91. Hz, C2), 122.43 (C5), 115.59 (d, J = 22.2 Hz, C3), 52.15 (C1), 42.19 (C6), 26.67 (C4), -2.33 (C7).

IR ν_{max} (film)/cm^{-1}: 2956, 1602, 1505, 1412, 1251, 1224, 1097, 1047, 856.

HRMS: (ESI+) m/z calculated. C20H23F2SSi [M+H]+ 404.1423; found 404.1415, Δ 2.00 ppm.

4-(((Bis(4-fluorophenyl)methyl)sulfinyl)methyl)-1-((trimethylsilyl)methyl)-1H-1,2,3-triazole (144)

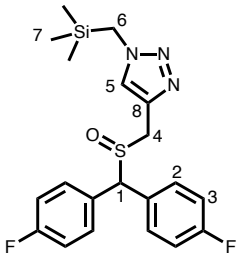

Following General procedure H: To alkyne **142** (49.3 mg, 0.17 mmol, 1.0 eq) was added copper sulfate pentahydrate (4.3 mg, 0.017 mmol, 0.10 eq) and sodium ascorbate (10.1 mg, 0.051 mmol, 0.30 eq), dissolving in 0.5 mL (THF) and 0.5 mL (Water), followed by (azidomethyl)trimethylsilane (0.12 mL mL, 0.18 mmol, 1.5 M, 1.05 eq). The crude was purified by FCC ramping up from 0% -> 25% ethyl acetate in hexane to afford 42.7 mg (59.9%) of a white solid.

^{1}HNMR (400 MHz, CDCl3) δ 7.55 (s, 1H, C5-H), 7.54 – 7.50 (m, 2H, C3-H), 7.42 – 7.35 (m, 2H, C3-H), 7.12 (td, *J* = 8.6, 2.2 Hz, 2H, C2-H), 7.05 (td, *J* = 8.5, 2.2 Hz, 2H, C2-H), 5.00 (s, 1H, C1-H), 4.02 (d, *J* = 14.1 Hz, 1H, C4-H$_a$*H$_b$*), 3.92 (dd, *J* = 15.1, 7.2 Hz, 2H, C6-H$_2$), 3.78 (d, *J* = 14.0 Hz, 1H, C4-*H$_a$*H$_b$), 0.16 (s, 9H, 3 x C7-H$_3$).

^{13}CNMR(101 MHz, CDCL3) δ 162.8 (C-F, d, J = 261.6 Hz), 135.69 (C8), 131.50 (d, J = 9.1 Hz, C2), 129.95 (C$_{AR}$), 125.57 (C5), 116.48 (d, J = 22.2 Hz, C3), 67.22 (C1), 45.04 (C4), 42.37 (C6), -2.37 (C7).

IR ν_{max} (film)/cm^{-1}: 1956, 1603, 1507, 1414, 1251, 1227, 1251, 1044, 856.

MP: 99-100

HRMS: (ESI+) m/z calculated. C20H23F2OSSi [M+H]+ 420.1372; found 420.1363, Δ 1.02 ppm.

4-(((Bis(4-fluorophenyl)methyl)thio)methyl)-1-methyl-1H-1,2,3-triazole (**145**):

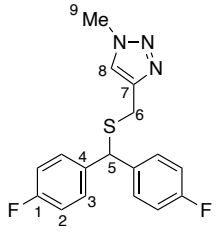

In a vial under argon, a solution of sulfoxide **143** (34.0 mg, 0.081 mmol, 1.00 eq) was prepared in THF (0.30 mL, 0.25M) and water (0.02 mL). To this solution was added TBAF (0.10 mL, 0.097 mmol, 1M in THF, 1.20 eq) in one portion, the reaction was then stirred at 20 °C for 18 hours under argon and then the solvent was removed under reduced pressure and the crude purified by FCC ramping up 0->100% ethyl acetate in hexanes to yield 6.8 mg (77.0%) of a colorless oil.

^{1}HNMR (400 MHz, CDCl3) δ 7.46 – 7.30 (m, 5H, 4 x C2-H + C8-H), 7.11 – 7.03 (m , 4H, 4 x C3-H), 5.12 (s, 1H, C1-H, C5-H), 3.87 (s, 2H, C6-H_2), 3.78 (s, 3H, C9-H_3).

^{13}CNMR(101 MHz, CDCL3) δ 161.97 (C-1, d, J = 247.5 Hz), 139.42 (C4), 130.13 (d, J = 9.1 Hz, C3), 130.04 (C7), 122.43 (C8), 116.02 (d, J = 21.2 Hz, C2), 51.33 (CC5), 39.21 (C9), 24.81 (C6).

IR ν_{max} (film)/cm^{-1}: 2933, 1501, 1484, 1414, 1224, 1058, 1047, 804.

HRMS: (ESI+) m/z calculated. C17H15F2N3S [M+H]+ 332.1027; found 332.1024, Δ 1.02 ppm.

4-(((Bis(4-fluorophenyl)methyl)sulfinyl)methyl)-1-methyl-1H-1,2,3-triazole (**146**):

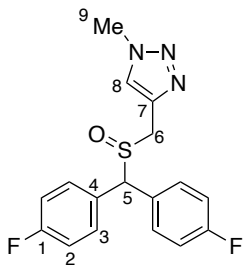

In a vial under argon, a solution of sulfoxide **144** (10.8 mg, 0.027 mmol, 1.00 eq) was prepared in THF (0.10 mL, 0.25M) and water (0.01 mL). To this solution was added TBAF (0.03 mL, 0.032 mmol, 1M in THF, 1.20 eq) in one portion, the reaction was then stirred at 20 °C for 18 hours under argon and then the solvent was removed under reduced pressure and the crude purified by FCC ramping up 0->50% ethyl acetate in hexanes to yield 24.2 mg (86.0%) of a white solid.

^{1}HNMR (400 MHz, CDCl3) δ 7.51 (s, 1H, C8-H), 7.55 – 7.46 (m, 4H, 4 x C2-H), 7.12 – 7.05 (m, 4H, 4 x C2-H), 5.06 (s, 1H, C5-H), 4.02 (d, *J* = 13.7 Hz, 1H, C6-H$_a$*H$_b$*), 3.94 (d, *J* = 13.8 Hz, 1H, C6-*H$_a$*H$_b$), 3.81 (s, 3H, C9-H$_3$).

^{13}CNMR(101 MHz, CDCL3) δ 164.23 (C-F, d, J = 247.2 Hz), 134.41 (C4), 131.74 (C7), 130.37 (d, J = 9.1 Hz, C3), 125.57 (C8), 116.36 (d, J = 24.2, C2), 67.83 (C5), 48.14 (C6), 38.85 (C9).

IR ν_{max} (film)/cm^{-1}: 2931, 1566, 1493, 1422, 1250, 1045, 981, 877, 804.

HRMS: (ESI+) m/z calculated. C17H15F2N3OS [M+H]+ 348.0977; found 348.0973, Δ 1.18 ppm.

(3-Bromoprop-1-yn-1-yl)triisopropylsilane (**147**)

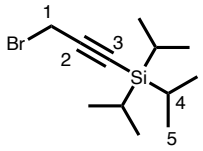

In a round bottom flask under argon was added a solution of lithium bis(trimethylsilyl)amide (2.20 mL, 2.20 mmol, 1 M in hexanes, 1.10 eq) and was diluted with dry diethyl ether (2.0 mL). The solution was then cooled to -78 °C and propargyl bromide (0.21 nL, 2.00 mL, 80% in toluene, 1.00 eq) was added dropwise. After stirring for 5 minutes, added triisopropylchlorosilane (0.43 mL, 2.00 mmol, 1.00 eq) dropwise and the reaction was warmed to -40 °C and stirred at that

temperature for 1 hour. The reaction was quenched at -40 °C with 10 mL of water and the aqueous layer was extracted twice with diethyl ether. The combined organic layers were then washed with brine and subsequently dried with Na2SO4 and filtered. The solvent was then removed under reduced pressure and the crude purified by flash chromaatography in 100% hexanes tp afford 381.0 mg (69.2%) of a colorless oil.

^{1}HNMR (400 MHz, CDCl3) δ 3.95 (s, 2H, C1-H_2), 1.07 (br s, 21H, 3 x C4-H + 6 x C5-H_3).

^{13}CNMR(101 MHz, CDCL3) δ 101.96 (C3), 89.29 (C2), 18.66 (C4), 15.17 (C5), 11.28 (C1).

Spectroscopic data matches literature.[6]

S-(3-(Triisopropylsilyl)prop-2-yn-1-yl) ethanethioate (**148**)

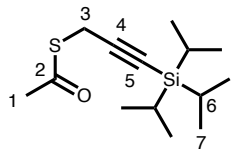

Bromide **147** (381.0 mg, 1.38 mmol, 1.00 eq) was dissolved in MeCN (2.8 mL, 0.50M) then added potassium ethanethioate (166.0 mg, 1.45 mmol, 1.05 eq) in one portion. The reaction was stirred at 20 °C for 18 hours, then filtered and the filtrate was concentrated under reduced pressure. The crude was carried on without further purification to yield 334.7 mg (89.4%) of a yellow oil.

^{1}HNMR (400 MHz, CDCl3) δ 3.71 (s, 2H, C3-H_2), 2.35 (s, 3H, C1-H_3), 1.05 (s, 21H, 3 x C4-H + 6 x C5-H_3).

^{13}CNMR(101 MHz, CDCL3) δ 194.24 (C2), 101.87 (C5), 84.46 (C4), 30.22 (C1), 19.05 (C6), 18.67 (C7), 11.27 (C3).

IR ν_{max} (film)/cm^{-1}: 2943, 2866, 2212, 1700, 1454, 132, 1032, 883, 676.

HRMS: (ESI+) m/z calculated. C14H26OSSi [M+H]+ 271.1526; found 271.1542, Δ 1.59 ppm.

3-(Triisopropylsilyl)prop-2-yne-1-thiol (149):

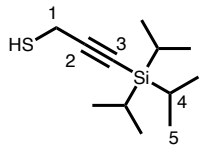

In a round bottom flask under argon, a suspension of lithium aluminum hydride (41.8 mg, 1.10 mmol, 1.00 eq) in diethyl ether (2.20 mL, 0.5M) was cooled to -30 °C. Then added thioacetate **148** (298.2 mg, 1.10 mmol, 1.00 eq) was addeddropwise and the reaction was stirred at -30 °C for 10 minutes before allowing to reach room temperature (22 °C). The reaction is stirred at 22 °C for 1 hour and then cooled to 0 °C and quenched with saaturated ammonium chloride solution, the organic layer was then separated and washed three times with water. The organic layer was then dried with Na2SO4 and solvent is removed with a stream of air flow. The crude is then used without further purification.

^{1}HNMR (400 MHz, CDCl3) δ 3.32 (d, J = 7.0 Hz, 2H, C1-H_2), 1.97 (t, J = 7.3 Hz, 1H, S-H), 1.06 (br s, 21H, 3 x C4-H + 6 x C5-H_3).

^{13}CNMR(101 MHz, CDCL3) δ 105.65 (C3), 83.72 (C2), 18.72 (C4), 13.55 (C5), 11.33 (C1).

IR ν_{max} (film)/cm^{-1}: 2942, 2892, 2865, 2174, 1463, 1383, 1240, 1030, 995, 882.

HRMS: (ESI-) m/z calculated. C12H24SSi [M-H]- 227.1295; found 227.1295, Δ 0.13 ppm.

(3-(Benzhydrylthio)prop-1-yn-1-yl)triisopropylsilane (**150**):

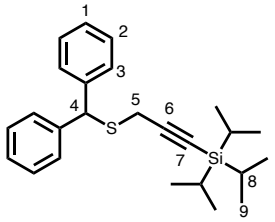

Using General procedure E: utilizing thiol **148** (142.0 mg mg, 0.54 mmol, 1.0 eq); for formation of mesylate used diphenylmethanol (100.0 mg, 0.54 mmol, 1.0 eq), TEA (0.08 mL, 0.54 mmol, 1 eq), MsCl (57 uL, 0.59 mmol, 1.10 eq). During reaction between thiol and mesylate, utilized DBU (0.08 mL, 0.0.54 mmol, 1.0 eq). Following removal of solvent and purification by FCC 100% in hexanes resulted in 59.6 mg (28.0%) of the product as a yellow oil.

^{1}HNMR (400 MHz, CDCl3) δ 7.43 (d, *J* = 7.6 Hz, 4H, 4 x C2-H), 7.31 (t, *J* = 7.5 Hz, 4H, 4 x C3-H), 7.24 (d, *J* = 6.9 Hz, 2H, 2 x C1-H), 5.50 (s, 1H, C4-H), 3.10 (s, 2H, C5-H_2), 1.15 – 1.05 (m, 21H, 3 x C8-H + 6 x C9-H_3).

^{13}CNMR(101 MHz, , CDCl3) δ 140.63 (C_{AR}), 128.74 (C_{AR}), 128.61 (C_{AR}), 127.46 (C_{AR}), 102.2 (C7), 83.3 (C6), 53.15 (C4), 21.24 (C8), 18.84 (C5), 11.45 (C9).

IR ν_{max} (film)/cm^{-1}: 2941, 2864, 2169, 1600, 1494, 1463, 1383, 1225, 1075, 1024, 995, 919, 882, 748, 699.

HRMS: (ESI+) m/z calculated. C25H34SSi [M+H]+ 395.2223; found 395.2222, Δ 0.40 ppm.

(3-((Bis(3-chlorophenyl)methyl)thio)prop-1-yn-1-yl)triisopropylsilane (151):

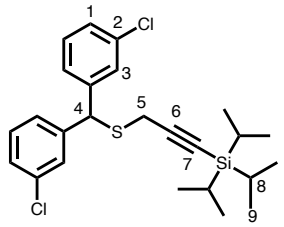

Using General procedure E: utilizing thiol **148** (90.2 mg, 0.39 mmol, 1.0 eq); for formation of mesylate used bis(3-chlorophenyl)methanol (100.0 mg, 0.39 mmol, 1.0 eq), TEA (0.06 mL, 0.40 mmol, 1 eq), MsCl (42 uL, 0.44 mmol, 1.10 eq). During reaction between thiol and mesylate, tilized DBU (0.06 mL, 0.40 mmol, 1.0 eq). Following removal of solvent and purification by FCC 100% in hexanes resulted in 88.8 mg (48.5%) of the product as a yellow oil.

^{1}HNMR (400 MHz, CDCl3) δ 7.39 (s, 2H, 2 x C3-H), 7.33 – 7.20 (m, 6H, 6 x C_{AR}-H), 5.43 (s, 1H, C4-H), 3.14 (s, 2H, C5-H_2), 1.12 (s, 21H, 3 x C8-H + 6 x C9-H_3).

^{13}CNMR(101 MHz, CDCL3) δ 142.05 (C_{AR}), 134.74 (C_{AR}), 130.14 (C_{AR}), 128.67 (C_{AR}), 127.98 (C_{AR}), 126.70 (C_{AR}), 102.51 (C7), 85.18 (C6), 52.12 (C4), 21.31 (C8), 18.83 (C5), 11.40 (C9).

IR ν_{max} (film)/cm^{-1}: 2942, 2864, 2169, 1590, 1572, 1473, 1425, 1227, 1079, 1023, 997, 919, 883, 786.

HRMS: (ESI+) m/z calculated. C25H32Cl2SSi [M+H]+ 463.1444; found 463.1440, Δ 0.80 ppm.

(3-((Bis(4-chlorophenyl)methyl)thio)prop-1-yn-1-yl)triisopropylsilane (**152**):

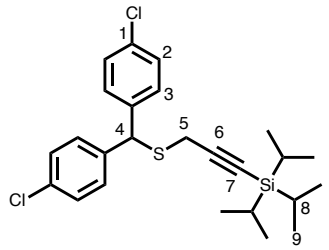

Using General procedure E: utilizing thiol **148** (90.2 mg, 0.39 mmol, 1.0 eq); for formation of mesylate used bis(4-chlorophenyl)methanol (100.0 mg, 0.39 mmol, 1.0 eq), TEA (0.06 mL, 0.40 mmol, 1 eq), MsCl (42 uL, 0.44 mmol, 1.10 eq). During reaction between thiol and mesylate, tilized DBU (0.06 mL, 0.40 mmol, 1.0 eq). Following removal of solvent and purification by FCC 100% in hexanes resulted in 53.1 mg (29.0%) of the product as a yellow oil.

^{1}HNMR (400 MHz, CDCl3) δ 7.37 – 7.24 (m, 8H, 8 x C_{AR}-H), 5.44 (s, 1H, C4-H), 3.11 (s, 2H, C5-H_2), 1.11 (br s, 21H, 3 x C8-H + 6 x C9-H_3).

^{13}CNMR(101 MHz, CDCL3) δ 138.71 (C_{AR}), 133.48 (C_{AR}), 129.86 (C_{AR}), 129.02 (C_{AR}), 102.68 (C7), 84.95 (C6), 51.76 (C4), 21.26 (C8), 18.77 (C5), 11.39 (C9).

IR ν_{max} (film)/cm^{-1}: 2942, 2864, 2169, 1489, 1463, 1403, 1226, 1090, 1015, 883, 798, 678.

HRMS: (ESI+) m/z calculated. C25H32Cl2SSi [M+H]+ 463.1444; found 463.1439, Δ 0.84 ppm.

(3-(Benzhydrylsulfinyl)prop-1-yn-1-yl)triisopropylsilane (156):

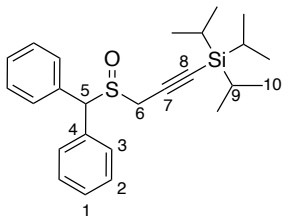

Following General procedure G: used sulfide **150** (116.0 mg, 0.29 mmol, 1.00 eq) and mCPBA (71.0 mg, 0.31 mmol, 1.05 eq). The crude product wass purified by FCC ramping up from 0->20% ethyl acetate in hexane to yield 53.1 mg (44.0%) of a colorless oil.

^{1}HNMR (400 MHz, CDCl3) δ 7.45 – 7.31 (m, 10H, 10 x C_{AR}-H), 5.35 (s, 1H, C5-H), 3.42 (s, 2H, C6-H_2), 1.14 (br s, 18H, 6 x C10-H_3), 1.11 – 1.03 (m, 3H, 3 x C9-H).

^{13}CNMR(101 MHz, CDCL3) δ 131.10 (C4), 130.03 (C3), 129.27 (C2), 128.4 (C1), 95.51 (C8), 90.76 (C7) 68.03 (C5), 41.59 (C6), 18.75 (C9), 11.28 (C10).

IR ν_{max} (film)/cm^{-1}: 2942, 2864, 2170, 1719, 1575, 1498, 1462, 1451, 1241, 1066, 1032, 882, 748, 698.

HRMS: (ESI+) m/z calculated. C25H34OSSi [M+Na]+ 433.1992; found 433.1984, Δ 1.89 ppm.

1-Benzyl-4-(bromomethyl)-1H-1,2,3-triazole (**159**)

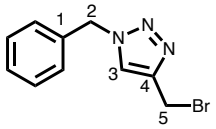

In a round bottom flask, **157** (1.00 g, 5.29 mmol, 1.0 eq) was dissolved in DCM (26.4 mL, 0.2M) and cooled to 0 °C under argon, to this solution was added triphenyl phosphine (1.53 g, 5.83 mmol, 1.1 eq) in one portion and carbon tetrabromide (1.93 mg, 5.83 mmol, 1.2 eq) portionwise over 2 minutes. The reaction was allowed to stir at 0 °C for 5 minutes and subsequently removed from the ice bath and allowed to reach room temperature. The reaction mixture was stirred at 20 °C for 24 h before being quenched with 10% sodium thiosulphate solution. The aqeous layer was extracted twice with DCM and the combined organic layers were dried with Na2SO4, the solvent was removed under reduced pressure and the crude purified by flash column chromatogrpahy ramping up 0 -> 35% ethyl acetate in hexanes to yield 1.029 g (77.2%) of a white solid.

^{1}HNMR (400 MHz, MeOH-d4) δ 8.00 (s, 1H, C3-H), 7.36 – 7.30 (m, 5H, 5 x C_{AR}-H), 5.59 (s, 2H, C2-H_2), 4.62 (s, 2H, C5-H_2).

^{13}CNMR(101 MHz, MeOHd4) δ 145.1(C1), 135.4 (C4), 128.7 (C_{AR}), 128.3 (C_{AR}), 127.5 (C_{AR}), 123.9 (C3), 53.5 (C2), 20.1 (C5).

IR ν_{max} (film)/cm^{-1}: 3118, 3076, 3035, 1551, 1455, 1074, 1226, 1216, 1052, 823, 746, 722, 701.

HRMS: (ESI^{+}) m/z calculated. $C_{10}H_{10}BrN_32[M+H]^{+}$252.1150; found at 252.0126, Δ 1.80 ppm.

MP: 124-125

S-((1-Benzyl-1H-1,2,3-triazol-4-yl)methyl) ethanethioate (**160**)

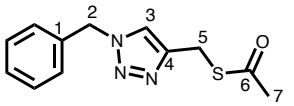

Bromide **159** (378.0 mg, 1.50 mmol, 1.00 eq) was dissolved in MeCN (5.9 mL, 0.25M). Then added potassium ethanethioate (205.6 mg, 1.80 mmol, 1.20 eq) in one portion and the reaction was stirred at 20 °C for 18 hours. Subsequently filtered and the filtrate was concentrated under reduced pressure. The crude was then purified by flash column chromatogrpahy ramping up 0 -> 40% ethyl acetate in hexane to yield 298.3 mg (80.4%) of a white solid.

^{1}HNMR (400 MHz, CDCl3) δ 7.40 (s, 1H, C3-H), 7.37 (d, *J* = 6.4 Hz, 3H, 3 x C_{AR}-H), 7.28 – 7.23 (m, 2H, 2 x C_{AR}-H), 5.48 (s, 2H, C2-H_2), 4.16 (s, 2H, C5-H_2), 2.33 (s, 3H, C7-H_3).

^{13}CNMR(101 MHz, CDCL3) δ 195.41 (C6), 144.91 (C1), 134.64 (C4), 129.23 (C_{AR}), 128.87 (C_{AR}), 128.19 (C_{AR}), 122.39 (C3), 54.28 (C2), 30.45 (C5), 24.12 (C7).

IR ν_{max} (film)/cm^{-1}: 3064, 1689, 1551, 1456, 1218, 1133, 1049, 959, 753, 702, 627.

HRMS: (ESI^{+}) m/z calculated. $C_{12}H_{13}N_3OS$ $[M+H]^+$ 248.0850; found at 248.046, Δ 2.50 ppm.

MP: 87-88

S-((1-Phenyl-1H-1,2,3-triazol-4-yl)methyl) ethanethioate (**162**)

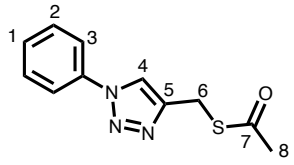

In a round bottom flask, **158** (250.0 mg, 1.43 mmol, 1.0 eq) was dissolved in DCM (7.0 mL, 0.2M) and cooled to 0 °C under argon, to this solution was added triphenyl phosphine (412.0 mg, 1.57 mmol, 1.1 eq) in one portion and carbon tetrabromide (520.6 mg, 1.57 mmol, 1.2 eq) portionwise over 2 minutes. The reaction was allowed to stir at 0 °C for 5 minutes and subsequently removed from the ice bath and allowed to reach room temperature. The reaction mixture was stirred at 20 °C for 24 h before being quenched with 10% sodium thiosulphate solution. The aqeous layer was extracted twice with DCM, and the combined organic layers dried with Na2SO4, the solvent was removed under reduced pressure. The crude was then redissolved in MeCN (7 mL) and potassium ethanethioate (195.6 mg, 1.71 mmol, 1.20 eq) was added in one portion. The reaction was stirred for 18 hours, then filtered and the filtrate was concentrated under reduced pressure. The crude was then purified by flash column chromatogrpahy ramping up 0 -> 15% ethyl acetate in hexanes to yield 58.8 mg (17.7%) of a coloreless oil.

^{1}HNMR (400 MHz, CDCl3) δ 7.94 (s, 1H, C4-H), 7.71 (d, *J* = 7.4 Hz, 2H, 2 x C3-H), 7.54 – 7.47 (m, 2H, 2 x C2-H), 7.47 – 7.38 (m, 1H, C1-H), 4.26 (s, 2H, C6-H_2), 2.37 (s, 3H, C8-H_3).

^{13}CNMR(101 MHz, CDCL3) δ 195.44 (C7), 145.27 (C_{AR}), 137.03 (C5), 129.79 (C_{AR}), 128.83 (C_{AR}), 120.76 (C_{AR}), 120.56 (C4)), 30.48 (C6), 24.09 (C8).

IR ν_{max} (film)/cm^{-1}: 3142, 1686, 1597, 1500, 1352, 1133, 1042, 956, 756, 688, 622.

Spectroscopic data matches literature.[7]

1-(Azidomethyl)-4-chlorobenzene (**163**):

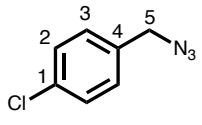

In a round bottom flask, added 1-(bromomethyl)-4-(tert-butyl)benzene (454.0 mg, 2.00 mmol, 1.0 eq) and dissolved in acetone:water (4:1; 10.0 mL; 0.2M) and subsequently added sodium azide (195.0 mg, 3.00 mmol, 1.50 eq) and stirred vigorously for 18 hours at 22 °C. Subsequently removed acetone through reduced pressure, and the aqueous layer was extracted with diethyl ether three times. The combined organic layers were then washed once with brine and were dried with Na2SO4. The crude was then concentrated and carried on without further purification, isolated 351.0 mg (92.7%) of colorless liquid.

^{1}HNMR (400 MHz, CDCl3) δ 7.36 (dt, *J* = 8.8, 2.6 Hz, 2H, 2 x C1-H), 7.25 (dt, *J* = 8.4, 2.2 Hz, 2H, 2 x C3-H), 4.31 (s, 2H, C5-H_2).

^{13}CNMR(101 MHz, CDCL3) δ 134.32 (C4), 133.98 (C1), 129.63 (C3), 129.15 (C2), 54.14 (C5).

IR ν_{max} (film)/cm^{-1}: 2931, 2092, 1598, 1492, 1248, 1090, 1016, 838, 796.

Spectroscopic data matches literature.[8]

1-(Azidomethyl)-4-(tert-butyl)benzene (**164**):

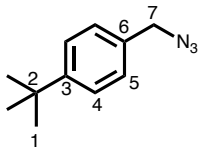

In a round bottom flask, added 1-(bromomethyl)-4-chlorobenzene (411.0 mg, 2.00 mmol, 1.0 eq) and dissolved in acetone:water (4:1; 10.0 mL; 0.2M). Subsequently added sodium azide (195.0 mg, 3.00 mmol, 1.50 eq) and stirred vigorously for 18 hours at 22 °C. Then removed acetone through reduced pressure, and extracted aqueous layer with diethyl ether three times, combined organic layers were then washed once with brine and were dried with Na_2SO_4 and filtered. The crude was then concentrated and carried on without further purification, isolated 303.1 mg (90.42%) of colorless liquid.

^{1}HNMR (400 MHz, CDCl3) δ 7.40 (d, *J* = 7.9 Hz, 2H, 2 x C5-H), 7.25 (d, *J* = 8.1 Hz, 2H, 2 x C4-H), 4.30 (s, 2H), 1.32 (s, 9H, 3 x C1-H_3).

^{13}CNMR(101 MHz, CDCL3) δ 151.46 (C3), 132.53 (C6), 128.13 (C5), 125.89 (C4), 54.66 (C7), 34.74 (C2), 31.42 (C1).

IR ν_{max} (film)/cm^{-1}: 2963, 2869, 2084, 1515, 1267, 1108, 802.

Spectroscopic data matches literature.[9]

S-((1-(4-Chlorobenzyl)-1H-1,2,3-triazol-4-yl)methyl) ethanethioate (165):

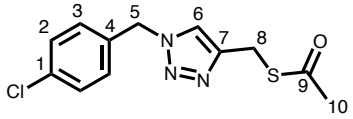

Following General procedure H: To alkyne **132** (170.0 mg, 1.49 mmol, 1.0 eq) was added copper sulfate pentahydrate (37.2 mg, 0.15 mmol, 0.10 eq) and sodium ascorbate (88.5 mg, 0.45 mmol, 0.30 eq), these were dissolved in 3.7 mL (THF) and 3.7 mL (Water). Then added azide **163** (262.1 mg, 1.56 mmol, 1.05 eq). The crude was purified ramping up from 0% -> 40% ethyl acetate in hexane to afford 287.6 mg (68.5%) of a white solid.

^{1}HNMR (400 MHz, CDCl3) δ 7.41 (s, 1H, C6-H), 7.35 (td, *J* = 9.0, 8.4, 2.6 Hz, 2H, 2 x C2-H), 7.20 (td, *J* = 8.5, 8.0, 2.3 Hz, 2H, 2 x C3-H), 5.45 (s, 2H, C5-H_2), 4.16 (s, 2H, C8-H_2), 2.33 (s, 3H, C10-H_3).

^{13}CNMR(101 MHz, CDCL3) δ 195.41 (C9), 145.14 (C4), 134.91 (C1), 133.14 (C_{AR}), 129.50 (C_{AR}), 129.42 (C_{AR}), 122.38 (C6), 53.51 (C5), 30.46 (C8), 24.08 (C10).

IR ν_{max} (film)/cm^{-1}: 3136, 1692, 1491, 1355, 1222, 1137, 1099, 954, 781, 623

HRMS: (ESI^{+}) m/z calculated. $C_{12}H_{12}ClN_3OS$ $[M+H]^{+}$ 282.0462; found at 282.0461, Δ 0.50 ppm.

MP: 96-97

S-((1-(4-(tert-Butyl)benzyl)-1H-1,2,3-triazol-4-yl)methyl) ethanethioate (**166**):

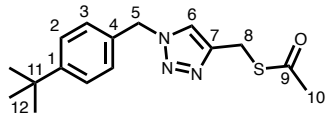

Following General procedure H: To alkyne **132** (180.0 mg, 1.58 mmol, 1.0 eq) was added copper sulfate pentahydrate (39.4 mg, 0.16 mmol, 0.10 eq) and sodium ascorbate (93.7 mg, 0.47 mmol, 0.30 eq). These were dissolved in 3.9 mL (THF) and 3.9 mL (Water), then added azide **164** (313.3 mg, 1.66 mmol, 1.05 eq). The crude was purified ramping up from 0% -> 40% ethyl acetate in hexane to afford 320.6 mg (67.0%) of a white solid.

^{1}HNMR (400 MHz, CDCl3) δ 7.40 (s, 1H, C6), 7.40 – 7.35 (m, 2H, 2 x C3-H), 7.24 – 7.16 (m, 2H, 2 x C2-H), 5.44 (s, 2H, C5-H_2), 4.16 (s, 2H, C8-H_2), 2.32 (s, 3H C10-H_3), 1.31 (s, 9H, 3 x C12-H_3).

^{13}CNMR(101 MHz, CDCL3) δ 195.38 (C9), 151.95 (C1), 144.72 (C4), 131.60 (C7), 128.01 (C3), 126.12 (C2), 122.34 (C6), 53.94 (C8), 34.72 (C8), 31.33 (C11), 30.42 (C12), 24.10 (C10).

IR ν_{max} (film)/cm^{-1}: 2962, 2868, 2689, 1461, 1354, 1133, 1047, 958, 786, 626.

HRMS: (ESI^{+}) m/z calculated. $C_{16}H_{21}N_3OS$ $[M+H]^+$ 304.1478; found at 304.1473, Δ 1.55 ppm.

MP: 85-86

1901-Benzyl-4-(((bis(4-fluorophenyl)methyl)thio)methyl)-1H-1,2,3-triazole (167)

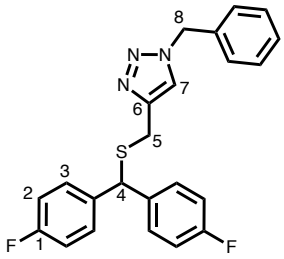

Using General procedure D: utilizing thiolacetate **160** (24.6 mg, 0.12 mmol, 1.0 eq) for formation of thiol; 4,4'-(bromomethylene)bis(fluorobenzene) (34.0 mg, 0.12 mmol, 1.0 eq). Utilized DBU (0.02 mL, 0.12 mmol, 1.0 eq). Following removal of solvent and purification by FCC 0->50% ethyl acetate in hexanes resulted in 14.9 mg (30.5%) of the product as a colorless oil.

^{1}HNMR (400 MHz, CDCl3) δ 7.42 – 7.35 (m, 3H, C7-H + 2 x C_{AR}-H), 7.35 – 7.28 (m, 4H, 4 x C2-H), 7.28 – 7.24 (m, 2H, 2 x C_{AR}-H), 7.22 (s, 1H, C_{AR}-H), 7.01 – 6.93 (m, 4H, 4 x C3-H), 5.48 (s, 2H, C8-H_2), 5.13 (s, 1H, C4-H), 3.62 (s, 2H, C5-H_2).

^{13}CNMR(101 MHz, CDCL3) δ 162.02 (d, J = 247.5 Hz, C1), 145.72 (C_{AR}), 136.61 (C_{AR}), 134.68 (C6), 130.11 (C_{AR}), 129.29 (C_{AR}), 128.97 (C_{AR}), 128.26 (C_{AR}), 121.78 (C7), 115.61 (d, J = 21.2 Hz, C2), 54.34 (C8), 52.31 (C4), 26.71 (C5).

IR ν_{max} (film)/cm^{-1}: 3064, 1602, 1505, 1223, 1157, 1047, 835, 572, 530.

HRMS: (ESI^{+}) m/z calculated. $C_{23}H_{19}F_2N_3S$ $[M+H]^+$ 408.1341; found at 408.1338, Δ 0.56 ppm.

4-(((Bis(4-fluorophenyl)methyl)thio)methyl)-1-phenyl-1H-1,2,3-triazole (168)

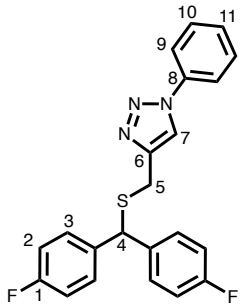

Using General procedure D: utilizing thiolacetate **162** (20.1 mg, 0.11 mmol, 1.0 eq) for formation of thiol; 4,4'-(bromomethylene)bis(fluorobenzene) (0.0 mg, 0.11 mmol, 1.0 eq). Utilized DBU (0.02 mL, 0.12 mmol, 1.0 eq). Following removal of solvent and purification by FCC 0->50% ethyl acetate in hexanes resulted in 13.2 mg (31.9%) of the product as a colorless oil.

^{1}HNMR (400 MHz, CDCl3) δ 7.78 (s, 1H, C7-H) , 7.70 (d, *J* = 8.1 Hz, 2 x C9-H), 7.53 (t, *J* = 7.8 Hz, 2H, 2 x C10-H), 7.45 (t, *J* = 7.4 Hz, 1H, C11-H), 7.42 – 7.36 (m, 4H, 4 x C2-H), 7.01 (t, *J* = 8.7 Hz, 4H, 4 x C3-H), 5.27 (s, 1H, C4-H) , 3.74 (s, 1H, C5-H) .

^{13}CNMR(101 MHz, CDCL3) δ 162.09 (d, J = 248.5 Hz, C1), 146.21 (C_{AR}), 137.09 (C_{AR}), 136.63 (C6), 130.18 (C_{AR}), 130.18 (C_{AR}), 129.93 (C_{AR}), 128.94 (C_{AR}), 120.52 (C7), 115.68 (d, J = 22.2 Hz, C2), 52.41 (C4), 26.64 (C5).

IR ν_{max} (film)/cm^{-1}: 3073, 1600, 1504, 1224, 1157, 1043, 835, 758, 835,572.

HRMS: (ESI^{+}) m/z calculated. $C_{22}H_{17}F_2N_3S$ $[M+H]^+$ 394.1184; found at 394.1179, Δ 1.24 ppm.

1-Benzyl-4-((((4-chlorophenyl)(phenyl)methyl)thio)methyl)-1H-1,2,3-triazole (169)

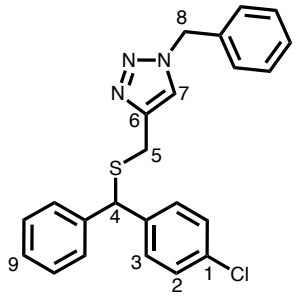

Using General procedure D: utilizing thiolacetate **160** (20.0 mg, 0.097 mmol, 1.0 eq) for formation of thiol; 1-chloro-4-(chloro(phenyl)methyl)benzene (23.1 mg, 0.097 mmol, 1.0 eq). Utilized DBU (0.02 mL, 0.12 mmol, 1.0 eq). Following removal of solvent and purification by FCC 0->50% ethyl acetate in hexanes resulted in 13.1 mg (33.1%) of the product as a colorless oil.

^{1}HNMR (400 MHz, CDCl3) δ 7.37 (s, 2H, 2 x C2-H), 7.35 – 7.21 (m, 12H, 12 x C_{AR}-H), 7.19 (s, 1H, C9-H), 5.47 (s, 2H, C8-H_2), 5.11 (s, 1H, C4-H), 3.64 (s, 2H, C5-H_2).

^{13}CNMR(101 MHz, CDCL3) δ 145.71 (C_{AR}), 140.50 (C_{AR}), 139.62 (C_{AR}), 134.70 (C_{AR}), 133.11 (C7), 129.94 (C_{AR}), 129.28 (C_{AR}), 128.94 (C_{AR}), 128.82 (C_{AR}), 128.43 (C_{AR}), 128.24 (C_{AR}), 127.57 (C_{AR}), 121.84 (C6), 54.31 (C8), 53.24 (C4), 26.76 (C5).

IR ν_{max} (film)/cm^{-1}: 3029, 1489, 1453, 1407, 1220, 1089, 1047, 1014, 803, 748, 698, 605, 516.

HRMS: (ESI^{+}) m/z calculated. $C_{23}H_{20}ClN_3S$ $[M+H]^+$ 406.1139; found at 406.1136, Δ 0.89 ppm.

4-((((4-Chlorophenyl)(phenyl)methyl)thio)methyl)-1-phenyl-1H-1,2,3-triazole (170)

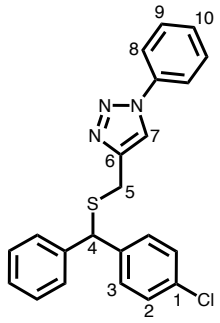

Using General procedure D: utilizing thiolacetate **160** (20.1 mg, 0.11 mmol, 1.0 eq) for formation of thiol; 1-chloro-4-(chloro(phenyl)methyl)benzene (24.9 mg, 0.11 mmol, 1.0 eq). Utilized DBU (0.02 mL, 0.12 mmol, 1.0 eq). Following removal of solvent and purification by FCC 0->50% ethyl acetate in hexanes resulted in 10.7 mg (25.9%) of the product as a colorless oil.

^{1}HNMR (400 MHz, CDCl3) δ 7.73 (s, 1H, C7-H), 7.69 (d, *J* = 8.1 Hz, 2H, 2 x C8-H), 7.53 (t, *J* = 7.8 Hz, 2H, 2 x C9-H), 7.43 – 7.36 (m, 4H, 2 x C2-H + C10-H + C_{AR}-H), 7.35 – 7.21 (m, 6H 2 x C3-H + 4 x C_{AR}-H), 5.24 (s, 1H, C4-H), 3.76 (s, 2H, C5-H_2).

^{13}CNMR(101 MHz, CDCL3) δ 146.21 (C_{AR}), 140.54 (C_{AR}), 137.04 (C_{AR}), 139.65 (C_{AR}), 133.22 (C6), 130.16 (C_{AR}), 130.01 (C_{AR}), 129.99 (C_{AR}), 129.91 (C_{AR}), 128.88 (C_{AR}), 128.49 (C_{AR}), 127.66 (C_{AR}), 120.54 (C7), 120.09 (C_{AR}), 53.40 (C4), 26.72 (C5).

IR ν_{max} (film)/cm^{-1}: 3061, 1598, 1489, 1089, 1043, 757, 689.

HRMS: (ESI^{+}) m/z calculated. $C_{22}H_{18}ClN_3S$ $[M+H]^{+}$ 392.0983; found at 392.0980, Δ 0.61 ppm.

1-Benzyl-4-((((3-bromophenyl)(phenyl)methyl)thio)methyl)-1H-1,2,3-triazole (171):

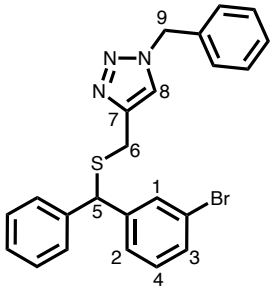

Using General procedure E: utilizing thiolacetate **160** (49.5 mg, 0.20 mmol, 1.0 eq) for formation of thiol; for formation of mesylate used (3-bromophenyl)(phenyl)methanol (52.6 mg, 0.20 mmol, 1.0 eq), TEA (0.03 mL, 0.20 mmol, 1 eq), MsCl (16 uL, 0.22 mmol, 1.10 eq). During reaction between thiol and mesylate, tilized DBU (0.03 mL, 0.20 mmol, 1.0 eq). Following removal of solvent and purification by FCC 0->50% ethyl acetate in hexanes resulted in 38.2 mg (42.4%) of the product as a colorless oil.

^{1}HNMR (400 MHz, CDCl3) δ 7.43 – 7.36 (m, 5H, C8-H + C3-H + 3 x C_{AR}-H), 7.35 – 7.29 (m, 2H, C1-H + C_{AR}-H), 7.29 – 7.23 (m, 7H, C4-H + 6 x C_{AR}-H), 7.19 (s, 1H, C2-H), 5.48 (s, 2H, C9-H_2), 5.09 (s, 1H, C5-H), 3.64 (s, 2H, C6-H_2).

^{13}CNMR(101 MHz, CDCL3) δ 145.66 (C_{AR}), 143.44 (C_{AR}), 140.27 (C_{AR}), 134.70 (C_{AR}), 131.49 (C8), 130.51 (C_{AR}), 130.23 (C_{AR}), 129.29 (C_{AR}), 128.95 (C_{AR}), 128.84 (C_{AR}), 128.47 (C_{AR}), 128.25 (C_{AR}), 127.65 (C_{AR}), 127.28 (C_{AR}), 122.74 (C7), 121.84(C_{AR}), 54.32 (C9), 53.44 (C5), 26.81 (C6).

IR ν_{max} (film)/cm^{-1}: 3029, 1453, 1221, 1072, 1047, 1010, 802, 749

HRMS: (ESI^{+}) m/z calculated. $C_{23}H_{20}BrN_3S$ $[M+H]^{+}$ 450.0634; found at 450.0633, Δ 0.33 ppm.

1-Benzyl-4-((((4-bromophenyl)(phenyl)methyl)thio)methyl)-1H-1,2,3-triazole (172):

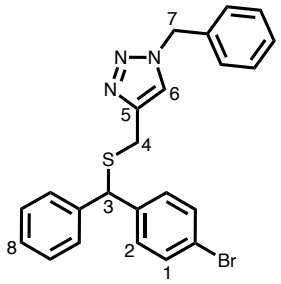

Using General procedure E: utilizing thiolacetate **160** (49.5 mg, 0.20 mmol, 1.0 eq) for formation of thiol; for formation of mesylate used (4-bromophenyl)(phenyl)methanol (52.6 mg, 0.20 mmol, 1.0 eq), TEA (0.03 mL, 0.20 mmol, 1 eq), MsCl (16 uL, 0.22 mmol, 1.10 eq). During reaction between thiol and mesylate, tilized DBU (0.03 mL, 0.20 mmol, 1.0 eq). Following removal of solvent and purification by FCC 0->50% ethyl acetate in hexanes resulted in 39.8 mg (44.2%) of the product as a colorless oil.

^{1}HNMR (400 MHz, CDCl3) δ 7.53 (t, *J* = 1.7 Hz, 1H, C6-H), 7.42 – 7.19 (m, 11 x C_{AR}-H + C1-H + C2-H), 7.14 (t, *J* = 7.6 Hz, 1H, C8-H), 5.48 (s, 2H, C7-H_2), 5.09 (s, 1H, C3-H), 3.65 (s, 2H, C4-H_2).

^{13}CNMR(101 MHz, CDCL3) δ 145.72 (C_{AR}), 140.43 (C_{AR}), 140.17 (C_{AR}), 134.71 (C5), 131.78 (C_{AR}), 130.32 (C_{AR}), 129.30 (C_{AR}), 128.96 (C_{AR}), 128.82 (C_{AR}), 128.43 (C_{AR}), 128.26 (C_{AR}), 127.60 (C_{AR}), 121.85 (C_{AR}), 121.26 (C6), 54.34 (C7), 53.31 (C3), 26.77 (C4).

IR ν_{max} (film)/cm^{-1}: 3061, 1586, 1566, 1453, 1341, 1219, 1073, 1046, 744, 701.

HRMS: (ESI^{+}) m/z calculated. $C_{23}H_{20}BrN_3S$ $[M+H]^+$ 450.0634; found at 450.0632, Δ 0.38 ppm.

1-Benzyl-4-((((3-chlorophenyl)(phenyl)methyl)thio)methyl)-1H-1,2,3-triazole (**173**):

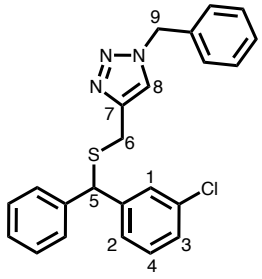

Using General procedure E: utilizing thiolacetate **160** (49.5 mg, 0.20 mmol, 1.0 eq) for formation of thiol; for formation of mesylate used (3-chloromophenyl)(phenyl)methanol (43.7 mg, 0.20 mmol, 1.0 eq), TEA (0.03 mL, 0.20 mmol, 1 eq), MsCl (16 uL, 0.22 mmol, 1.10 eq). During reaction between thiol and mesylate, tilized DBU (0.03 mL, 0.20 mmol, 1.0 eq). Following removal of solvent and purification by FCC 0->50% ethyl acetate in hexanes resulted in 42.0 mg (51.7%) of the product as a colorless oil.

^{1}HNMR (400 MHz, CDCl3) δ 7.42 – 7.32 (m, 6H, C1-H + C3-H + 4 x C_{AR}-H), 7.31 – 7.23 (m, 6H, C4-H + 5 x C_{AR}-H), 7.23 – 7.17 (m, 3H, C2-H + 2 x C_{AR}-H), 5.48 (s, 2H, C9-H_2), 5.10 (s, 1H, C5-H), 3.65 (s, 2H, C6-H_2).

^{13}CNMR(101 MHz, CDCL3) δ 145.67 (C_{AR}), 143.16 (C_{AR}), 140.29 (C_{AR}), 134.70 (C_{AR}), 134.51 (C7), 129.93 (C_{AR}), 129.28 (C_{AR}), 128.94 (C_{AR}), 128.84 (C_{AR}), 128.56 (C_{AR}), 128.47 (C_{AR}), 128.24 (C_{AR}), 127.64 (C_{AR}), 127.58 (C_{AR}), 126.81 (C_{AR}), 121.85 (C8), 54.31 (C9), 53.46 (C5), 26.80 (C6).

IR ν_{max} (film)/cm^{-1}: 3061, 1592, 1571, 1453, 1220, 1078, 1046,894, 782, 745, 704.

HRMS: (ESI^{+}) m/z calculated. $C_{23}H_{20}ClN_3S$ $[M+H]^{+}$ 406.1139; found at 406.1135, Δ 0.94 ppm.

1-Benzyl-4-(((phenyl(p-tolyl)methyl)thio)methyl)-1H-1,2,3-triazole (**174**):

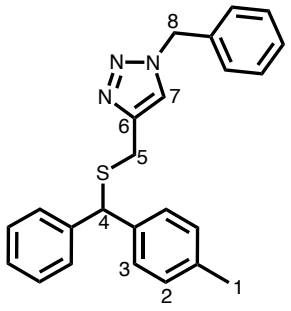

Using General procedure E: utilizing thiolacetate **165** (93.8 mg, 0.33 mmol, 1.0 eq) for formation of thiol; for formation of mesylate used (4-methylmophenyl)(phenyl)methanol (65.4 mg, 0.33 mmol, 1.0 eq), TEA (0.05 mL, 0.33 mmol, 1 eq), MsCl (26 uL, 0.36 mmol, 1.10 eq). During reaction between thiol and mesylate, tilized DBU (0.05 mL, 0.33 mmol, 1.0 eq). Following removal of solvent and purification by FCC 0->50% ethyl acetate in hexanes resulted in 47.1 mg (33.7%) of the product as a colorless solid.

^{1}HNMR (400 MHz, CDCl3) δ 7.43 – 7.33 (m, 5H, C7-H + 4 x C_{AR}-H), 7.30 – 7.23 (m, 6H, 6 x C_{AR}-H), 7.22 – 7.15 (m, 2H, 2 x C3-H), 7.08 (d, *J* = 7.9 Hz, 2H, 2 x C2-H), 5.47 (s, 2H, C8-H_2), 5.08 (s, 1H, C4-H), 3.64 (s, 2H, C5-H_2), 2.30 (s, 3H, C1-H_3).

^{13}CNMR(101 MHz, CDCL3) δ 145.90 (C_{AR}), 141.17 (C_{AR}), 137.94 (C_{AR}), 137.06 (C_{AR}), 134.78 (C6), 129.39 (C_{AR}), 129.25 (C_{AR}), 128.89 (C_{AR}), 128.66 (C_{AR}), 128.47 (C_{AR}), 128.39 (C_{AR}), 128.21 (C_{AR}), 127.29 (C_{AR}), 121.89 (C7), 54.27 (C8), 53.75 (C4), 26.83 (C5), 21.18 (C1).

IR ν_{max} (film)/cm^{-1}: 3028, 1510, 1495, 1453, 1220, 1046, 798, 733, 698.

HRMS: (ESI^{+}) m/z calculated. $C_{24}H_{23}N_3S$ $[M+H]^{+}$ 386.1686; found at 386.1682, Δ 1.01 ppm.

1-(4-Chlorobenzyl)-4-(((phenyl(p-tolyl)methyl)thio)methyl)-1H-1,2,3-triazole (175):

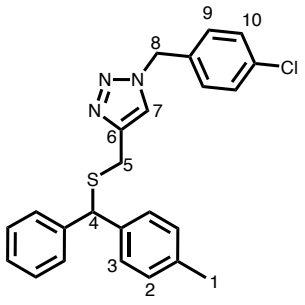

Using General procedure E: utilizing thiolacetate **160** (82.4 mg, 0.33 mmol, 1.0 eq) for formation of thiol; for formation of mesylate used (4-methylmophenyl)(phenyl)methanol (65.4 mg, 0.33 mmol, 1.0 eq), TEA (0.05 mL, 0.33 mmol, 1 eq), MsCl (26 uL, 0.36 mmol, 1.10 eq). During reaction between thiol and mesylate, tilized DBU (0.05 mL, 0.33 mmol, 1.0 eq). Following removal of solvent and purification by FCC 0->50% ethyl acetate in hexanes resulted in 18.0 mg (14.0%) of the product as a white solid.

^{1}HNMR (400 MHz, CDCl3) δ 7.40 – 7.31 (m, 4H, C7-H + 2 x C10-H + C_{AR}-H), 7.30 – 7.23 (m, 4H, 4 x C_{AR}-H), 7.22 – 7.15 (m, 4H, 2 x C9-H + 2 x C3-H), 7.09 (d, *J* = 7.9 Hz, 2H, 2 x C2-H), 5.42 (s, 2H, C8-H_2), 5.10 (s, 1H, C4-H), 3.64 (s, 2H, C5-H_2), 2.29 (s, 3H, C1-H_3).

^{13}CNMR(101 MHz, CDCL3) δ 146.10 (C_{AR}), 141.14 (C_{AR}), 137.90 (C_{AR}), 137.07 (C_{AR}), 134.88 (C_{AR}), 133.26 (C6), 129.49 (C_{AR}), 129.41 (C_{AR}), 129.38 (C_{AR}), 128.65 (C_{AR}), 128.43 (C_{AR}), 128.34 (C_{AR}), 127.30 (C_{AR}), 121.83 (C7), 53.80 (C8), 53.45 (C4), 26.76 (C5), 21.15 (C1).

IR ν_{max} (film)/cm^{-1}: 3025, 2920, 1510, 1492, 1451, 1341, 1088, 1046, 1016, 805, 733, 698.

HRMS: (ESI^{+}) m/z calculated. $C_{24}H_{22}ClN_3S$ $[M+H]^+$ 420.1296; found at 420.1294, Δ 0.40 ppm.

1-(4-(tert-Butyl)benzyl)-4-(((phenyl(p-tolyl)methyl)thio)methyl)-1H-1,2,3-triazole (176):

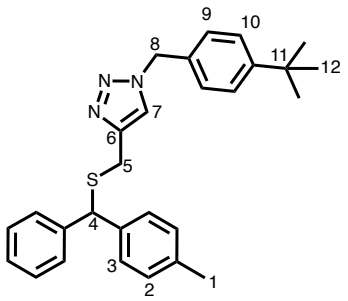

Using General procedure E: utilizing thiolacetate **166** (101.0 mg, 0.33 mmol, 1.0 eq) for formation of thiol; for formation of mesylate used (4-methylmophenyl)(phenyl)methanol (65.4 mg, 0.33 mmol, 1.0 eq), TEA (0.05 mL, 0.33 mmol, 1 eq), MsCl (26 uL, 0.36 mmol, 1.10 eq). During reaction between thiol and mesylate, tilized DBU (0.05 mL, 0.33 mmol, 1.0 eq). Following removal of solvent and purification by FCC 0->50% ethyl acetate in hexanes resulted in 18.0 mg (14.0%) of the product as a colorless solid.

^{1}HNMR (400 MHz, CDCl3) δ 7.42 – 7.33 (m, 4H, C7-H + 3 x C_{AR}-H), 7.29 – 7.22 (m, 4H, 2 x C10-H + 2 x C_{AR}-H), 7.22 – 7.16 (m, 4H, 2 x C9-H + 2 x C3-H), 7.08 (d, *J* = 7.8 Hz, 2H, 2 x C2-H_2), 5.43 (s, 2H, C8-H_2), 5.08 (s, 1H, C4-H), 3.64 (s, 2H, C5-H_2), 2.29 (s, 3H, C1-H_3), 1.31 (s, 9H, 3 x C12-H_3).

^{13}CNMR(101 MHz, CDCL3) δ 152.02 (C_{AR}), 145.73 (C_{AR}), 141.18 (C_{AR}), 137.95 (C_{AR}), 137.03 (C_{AR}), 131.74 (C6), 129.38 (C_{AR}), 128.65 (C_{AR}), 128.47 (C_{AR}), 128.38 (C_{AR}), 128.03 (C_{AR}), 127.28 (C_{AR}), 126.16 (C_{AR}), 121.87 (C7), 53.97 (C8), 53.70 (C4), 34.77 (C11), 31.38 (C12), 26.82 (C5), 21.18 (C1).

IR ν_{max} (film)/cm^{-1}: 2962, 1510, 1451, 1046, 786, 698.

HRMS: (ESI$^+$) m/z calculated. $C_{28}H_{31}N_3S$ $[M+H]^+$ 442.2312; found at 442.2307, Δ 0.93 ppm.

1-Benzyl-4-(((bis(4-chlorophenyl)methyl)sulfinyl)methyl)-1H-1,2,3-triazole (177):

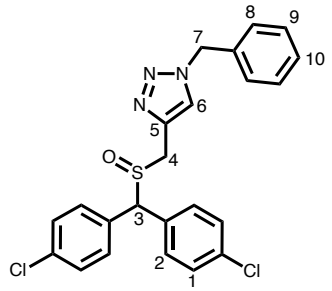

Compound **177** was prepared through General procedure G. Starting from 1-benzyl-4-(((bis(4-chlorophenyl)methyl)thio)methyl)-1H-1,2,3-triazole (20.0 mg, 0.045 mmol, 1.0 eq) and mCPBA (8.2 mg, 0.048 mmol, 1.05 eq). Following concentration under reduced pressure, the sulfoxide was purified by FCC 0->50% ethyl acetate in hexanes to yield 15.8 mg (76.2%) of the product as a white solid.

^{1}HNMR (400 MHz, CDCl3) δ 7.58 (s, 1H, C6-H), 7.46 (dd, *J* = 8.6, 2.4 Hz, 2H, 2 x C2-H), 7.42 – 7.35 (m, 5H, 2 x C2-H + 2 x C8-H + C10-H), 7.35 – 7.26 (m, 6H, 2 x C9-H + 4 x C2-H), 5.55 (d, *J* = 14.9 Hz, 2H, C7-H), 4.96 (s, 1H, C3-H), 4.00 (d, *J* = 14.1 Hz, 1H, C4-H_aH_b), 3.76 (d, *J* = 14.1 Hz, 1H, C4-H_aH_b).

^{13}CNMR(101 MHz, CDCL3) δ 136.45 (C_{AR}), 134.85 (C_{AR}), 134.35 (C_{AR}), 133.53 (C5), 131.09 (C_{AR}), 131.09 (C_{AR}), 130.64 (C_{AR}), 129.69 (C_{AR}), 128.31 (C_{AR}), 124.85 (C6), 67.61 (C3), 54.55 (C7), 45.27 (C4).

IR ν_{max} (film)/cm^{-1}: 3065, 1491, 1406, 1090, 1044, 1014, 800, 729, 525.

HRMS: (ESI$^+$) m/z calculated. $C_{23}H_{19}Cl_2N_3OS$ $[M+H]^+$ 456.0699; found at 456.0698, Δ 0.13 ppm.

4-(((Bis(3-chlorophenyl)methyl)sulfinyl)methyl)-1-phenyl-1H-1,2,3-triazole (178):

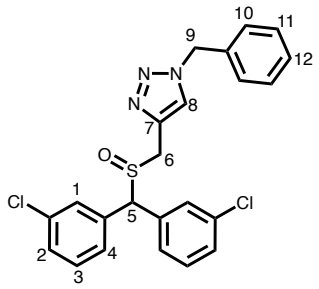

Compound **178** was prepared through General procedure G. Starting from 1-benzyl-4-(((bis(3-chlorophenyl)methyl)thio)methyl)-1H-1,2,3-triazole (15.4 mg, 0.035 mmol, 1.0 eq) and mCPBA (8.2 mg, 0.037 mmol, 1.05 eq). Following concentration under reduced pressure, the sulfoxide was purified by FCC 0->50% ethyl acetate in hexanes to yield 8.1 mg (50.8%) of the product as a white solid.

^{1}HNMR (400 MHz, CDCl3) δ 7.58 (s, 1H, C8-H), 7.49 (d, *J* = 1.8 Hz, 2H, 2 x C2-H), 7.44 (dd, *J* = 7.0, 2.0 Hz, 1H, C12-H), 7.41 – 7.35 (m, 6H, 2 x C1-H + 2 x C10-H + 2 x C11-H), 7.32 – 7.27 (m, 4H, 2 x C3-H + 2 x C4-H), 5.64 – 5.43 (m, 2H, C9-H$_2$), 4.95 (s, 1H, C5-H), 4.02 (d, *J* = 14.1 Hz, 1H, C6-*H$_a$*H$_b$), 3.79 (d, *J* = 14.1 Hz, 1H, C6-H$_a$*H$_b$*).

^{13}CNMR(101 MHz, CDCL3) δ 136.87 (C_{AR}), 135.76 (C_{AR}), 134.36 (C7), 130.82 (C_{AR}), 129.85 (C_{AR}), 129.09 (C_{AR}), 128.89 (C_{AR}), 128.31 (C_{AR}), 127.96 (C_{AR}), 127.50 (C_{AR}), 124.92 (C8), 68.24 (C5), 54.57 (C9), 45.47 (C6).

IR ν_{max} (film)/cm^{-1}: 2922, 1591, 1570, 1474, 1428, 1227, 1049, 705.

HRMS: (ESI^+) m/z calculated. $C_{23}H_{20}Cl_22N_3OS$ $[M+H]^+$ 456.0699; found at 456.0694, Δ 0.99 ppm.

1-Benzyl-4-(((bis(4-fluorophenyl)methyl)sulfinyl)methyl)-1H-1,2,3-triazole (179)

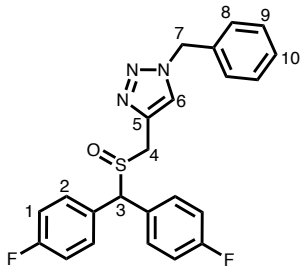

Compound **179** was prepared through General procedure G. Starting from 1-benzyl-4-(((bis(4-fluorophenyl)methyl)thio)methyl)-1H-1,2,3-triazole (77.7 mg, 0.19 mmol, 1.0 eq) and mCPBA (34.2 mg, 0.20 mmol, 1.05 eq). Following concentration under reduced pressure, the sulfoxide was purified by FCC 0->50% ethyl acetate in hexanes to yield 61.6 mg (76.9%) of the product as a white solid.

^{1}HNMR (400 MHz, CDCl3) δ 7.60 (s, 1H, C6-H), 7.53 – 7.48 (m, 2H, 2 x C_a1-H), 7.40 – 7.33 (m, 5H, 5 x C8,9,10-H), 7.31 – 7.25 (m, 2H, 2 x C_b1-H), 7.11 (t, J = 8.4 Hz, 2H, 2 x C_a2-H), 7.03

(t, *J* = 8.4 Hz, 2H, 2 x C_b2-H), 5.54 (dd, *J* = 14.9, 10.4 Hz, 2H, C7-H_2), 4.99 (s, 1H, C3-H), 3.88 (dd, J = 80.2, 13.0 Hz, 2H, C7-H_2).

^{13}CNMR(101 MHz, CDCL3) δ 162.84 (d, J = 248.5, C-F), 162.72 (d, J = 50.5, C-F), 134.37 (C_{AR}), 131.49 (C_{AR}), 131.40 (C_{AR}), 131.07 (C_{AR}), 129.00 (C_{AR}), 124.81 (C6), 116.45 (d, J = 21.2, C_{AR}), 115.79 (d, J = 21.2, C_{AR}), 67.44 (C3), 54.47 (C7), 45.16 (C4).

^{19}F NMR (376 MHz, CDCL3) δ -112.89 (d, J = 297.0 Hz).

IR ν_{max} (film)/cm^{-1}: 3068, 1603, 1506, 1227, 1159, 1043, 907, 835, 725, 646, 572.

HRMS: (ESI+) m/z calculated for $[C_{23}H_{19}F_2N_3OS+H]^+$ 424.1289; found 424.1285, Δ -1.04 ppm.

1-Benzyl-4-((((3-chlorophenyl)(phenyl)methyl)sulfinyl)methyl)-1H-1,2,3-triazole (**180**):

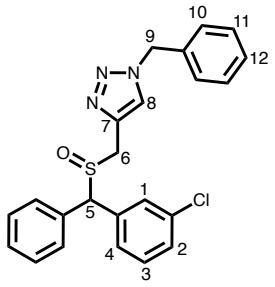

Compound **180** was prepared through General procedure G. Starting from **173** (14.9 mg, 0.037 mmol, 1.0 eq) and mCPBA (8.9 mg, 0.039 mmol, 1.05 eq). Following concentration under reduced pressure, the sulfoxide was purified by FCC 0->50% ethyl acetate in hexanes to yield 11.3 mg (72.9%) of the product as a white solid.

^{1}HNMR (400 MHz, CDCl3) δ 7.59 (d, *J* = 10.4 Hz, 1H, C8-H), 7.52 – 7.43 (m, 3H, 3 x C1,2,3-H), 7.42 – 7.32 (m, 7H, 2 x CAR-H + 5 x C8,9,10-H), 7.32 – 7.26 (m, 4H, C4-H + 3 x C_{AR}-H), 5.65 – 5.43 (m, 2H, C9-H_2), 4.94 (d, *J* = 8.9 Hz, 1H, C5-H), 4.01 (dd, *J* = 14.1, 8.3 Hz, 1H, C9-$H_a$$H_b$), 3.78 (dd, *J* = 14.1, 8.5 Hz, 1H, C9-$H_a$$H_b$).

Note mixture of diastereomers:

^{13}CNMR(101 MHz, CDCL3) δ 137.58 (C_{AR}), 136.80 (C_{AR}), 136.65 (C_{AR}), 135.20 (C_{AR}), 134.69 (C_{AR}), 134.61 (C_{AR}), 134.45 (C_{AR}), 134.40 (C_{AR}), 133.66 (C7), 130.64 (C_{AR}), 129.99 (C_{AR}), 129.98 (C_{AR}), 129.79 (C_{AR}), 129.73 (C_{AR}), 129.61 (C_{AR}), 129.60 (C_{AR}), 129.34 (C_{AR}), 129.34 (C_{AR}), 129.28 (C_{AR}), 129.24 (C_{AR}), 129.04 (C_{AR}), 128.98 (C_{AR}), 128.90 (C_{AR}), 128.79 (C_{AR}), 128.67 (C_{AR}), 128.62 (C_{AR}), 128.32 (C_{AR}), 128.28 (C_{AR}), 127.93 (C_{AR}), 127.53 (C_{AR}), 124.88 ($C8_a$), 124.75 ($C8_b$), 69.43 ($C5_a$), 69.03 ($C5_b$), 54.52 (C9), 45.63 ($C6_a$), 45.46 ($C6_b$).

IR ν_{max} (film)/cm^{-1}: 3063, 1591, 1570, 1496, 1474, 1454, 1045, 704.

HRMS: (ESI^{+}) m/z calculated. $C_{23}H_{20}ClN_3OS$ $[M+H]^{+}$ 422.1088; found at 422.1085, Δ 0.71 ppm.

1-Benzyl-4-((((3-bromophenyl)(phenyl)methyl)sulfinyl)methyl)-1H-1,2,3-triazole (**181**):

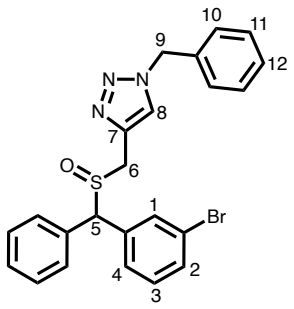

Compound **181** was prepared through General procedure G. Starting from **171** (7.7 mg, 0.017 mmol, 1.0 eq) and mCPBA (4.1 mg, 0.018 mmol, 1.05 eq). Following concentration under reduced pressure, the sulfoxide was purified by FCC 0->50% ethyl acetate in hexanes to yield 5.8 mg (72.7%) of the product as a white solid.

^{1}HNMR (400 MHz, CDCl3) δ 7.59 – 7.51 (m, 2H, C8-H), 7.51 – 7.40 (m, 4H), 7.40 – 7.31 (m, 5H), 7.31 – 7.26 (m, 3H, C4-H + 2 x C_{AR}-H), 5.54 (dq, *J* = 14.9, 1.7 Hz, 2H, C9-H_2), 4.93 (d, *J* = 6.3 Hz, 1H, C5-H), 4.00 (dd, *J* = 14.1, 5.8 Hz, 1H, C9-$H_a$$H_b$), 3.77 (dd, *J* = 14.2, 8.0 Hz, 1H, C9-$H_a$$H_b$).

Note mixture of diastereomers:

^{13}CNMR(101 MHz, CDCL3) δ 137.86 (C_{AR}), 136.91 (C_{AR}), 136.79 (C_{AR}), 136.63 (C_{AR}), 134.59 (C_{AR}), 134.43 (C_{AR}), 134.38 (C_{AR}), 133.62 (C_{AR}), 132.57 (C_{AR}), 132.07 (C_{AR}), 131.70 (C_{AR}), 131.52 (C_{AR}), 130.89 ($C7_a$), 130.25 ($C7_a$), 129.78 (C_{AR}), 129.78 (C_{AR}), 129.60 (C_{AR}), 129.33 (C_{AR}), 129.25 (C_{AR}), 129.02 (C_{AR}), 128.97 (C_{AR}), 128.89 (C_{AR}), 128.67 (C_{AR}), 128.36 (C_{AR}), 128.31 (C_{AR}), 128.27 (C_{AR}), 127.97 (C_{AR}), 124.87 ($C8_a$), 124.74 ($C8_b$), 123.33 (C_{AR}), 122.87 (C_{AR}), 69.38 ($C5_a$), 68.94 ($C5_b$), 54.51 (C9), 45.65 ($C6_a$), 45.44 ($C6_b$).

IR ν_{max} (film)/cm^{-1}: 3053, 1587, 1566, 1496, 1473, 1454, 1044, 703

HRMS: (ESI^{+}) m/z calculated. $C_{23}H_{20}BrN_3OS$ $[M+H]^+$ 466.0583; found at 466.0582, Δ 0.36 ppm.

1-(4-Chlorobenzyl)-4-(((phenyl(p-tolyl)methyl)sulfinyl)methyl)-1H-1,2,3-triazole (**182**):

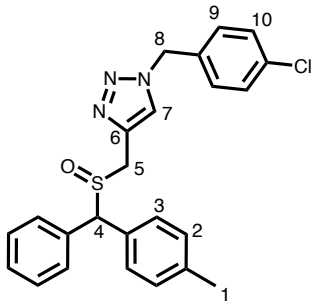

Compound **182** was prepared through General procedure G. Starting from **175** (40.0 mg, 0.095 mmol, 1.0 eq) and mCPBA (23.0 mg, 0.100 mmol, 1.05 eq). Following concentration under reduced pressure, the sulfoxide was purified by FCC 0->50% ethyl acetate in hexanes to yield 25.2 mg (60.7%) of the product as a white solid.

^{1}HNMR (400 MHz, CDCl3) δ 7.61 (d, *J* = 7.0 Hz, 1H, C7-H), 7.51 (d, *J* = 7.7 Hz, 1H, C10-H), 7.42 – 7.37 (m, 3H, C10-H + 2 x C_{AR}-H), 7.37 – 7.26 (m, 5H, 2 x C3-H + 3 x C_{AR}-H), 7.25 – 7.19 (m, 3H, C2-H + 2 x C9-H), 7.15 (d, *J* = 7.9 Hz, 1H, C2-H), 5.58 – 5.44 (m, 2H, C8-H_2), 4.88 (d, *J* = 3.0 Hz, 1H, C4-H), 3.99 (dd, *J* = 13.9, 1.5 Hz, 1H, C5-H_aH$_b$), 3.77 (dd, *J* = 14.0, 6.6 Hz, 1H, C5-H$_a$$H_b$), 2.33 (d, *J* = 16.7 Hz, 3H, C1-H_3).

Note mixture of diastereomers:

^{13}CNMR(101 MHz, CDCL3) δ 138.59 (C_{AR}), 138.31 (C_{AR}), 137.31 (C_{AR}), 137.26 (C_{AR}), 135.47 (C_{AR}), 135.03 (C_{AR}), 134.83 (C_{AR}), 133.02 (C_{AR}), 133.01 (C_{AR}), 132.07 (C_{AR}), 131.42 (C_{AR}), 130.15 (C6), 129.60 (C_{AR}), 129.58 (C_{AR}), 129.54 (C_{AR}), 129.51 (C_{AR}), 129.50 (C_{AR}), 129.40 (C_{AR}), 129.19 (C_{AR}), 129.12 (C_{AR}), 128.83 (C_{AR}), 128.55 (C_{AR}), 128.33 (C_{AR}), 124.71 (C7$_a$), 124.67 (C7$_b$), 70.17 (C4$_a$), 70.11 (C4$_b$), 53.70 (C8), 45.54 (C5$_a$), 45.42 (C5$_b$), 21.29 (C1$_a$), 21.25 (C1$_b$).

IR ν_{max} (film)/cm^{-1}: 2922, 1493, 1452, 1042, 782, 728, 698.

HRMS: (ESI$^+$) m/z calculated. $C_{24}H_{22}ClN_3OS$ $[M+H]^+$ 436.1245; found at 436.1243, Δ 0.48 ppm.

1-(4-(tert-Butyl)benzyl)-4-(((phenyl(p-tolyl)methyl)sulfinyl)methyl)-1H-1,2,3-triazole (183):

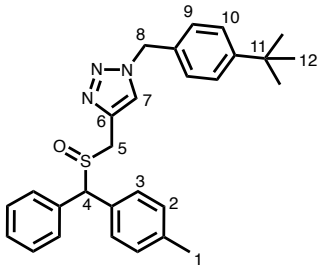

Compound **183** was prepared through General procedure G. Starting from **176** (20.0 mg, 0.045 mmol, 1.0 eq) and mCPBA (10.9 mg, 0.047 mmol, 1.05 eq). Following concentration under reduced pressure, the sulfoxide was purified by FCC 0->50% ethyl acetate in hexanes to yield 14.8 mg (71.4%) of the product as a white solid.

^{1}HNMR (400 MHz, CDCl3) δ 7.58 (d, *J* = 8.4 Hz, 1H), 7.51 (d, *J* = 7.6 Hz, 1H, C10-H), 7.43 – 7.36 (m, 5H, C10-H + 4 x C_{AR}-10), 7.36 – 7.28 (m, 3H, C_{AR}-H + 2 x C3-H), 7.24 – 7.18 (m, 3H, 2 x C9-H + C2-H), 7.15 (d, *J* = 7.9 Hz, 1H, C2-H), 5.60 – 5.41 (m, 2H, C8-H_2), 4.90 (d, *J* = 3.9 Hz, 1H, C4-H), 3.99 (dd, *J* = 14.1, 1.5 Hz, 1H, C5-H_aH$_b$), 3.76 (dd, *J* = 14.2, 6.1 Hz, 1H, C5-H$_a$$H_b$), 2.33 (d, *J* = 16.1 Hz, 3H, C1-H_3), 1.30 (s, 9H, 3 x C12-H_3).

Note mixture of diastereomers:

^{13}CNMR(101 MHz, CDCL3) δ 152.10 (C-tBu), 138.53 (C_{AR}), 138.26 (C_{AR}), 137.08 (C_{AR}), 137.03 (C_{AR}), 135.62 (C_{AR}), 134.85 (C_{AR}), 132.21 (C_{AR}), 131.43 (C_{AR}), 130.12 (C6), 129.60 (C_{AR}), 129.56 (C_{AR}), 129.37 (C_{AR}), 129.20 (C_{AR}), 129.12 (C_{AR}), 128.81 (C_{AR}), 128.50 (C_{AR}), 128.30 (C_{AR}), 128.13 (C_{AR}), 128.12 (C_{AR}), 128.11 (C_{AR}), 126.23 (C_{AR}), 124.65 ($C7_a$), 124.60 ($C7_b$), 70.08 ($C4_a$), 70.00 ($C4_b$), 54.18 (C8), 45.76 ($C5_a$), 45.64 ($C5_b$), 34.78 (C11), 31.38 (C12), 21.30 (C1).

IR ν_{max} (film)/cm^{-1}: 2962, 1513, 1453, 1111, 1044, 787, 699

HRMS: (ESI^+) m/z calculated. $C_{24}H_{22}ClN_3OS$ $[M+H]^+$ 458.2261; found at 458.2258, Δ 0.65 ppm.

4-(1-((Trimethylsilyl)methyl)-1H-1,2,3-triazol-4-yl)butan-1-ol (184):

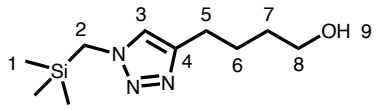

Following General procedure H: To hex-5-yn-1-0l (500.0 mg, 5.09 mmol, 1.0 eq) was added copper sulfate pentahydrate (127.2 mg, 0.51 mmol, 0.10 eq) and sodium ascorbate (302.8 mg, 1.53 mmol, 0.30 eq), these were dissolved in 12.7 mL (THF) and 12.7 mL (Water). Then added (azidomethyl)trimethylsilane (3.57 mL, 5.35 mmol, 1.5M in tert-butyl methyl ether, 1.05 eq). The crude was purified ramping up from 0% -> 5% MeOH in DCM to afford 733.4 mg (63.3%) of a white solid.

^{1}HNMR (400 MHz, CDCl3) δ 7.16 (s, 1H, C3-H), 3.87 (s, 2H, C2-H_2), 3.68 (q, *J* = 5.7 Hz, 2H, C8-H_2), 2.73 (t, *J* = 7.5 Hz, 2H, C5-H_2), 1.81 – 1.60 (m, 5H, 2 x C6-H_2 + 2 x C7-H_2 + OH), 0.13 (s, 9H, 3 x C1-H_3)

^{13}CNMR(101 MHz, CDCL3) δ 130.39 (C4), 122.25 (C3), 62.47 (C8), 42.01 (C2), 32.26 (C5), 25.68 (C7), 25.39 (C6), -2.36 (C1).

HRMS: (ESI+) m/z calculated for $[C_{13}H_{17}N_3O+H]^+$ 232.1444; found 232.1442, Δ -1.25 ppm.

MP: 80-82 C

Data matches literature.[10]

4-(4-Bromobutyl)-1-((trimethylsilyl)methyl)-1H-1,2,3-triazole (**185**):

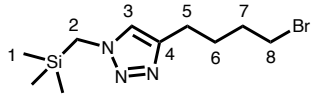

In a round bottom flask, **184** (215.8 mg, 0.95 mmol, 1.0 eq) was dissolved in DCM (5.0 mL, 0.2M) and cooled to 0 °C under argon, to this solution was added triphenyl phosphine (299.0 mg, 1.14 mmol, 1.2 eq) in one portion and carbon tetrabromide (378.0 mg,1.14 mmol, 1.2 eq) portionwise over 2 minutes. The reaction was allowed to stir at 0 °C for 5 minutes and subsequently removed from the ice bath and allowed to reach room temperature. The reaction mixture was stirred at 20 °C for 24 h before being quenched with 10% sodium thiosulphate solution. The aqeous layer was extracted twice with DCM and the combined organic layers were dried with Na2SO4, the solvent was removed under reduced pressure and the crude purified by flash column chromatogrpahy ramping up 0 -> 25% ethyl acetate in hexanes to yield 132.5 mg (48.1%) of a white solid.

^{1}HNMR (400 MHz, CDCl3) δ 9.41 (s, 1H, C3-H), 4.50 (t, *J* = 6.2 Hz, 2H, C8-H_2), 4.42 (s, 2H, C2-H_2), 3.10 (t, *J* = 6.4 Hz, 2H, C5-H_2), 2.31 – 2.19 (m, 2H, C7-H_2), 2.11 – 1.99 (m, 2H, C6-H_2), 0.17 (s, 9H, 3 x C1-H_3).

^{13}CNMR(101 MHz, CDCL3) δ 139.82 (C4), 129.43 (C3), 48.95 (C8), 46.02 (C2), 21.67 (C7), 20.59 (C5), 18.29 (C6), -2.52 (C1).

IR ν_{max} (film)/cm^{-1}: 3412, 2955, 1626, 1575, 1447, 1251, 853.

HRMS: (ESI+) m/z calculated for $[C_{10}H_{19}N_3Si+H]^+$ 210.1421; found 210.1419, Δ -0.71 ppm.

S-(4-(1-((Trimethylsilyl)methyl)-1H-1,2,3-triazol-4-yl)butyl) ethanethioate (186):

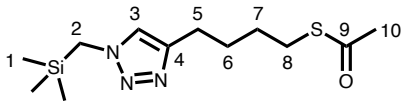

Bromide **185** (255.0 mg, 0.88 mmol, 1.0 eq))was dissolved in MeCN (3.5 mL, 0.25M) then added potassium ethanethioate (120.4 mg, 1.05 mmol, 1.20 eq) in one portion and the reaction was stirred at 20 °C for 18 hours. Reaction was then filtered and the filtrate was concentrated under reduced pressure. The crude was then purified by flash column chromatogrpahy ramping up 0 -> 40% ethyl acetate in hexane to yield 180.2 mg (71.9%) of a colorless oil.

^{1}HNMR (400 MHz, CDCl3) δ 7.09 (s, 1H, C3-H), 3.75 (s, 2H, C2-H_2), 2.76 (t, *J* = 7.3 Hz, 2H, C8-H_2), 2.58 (t, *J* = 7.4 Hz, 2H, C5-H_2), 2.17 (s, 3H, C10-H_3), 1.67 – 1.56 (m, 2H, C7-H_2), 1.55 – 1.43 (m, 2H, C6-H_2), -0.00 (s, 9H, 3 x C1-H_3).

^{13}CNMR(101 MHz, CDCL3) δ 195.57 (C9), 147.07 (C4), 121.33 (C3), 41.55 (C2), 30.44 (C10), 28.84 (C8), 28.56 (C7), 28.33 (C6), 24.88 (C5), -2.64 (C1).

IR ν_{max} (film)/cm^{-1}: 2939, 2859, 1687, 1417, 1354, 1249, 1133, 1108, 845, 625

HRMS: (ESI+) m/z calculated for $[C_{12}H_{23}N_3OSSi+H]^+$ 286.1404; found 286.1401, Δ -1.19 ppm.

4-(1-Benzyl-1H-1,2,3-triazol-4-yl)butan-1-ol (**187**):

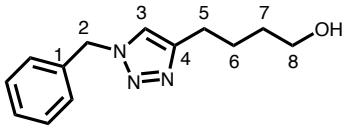

Following General procedure H: To hex-5-yn-1-0l (500.0 mg, 5.09 mmol, 1.0 eq) was added copper sulfate pentahydrate (127.2 mg, 0.51 mmol, 0.10 eq) and sodium ascorbate (302.8 mg, 1.53 mmol, 0.30 eq), these were dissolved in 12.7 mL (THF) and 12.7 mL (Water). Then added benzyl azide (10.7 mL, 5.35 mmol, 0.5M in toluene, 1.05 eq). The crude was purified ramping up from 0% -> 5% MeOH in DCM to afford 423.0 mg (35.9%) of a white solid.

^{1}HNMR (400 MHz, CDCl3) δ 7.40 – 7.34 (m, 3H, C3-H + 2 x C_{AR}-H), 7.27 – 7.23 (m, 3H, 3 x C_{AR}-H), 5.49 (s, 2H, C2-H_2), 3.66 (q, *J* = 5.7 Hz, 2H, C8-H_2), 2.73 (t, *J* = 7.4 Hz, 2H, C5-H_2), 2.07 (br s, 1H, O-H), 1.83 – 1.69 (m, 2H, C7-H_2), 1.69 – 1.54 (m, 2H, C6-H_2).

^{13}CNMR(101 MHz, $CDCl_3$): δ=148.4 (C_{AR}), 134.8 (C4), 128.9 (C_{AR}), 128.2 (C_{AR}), 127.9 (C_{AR}), 120.5 (C3), 62.2 (C8), 53.8 (C2), 31.7 (C5), 25.3 (C7), 25.1 (C6)

HRMS: (ESI+) m/z calculated for $[C_{10}H_{21}N_3OSi+H]^+$ 228.1527; found 228.1524, Δ -1.14 ppm.

Spectroscopic data matches literature.[10]

1-Benzyl-4-(4-bromobutyl)-1H-1,2,3-triazole (**188**):

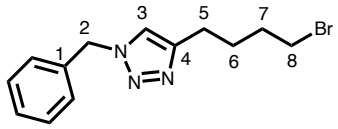

In a round bottom flask, **187** (124.6 mg, 0.54 mmol, 1.0 eq) was dissolved in DCM (5.0 mL, 0.2M) and cooled to 0 °C under argon, to this solution was added triphenyl phosphine (170.5 mg, 0.65 mmol, 1.2 eq) in one portion and carbon tetrabromide (215.5 mg,1.14 mmol, 1.2 eq) portionwise over 2 minutes. The reaction was allowed to stir at 0 °C for 5 minutes and subsequently removed from the ice bath and allowed to reach room temperature. The reaction mixture was stirred at 20 °C for 24 h before being quenched with 10% sodium thiosulphate solution. The aqeous layer was extracted twice with DCM and the combined organic layers were dried with Na2SO4, the solvent was removed under reduced pressure and the crude purified by flash column chromatogrpahy ramping up 0 -> 25% ethyl acetate in hexanes to yield 49.6 mg (31.3%) of a waxy solid.

^{1}HNMR (400 MHz, CDCl3) δ 9.66 (s, 1H, C3-H), 7.77 – 7.60 (m, 2H, 2 x C_{AR}-H), 7.51 – 7.33 (m, 3H, 3 x C_{AR}-H), 6.05 (s, 2H, C2-H_2), 4.54 (t, *J* = 6.2 Hz, 2H, C8-H_2), 3.08 (t, *J* = 6.5 Hz, 2H, C5-H_2), 2.25 (p, *J* = 6.2 Hz, 2H, C7-H_2), 2.05 (p, *J* = 6.4 Hz, 2H, C6-H_2).

^{13}CNMR(101 MHz, CDCL3) δ 140.05 (C4), 132.07 (C_{AR}), 129.88 (C_{AR}), 129.85 (C_{AR}), 129.43 (C_{AR}), 129.02 (C3), 57.23 (C2), 49.22 (C8), 21.60 (C7), 20.61 (C5), 18.26 (C6).

IR ν_{max} (film)/cm^{-1}: 3416, 2957, 1626, 1575, 1497, 1456, 1330, 1160, 1053, 748, 708.

HRMS: (ESI+) m/z calculated for $[C_{13}H_{15}N_3+H]^+$ 214.1339; found 214.1337, Δ -0.89 ppm.

S-(4-(1-Benzyl-1H-1,2,3-triazol-4-yl)butyl) ethanethioate (**189**):

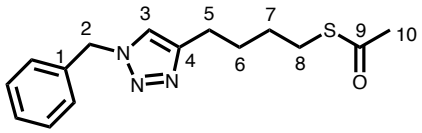

Bromide **188** (435.0 mg, 1.48 mmol, 1.0 eq) was dissolved in MeCN (5.9 mL, 0.25M) then added potassium ethanethioate (202.6 mg, 1.77 mmol, 1.20 eq) in one portion and the reaction was stirred at 20 °C for 18 hours, then filtered and the filtrate was concentrated under reduced pressure. The crude was then purified by flash column chromatogrpahy ramping up 0 -> 40% ethyl acetate in hexane to yield 316.5 mg (73.9%) of a white solid.

^{1}HNMR (400 MHz, CDCl3) δ 7.40 – 7.30 (m, 4H, C3-H + 3 x C_{AR}-H), 7.27 – 7.18 (m, 2H, 2 x C_{AR}-H), 5.47 (s, 2H, C2-H_2), 2.85 (t, *J* = 7.2 Hz, 2H, C8-H_2), 2.69 (t, *J* = 7.5 Hz, 2H, C5-H_2), 2.27 (s, 3H, C10-H_3), 1.81 – 1.66 (m, 2H, C6-H_2), 1.65 – 1.53 (m, 2H, C7-H_2).

^{13}CNMR(101 MHz, CDCL3) δ 195.46 (C9), 147.74 (C4), 134.83 (C_{AR}), 128.74 (C_{AR}), 128.26 (C_{AR}), 127.64 (C_{AR}), 120.62 (C3), 53.59 (C2), 30.36 (C10), 28.79 (C7), 28.46 (C6), 28.16 (C8), 24.87 (C5).

IR ν_{max} (film)/cm^{-1}: 3136, 2935, 2858 ,1683, 1550, 1456, 1353, 1216, 1131, 1050, 953, 720, 697, 625

HRMS: (ESI+) m/z calculated for $[C_{15}H_{19}N_3OS+H]^+$ 290.1322; found 290.1319, Δ -1.03 ppm.

4-(3-Bromopropyl)-1-((trimethylsilyl)methyl)-1H-1,2,3-triazole (190):

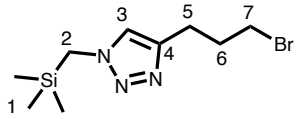

Following General procedure H: To 5-bromopent-1-yne (250.0 mg, 1.70 mmol, 1.0 eq) was added copper sulfate pentahydrate (42.5 mg, 0.17 mmol, 0.10 eq) and sodium ascorbate (101.1 mg, 0.51 mmol, 0.30 eq), these were dissolved in 4.3 mL (THF) and 4.3 mL (Water). Then added (azidomethyl)trimethylsilane (1.19 mL, 1.76 mmol, 1.5M in tert-butyl methyl ether, 1.05 eq). The crude was purified ramping up from 0% -> 25% ethyl acetate in hexane to afford 261.7 mg (55.7%) of a white solid.

^{1}HNMR (400 MHz, CDCl3) δ 7.19 (s, 1H, C3-H), 3.85 (s, 2H, C2-H_2), 3.41 (t, *J* = 6.4 Hz, 2H, C7-H_2), 2.85 (t, *J* = 7.2 Hz, 2H, C5-H_2), 2.22 (p, *J* = 6.6 Hz, 2H, C6-H_2), 0.11 (s, 9H, 3 x C1-H_3).

^{13}CNMR(101 MHz, CDCL3) δ 145.91 (C4), 121.94 (C3), 41.94 (C2), 33.26 (C7), 32.02 (C6), 23.94 (C5), -2.38 (C1).

IR ν_{max} (film)/cm^{-1}: 3408, 2955, 1548, 1427, 1250, 1049, 854.

HRMS: (ESI+) m/z calculated for $[C_9H_{18}BrN_3Si+H]^+$ 276.0453; found 276.0450, Δ -1.09 ppm.

S-(3-(1-((Trimethylsilyl)methyl)-1H-1,2,3-triazol-4-yl)propyl) ethanethioate (191):

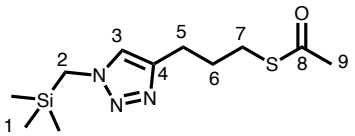

Bromide **190** (220.0 mg, 0.79 mmol, 1.0 eq))was dissolved in MeCN (3.2 mL, 0.25M) then added potassium ethanethioate (100.0 mg, 0.88 mmol, 1.10 eq) in one portion and the reaction was stirred at 20 °C for 18 hours, then filtered and the filtrate was concentrated under reduced pressure. The crude was then purified by flash column chromatogrpahy ramping up 0 -> 40% ethyl acetate in hexane to yield 164.8 mg (76.2%) of a colorless oil.

^{1}HNMR (400 MHz, CDCl3) δ 7.14 (s, 1H, C3-H), 3.76 (s, 2H, C2-H_2), 2.79 (t, *J* = 7.2 Hz, 2H, C7-H_2), 2.65 (t, *J* = 7.5 Hz, 2H, C5-H_2), 2.20 (s, 3H, C9-H_3), 1.83 (p, *J* = 7.3 Hz, 2H, C6-H_2), 0.01 (s, 9H, 3 x C1-H_3).

^{13}CNMR(101 MHz, CDCL3) δ 195.56 (C8), 146.34 (C4), 121.54 (C3), 41.63 (C2), 30.49 (C9), 29.05 (C6), 28.22 (C7), 24.43 (C5), -2.62 (C1).

IR ν_{max} (film)/cm^{-1}: 2953, 1688, 1417, 1354, 1250, 1134, 1049, 951, 846, 702, 625.

HRMS: (ESI+) m/z calculated for $[C_{11}H_{21}N_3OSSi+H]^+$ 272.1247; found 272.1245, Δ -1.03 ppm.

1-Benzyl-4-(3-bromopropyl)-1H-1,2,3-triazole (192):

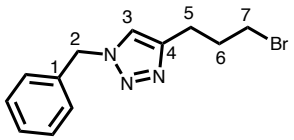

Following General procedure H: To 5-bromopent-1-yne (250.0 mg, 1.70 mmol, 1.0 eq) was added copper sulfate pentahydrate (42.5 mg, 0.17 mmol, 0.10 eq) and sodium ascorbate (101.1 mg, 0.51 mmol, 0.30 eq), these were dissolved in 4.3 mL (THF) and 4.3 mL (Water). Then added benzyl azide (3.57 mL, 1.78 mmol, 0.5M in toluene, 1.05 eq). The crude was purified ramping up from 0% -> 25% ethyl acetate in hexane to afford 390.0 mg (81.9%) of a white solid.

^{1}HNMR (400 MHz, CDCl3) δ 7.37 (d, *J* = 6.9 Hz, 4H, C3-H + 3 x C_{AR}-H), 7.26 (d, *J* = 8.5 Hz, 2H, 2 x C_{AR}-H), 5.50 (s, 2H, C2-H_2), 3.42 (t, *J* = 6.9 Hz, 2H, C7-H_2), 2.85 (t, *J* = 7.4 Hz, 2H, C5-H_2), 2.22 (dt, *J* = 13.8, 6.7 Hz, 2H, C6-H_2).

^{13}CNMR(101 MHz, CDCL3) δ 146.71 (C4), 134.86 (C1), 129.14 (C_{AR}), 128.73 (C_{AR}), 128.04 (C_{AR}), 121.14 (C3), 54.07 (C2), 33.14 (C7), 31.96 (C6), 24.02 (C5).

IR ν_{max} (film)/cm^{-1}: 3408, 3032, 2940, 1550, 1497, 1455, 1435, 1336, 1216, 1048, 804, 725, 698.

HRMS: (ESI+) m/z calculated for $[C_{12}H_{14}BrN_3+H]^+$ 280.0371; found 280.0369, Δ -0.71 ppm.

S-(3-(1-Benzyl-1H-1,2,3-triazol-4-yl)propyl) ethanethioate (**193**):

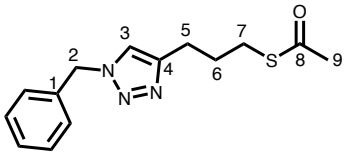

Bromide **192** (350.0 mg, 1.25 mmol, 1.0 eq) was dissolved in MeCN (5.0 mL, 0.25M) then added potassium ethanethioate (157.0 mg, 1.37 mmol, 1.10 eq) in one portion and the reaction was stirred at 20 °C for 18 hours, then filtered and the filtrate was concentrated under reduced pressure. The crude was then purified by flash column chromatogrpahy ramping up 0 -> 40% ethyl acetate in hexane to yield 259.9 mg (75.5%) of a off-white solid.

^{1}HNMR (400 MHz, CDCl3) δ 7.38 – 7.28 (m, 4H, C3-H + 3 x C_{AR}-H), 7.27 – 7.20 (m, 2H, 2 x C_{AR}-H), 5.47 (s, 2H, C2-H_2), 2.88 (t, *J* = 7.3 Hz, 2H, C7-H_2), 2.74 (t, *J* = 7.6 Hz, 2H, C5-H_2), 2.28 (s, 3H, C9-H_3), 1.92 (p, *J* = 7.4 Hz, 2H, C6-H_2).

^{13}CNMR(101 MHz, CDCL3) δ 195.37 (C8), 146.99 (C4), 134.78 (C1), 128.74 (C_{AR}), 128.28 (C_{AR}), 127.65 (C_{AR}), 120.80 (C4), 53.61 (C2), 30.36 (C9), 28.89 (C6), 28.14 (C7), 24.37 (C5).

IR ν_{max} (film)/cm^{-1}: 3136, 2927, 1683, 1497, 1455, 1433, 1354, 1213, 1131, 1048, 951, 724, 697, 624

HRMS: (ESI+) m/z calculated for $[C_{14}H_{17}N_3OS+H]^+$ 276.1165; found 276.1162, Δ -1.12 ppm.

1-Benzyl-4-(2-bromoethyl)-1H-1,2,3-triazole (**195**):

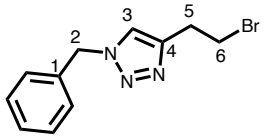

In a round bottom flask, **194** (100.0 mg, 0.49 mmol, 1.0 eq) was dissolved in DCM (2.5 mL, 0.2M) and cooled to 0 °C under argon, to this solution was added triphenyl phosphine (142.0 mg, 0.54 mmol, 1.1 eq) in one portion and carbon tetrabromide (179.5 mg, 0.54 mmol, 1.2 eq) portionwise over 2 minutes. The reaction was allowed to stir at 0 °C for 5 minutes and subsequently removed from the ice bath and allowed to reach room temperature. The reaction mixture was stirred at 20 0 °C for 24 h before being quenched with 10% sodium thiosulphate solution. The aqeous layer was extracted twice with DCM and the combined organic layers were dried with Na2SO4, the solvent was removed under reduced pressure and the crude purified by flash column chromatogrpahy ramping up 0 -> 25% ethyl acetate in hexanes to yield 51.7 mg (39.5%) of a waxy solid.

^{1}HNMR (400 MHz, CDCl3) δ 7.37 (d, *J* = 7.2 Hz, 4H, C3-H + 3 x C_{AR}-H), 7.29 – 7.23 (m, 2H, 2 x C_{AR}-H), 5.52 (s, 2H, C2-H_2), 3.64 (t, *J* = 7.1 Hz, 2H, C6-H_2), 3.27 (t, *J* = 6.7 Hz, 2H, C5-H_2).

^{13}CNMR(101 MHz, CDCL3) δ 145.41 (C4), 134.82 (C1), 129.24 (C_{AR}), 128.85 (C_{AR}), 128.10 (C_{AR}), 121.74 (C3), 54.23 (C2), 31.63 (C6), 29.60 (C5).

IR ν_{max} (film)/cm^{-1}: 3137, 1551, 1497, 1455, 1260, 1219, 1050, 725, 697.

Spectroscopic data matches literature.[15]

S-(2-(1-Benzyl-1H-1,2,3-triazol-4-yl)ethyl) ethanethioate (196):

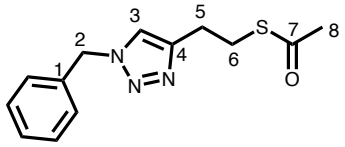

Bromide **195** (85.0 mg, 0.32 mmol, 1.0 eq) was dissolved in MeCN (1.6 mL, 0.25M) then added potassium ethanethioate (44.0 mg, 0.38 mmol, 1.20 eq) in one portion and the reaction was stirred at 20 °C for 18 hours, then filtered and the filtrate was concentrated under reduced pressure. The crude was then purified by flash column chromatogrpahy ramping up 0 -> 40% ethyl acetate in hexane to yield 67.5 mg (80.9%) of a off-white solid.

^{1}HNMR (400 MHz, CDCl3) δ 7.41 – 7.33 (m, 3H, 3 x C_{AR}-H), 7.30 (s, 1H, C3-H), 7.28 – 7.21 (m, 2H, 2 x C_{AR}-H), 5.50 (s, 2H, C2-H_2), 3.17 (t, J = 7.3 Hz, 2H, C6-H_2), 2.97 (t, J = 7.4 Hz, 2H, C5-H_2), 2.29 (s, 3H, C8-H_3).

^{13}CNMR(101 MHz, CDCL3) δ 195.62 (C7), 146.27 (C4), 134.83 (C1), 129.11 (C_{AR}), 128.70 (C_{AR}), 128.02 (C_{AR}), 121.27 (C3), 54.07 (C2), 30.66 (C8), 28.60 (C6), 26.08 (C5).

IR ν_{max} (film)/cm^{-1}: 3136, 2934, 1686, 1497, 1456, 1432, 1355, 1219, 1133, 1050, 955, 729, 698, 625.

HRMS: (ESI+) m/z calculated for $[C_{13}H_{15}N_3OS+H]^+$ 262.1009; found 262.1006, Δ -1.14 ppm.

4-(2-Chloroethyl)-1-methyl-1H-1,2,3-triazole (198):

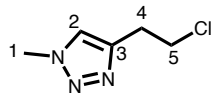

Dissolved **197** (150.0 mg, 1,18 mmol, 1.0 eq) in thionyl chloride (0.43 mL, 5.90 mmol, 5.0 eq) at 20 °C under an argon atmosphere, stired at room temperature for 18 hours, then removed solvent under reduced pressure and carried on without further purification. Isolated 162.2 mg (94.4%) of a yellow oil.

^{1}HNMR (400 MHz, CDCl3) δ 8.61 (s, 1H, C2-H), 4.44 (s, 3H, C1-H_3), 3.98 (t, *J* = 5.9 Hz, 2H, C5-H_2), 3.51 (t, *J* = 6.1 Hz, 2H, C4-H_2).

^{13}CNMR(101 MHz, CDCL3) δ 140.67 (C3), 128.33 (C2), 41.80 (C1), 40.11 (C5), 26.75 (C4).

IR ν_{max} (film)/cm^{-1}: 3094, 2214, 1885, 1505, 1448, 1165, 908, 723

HRMS: (ESI+) m/z calculated for $[C_5H_8ClN_3O+H]^+$ 146.04795; found 146.04794, Δ -0.07 ppm.

S-((1-Benzyl-1H-imidazol-4-yl)methyl) ethanethioate (202):

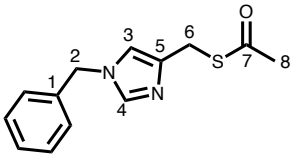

To a flame dried round bottom flask, placed carboxylic acid **201** (250.0 mg, 1.24 mmol, 1.0 eq) under argon atmosphere. Dissolved in THF (6.9 mL, 0.18M) and cooled to 0 °C, subsequently

added lithium aluminum hydride (0.80 mL, 1.61 mmol, 2M, 1.30 eq) dropwise over 5 minutes to the reaction mixture and the removed from ice bath and allowed to stir at 20 °C for 18 hours. After 18 hours the reaction was placed in a hot bath at 50 °C for 1 hour, then cooled back to 20 °C and quenched with 0.05 mL of water and stirring viguriously for 1 hour, then added 3.0 g of Na2SO4 and continued to stir vigurously for 1 hour before filtering and concentrated the filtrate. The crude material was then dissolved in thionyl chloride (0.45 mL, 6.18 mmol, 5.0 eq) under argon and stirred for 20 hours at 20 °C. Subsequently removed the thionyl chloride under reduces pressure and resuspended the resulting crude in acetone (6.9 mL, 0.18M) and added potassium ethanethioate (169.4 mg, 1.48 mmol, 1.20 eq) and stirred for 72 hours. The reaction was then filtered and the filtrate concentrated under reduced pressure. The crude was subsequently purified by FCC with 2% methanol in DCM isocratic to yield 90.1 mg (29.6%) of a brown oil.

^{1}HNMR (400 MHz, CDCl3) δ 7.53 (s, 1H, C4-H), 7.38 – 7.27 (m, 3H, 3 x C_{AR}-H), 7.19 – 7.11 (m, 2H, 2 x C_{AR}-H), 6.83 (s, 1H, C3-H), 5.03 (s, 2H, C2-H_2), 4.06 (s, 2H, C6-H_2), 2.30 (s, 3H, C8-H_3).

^{13}CNMR(101 MHz, CDCL3) δ 195.44 (C7), 138.13 (C5), 136.96 (C4), 135.59 (C1), 128.99 (C_{AR}), 128.38 (C_{AR}), 127.47 (C_{AR}), 117.45 (C3), 51.03 (C2), 30.35 (C8), 26.59 (C6).

IR ν_{max} (film)/cm^{-1}: 2927, 2854, 1683, 1498, 1454, 1354, 1233, 1134, 985, 956, 737, 703.

HRMS: (ESI+) m/z calculated for $[C_{13}H_{14}N_2OS+H]^+$ 247.0899; found 247.0898, Δ -0.61 ppm.

S-((2-Benzyl-1H-imidazol-4-yl)methyl) ethanethioate (204):

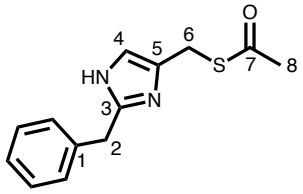

Salt **203** (328.0 mg, 1.35 mmol, 1.0 eq))was suspended in MeCN (5.4 mL, 0.25M) and DIPEA (0.24 mL, 1.35 mmol, 1.0 eq) was added to deprotonate the salt and solubilize it. Subsequently added potassium ethanethioate (169.5 mg, 1.48 mmol, 1.10 eq) was added in one portion and the reaction was stirred at 20 °C for 18 hours, then filtered and the filtrate was concentrated under reduced pressure. The crude was then purified by flash column chromatogrpahy ramping up 0 -> 50% ethyl acetate in hexane to yield 92.8 mg (27.9%) of a waxy solid.

^{1}HNMR (400 MHz, CDCl3) δ 9.89 (br s, 1H, N-H), 7.30 – 7.18 (m, 3H, 3 x C_{AR}-H), 7.12 (d, *J* = 7.4 Hz, 2H, 2 x C_{AR}-H), 6.73 (s, 1H, C4-H), 3.99 (s, 2H, C6-H_2), 3.93 (s, 2H, C2-H_2), 2.29 (s, 3H, C8-H_3).

^{13}CNMR(101 MHz, CDCL3) δ 196.34 (C7), 147.28 (C5), 137.22 (C3), 133.76 (C1), 128.81 (C_{AR}), 128.71 (C_{AR}), 126.94 (C_{AR}), 117.74 (C4), 34.94 (C2), 30.48 (C8), 26.00 (C6).

IR ν_{max} (film)/cm^{-1}: 3027, 2927, 1687, 1578, 1495, 1455, 1427, 1133, 957, 731, 695, 628

HRMS: (ESI+) m/z calculated for $[C_{12}H_{14}N_2O_2Si+H]^+$ 247.0897; found 247.0896, Δ -0.24 ppm.

S-((1-Methyl-1H-imidazol-4-yl)methyl) ethanethioate (206):

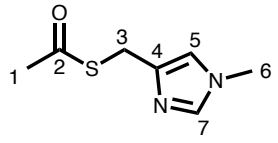

Salt **205** (200.0 mg, 1.19 mmol, 1.0 eq))was suspended in MeCN (5 mL, 0.25M) and DIPEA (0.21 mL, 1.19 mmol, 1.0 eq) was added to deprotonate the salt and solubilize it. Subsequently added potassium ethanethioate (150.0 mg, 1.32 mmol, 1.10 eq) was added in one portion and the reaction was stirred at 20 °C for 18 hours, then filtered and the filtrate was concentrated under reduced pressure. The crude was then purified by flash column chromatogrpahy ramping up 0 -> 5% methanol in DCM to yield 126.2 mg (61.9%) of a yellow oil.

^{1}HNMR (400 MHz, CDCl3) δ 7.34 (s, 1H, C7-H), 6.82 (s, 1H, C5-H), 4.06 (s, 2H C3-H_2), 3.63 (s, 3H, C6-H_3), 2.32 (s, 3H, C1-H_3).

^{13}CNMR(101 MHz, CDCL3) δ 195.31 (C2), 137.24 (C4), 137.22 (C7), 118.01 (C5), 33.16 (C3), 30.18 (C6), 26.67 (C3).

IR ν_{max} (film)/cm^{-1}: 3357, 1681, 1507, 1420, 1355, 1233, 1135, 1106, 993, 828, 754

HRMS: (ESI+) m/z calculated for $[C_7H_{10}N_2OS+H]^+$ 171.0587; found 171.0585, Δ -1.23 ppm.

1-Benzyl-4-(3-((bis(4-fluorophenyl)methyl)thio)propyl)-1H-1,2,3-triazole (207)

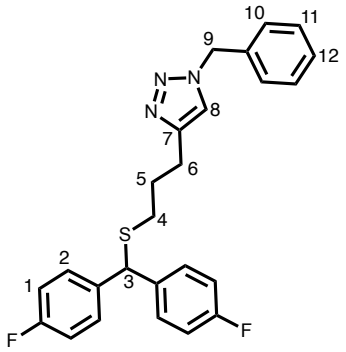

Using General procedure D: utilizing thiolacetate **193** (50.0 mg, 0.18 mmol, 1.0 eq) for formation of thiol; 4,4'-(bromomethylene)bis(fluorobenzene) (51.4 mg, 0.18 mmol, 1.0 eq). Utilized DBU (0.02 mL, 0.36 mmol, 1.0 eq). Following removal of solvent and purification by FCC 0->50% ethyl acetate in hexanes resulted in 57.0 mg (72.1%) of the product as a colorless oil.

^{1}HNMR (400 MHz, CDCl3) δ 7.41 – 7.29 (m, 7H, 4 x C1-H + 2 x C10-H + C12-H), 7.28 – 7.21 (m, 2H, 2 x C11-H), 7.10 (s, 1H, C8-H), 7.03 – 6.93 (m, 4H, 4 x C2-H), 5.47 (s, 2H, C9-H_2), 5.10 (s, 1H, C3-H), 2.75 (t, *J* = 7.4 Hz, 2H, C4-H_2), 2.39 (t, *J* = 7.3 Hz, 2H, C6-H_2), 1.91 (p, *J* = 7.3 Hz, 2H, C5-H_2).

^{13}CNMR(101 MHz, CDCL3) δ 161.98 (d, J = 247.5 Hz, C1), 147.63 (C_{AR}), 137.14 (C_{AR}), 134.98 (C7), 129.95 (C_{AR}), 129.87 (C_{AR}), 128.83 (C_{AR}), 128.12 (C_{AR}), 120.83 (C8), 115.59 (d, J = 21.2 Hz, C2), 54.15 (C9), 52.49 (C3), 31.62 (C6), 28.65 (C5), 24.75 (C4).

^{19}F NMR (376 MHz, CDCL3) δ -115.04.

IR ν_{max} (film)/cm^{-1}: 2928, 1602, 1505, 1456, 1222, 1157, 1049, 834, 728, 573.

HRMS: (ESI+) m/z calculated for $[C_{25}H_{23}F_2N_3S+H]^+$ 436.1653; found 436.1649, Δ -0.92 ppm.

4-(4-(((3-Bromophenyl)(phenyl)methyl)thio)butyl)-1-methyl-1H-1,2,3-triazole (208):

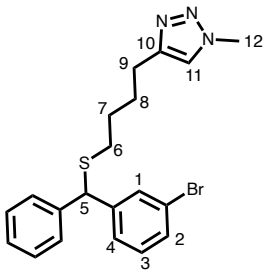

Using General procedure F: utilizing thiolacetate **186** (114.0 mg, 0.40 mmol, 1.0 eq) for formation of thiol; (3-bromophenyl)(phenyl)methanol (105.0 mg, 0.40 mmol, 1.0 eq) and HBr (33% in AcOH, 1.0 mL, 0.4M). Upon formation of thiol and benzhydryl bromide, utilized DBU (0.06 mL, 0.40 mmol, 1.0 eq). Following removal of solvent and purification by FCC 0->50% ethyl acetate in hexanes resulted in 90.2 mg (54.2%) of the product as a colorless oil.

^{1}HNMR (400 MHz, CDCl3) δ 7.57 (t, *J* = 1.9 Hz, 1H, C2-H), 7.42 – 7.21 (m, 8H, 3 x C1,3,4-H + 5 x C_{AR}-H), 7.16 (dd, *J* = 8.2, 7.4 Hz, 1H, C11-H), 5.07 (s, 1H, C5-H), 4.02 (s, 3H, C12-H_3), 2.66 (t, *J* = 7.4 Hz, 2H, C6-H_2), 2.41 (t, *J* = 7.2 Hz, 2H, C8-H_2), 1.77 – 1.67 (m, 2H, C7-H_2), 1.65 – 1.55 (m, 2H, C8-H_2).

^{13}CNMR(101 MHz, CDCL3) δ 148.02 (C_{AR}), 143.99 (C_{AR}), 140.76 (C9), 131.28 (C_{AR}), 131.28 (C_{AR}), 130.30 (C_{AR}), 130.15 (C_{AR}), 128.72 (C_{AR}), 128.23 (C_{AR}), 127.45 (C_{AR}), 127.02 (C_{AR}), 122.61 (C-Br), 121.73 (C11), 53.64 (C5), 36.56 (C12), 32.08 (C9), 28.56 (C7), 28.38 (C8), 25.18 (C6).

IR ν_{max} (film)/cm^{-1}: 2941, 2856, 1586, 1566, 1471, 1451, 1214, 1072, 1052, 778, 703.

HRMS: (ESI+) m/z calculated for $[C_{20}H_{22}BrN_3S+H]^+$ 418.0769; found 418.0766, Δ -0.84 ppm.

4-(3-(((3-Bromophenyl)(phenyl)methyl)thio)propyl)-1-methyl-1H-1,2,3-triazole (209):

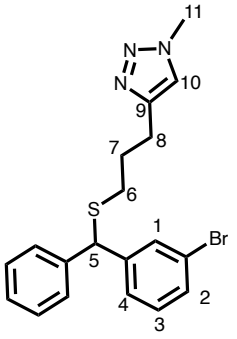

Using General procedure F: utilizing thiolacetate **191** (108.6 mg, 0.40 mmol, 1.0 eq) for formation of thiol; (3-bromophenyl)(phenyl)methanol (105.0 mg, 0.40 mmol, 1.0 eq) and HBr (33% in AcOH, 1.0 mL, 0.4M). Upon formation of thiol and benzhydryl bromide, utilized DBU (0.06 mL, 0.40 mmol, 1.0 eq). Following removal of solvent and purification by FCC 0->50% ethyl acetate in hexanes resulted in 49.0 mg (30.5%) of the product as a colorless oil.

^{1}HNMR (400 MHz, CDCl3) δ 7.57 (t, *J* = 1.7 Hz, 1H, C2-H), 7.43 – 7.21 (m, 7H, C1-H + C3-H + 5 x C_{AR}-H), 7.18 (d, *J* = 7.6 Hz, 1H, C4-H), 7.15 (s, 1H, C10-H), 5.09 (s, 1H, C5-H), 4.02 (s, 3H, C11-H_3), 2.77 (t, *J* = 7.4 Hz, 2H, C6-H_2), 2.43 (t, *J* = 7.2 Hz, 2H, C8-H_2), 1.93 (p, *J* = 7.3 Hz, 2H, C7-H_2).

^{13}CNMR(101 MHz, CDCL3) δ 147.34 (C_{AR}), 143.97 (C_{AR}), 140.77 (C10), 131.35 (C_{AR}), 130.39 (C_{AR}), 130.22 (C_{AR}), 128.32 (C_{AR}), 127.53 (C_{AR}), 127.12 (C_{AR}), 122.68 (C-Br), 121.95 (C11), 53.55 (C5), 36.63 (C11), 31.54 (C8), 28.60 (C7), 24.54 (C6).

IR ν_{max} (film)/cm^{-1}: 2945, 1586, 1567, 1493, 1471, 1451, 1215, 1072, 1051, 780, 703.

HRMS: (ESI+) m/z calculated for $[C_{19}H_{20}BrN_3S+H]^+$ 404.0613; found 404.0609, Δ -0.85 ppm.

1-Benzyl-4-(4-(((3-bromophenyl)(phenyl)methyl)thio)butyl)-1H-1,2,3-triazole (210):

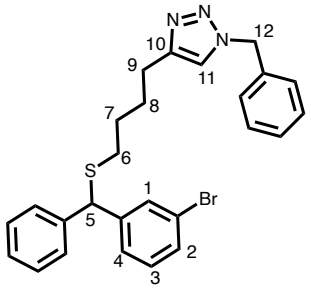

Using General procedure F: utilizing thiolacetate **189** (100.0 mg, 0.35 mmol, 1.0 eq) for formation of thiol; (3-bromophenyl)(phenyl)methanol (72.6 mg, 0.36 mmol, 1.0 eq) and HBr (33% in AcOH, 0.90 mL, 0.4M). Upon formation of thiol and benzhydryl bromide, utilized DBU (0.05 mL, 0.35 mmol, 1.0 eq). Following removal of solvent and purification by FCC 0->50% ethyl acetate in hexanes resulted in 117.2 mg (68.9%) of the product as a colorless oil.

^{1}HNMR (400 MHz, CDCl3) δ 7.55 (d, *J* = 1.8 Hz, 1H, C2-H), 7.39 – 7.29 (m, 8H, C1-H + C3-H + 6 x C_{AR}-H), 7.27 – 7.18 (m, 4H, 4 x C_{AR}-H), 7.17 – 7.10 (m, 2H, C11-H + C4-H), 5.45 (s, 2H, C12-H_2), 5.05 (s, 1H, C5-H), 2.63 (t, *J* = 7.5 Hz, 2H, C6-H_2), 2.38 (t, *J* = 7.1 Hz, 2H, C9-H_2), 1.69 (p, *J* = 7.3 Hz, 2H, C7-H_2), 1.58 (p, *J* = 7.2 Hz, 2H, C8-H_2).

^{13}CNMR(101 MHz, CDCL3) δ 148.23 (C_{AR}), 143.94 (C_{AR}), 140.71 (C_{AR}), 134.95 (C10), 131.24 (C_{AR}), 130.26 (C_{AR}), 130.12 (C_{AR}), 129.06 (C_{AR}), 128.69 (C_{AR}), 128.62 (C_{AR}), 128.20 (C_{AR}), 127.96 (C_{AR}), 127.41 (C_{AR}), 126.98 (C_{AR}), 122.58 (C-Br), 120.62 (C11), 53.96 (C12), 53.56 (C5), 32.00 (C9), 28.43 (C8), 28.38 (C7), 25.21 (C6).

IR ν_{max} (film)/cm^{-1}: 3060, 2931, 2855, 1586, 1566, 1494, 1453, 1303, 1215, 1073, 1049, 1029, 778, 726, 701.

HRMS: (ESI+) m/z calculated for $[C_{26}H_{26}BrN_3S+H]^+$ 494.1083; found 494.1080, Δ -0.92 ppm.

1-Benzyl-4-(3-(((3-bromophenyl)(phenyl)methyl)thio)propyl)-1H-1,2,3-triazole (211):

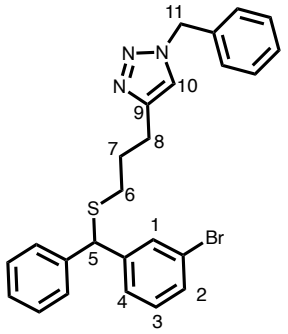

Using General procedure F: utilizing thiolacetate **193** (100.0 mg, 0.36 mmol, 1.0 eq) for formation of thiol; (3-bromophenyl)(phenyl)methanol (72.6 mg, 0.36 mmol, 1.0 eq) and HBr (33% in AcOH, 0.90 mL, 0.4M). Upon formation of thiol and benzhydryl bromide, utilized DBU (0.06 mL, 0.36 mmol, 1.0 eq). Following removal of solvent and purification by FCC 0->50% ethyl acetate in hexanes resulted in 127.2 mg (73.2%) of the product as a colorless oil.

^{1}HNMR (400 MHz, CDCl3) δ 7.55 (t, *J* = 1.9 Hz, 1H, C2-H), 7.38 – 7.28 (m, 8H, C1-H + 7 x C_{AR}-H), 7.26 – 7.19 (m, 4H, C3-H + 3 x C_{AR}-H), 7.15 – 7.09 (m, 2H, C10-H + C4-H), 5.44 (s, 2H, C11-H_2), 5.06 (s, 1H, C5-H), 2.74 (t, *J* = 7.5 Hz, 2H, C6-H_2), 2.40 (t, *J* = 7.2 Hz, 2H, C8-H_2), 1.89 (p, *J* = 7.3 Hz, 2H, C7-H_2).

^{13}CNMR(101 MHz, CDCL3) δ 147.46 (C_{AR}), 143.89 (C_{AR}), 140.68 (C_{AR}), 134.91 (C9), 131.23 (C_{AR}), 130.27 (C_{AR}), 130.12 (C_{AR}), 129.06 (C_{AR}), 128.68 (C_{AR}), 128.63 (C_{AR}), 128.21 (C_{AR}), 127.96

(C_{AR}), 127.42 (C_{AR}), 127.00 (C_{AR}), 122.57 (C-Br), 120.82 (C10), 53.95 (C11), 53.46 (C5), 31.56 (C8), 28.48 (C7), 24.57 (C6).

IR ν_{max} (film)/cm^{-1}: 3061, 2927, 1586, 1566, 1458, 1216, 1073, 1048, 778, 727, 702.

HRMS: (ESI+) m/z calculated for $[C_{25}H_{24}BrN_3S+H]^+$ 480.0926; found 480.0924, Δ -0.38 ppm.

4-((((3-Bromophenyl)(phenyl)methyl)thio)methyl)-1H-imidazole (212):

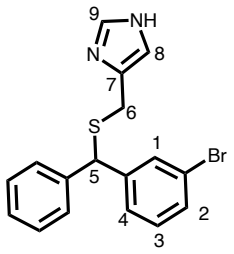

Using General procedure F: utilizing thiolacetate **200** (50.0 mg, 0.33 mmol, 1.0 eq) for formation of thiol; (3-bromophenyl)(phenyl)methanol (66.6 mg, 0.33 mmol, 1.0 eq) and HBr (33% in AcOH, 0.80 mL, 0.4M). Upon formation of thiol and benzhydryl bromide, utilized DBU (0.05 mL, 0.40 mmol, 1.0 eq). Following removal of solvent and purification by FCC 0->50% ethyl acetate in hexanes resulted in 50.2 mg (42.1%) of the product as a waxy solid.

^{1}HNMR (400 MHz, CDCl3) δ 7.57 (s, 1H, C9-H), 7.51 (s, 1H, C2-H), 7.40 – 7.19 (m, 7H, C1-H + C3-H + 5 x C_{AR}-H), 7.13 (t, J = 7.8 Hz, 1H, C4-H), 6.80 (s, 1H, C8-H), 5.00 (s, 1H, C5-H), 3.58 (s, 2H, C6-H_2).

^{13}CNMR(101 MHz, CDCL3) δ 143.57 (C_{AR}), 140.37 (C_{AR}), 135.61 (C9), 131.48 (C7), 130.43 (C_{AR}), 130.22 (C_{AR}), 128.83 (C8), 128.46 (C_{AR}), 127.60 (C_{AR}), 127.21 (C_{AR}), 122.70 (C-Br), 60.57 (C6), 53.06 (C5).

IR ν_{max} (film)/cm^{-1}: 3061, 2924, 2853, 1585, 1566, 1492, 1471, 1451, 1073, 995, 827, 775, 702.

HRMS: (ESI+) m/z calculated for $[C_{17}H_{15}BrN_2S+H]^+$ 361.0191; found 361.0188, Δ -0.61 ppm.

4-((((3-Bromophenyl)(phenyl)methyl)thio)methyl)-1-methyl-1H-imidazole (213):

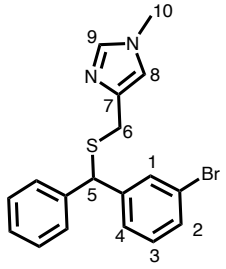

Using General procedure F: utilizing thiolacetate **206** (68.1 mg, 0.40 mmol, 1.0 eq) for formation of thiol; (3-bromophenyl)(phenyl)methanol (105.0 mg, 0.40 mmol, 1.0 eq) and HBr (33% in AcOH, 1.0 mL, 0.4M). Upon formation of thiol and benzhydryl bromide, utilized DBU (0.06 mL, 0.40 mmol, 1.0 eq). Following removal of solvent and purification by FCC 0->50% ethyl acetate in hexanes resulted in 49.5 mg (33.1%) of the product as a colorless oil.

^{1}HNMR (400 MHz, CDCl3) δ 7.56 (t, *J* = 1.7 Hz, 1H, C9-H), 7.43 – 7.19 (m, 8H, 3 x C1,2,3-H + 5 x C_{AR}-H), 7.15 (t, *J* = 7.8 Hz, 1H, C4-H), 6.63 (s, 1H, C8-H), 5.16 (s, 1H, C5-H), 3.60 (s, 3H, C10-H_3), 3.54 (s, 2H, C6-H_2).

^{13}CNMR(101 MHz, CDCL3) δ 143.98 (C_{AR}), 140.76 (C_{AR}), 139.20 (C9), 137.68 (C7), 131.54 (C_{AR}), 130.22 (C_{AR}), 130.09 (C_{AR}), 128.70 (C_{AR}), 128.48 (C_{AR}), 127.40 (C_{AR}), 127.26 (C_{AR}), 122.57 (C-Br), 117.85 (C8), 53.35 (C5), 33.44 (C10), 29.86 (C6).

IR ν_{max} (film)/cm^{-1}: 3058, 2923, 2589, 2566, 1506, 1471, 1420, 1231, 1165, 1072, 984, 753, 702

HRMS: (ESI+) m/z calculated for $[C_{18}H_{17}BrN_2S+H]^+$ 375.0347; found 375.0345, Δ -0.59 ppm.

1-Benzyl-4-(2-(((3-bromophenyl)(phenyl)methyl)thio)ethyl)-1H-1,2,3-triazole (214):

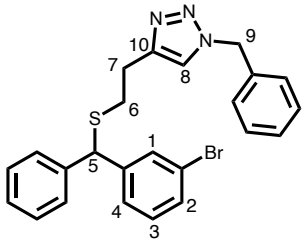

Using General procedure F: utilizing thiolacetate **196** (61.0 mg, 0.23 mmol, 1.0 eq) for formation of thiol; (3-bromophenyl)(phenyl)methanol (46.4 mg, 0.36 mmol, 1.0 eq) and HBr (33% in AcOH, 0.60 mL, 0.4M). Upon formation of thiol and benzhydryl bromide, utilized DBU (0.04 mL, 0.36 mmol, 1.0 eq). Following removal of solvent and purification by FCC 0->50% ethyl acetate in hexanes resulted in 45.6 mg (42.1%) of the product as a colorless oil.

^{1}HNMR (400 MHz, CDCl3) δ 7.53 (d, *J* = 1.8 Hz, 1H, C2-H), 7.39 – 7.20 (m, 13H, C8-H + 2 x C1,3-H + 10 x C_{AR}-H), 7.14 (t, *J* = 7.8 Hz, 1H, C4-H), 5.46 (s, 2H, C9-H_2), 5.05 (s, 1H, C5-H), 2.92 (t, *J* = 7.3 Hz, 2H, C6-H_2), 2.71 (t, *J* = 7.3 Hz, 2H, C7-H_2).

^{13}CNMR(101 MHz, CDCL3) δ 146.51 (C_{AR}), 143.79 (C_{AR}), 140.60 (C_{AR}), 134.90 (C10), 131.31 (C_{AR}), 130.43 (C_{AR}), 130.22 (C_{AR}), 129.16 (C_{AR}), 128.80 (C_{AR}), 128.75 (C_{AR}), 128.27 (C_{AR}), 128.07 (C_{AR}), 127.57 (C_{AR}), 127.06 (C_{AR}), 122.69 (C-Br), 121.34 (C8), 54.10 (C9), 53.82 (C5), 31.90 (C7), 25.79 (C6).

IR ν_{max} (film)/cm^{-1}: 3029, 2922, 1953, 1881, 1808, 1586, 1494, 1470, 1453, 1218, 1073, 1048, 728, 701.

HRMS: (ESI+) m/z calculated for $[C_{24}H_{22}BrN_3S+H]^+$ 466.0769; found 466.0768, Δ -0.60 ppm.

4-(4-(((3-Bromophenyl)(phenyl)methyl)sulfinyl)butyl)-1-methyl-1H-1,2,3-triazole (215):

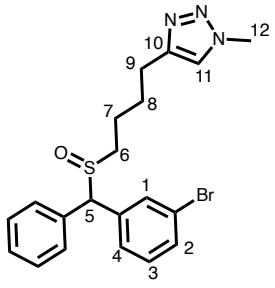

Compound **215** was prepared through General procedure G. Starting from sulfide **208** (75.9 mg, 0.18 mmol, 1.0 eq) and mCPBA (33.0 mg, 0.19 mmol, 1.05 eq). Following concentration under

reduced pressure, the sulfoxide was purified by FCC 0->2% methanol in DCM to yield 45.5 mg (57.7%) of the product as a colorless oil.

^{1}HNMR (400 MHz, CDCl3) δ 7.58 (dt, *J* = 16.2, 1.7 Hz, 1H, C2-H), 7.49 – 7.34 (m, 7H), 7.26 (d, *J* = 7.3 Hz, 2H, C11-H + C4-H), 4.75 (d, *J* = 10.1 Hz, 1H, C5-H), 4.04 (s, 3H, C12-H_3), 2.69 (t, *J* = 6.4 Hz, 2H, C6-H_2), 2.50 (t, *J* = 7.2 Hz, 2H, C9-H_2), 1.78 (qd, *J* = 19.7, 17.5, 8.1 Hz, 4H, C7-H_2 + C8-H_2).

Note corresponds to mixture of diastereomers:

^{13}CNMR(101 MHz, CDCL3) δ 147.50 (C_{AR}), 138.43 (C_{AR}), 137.53 (C_{AR}), 135.18 (C_a10), 134.14 (C_b10), 132.22 (C_{AR}), 131.61 (C_{AR}), 131.56 (C_{AR}), 131.51 (C_{AR}), 130.85 (C_{AR}), 130.35 (C_{AR}), 129.59 (C_{AR}), 129.42 (C_{AR}), 129.00 (C_{AR}), 128.77 (C_{AR}), 128.67 (C_{AR}), 128.57 (C_{AR}), 128.03 (C_{AR}), 127.26 (C_{AR}), 123.33 (C_a-Br), 122.90 (C_b-Br), 121.96 (C11), 72.15 (C_a5), 71.36 (C_b5), 50.84 (C_a9), 50.77 (C_b9), 36.65 (C12), 28.49 (C_a7), 28.44 (C_b7), 25.16 (C6), 22.32 (C_a8), 22.19 (C_b8).

IR ν_{max} (film)/cm^{-1}: 3439, 3061, 2938, 1587, 1565, 1495, 1473, 1453, 1214, 1047, 885, 788, 705.

HRMS: (ESI+) m/z calculated for $[C_{20}H_{22}BrN_3OS+H]^+$ 434.0719; found 434.0714, Δ -0.65 ppm.

1-Benzyl-4-(4-(((3-bromophenyl)(phenyl)methyl)sulfinyl)butyl)-1H-1,2,3-triazole (216):

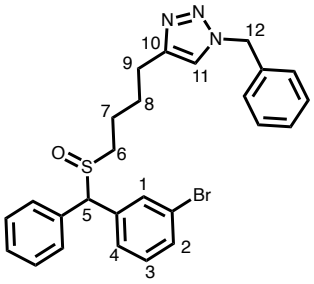

Compound **216** was prepared through General procedure G. Starting from sulfide **210** (100.0 mg, 0.20 mmol, 1.0 eq) and mCPBA (36.8 mg, 0.21 mmol, 1.05 eq). Following concentration under reduced pressure, the sulfoxide was purified by FCC 0->50% ethyl acetate in hexanes to yield 55.5 mg (53.8%) of the product as a colorless oil.

^{1}HNMR (400 MHz, CDCl3) δ 7.57 (td, *J* = 17.2, 16.9, 2.0 Hz, 1H, C2-H), 7.48 – 7.40 (m, 3H), 7.40 – 7.31 (m, 7H), 7.25 (q, *J* = 4.7, 3.3 Hz, 3H), 7.18 (d, *J* = 3.6 Hz, 1H, C11-H), 5.47 (s, 2H, C12-H_2), 4.74 (d, *J* = 10.3 Hz, 1H, C5-H), 2.66 (q, *J* = 6.6 Hz, 2H, C6-H_2), 2.49 (t, *J* = 7.3 Hz, 2H, C9-H_2), 1.88 – 1.63 (m, 4H, C7-H_2 + C8-H_2).

Note corresponds to mixture of diastereomers:

^{13}CNMR(101 MHz, CDCL3) δ 147.72 (C_{AR}), 138.42 (C_{AR}), 137.51 (C_{AR}), 135.16 (C_{AR}), 134.92 (C_a10), 134.10 (C_b10), 132.20 (C_{AR}), 131.59 (C_{AR}), 131.53 (C_{AR}), 131.49 (C_{AR}), 130.82 (C_{AR}), 130.32 (C_{AR}), 129.56 (C_{AR}), 129.41 (C_{AR}), 129.17 (C_{AR}), 128.97 (C_{AR}), 128.75 (C_{AR}), 128.74 (C_{AR}), 128.64 (C_{AR}), 128.54 (C_{AR}), 128.09 (C_{AR}), 128.01 (C_{AR}), 127.24 (C_{AR}), 123.30 (C_aBr), 122.88 (C_bBr), 120.83 (C11), 72.07 (C_a5), 71.26 (C_b5), 54.10 (C12), 50.76 (C_a9), 50.72 (C_b9), 28.43 (C_a8), 28.38 (C_b8), 25.25 (C6), 22.39 (C_a7), 22.24 (C_b7).

IR ν_{max} (film)/cm^{-1}: 3443, 3062, 2934, 1587, 1565, 1496, 1454, 1215, 1048, 1028, 909, 726, 702.

HRMS: (ESI+) m/z calculated for $[C_{26}H_{26}BrN_3OS+H]^+$ 510.1032; found 510.1028, Δ -0.79 ppm.

1-Benzyl-4-(3-(((3-bromophenyl)(phenyl)methyl)sulfinyl)propyl)-1H-1,2,3-triazole (217):

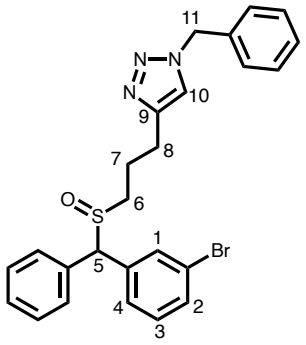

Compound **217** was prepared through General procedure G. Starting from sulfide **211** (110.0 mg, 0.23 mmol, 1.0 eq) and mCPBA (41.7 mg, 0.24 mmol, 1.05 eq). Following concentration under reduced pressure, the sulfoxide was purified by FCC 0->50% ethyl acetate in hexanes to yield 55.6 mg (48.9%) of the product as a colorless oil.

^{1}HNMR (400 MHz, CDCl3) δ 7.57 (td, *J* = 15.2, 15.1, 1.7 Hz, 1H, C2-H), 7.48 – 7.31 (m, 10H, C1-H + 9 x C_{AR}-H), 7.24 (d, *J* = 5.4 Hz, 3H, C4-H + C3-H + C_{AR}-H), 7.17 (d, *J* = 5.6 Hz, 1H, C10-H), 5.46 (s, 2H, C11-H_2), 4.74 (d, *J* = 10.1 Hz, 1H, C5-H), 2.87 – 2.69 (m, 2H, C6-H_2), 2.63 – 2.43 (m, 2H, C8-H_2), 2.11 (p, *J* = 7.5 Hz, 2H, C7-H_2).

Note corresponds to mixture of diastereomers:

^{13}CNMR(101 MHz, CDCL3) δ 146.87 (C_{AR}), 146.84 (C_{AR}), 138.40 (C_{AR}), 137.37 (C_{AR}), 135.13 (C_a9), 134.81 (C_b9), 133.97 (C_{AR}), 132.22 (C_{AR}), 131.56 (C_{AR}), 131.50 (C_{AR}), 130.81 (C_{AR}), 130.30 (C_{AR}), 129.53 (C_{AR}), 129.45 (C_{AR}), 129.19 (C_{AR}), 128.95 (C_{AR}), 128.80 (C_{AR}), 128.80 (C_{AR}), 128.71 (C_{AR}), 128.64 (C_{AR}), 128.57 (C_{AR}), 128.09 (C_{AR}), 128.06 (C_{AR}), 127.28 (C_{AR}), 123.25 (C_aBr), 122.86 (C_bBr), 121.09 (C_a10), 121.06 (C_b10), 71.80 (C_a5), 71.01 (C_b5), 54.13 (C11), 50.11 (C_a8), 50.06 (C_b8), 24.59 (C6), 22.57 (C_a7), 22.45 (C_b7).

IR ν_{max} (film)/cm^{-1}: 3443, 3062, 2930, 1587, 1565, 1496, 1454, 1217, 1047, 789, 704.

HRMS: (ESI+) m/z calculated for $[C_{25}H_{24}BrN_3OS+H]^+$ 496.0875; found 496.0872, Δ -0.55 ppm.

Chiral HPLC: Chiralpak IA with guard, 50% IPA, 50% hexane, 0.7 mL/min, 25 °C, , λ = 210 nm, 10 μL injection; τR (A) = 17.1 min, 28%, τR (B) = 18.8 min, 28%, τR (C) = 21.6 min, 22%, τR (B) = 21.6 min, 22%.

4-((((3-Bromophenyl)(phenyl)methyl)sulfinyl)methyl)-1H-imidazole (218):

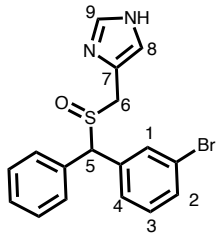

Compound **218** was prepared through General procedure G. Starting from sulfide **212** (43.2 mg, 0.12 mmol, 1.0 eq) and mCPBA (21.8 mg, 0.13 mmol, 1.05 eq). Following concentration under

reduced pressure, the sulfoxide was purified by FCC 0->4% Methanol in DCM to yield 14.5 mg (32.1%) of the product as a colorless oil.

^{1}HNMR (400 MHz, CDCl3) δ 7.61 (br s, 1H, C9-H), 7.57 – 7.53 (m, 1H, N-H), 7.52 – 7.34 (m, 7H, C2-H + C1-H + 5 x C_{AR}-H), 7.32 – 7.20 (m, 2H, C4-H + C3-H), 6.91 (s, 1H, C8-H), 5.10 (d, *J* = 9.1 Hz, 1H, C5-H), 3.95 (dd, *J* = 14.0, 7.7 Hz, 1H, C6-H_aH_b), 3.67 (d, *J* = 13.9 Hz, 1H, C6-H_aH_b).

Note corresponds to mixture of diastereomers:

^{13}CNMR(101 MHz, CDCL3) δ 138.11 (C_{AR}), 137.23 (C_{AR}), 136.20 (C9), 134.86 (C_{AR}), 134.02 (C_{AR}), 132.59 (C_{AR}), 131.99 (C_{AR}), 131.72 (C_{AR}), 131.59 (C_{AR}), 130.93 (C_{AR}), 130.35 (C_{AR}), 129.75 (C_{AR}), 129.66 (C_{AR}), 129.05 (C_{AR}), 128.92 (C_{AR}), 128.73 (C_{AR}), 128.29 (C_{AR}), 127.74 (C_{AR}), 123.39 (C_aBr), 122.92 (C_bBr), 69.37 (C_a5), 68.96 (C_a5), 47.61 (C_a6), 47.26 (C_b6).

IR ν_{max} (film)/cm^{-1}: 3149, 2924, 1587, 1566, 1495, 1473, 1426, 1032, 829, 732, 703.

HRMS: (ESI+) m/z calculated for $[C_{17}H_{15}BrN_2OS+H]^+$ 377.0139; found 377.017, Δ -0.64 ppm.

4-((((3-Bromophenyl)(phenyl)methyl)sulfinyl)methyl)-1-methyl-1H-imidazole (219):

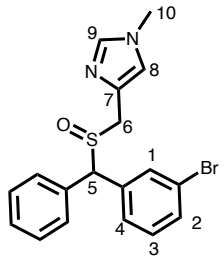

Compound **219** was prepared through General procedure G. Starting from sulfide **213** (39.8 mg, 0.107 mmol, 1.0 eq) and mCPBA (20.2 mg, 0.112 mmol, 1.05 eq). Following concentration under reduced pressure, the sulfoxide was purified by FCC 0->2% Methanol in DCM to yield 26.2 mg (63.1%) of the product as a colorless oil.

^{1}HNMR (400 MHz, CDCl3) δ 7.62 (dd, *J* = 16.1, 1.7 Hz, 1H, C9-H), 7.56 – 7.30 (m, 8H, C1-H + C2-H + C3-H + 5 x C_{AR}-H), 7.25 (q, *J* = 7.7 Hz, 1H, C4-H), 6.94 (d, *J* = 10.1 Hz, 1H, C8-H), 5.15 (d, *J* = 3.4 Hz, 1H, C5-H), 3.87 (dd, *J* = 13.8, 7.1 Hz, 1H, C6-H_aH$_b$), 3.73 – 3.62 (m, 4H, C6-H$_a$$H_b$ + C10-H$_3$).

Note corresponds to mixture of diastereomers:

^{13}CNMR(101 MHz, CDCL3) δ 138.16 (C_{AR}), 138.14 (C_{AR}), 137.17 (C_{AR}), 135.69 (C_{AR}), 133.75 (C_a9), 132.88 (C_b9), 131.31 (C_{AR}), 131.28 (C_{AR}), 130.94 (C_{AR}), 130.74 (C_{AR}), 130.13 (C_{AR}), 129.39 (C_{AR}), 129.16 (C_{AR}), 128.82 (C_{AR}), 128.62 (C_{AR}), 128.50 (C_{AR}), 127.82 (C_{AR}), 123.10 (C_aBr), 122.71 (C_bBr), 121.46 (C_a8), 121.23 (C_b8), 68.75 (C_a5), 68.29 (C_b5), 49.29 (C_a6), 49.03 (C_b6), 33.70 (C10).

IR ν_{max} (film)/cm^{-1}: 3437, 3060, 2922, 1564, 1506, 1473, 1163, 1042, 986, 704.

HRMS: (ESI+) m/z calculated for $[C_{18}H_{17}BrN_2OS+H]^+$ 391.0297; found 391.0294, Δ -0.64 ppm.

1-Benzyl-4-(3-((bis(4-fluorophenyl)methyl)sulfinyl)propyl)-1H-1,2,3-triazole (220)

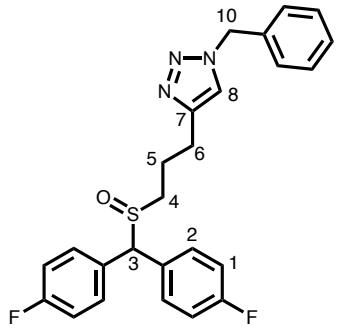

Compound **220** was prepared through General procedure G. Starting from sulfide **207** (45.0 mg, 0.103 mmol, 1.0 eq) and mCPBA (18.7 mg, 0.11 mmol, 1.05 eq). Following concentration under reduced pressure, the sulfoxide was purified by FCC 0->50% Ethyl Acetate in Hexanes to yield 27.3 mg (58.5%) of the product as a colorless oil.

^{1}HNMR (400 MHz, CDCl3) δ 7.43 – 7.32 (m, 7H, 4 x C1-H + 3 x C_{AR}-H), 7.26 – 7.22 (m, 2H, 2 x C_{AR}-H), 7.17 (s, 1H, C8-H), 7.12 – 7.02 (m, 4H, 4 x C2-H), 5.47 (s, 2H, C10-H_2), 4.80 (s, 1H, C3-H), 2.79 (t, *J* = 8.5 Hz, 2H, C4-H_2), 2.65 – 2.44 (m, 2H, C6-H_2), 2.12 (p, *J* = 7.5 Hz, 2H, C5-H_2).

^{13}CNMR(101 MHz, CDCL3) δ 162.78 (d, J = 223.2 Hz, C-F), 146.84 (C_{AR}), 134.76 (C7), 131.68 (d, J = 4.0 Hz, C_{AR}), 131.17 (d, J = 8.1 Hz, C_{AR}), 130.44 (C_{AR}), 129.25 (C_{AR}), 128.89 (C_{AR}), 121.13 (C8), 116.46 (d, J = 22.2 Hz, C2), 69.90 (C3), 54.22 (C10), 49.95 (C6), 24.59 (C4), 22.55 (C5).

^{19}F NMR (376 MHz, CDCL3) δ -112.61, -113.24.

IR ν_{max} (film)/cm^{-1}: 3070, 2929, 1708, 1603, 1507, 1226, 1160, 1048, 838, 727, 573.

HRMS: (ESI+) m/z calculated for $[C_{25}H_{23}F_2N_3OS+H]^+$ 452.1603; found 452.1597, Δ -1.13 ppm.

1-Benzyl-4-(2-(((3-bromophenyl)(phenyl)methyl)sulfinyl)ethyl)-1H-1,2,3-triazole (221):

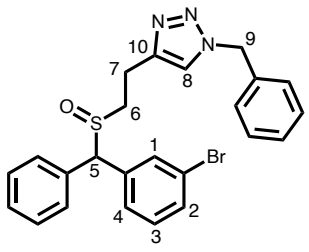

Compound **221** was prepared through General procedure G. Starting from sulfide **214** (45.6 mg, 0.98 mmol, 1.0 eq) and mCPBA (17.8 mg, 0.10 mmol, 1.05 eq). Following concentration under reduced pressure, the sulfoxide was purified by FCC 0->5% Methanol in DCM to yield 15.8 mg (33.5%) of the product as a colorless oil.

^{1}HNMR (400 MHz, CDCl3) δ 7.56 (d, *J* = 18.7 Hz, 1H, C2-H), 7.48 – 7.19 (m, 14H, C8-H + 10 x C_{AR}-H + 3 x C1,3,4-H), 5.56 – 5.38 (m, 2H, C9-H_2), 4.78 (d, *J* = 10.0 Hz, 1H, C5-H), 3.15 (t, *J* = 7.4 Hz, 2H, C7-H), 3.05 – 2.89 (m, 1H, C6-H_aH$_b$), 2.78 (dq, *J* = 20.5, 6.5 Hz, 1H, C6-H$_a$$H_b$).

Note corresponds to mixture of diastereomers:

^{13}CNMR(101 MHz, CDCL3) δ 145.05 (C_{AR}), 138.17 (C_{AR}), 137.39 (C_{AR}), 134.88 (C_a10), 134.68 (C_b10), 134.02 (C_{AR}), 132.26 (C_{AR}), 131.67 (C_{AR}), 131.64 (C_{AR}), 131.61 (C_{AR}), 130.88 (C_{AR}), 130.37 (C_{AR}), 129.64 (C_{AR}), 129.50 (C_{AR}), 129.27 (C_{AR}), 129.04 (C_{AR}), 128.93 (C_{AR}), 128.87 (C_{AR}), 128.75 (C_{AR}), 128.60 (C_{AR}), 128.19 (C_{AR}), 128.10 (C_{AR}), 127.28 (C_{AR}), 123.39 (C_aBr), 122.96 (C_bBr), 121.87 (C8), 72.20 (C_a5), 71.41 (C_b5), 54.28 (C9), 50.26 (C_a6), 50.20 (C_b6), 19.36 (C_a7), 19.27 (C_b7).

IR ν_{max} (film)/cm^{-1}: 3062, 2927, 1565, 1496, 1473, 1454, 1220, 1048, 728, 704.

HRMS: (ESI+) m/z calculated for $[C_{24}H_{22}BrN_3OS+H]^+$ 482.0719; found 482.0717, Δ -0.37 ppm.

8.2.4 Computational Methods

QSAR modeling prediction

Machine learning (ML)-based QSAR models were built to predict the hDAT binding affinities of the bisphenyl DAT inhibitors. ML-based QSAR models trained with the hDAT binding Ki dataset and eXtreme Gradient Boosting (XGBoost) algorithm was used for modeling prodiction.

Data was obtained from ChEMBL database using the same filtering pipeline used in previous study.[11] We updated the training dataset using ChEMBL version 34, and only kept the largest pChEMBL value among the compounds with the same chemical structure (Tanimoto similarity > 0.999). The binding dataset comprise 1259 Ki data points. This dataset was used to search the hyper-parameter space as described previously. Ten production models were then generated using the resulting hyper-parameters and 100% of the data. These QSAR models were used to predict the hDAT binding affinities (pKi) for the DAT inhibitors. For each compound, the mean and the standard deviation of the ten predicted pKi values were calculated.

Molecular docking and molecular dynamics simulation

The molecular modeling and docking were carried out with the Schrodinger Suite (version 2025-3). The pKa predictions of the protonation state of the ligands were performed using Epik.[12] The 3D structures of the ligands were then generated using LigPrep. The hDAT model was constructed from the cryo-EM structure of the human dopamine transporter co-crystallized with benztropine (PDB ID: 8Y2E).[13] The hDAT structure was prepared using the protein preparation protocol.

Finally, the induced fitted docking (IFD)[14] was used to perform molecular docking. The final binding poses were selected based on the best IFD scores obtained.

8.2.5 References for Experimental section

(1) Camacho-Hernandez, G. A.; Gopinath, A.; Okorom, A. V.; Khoshbouei, H.; Newman, A. H. Development of a Fluorescently Labeled Ligand for Rapid Detection of DAT in Human and Mouse Peripheral Blood Monocytes. *JACS Au* **2024**, *4* (2), 657–665. https://doi.org/10.1021/jacsau.3c00719.

(2) Akhtar, W. M.; Armstrong, R. J.; Frost, J. R.; Stevenson, N. G.; Donohoe, T. J. Stereoselective Synthesis of Cyclohexanes via an Iridium Catalyzed (5 + 1) Annulation Strategy. *J. Am. Chem. Soc.* **2018**, *140* (38), 11916–11920. https://doi.org/10.1021/jacs.8b07776.

(3) Smith, L. B.; Armstrong, R. J.; Matheau-Raven, D.; Donohoe, T. J. Chemo- and Regioselective Synthesis of Acyl-Cyclohexenes by a Tandem Acceptorless Dehydrogenation-[1,5]-Hydride Shift Cascade. *J. Am. Chem. Soc.* **2020**, *142* (5), 2514–2523. https://doi.org/10.1021/jacs.9b12296.

(4) Kuehne, M. E.; Bornmann, W. G.; Markó, I.; Qin, Y.; LeBoulluec, K. L.; Frasier, D. A.; Xu, F.; Mulamba, T.; Ensinger, C. L.; Borman, L. S.; Huot, A. E.; Exon, C.; Bizzarro, F. T.; Cheung, J. B.; Bane, S. L. Syntheses and Biological Evaluation of Vinblastine Congeners. *Org Biomol Chem* **2003**, *1* (12), 2120–2136. https://doi.org/10.1039/B209990J.

(5) Das, J.; Singh, K.; Vellakkaran, M.; Banerjee, D. Nickel-Catalyzed Hydrogen-Borrowing Strategy for α-Alkylation of Ketones with Alcohols: A New Route to

Branched *Gem* -Bis(Alkyl) Ketones. *Org. Lett.* **2018**, *20* (18), 5587–5591. https://doi.org/10.1021/acs.orglett.8b02256.

(6) Masuda, M.; Miyazawa, S.; Ito, Y.; Matsuo, I. Synthesis of a Versatile Probe for Analysis of Cytoplasmic Peptide- *N* -Glycanase. *J. Chin. Chem. Soc.* **2012**, *59* (3), 269–272. https://doi.org/10.1002/jccs.201100631.

(7) Pokhodylo, N. T.; Tupychak, M. A.; Shyyka, O. Ya.; Obushak, M. D. Some Aspects of the Azide-Alkyne 1,3-Dipolar Cycloaddition Reaction. *Russ. J. Org. Chem.* **2019**, *55* (9), 1310–1321. https://doi.org/10.1134/S1070428019090082.

(8) Huy, P. H.; Motsch, S.; Kappler, S. M. Formamides as Lewis Base Catalysts in S_N Reactions—Efficient Transformation of Alcohols into Chlorides, Amines, and Ethers. *Angew. Chem. Int. Ed.* **2016**, *55* (34), 10145–10149. https://doi.org/10.1002/anie.201604921.

(9) Valderrama-Callejón, R.; Vargas, E. L.; Alonso, I.; Tortosa, M.; Belén Cid, M. Diboron Reagents in N−N Bond Cleavage of Hydrazines, *N* -Nitrosamines, and Azides: Reactivity and Mechanistic Insights. *Chem. – Eur. J.* **2025**, *31* (26), e202404081. https://doi.org/10.1002/chem.202404081.

(10) Chassaing, S.; Sani Souna Sido, A.; Alix, A.; Kumarraja, M.; Pale, P.; Sommer, J. “Click Chemistry” in Zeolites: Copper(I) Zeolites as New Heterogeneous and Ligand-Free Catalysts for the Huisgen [3+2] Cycloaddition. *Chem. – Eur. J.* **2008**, *14* (22), 6713–6721. https://doi.org/10.1002/chem.200800479.

(11) Lee, K. H.; Fant, A. D.; Guo, J.; Guan, A.; Jung, J.; Kudaibergenova, M.; Miranda, W. E.; Ku, T.; Cao, J.; Wacker, S.; Duff, H. J.; Newman, A. H.; Noskov, S. Y.; Shi, L. Toward Reducing hERG Affinities for DAT Inhibitors with a Combined Machine Learning and

Molecular Modeling Approach. *J. Chem. Inf. Model.* **2021**, *61* (9), 4266–4279. https://doi.org/10.1021/acs.jcim.1c00856.

(12) Li, Y.; Wang, X.; Meng, Y.; Hu, T.; Zhao, J.; Li, R.; Bai, Q.; Yuan, P.; Han, J.; Hao, K.; Wei, Y.; Qiu, Y.; Li, N.; Zhao, Y. Dopamine Reuptake and Inhibitory Mechanisms in Human Dopamine Transporter. *Nature* **2024**, *632* (8025), 686–694. https://doi.org/10.1038/s41586-024-07796-0.

(13) Shelley, J. C.; Cholleti, A.; Frye, L. L.; Greenwood, J. R.; Timlin, M. R.; Uchimaya, M. Epik: A Software Program for pK a Prediction and Protonation State Generation for Drug-like Molecules. *J. Comput. Aided Mol. Des.* **2007**, *21* (12), 681–691. https://doi.org/10.1007/s10822-007-9133-z.

(14) Sherman, W.; Beard, H. S.; Farid, R. Use of an Induced Fit Receptor Structure in Virtual Screening. *Chem. Biol. Drug Des.* **2006**, *67* (1), 83–84. https://doi.org/10.1111/j.1747-0285.2005.00327.x.

(15) Vidal, C.; Garcia-Alvarez, J. Glycerol: a biorenewable solvent for base-free Cu(I)-catalyzed 1,3-dipolar cycloaddition of azides with terminal and 1-iodoalkynes. Highly efficient transformations and catalyst recycling. *Green Chem.* **2014**, *16* (7), 3515–3521.

9 Appendix

Protocol for radioligand binding assays:

HEK293 cells stably expressing human DAT were grown in Dulbecco's modified Eagle medium (DMEM), supplemented with 5% fetal bovine serum, 5% calf bovine serum, 100 units/mL S20 penicillin/ 100 ug/mL streptomycin and 2 ug/mL puromycin and kept in an incubator at 37 °C and 10% CO2. Upon reaching 80−90% confluence, cells were harvested using premixed Earle's balanced salt solution with 5 mM ethylenediaminetetraacetic acid (EDTA) (Life Technologies) and centrifuged at 3000 rpm for 10 min at 21 °C. The supernatant was removed, and the pellet was resuspended in 10 mL of hypotonic lysis buffer (5 mM MgCl2, 5 mM Tris, pH 7.4 at 4 °C) and centrifuged at 14,500 rpm (∼25,000 g) for 30 min at 4 °C. The pellet was then resuspended in binding buffer (50mM Tris, 120 mM NaCl, pH 7.4) Bradford protein assay (Bio- Rad, Hercules, CA) was used to determine the protein concentration and the membranes were diluted to 1000 μg/mL and stored in a −80 °C freezer for later use. Radioligand binding assays were conducted similar to those previously described.9 Experiments were conducted in 96-well polypropylene plates containing 50 μL of various concentrations of the test compound, diluted using 30% DMSO vehicle, 300 μL of binding buffer (50 mM Tris, 120 mM NaCl, pH 7.4) 50 μL of [3H]WIN35,4288 (final concentration 1.5 nM; Kd = 38.1 nM; NOVANDI Chemistry AB, 78 Ci/mmol SA), and 100 μL of membranes 30 μg/well). All compound dilutions were tested in triplicate and the competition reactions started with the addition of tissue; the plates were incubated for 120 min at 4 °C. Nonspecific binding was determined using 10 μM final concentration of indatraline. For all binding assays, incubations were terminated by rapid filtration through PerkinElmer Uni-Filter-96 GF/B or GF/C (rDAT, rSERT, hDAT) or Whatman GF/B filters (rNET), presoaked in either 0.3% (rSERT and rNET), 0.05% (RDAT) or 0.2% (hDAT) polyethylenimine, using a Brandel 96-Well

Plates Harvester manifold or Brandel R48 filtering manifold (Brandel Instruments, Gaithersburg, MD). The filters were washed a total of three times with 3 mL (3 × 1 mL/well or 3 × 1 mL/tube) of ice-cold binding buffer. For rDAT, rSERT and hDAT binding experiment 65 µL PerkinElmer MicroScint20 Scintillation Cocktail was added to each filter well. For rNET binding experiment, the filters were transferred in 24-well scintillation plates and 600 µL of CytoScint was added to each well. All the plates/filters were counted using a PerkinElmer MicroBeta Microplate Counter. For each experiment, aliquots of the prepared radioligand solutions were measured to calculate the exact amount of radioactivity added, taking in account the experimentally determined top-counter efficiency for each radioligand. Ki values have been extrapolated by constraining the bottom of the dose−response curves (= 0% residual specific binding) in the nonlinear regression analysis. Ki values were calculated using GraphPad Prism 8 version 8.4.0 for Macintosh (GraphPad Software, San Diego, CA) utilizing One site- Fit Ki model. Kd values for the radioligands were determined S21 via separate homologous competitive binding or radioligand binding saturation experiments. Ki values were determined from at least three independent experiments performed in triplicate and are reported as mean +/- SEM.

Table A1: Optimization of Aerobic Oxidation

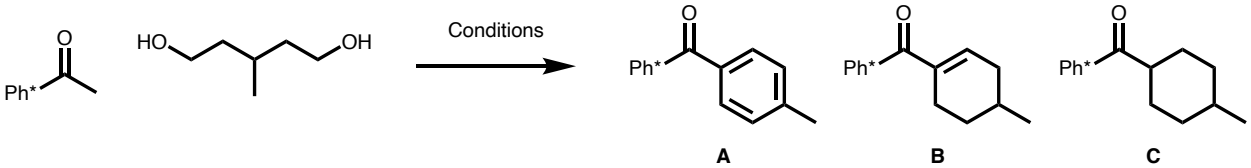

Full Table

Entry	PdX_2 (x mol%)	Oxidant (x eq)	Ligand (x mol%)	Additive (x eq)	Solvent (x M)	HNMR Yield A	HNMR Yield B	HNMR Yield C
1	$Pd(OAc)_2$ (1)	O_2 (g)	n/a	n/a	PhMe (2.5 M)	10.5	n/a	n/a

2	$Pd(OAc)_2$ (1)	CuCl2 (0.5 eq) + O_2(g)	n/a	n/a	PhMe (2.5 M)	10	0	0
3	$PdCl_2$ (1)	CuCl2 (0.5 eq) + O_2(g)	n/a	n/a	PhMe (1 M)	5	11	40
4	$Pd(OAc)_2$ (1)	O_2 (g)	n/a	n/a	PhMe (1 M)	9	3	32
5	$PdCl_2$ (1)	O_2 (g)	n/a	n/a	PhMe (1 M)	10	15	44
6	$Pd(TFA)_2$ (1)	O_2 (g)	n/a	n/a	PhMe (1 M)	7	3	0
7	$Pd(OAc)_2$ (1)	O_2 (g)	n/a	Neohexene (2 eq)	PhMe (1 M)	21	0	13
8	$Pd(OAc)_2$ (1)	O_2 (g)	n/a	Neohexene (4 eq)	n/a	10	n/a	7
9	$PdCl_2$ (1)	O_2 (g)	n/a	Neohexene (2 eq)	PhMe (1 M)	7	19	37
10	$PdCl_2$ (1)	O_2 (g)	n/a	Neohexene (4 eq)	PhMe (1 M)	10	4	n/a
11	$PdCl_2$ (2)	O_2 (g)	n/a	Neohexene (4 eq)	n/a	trace	trace	trace
12	$Pd(OAc)_2$ (2.5)	O_2 (g)	Xantphos (2.5)	Neohexene (2 eq)	PhMe (1 M)	10	16	44
13	$Pd(OAc)_2$ (2.5)	O_2 (g)	DPPE (2.5)	Neohexene (2 eq)	PhMe (1 M)	12	3	38
14	$Pd(OAc)_2$ (2.5)	O_2 (g)	DPPF (2.5)	Neohexene (2 eq)	PhMe (1 M)	5	17	n/a
15	$PdCl_2$ (1)	O_2 (g)	cataCXium A (2)	n/a	PhMe (1 M)	19	16	n/a
16	$PdCl_2$ (1)	O_2 (g)	Xantphos (1)	n/a	PhMe (1 M)	15	0	n/a
17	$PdCl_2$ (1)	O_2 (g)	DPPE (1)	n/a	PhMe (1 M)	7	20	37
18	$PdCl_2$ (5)	O_2 (g)	cataCXium A (10)	n/a	PhMe (1 M)	10	3	n/a
19	$Pd(OAc)_2$ (1)	O_2 (g)	n/a	n/a	PhMe (2.5 M)	10	n/a	n/a
20	$Pd(OAc)_2$ (1)	O_2 (g)	n/a	n/a	PhMe (1 M)	14	7	11
21	$Pd(OAc)_2$ (1)	O_2 (g)	n/a	n/a	PhMe (0.25M)	8	n/a	n/a
22	$Pd(OAc)_2$ (2)	O_2 (g)	n/a	NaOAc (0.5)	tBuOH (1 M)	trace	30	40

23	$Pd(OAc)_2$ (2)	O_2 (g)	n/a	NaOAc (0.5)	DMF (1 M)	2	0	n/a
24	$Pd(OAc)_2$ (2)	O_2 (g)	n/a	n/a	tBuOH (1 M)	1.5	30	50
25	$Pd(OAc)_2$ (2)	O_2 (g)	n/a	n/a	DMF (1 M)	2	4	n/a
26	$PdCl_2$ (1)	O_2 (g)	n/a	KCl (0.05)	PhMe (1 M)	3.5	12	0
27	$Pd(OAc)_2$ (1)	O_2 (g)	n/a	NaOAc (0.05)	PhMe (1 M)	18	19	n/a
28	$Pd(OAc)_2$ (1)	O_2 (g)	cataCXium A (2)	NaOAc (0.05)	PhMe (1 M)	10	0	n/a
29	$Pd(OAc)_2$ (2)	O_2 (g)	n/a	NaOAc (0.5)	PhMe (1 M)	6	43	n/a
30	$Pd(OAc)_2$ (2)	O_2 (g)	n/a	NaOAc (1)	PhMe (1 M)	4	36	46
All conditions use 1 eq. of Ph*COMe, 2 eq of diol, 2 eq. of KOtBu base, ran at 115 degrees C, for 24 hrs.								

Table A2: Optimization of Aromatization Reaction

Entry	**Substrate**	**PdX_2 (x mol%)**	**Oxidant (x eq)**	**Ligand (x mol%)**	**Additive (x eq)**	**Solvent (x M)**	**HNMR Yield (Isolated)**
1	Cy0	$Pd(TFA)_2$ (5)	$CuCl_2$ (2 eq)	n/a	n/a	DMF (2 M)	(25)
2	S3	$Pd(TFA)_2$ (5)	$CuCl_2$ (2 eq)	n/a	n/a	DMF (2 M)	(55)
3	S2	$Pd(TFA)_2$ (5)	$CuCl_2$ (2 eq)	n/a	n/a	DMF (2 M)	83 (63)
4	S4	$Pd(TFA)_2$ (5)	$CuCl_2$ (2 eq)	n/a	n/a	DMF (2 M)	(25)
5	S2	$Pd(OAc)_2$ (5)	$CuCl_2$ (2 eq)	n/a	n/a	DMF (2 M)	57

6	S2	$PdCl_2$ (5)	$CuCl_2$ (2 eq)	n/a	n/a	DMF (2 M)	50
7	S2	$Pd(TFA)_2$ (5)	$CuCl_2$ (1 eq)	n/a	n/a	DMF (2 M)	67
8	S2	$Pd(TFA)_2$ (5)	$CuCl_2$ (3 eq)	n/a	n/a	DMF (2 M)	37
9	S2	$Pd(TFA)_2$ (5)	$CuCl_2$ (2 eq)	2-NH_2-py (10)	n/a	DMF (2 M)	66
10	S2	$Pd(TFA)_2$ (5)	$CuCl_2$ (2 eq)	2-Me-py (10)	n/a	DMF (2 M)	40
11	S2	$Pd(TFA)_2$ (5)	$CuCl_2$ (2 eq)	2-COOH-py (10)	n/a	DMF (2 M)	44
12	S2	$Pd(TFA)_2$ (5)	$CuCl_2$ (2 eq)	2-F-py (10)	n/a	DMF (2 M)	50
15	S2	$Pd(TFA)_2$ (5)	$CuCl_2$ (2 eq)	2-NO_2-py (10)	n/a	DMF (2 M)	85
16	S2	$Pd(TFA)_2$ (5)	$CuCl_2$ (2 eq)	n/a	AcOH (2 drops)	DMF (1 M)	50
17	S2	$Pd(TFA)_2$ (5)	O_2 (g)	n/a	n/a	DMF (1 M)	trace
18	S2	$Pd(TFA)_2$ (5)	O_2 (g)	n/a	n/a	DMSO (1 M)	45
19	S2	$Pd(TFA)_2$ (5)	$CuCl_2$ (2 eq)	n/a	n/a	DMSO (1 M)	50
20	S2	$Pd(TFA)_2$ (5)	$CuCl_2$ (2 eq)	2-NO_2-py (20)	n/a	DMF (1 M)	46
21	S2	$Pd(TFA)_2$ (5)	$CuCl_2$ (2 eq)	2-NO_2-py (20)	n/a	DMSO (1 M)	44
22	S2	$Pd(TFA)_2$ (5)	O_2 (g)	2-NO_2-py (20)	n/a	DMSO (1 M)	33
23	S2	$Pd(TFA)_2$ (5)	$CuCl_2$ (2 eq)	Phenanthroline (20)	n/a	DMF (1 M)	40
24	S2	$Pd(TFA)_2$ (5)	$CuCl_2$ (2 eq)	2,2'-bipy. (20)	n/a	DMF (1 M)	40
25	S2	$Pd(TFA)_2$ (5)	$CuCl_2$ (2 eq)	n/a	NaTFA (0.2)	DMF (1 M)	60
26	Cy0	$Pd(TFA)_2$ (5)	$CuCl_2$ (2 eq)	n/a	NaTFA (0.2)	DMF (1 M)	35
27	Cy0	$Pd(TFA)_2$ (5)	$CuCl_2$ (2 eq)	n/a	n/a	DMF (1 M)	(21)
28	Cy0	$Pd(TFA)_2$ (5)	O_2 (g)	n/a	n/a	DMSO (1 M)	(16)
29[a]	S4	$Pd(TFA)_2$ (5)	$CuCl_2$ (2 eq)	n/a	n/a	DMF (0.5M)	(13)

30	S2	$Pd(TFA)_2$ (5)	O_2 (g)	n/a	n/a	Heptane (0.5M)	25
31	S2	$Pd(TFA)_2$ (5)	O_2 (g)	n/a	Norbornene (3)	DMSO (0.5M)	36
32	S2	$Pd(TFA)_2$ (5)	O_2 (g)	n/a	Et_3N (3)	DMSO (0.5M)	0
33	S2	$Pd(TFA)_2$ (5)	O_2 (g)	n/a	K_2CO_3 (3)	DMSO (0.5M)	0
34	S4	$Pd(TFA)_2$ (5)	O_2 (g)	n/a	n/a	NMP (0.5M)	0
35	S4	$Pd(TFA)_2$ (5)	$CuCl_2$ (2 eq)	n/a	n/a	NMP (0.5M)	26
36[f]	S4	$Pd(TFA)_2$ (5)	$CuCl_2$ (2 eq)	n/a	n/a	NMP (0.5M)	25
37	S4	$Pd(TFA)_2$ (5)	$CuCl_2$ (2 eq)	n/a	n/a	$PhNO_2$ (0.5M)	33 (31)
38	S4	$Pd(TFA)_2$ (5)	$CuCl_2$ (4 eq)	n/a	n/a	DMF (0.5M)	13
39	S4	$Pd(TFA)_2$ (5)	$CuCl_2$ (2 eq)	n/a	n/a	DMA (0.5M)	24
40	Cy0	$Pd(TFA)_2$ (5)	$CuCl_2$ (2 eq)	n/a	n/a	$PhNO_2$ (0.5M)	(44)
41	S4	$Pd(TFA)_2$ (5)	$CuCl_2$ (2 eq)	di-Me-phen (10)	n/a	DMF (0.5M)	(26)
42	S4	$Pd(TFA)_2$ (5)	$CuCl_2$ (2 eq)	2-NH_2-py (10)	n/a	DMF (0.5M)	(42)
43	S4	$Pd(TFA)_2$ (5)	$CuCl_2$ (2 eq)	2-NH_2-py (10)	TFA (2 drops)	DMF (0.5M)	trace
44	S4	$Pd(TFA)_2$ (5)	$CuCl_2$ (2 eq)	n/a	AgF (0.2)	DMF (0.5M)	(75)
45	S4	$Pd(TFA)_2$ (5)	$CuCl_2$ (2 eq)	n/a	AgTFA (0.2)	DMF (0.5M)	(69)
46	Cy0	$Pd(TFA)_2$ (5)	$CuCl_2$ (2 eq)	n/a	AgF (0.2)	DMF (0.5M)	(33)
47	S4	$Pd(TFA)_2$ (5)	$CuCl_2$ (2 eq)	n/a	AgF (0.2)	DMF (0.5M)	(31)
48[b]	S4	$Pd(TFA)_2$ (5)	$CuCl_2$ (2 eq)	n/a	AgF (0.2)	DMF (0.5M)	(35)
49[c]	S4	$Pd(TFA)_2$ (5)	$CuCl_2$ (2 eq)	n/a	AgF (0.2)	DMF (0.5M)	(34)
50	S4	$Pd(TFA)_2$ (5)	$CuCl_2$ (2 eq) + O_2 (g)	n/a	AgF (0.2)	DMF (0.5M)	(11)
51	S4	$Pd(TFA)_2$ (5)	$CuCl_2$ (2 eq)	n/a	AgF (0.5)	DMF (0.5M)	35

52[d]	S4	$Pd(TFA)_2$ (5)	$CuCl_2$ (2 eq)	n/a	AgF (0.2)	DMF (0.5M)	(50)
53	S4	$Pd(TFA)_2$ (10)	$CuCl_2$ (2 eq)	n/a	AgF (0.2)	DMF (0.5M)	(23)
54	S4	$Pd(TFA)_2$ (5)	$CuCl_2$ (2 eq)	n/a	Ag(TFA) (0.2)	DMF (0.5M)	(7)
55[e]	S4	$Pd(TFA)_2$ (5)	$CuCl_2$ (2 eq)	n/a	AgF (0.2)	DMF (0.5M)	(28)
56	Cy0	$Pd(TFA)_2$ (5)	$CuCl_2$ (2 eq)	n/a	AgF (0.2)	DMF (0.5M)	(38)
57	S4	$Pd(TFA)_2$ (5)	$CuCl_2$ (2 eq)	n/a	AgF (0.2)	DMF (0.5M)	(33)
58	S3	$Pd(TFA)_2$ (5)	$CuCl_2$ (2 eq)	n/a	AgF (0.2)	DMF (0.5M)	(40)
59	S2	$Pd(TFA)_2$ (5)	$CuCl_2$ (2 eq)	n/a	AgF (0.2)	DMF (0.5M)	(60)
60	S4	$Pd(TFA)_2$ (5)	$CuCl_2$ (2 eq)	2-NH_2-py (10)	n/a	DMF (0.5M)	(26)
61	Cy0	$Pd(TFA)_2$ (5)	$CuCl_2$ (2 eq)	2-NH_2-py (10)	n/a	DMF (0.5M)	(18)
62	Cy0	$Pd(TFA)_2$ (5)	$CuCl_2$ (2 eq)	2-NH_2-py (20)	AgF (0.2)	DMF (0.5M)	(28)
63	S3	$Pd(TFA)_2$ (5)	$CuCl_2$ (2 eq)	2-NH_2-py (20)	AgF (0.2)	DMF (0.5M)	n/a
64	S2	$Pd(TFA)_2$ (5)	$CuCl_2$ (2 eq)	2-NH_2-py (20)	AgF (0.2)	DMF (0.5M)	(35)
65	Cy0	$Pd(TFA)_2$ (5)	$CuCl_2$ (4 eq)	n/a	n/a	DMF (0.5M)	31
66	Cy0	$Pd(TFA)_2$ (5)	$CuOTf_2$ (2 eq)	n/a	n/a	DMF (0.5M)	13
67	Cy0	$Pd(TFA)_2$ (5)	$CuOTf_2$ (4 eq)	n/a	n/a	DMF (0.5M)	46 (49)
68[g]	Cy0	$Pd(TFA)_2$ (5)	$CuOTf_2$ (4 eq)	n/a	n/a	DMF (0.5M)	(45)
69[g]	Cy0	$Pd(TFA)_2$ (5)	$CuTFA_2 \cdot H_2O$ (4 eq)	n/a	n/a	DMF (0.5M)	3
70[h]	Cy0	$Pd(TFA)_2$ (5)	$CuTFA_2 \cdot H_2O$ (4 eq)	n/a	n/a	DMF (0.5M)	2
71i	Cy0	$Pd(TFA)_2$ (5)	$CuOTf_2$ (4 eq)	n/a	n/a	DMF (0.5M)	4
72j	Cy0	$Pd(TFA)_2$ (5)	$CuOTf_2$ (4 eq)	n/a	n/a	DMF (0.5M)	trace
73	Cy0	$Pd(TFA)_2$ (5)	$CuOTf_2$ (4 eq)	n/a	n/a	DMF (0.25M)	23

74	Cy0	$Pd(TFA)_2$ (5)	$CuOTf_2$ (4 eq)	n/a	n/a	DMF (0.1M)	10

All reactions ran at 115 degrees C over 18 hrs, following general procedure for aromatization.

[a] 48 hrs, [b] 10 hrs, [c] 24 hrs, [d]N2 atmosphere, [e] Aqueous work-up, [f] Temp 130 C. [g]45 hrs. [h] +3ÅMS. [i]Temp 90 C, [j]Temp 70 C.

Cy0: cyclohex-1-en-1-yl(2,3,4,5,6-pentamethylphenyl)methanone

S2: (4-methylcyclohex-1-en-1-yl)(2,3,4,5,6-pentamethylphenyl)methanone

S3: (3-methylcyclohex-1-en-1-yl)(2,3,4,5,6-pentamethylphenyl)methanone

S4: (2-methylcyclohex-1-en-1-yl)(2,3,4,5,6-pentamethylphenyl)methanone

Table A3: Optimization of TEMPO mediated aromatization

Entry	Hydrogen Borrowing Condition	[M] (x mol %) [L] (x mol %)	Additive (xeq)/change	TEMPO (eq)	Temp (C)	NMR yield (isolated)
1[a]	A	Cu(OAc)2 (10) Phen(10)	KOAc (3)	4	115	(41)
2	A	Cu(OAc)2 (10) Phen(10)	KOAc (3)	3	115	33 (11)
3	A	Cu(OAc)2 (10) Phen(10)	n.a	4	125	63
4	A	Cu(OAc)2 (10) 4,4'-$(CF_3)_2$bpy (10)	KOAc (3)	4	115	40
5	A	Cu(OTf)2 (10) Phen(10)	KOTf (3)	4	115	23
6	A	Cu(OAc)2 (20)	n.a	4	125	68

		Phen(20)				
7	A	Cu(OAc)2 (20) Phen(20)	Tert-amyl-OH:1,2-diCl-benzene (1:1)	4	125	65
8	A	Cu(OAc)2 (10) Phen(10)	n.a	4	135	72 (47)
9	A	Cu(OAc)2 (15) Phen(15)	n.a	4	135	49
10	A	Cu(OAc)2 (15) Phen(15)	NHIP (4 eq) + O2 instead of TEMPO.	0	125	0
11	A	Cu(OAc)2 (10) Phen(10)	tert-amyl-OH (0.1M)	4	125	31
12[b,c]	B	Cu(OAc)2 (10) Phen(10)	tert-amyl-OH (0.1M), diol (1.1 eq)	4	125	0
13	B	Cu(OAc)2 (10) Phen(10)	Diol (1.1 eq)	4	125	70 (53)
14	B	Cu(OAc)2 (10) Phen(10)	n.a.	6	125	(64)
15	B	Cu(OAc)2 (10) Phen(10)	O_2 (g) as oxidant	2	125	Trace
16	B	Cu(OAc)2 (10) Phen(10)	ABNO (6 eq) instead of TEMPO	0	125	19
17[d]	B	Cu(OAc)2 (10) Phen(10)	n.a	6	125	48
18	B	FeCl3-6H2O (10)	NaNO2 (0.1) O2 atm.	0.4	115	0
19	B	n.a.	Chloranil (2.5)		115	0
20	B	Cu(OAc)2 (10) Phen(10)	NHIP (5 eq) + O2 instead of TEMPO.	0	125	0
21	B	Cu(OAc)2 (10) Phen(10)	TFA (4 eq)	6	125	34
22	B	n.a.	n.a.	6	125	trace
23[e]	B	Cu(OAc)2 (10) Phen(10)	n.a.	6	125	54
24[f]	B	Cu(OAc)2 (10) Phen(10)	n.a.	6	125	34
25	B	Cu(OAc)2 (10) Phen(10)	NBS (4 eq) instead of TEMPO.	0	125	0
26[g]	B	Cu(OAc)2 (10)	n.a.	6	125	65

		Phen(10)				
27[g,h]	B	Cu(OAc)2 (10) Phen(10)	n.a.	6	125	56
28	B	Cu(OAc)2 (10) Phen(10)	n.a.	6	140	67
29	B	Cu(OAc)2 (10) Phen(10)	KOAc(1 eq)	6	140	61

All aromatizations following Conditions A proceeded in tert-amyl alcohol (0.5M), aromatizations following Conditions B in toluene (0.25M).
Condition A: Ph*COMe (0.3 mmol, 1 eq), 3-Me diol (1.1 eq), , KOtBu (0.5 eq), $[IrCp^*Cl_2]_2$ (2 mol %), tert-amyl-OH (1M), 115C.
Conditions B: Ph*COMe (0.3 mmol, 1 eq), 3-Me diol (1.5 eq), , KOtBu (1 eq), $[Ir(cod)Cl]_2$ (0.5 mol %), catacXium A(2 mol %) toluene (0.25M), 115C.
phen=1,10-phenanthroline.
4,4'-$(CF_3)_2$bpy = 4,4′-Di(trifluoromethyl)-2,2′-bypyridine
[a]Done at 1M instead of 0.5M
[b]Used $[IrCp^*Cl_2]_2$ instead of $[Ir(cod)Cl]_2$.
[c]tert-amyl-OH (0.25M) instead of toluene (0.25M)
[d]Used KOH (4eq) instead of KOtBu (1eq) during cyclyzation step.
[e]2 equivalents of diol used during cyclization.
[f]2 equivalents of KOtBu used during cyclization.
[g]degassing of solvent before cyclization step and before aromatization step.
[h]used 1,2-diCl-benzene as solvent.

TableA4: Computationally Predicted Values for triazole bearing compounds

compound	SMILES	hDAT_c34_inhibitor_Ki (log)	hDAT_c34+Newman (log)	hDAT_c34_uptake_IC50 (log)	hERG_c34_clamp_IC50 (log)
TC-001	CN1N=NC(CS(C(C2=CC=CC=C2)C3=CC=C(C)C=C3)=O)=C1	5.7	5.9	4.49	5.3
TC-002	CN1N=NC(CS(C(C2=CC=CC=C2)C3=CC=C(C(F)(F)F)C=C3)=O)=C1	5.56	5.63	4.47	5.3
TC-003	CN1N=NC(CS(C(C2=CC=CC=C2)C3=CC=C(CF)C=C3)=O)=C1	5.64	5.88	4.57	5.16
TC-004	CC(C)C(S(CC1=CN(C)N=N1)=O)C2=CC=C(F)C=C2	5.6	5.72	4.45	5.04
TC-005	CN1N=NC(CS(C(C2=CC=C(F)C=C2)C3=CC=CC=C3)=O)=C1	5.61	5.79	4.62	5.34
TC-006	CN1N=NC(CS(C(C2=CC=CC(F)=C2)C3=CC=CC=C3)=O)=C1	5.72	5.88	4.55	5.35
TC-007	CN1N=NC(CS(C(C2=CC=C(O)C=C2)C3=CC=CC=C3)=O)=C1	5.74	5.82	4.67	5.04
TC-008	CN1N=NC(CS(C(C2=CC=CC(O)=C2)C3=CC=CC=C3)=O)=C1	5.75	5.97	4.73	4.92

TC-009	CN1N=NC(CS(C(C2=CC=C(OC)C=C2)C3=CC=CC=C3)=O)=C1	5.63	5.72	4.49	5.25
TC-010	CN1N=NC(CS(C(C2=CC=CC(OC)=C2)C3=CC=CC=C3)=O)=C1	5.6	5.81	4.49	5.16
TC-011	CN1N=NC(CS(C(C2=CC=NC=C2)C3=CC=CC=C3)=O)=C1	5.52	5.57	4.6	4.89
TC-012	CN1N=NC(CS(C(C2=NC=NC=N2)C3=CC=CC=C3)=O)=C1	5.58	5.55	4.47	4.38
TC-013	CN1N=NC(CS(C(C2=CC=C(C#N)C=C2)C3=CC=CC=C3)=O)=C1	5.67	5.8	4.54	4.91
TC-014	CN1N=NC(CS(C(C2=CC=CC(C#N)=C2)C3=CC=CC=C3)=O)=C1	5.7	5.87	4.53	5
TC-015	CN1N=NC(CS(C(C2=CC=CC(Cl)=C2)C3=CC=CC=C3)=O)=C1	5.88	6.2	4.75	5.35
TC-016	CN1N=NC(CS(C(C2=CC=CC(Br)=C2)C3=CC=CC=C3)=O)=C1	5.84	6.2	4.7	5.46
TC-017	CN1N=NC(CS(C(C2=CC=C(C(N)=O)C=C2)C3=CC=CC=C3)=O)=C1	5.59	5.63	4.65	4.6
TC-018	CN1N=NC(CS(C(C2=CC=C(C(O)=O)C=C2)C3=CC=CC=C3)=O)=C1	5.6	5.65	4.6	4.75
TC-019	CN1N=NC(CS(C(C2=CC=CC(C(N)=O)=C2)C3=CC=CC=C3)=O)=C1	5.64	5.75	4.62	4.75
TC-020	CN1N=NC(CS(C(C2=CC=C(Cl)C=C2)C3=CC=CC=C3)=O)=C1	5.75	5.99	4.8	5.41
TC-021	CN1N=NC(CS(C(C2=CC=C(Br)C=C2)C3=CC=CC=C3)=O)=C1	5.72	6.01	4.73	5.44
TC-022	CN1N=NC(CS(C(C2=CC=CC(C(O)=O)=C2)C3=CC=CC=C3)=O)=C1	5.7	5.76	4.54	4.87
TC-023	CN1N=NC(CS(C(C2=CC=CC(C(OC)=O)=C2)C3=CC=CC=C3)=O)=C1	5.59	5.6	4.43	4.95
TC-024	CN1N=NC(CS(C(C2=CC=C(C(OC)=O)C=C2)C3=CC=CC=C3)=O)=C1	5.59	5.51	4.46	4.86
TC-025	O=S(CC1=CN(CC2=CC=CC=C2)N=N1)C(C3=CC=CC=C3)C4=CC=C(C)C=C4	5.89	6.16	4.56	5.53
TC-026	O=S(CC1=CN(CC2=CC=CC=C2)N=N1)C(C3=CC=CC=C3)C4=CC=C(C(F)(F)F)C=C4	5.83	5.99	4.43	5.53
TC-027	O=S(CC1=CN(CC2=CC=CC=C2)N=N1)C(C3=CC=CC=C3)C4=CC=C(CF)C=C4	5.83	6.09	4.49	5.44
TC-028	CC(C)C(S(CC1=CN(CC2=CC=CC=C2)N=N1)=O)C3=CC=C(F)C=C3	5.85	6.1	4.43	5.48
TC-029	O=S(CC1=CN(CC2=CC=CC=C2)N=N1)C(C3=CC=C(F)C=C3)C4=CC=CC=C4	5.87	6.1	4.62	5.45
TC-030	O=S(CC1=CN(CC2=CC=CC=C2)N=N1)C(C3=CC=CC(F)=C3)C4=CC=CC=C4	5.91	6.09	4.56	5.45
TC-031	O=S(CC1=CN(CC2=CC=CC=C2)N=N1)C(C3=CC=C(O)C=C3)C4=CC=CC=C4	5.88	6.07	4.4	5.27
TC-032	O=S(CC1=CN(CC2=CC=CC=C2)N=N1)C(C3=CC=CC(O)=C3)C4=CC=CC=C4	5.9	6.06	4.57	5.06
TC-033	O=S(CC1=CN(CC2=CC=CC=C2)N=N1)C(C3=CC=C(OC)C=C3)C4=CC=CC=C4	5.77	5.99	4.38	5.52
TC-034	O=S(CC1=CN(CC2=CC=CC=C2)N=N1)C(C3=CC=CC(OC)=C3)C4=CC=CC=C4	5.82	6.07	4.36	5.35
TC-035	O=S(CC1=CN(CC2=CC=CC=C2)N=N1)C(C3=CC=NC=C3)C4=CC=CC=C4	5.87	6.03	4.43	5.24
TC-036	O=S(CC1=CN(CC2=CC=CC=C2)N=N1)C(C3=NC=NC=N3)C4=CC=CC=C4	5.61	5.87	4.31	4.9
TC-037	O=S(CC1=CN(CC2=CC=CC=C2)N=N1)C(C3=CC=C(C#N)C=C3)C4=CC=CC=C4	5.87	5.99	4.44	5.22

TC-038	O=S(CC1=CN(CC2=CC=CC=C2)N=N1)C(C3=CC=CC(C#N)=C3)C4=CC=CC=C4	5.84	5.99	4.42	5.28
TC-039	O=S(CC1=CN(CC2=CC=CC=C2)N=N1)C(C3=CC=CC(Cl)=C3)C4=CC=CC=C4	5.92	6.18	4.58	5.53
TC-040	O=S(CC1=CN(CC2=CC=CC=C2)N=N1)C(C3=CC=CC(Br)=C3)C4=CC=CC=C4	5.89	6.21	4.55	5.61
TC-041	O=S(CC1=CN(CC2=CC=CC=C2)N=N1)C(C3=CC=C(C(N)=O)C=C3)C4=CC=CC=C4	5.75	5.97	4.55	4.91
TC-042	O=S(CC1=CN(CC2=CC=CC=C2)N=N1)C(C3=CC=C(C(O)=O)C=C3)C4=CC=CC=C4	5.73	5.83	4.54	5
TC-043	O=S(CC1=CN(CC2=CC=CC=C2)N=N1)C(C3=CC=CC(C(N)=O)=C3)C4=CC=CC=C4	5.78	6.02	4.58	5.11
TC-044	O=S(CC1=CN(CC2=CC=CC=C2)N=N1)C(C3=CC=C(Cl)C=C3)C4=CC=CC=C4	5.87	6.15	4.63	5.55
TC-045	O=S(CC1=CN(CC2=CC=CC=C2)N=N1)C(C3=CC=C(Br)C=C3)C4=CC=CC=C4	5.82	6.18	4.61	5.61
TC-046	O=S(CC1=CN(CC2=CC=CC=C2)N=N1)C(C3=CC=C(C(OC)=O)C=C3)C4=CC=CC=C4	5.7	5.86	4.47	5.17
TC-047	O=S(CC1=CN(CC2=CC=CC=C2)N=N1)C(C3=CC=CC(C(OC)=O)=C3)C4=CC=CC=C4	5.63	5.78	4.48	5.23
TC-048	O=S(CC1=CN(CC2=CC=CC=C2)N=N1)C(C3=CC=CC(C(O)=O)=C3)C4=CC=CC=C4	5.86	6.03	4.5	5.14
TC-049	CC1=CC=C(C(SCC2=CN(CC3=CC=CC=C3)N=N2)C4=CC=CC=C4)C=C1	6.22	6.39	5.03	5.34
TC-050	FC(C1=CC=C(C(SCC2=CN(CC3=CC=CC=C3)N=N2)C4=CC=CC=C4)C=C1)(F)F	6.09	6.08	5	5.53
TC-051	FCC1=CC=C(C(SCC2=CN(CC3=CC=CC=C3)N=N2)C4=CC=CC=C4)C=C1	6.1	6.25	5.1	5.53
TC-052	CC(C)C(SCC1=CN(CC2=CC=CC=C2)N=N1)C3=CC=C(F)C=C3	5.86	6.14	5.2	5.62
TC-053	FC(C=C1)=CC=C1C(SCC2=CN(CC3=CC=CC=C3)N=N2)C4=CC=CC=C4	6.09	6.3	5.1	5.55
TC-054	FC1=CC(C(SCC2=CN(CC3=CC=CC=C3)N=N2)C4=CC=CC=C4)=CC=C1	6.05	6.2	5.05	5.6
TC-055	OC(C=C1)=CC=C1C(SCC2=CN(CC3=CC=CC=C3)N=N2)C4=CC=CC=C4	6.1	6.24	5.02	5.36
TC-056	OC1=CC(C(SCC2=CN(CC3=CC=CC=C3)N=N2)C4=CC=CC=C4)=CC=C1	6.13	6.26	5.09	5.33
TC-057	COC(C=C1)=CC=C1C(SCC2=CN(CC3=CC=CC=C3)N=N2)C4=CC=CC=C4	5.96	6.11	4.96	5.49
TC-058	O=S(CC1=CN(CC2=CC=CC=C2)N=N1)C(C3=CC=CC(OC)=C3)C4=CC=CC=C4	5.82	6.07	4.36	5.35
TC-059	C1(C(SCC2=CN(CC3=CC=CC=C3)N=N2)C4=CC=NC=C4)=CC=CC=C1	6.05	6.24	4.99	5.42
TC-060	C1(C(SCC2=CN(CC3=CC=CC=C3)N=N2)C4=NC=NC=N4)=CC=CC=C1	5.8	5.93	4.8	5.05
TC-061	N#CC(C=C1)=CC=C1C(SCC2=CN(CC3=CC=CC=C3)N=N2)C4=CC=CC=C4	6.14	6.16	5.06	5.42
TC-062	N#CC1=CC(C(SCC2=CN(CC3=CC=CC=C3)N=N2)C4=CC=CC=C4)=CC=C1	6.04	6.12	5.15	5.49
TC-063	ClC1=CC(C(SCC2=CN(CC3=CC=CC=C3)N=N2)C4=CC=CC=C4)=CC=C1	6.07	6.23	5.16	5.53
TC-064	BrC1=CC(C(SCC2=CN(CC3=CC=CC=C3)N=N2)C4=CC=CC=C4)=CC=C1	6.07	6.27	5.05	5.42
TC-065	O=C(N)C(C=C1)=CC=C1C(SCC2=CN(CC3=CC=CC=C3)N=N2)C4=CC=CC=C4	5.92	6.04	5.47	4.96
TC-066	O=C(O)C(C=C1)=CC=C1C(SCC2=CN(CC3=CC=CC=C3)N=N2)C4=CC=CC=C4	6	5.96	5.23	5

TC-067	NC(C1=CC(C(SCC2=CN(CC3=CC=CC=C3)N=N2)C4=CC=CC=C4)=CC=C1)=O	5.81	6.08	5.49	5.14
TC-068	ClC(C=C1)=CC=C1C(SCC2=CN(CC3=CC=CC=C3)N=N2)C4=CC=CC=C4	6.18	6.37	5.18	5.56
TC-069	BrC(C=C1)=CC=C1C(SCC2=CN(CC3=CC=CC=C3)N=N2)C4=CC=CC=C4	6.16	6.39	5.05	5.44
TC-070	O=C(OC)C(C=C1)=CC=C1C(SCC2=CN(CC3=CC=CC=C3)N=N2)C4=CC=CC=C4	5.91	5.89	5.29	5.42
TC-071	O=C(OC)C1=CC(C(SCC2=CN(CC3=CC=CC=C3)N=N2)C4=CC=CC=C4)=CC=C1	5.75	5.82	5.3	5.47
TC-072	OC(C1=CC(C(SCC2=CN(CC3=CC=CC=C3)N=N2)C4=CC=CC=C4)=CC=C1)=O	5.9	5.96	5.22	5.21
TC-073	CN1N=NC(CSC(C2=CC=CC=C2)C3=CC=C(C)C=C3)=C1	5.68	5.88	4.87	5.34
TC-074	CN1N=NC(CSC(C2=CC=CC=C2)C3=CC=C(C(F)(F)F)C=C3)=C1	5.68	5.77	4.93	5.34
TC-075	CN1N=NC(CSC(C2=CC=CC=C2)C3=CC=C(CF)C=C3)=C1	5.47	5.64	4.95	5.34
TC-076	CC(C)C(SCC1=CN(C)N=N1)C2=CC=C(F)C=C2	5.48	5.78	5.08	5.41
TC-077	CN1N=NC(CSC(C2=CC=C(F)C=C2)C3=CC=CC=C3)=C1	5.53	5.71	4.93	5.45
TC-078	CN1N=NC(CSC(C2=CC=CC(F)=C2)C3=CC=CC=C3)=C1	5.64	5.83	4.86	5.46
TC-079	CN1N=NC(CSC(C2=CC=C(O)C=C2)C3=CC=CC=C3)=C1	5.75	5.8	5.01	5.14
TC-080	CN1N=NC(CSC(C2=CC=CC(O)=C2)C3=CC=CC=C3)=C1	5.81	5.9	5.08	5.17
TC-081	CN1N=NC(CSC(C2=CC=C(OC)C=C2)C3=CC=CC=C3)=C1	5.52	5.68	4.85	5.24
TC-082	CN1N=NC(CS(C(C2=CC=CC(OC)=C2)C3=CC=CC=C3)=O)=C1	5.6	5.81	4.49	5.16
TC-083	CN1N=NC(CSC(C2=CC=NC=C2)C3=CC=CC=C3)=C1	5.74	5.82	4.87	5.32
TC-084	CN1N=NC(CSC(C2=NC=NC=N2)C3=CC=CC=C3)=C1	5.53	5.63	4.66	4.71
TC-085	CN1N=NC(CSC(C2=CC=C(C#N)C=C2)C3=CC=CC=C3)=C1	5.5	5.73	4.88	5.2
TC-086	CN1N=NC(CSC(C2=CC=CC(C#N)=C2)C3=CC=CC=C3)=C1	5.4	5.76	4.95	5.35
TC-087	CN1N=NC(CSC(C2=CC=CC(Cl)=C2)C3=CC=CC=C3)=C1	5.81	6.02	5.06	5.55
TC-088	CN1N=NC(CSC(C2=CC=CC(Br)=C2)C3=CC=CC=C3)=C1	5.88	6.19	4.93	5.53
TC-089	CN1N=NC(CSC(C2=CC=C(C(N)=O)C=C2)C3=CC=CC=C3)=C1	5.65	5.76	5.32	4.85
TC-090	CN1N=NC(CSC(C2=CC=C(C(O)=O)C=C2)C3=CC=CC=C3)=C1	5.65	5.78	5.08	4.9
TC-091	CN1N=NC(CSC(C2=CC=CC(C(N)=O)=C2)C3=CC=CC=C3)=C1	5.68	5.88	5.32	5
TC-092	CN1N=NC(CSC(C2=CC=C(Cl)C=C2)C3=CC=CC=C3)=C1	5.8	5.96	5.1	5.51
TC-093	CN1N=NC(CSC(C2=CC=C(Br)C=C2)C3=CC=CC=C3)=C1	5.79	6.05	4.93	5.49
TC-094	CN1N=NC(CSC(C2=CC=C(C(OC)=O)C=C2)C3=CC=CC=C3)=C1	5.63	5.71	5.17	5.14
TC-095	CN1N=NC(CSC(C2=CC=CC(C(OC)=O)=C2)C3=CC=CC=C3)=C1	5.56	5.72	5.18	5.23

TC-096	CN1N=NC(CSC(C2=CC=CC(C(O)=O)=C2)C3=CC=CC=C3)=C1	5.73	5.82	5.09	5.08
TC-097	ClC(C=C1)=CC=C1C(SCC2=CN(CC3=CC=CC=C3)N=N2)C4=CC=C(C)C=C4	6.21	6.34	5.18	5.6
TC-098	ClC(C(Cl)=C1)=CC=C1C(SCC2=CN(CC3=CC=CC=C3)N=N2)C4=CC=CC=C4	6.23	6.33	5.3	5.83
TC-099	BrC(C(Br)=C1)=CC=C1C(SCC2=CN(CC3=CC=CC=C3)N=N2)C4=CC=CC=C4	6.23	6.28	5.17	5.72
TC-100	BrC1=CC=C(C(C2=CC=CC=C2)SCC3=CN(C4=CC=CC=C4)N=N3)C=C1	6.11	6.37	4.91	5.54
TC-101	ClC1=CC=C(C(C2=CC=CC=C2)SCC3=CN(C4=CC=CC=C4)N=N3)C=C1	6.18	6.34	5.04	5.59
TC-102	BrC1=CC(C(SCC2=CN(CC3=CC=CC=C3)N=N2)C4=CC=NC=C4)=CC=C1	6.04	6.21	4.96	5.57
TC-103	BrC1=CC(C(SCC2=CN(CC3=CC=CC=C3)N=N2)C4=NC=CC=N4)=CC=C1	5.93	6.01	4.99	5.37
TC-104	BrC(C=C1)=CC=C1C(SCC2=CN(CC3=CC=CC=C3)N=N2)C4=CC=C(C)C=C4	6.2	6.36	5.06	5.5
TC-105	CC1=CC=C(C(C2=CC=CC(Br)=C2)SCC3=CN(CC4=CC=CC=C4)N=N3)C=C1	6.17	6.28	5.12	5.48
TC-106	CC1=CC=C(C(C2=CC=CC(Cl)=C2)SCC3=CN(CC4=CC=CC=C4)N=N3)C=C1	6.17	6.26	5.2	5.58
TC-107	BrC1=CC=CC(C(C2=CC=CC=C2)SCC3=CN(C4=CC=CC=C4)N=N3)=C1	6.09	6.37	4.98	5.5
TC-108	ClC1=CC=CC(C(C2=CC=CC=C2)SCC3=CN(C4=CC=CC=C4)N=N3)=C1	6.16	6.36	5.05	5.56
TC-109	BrC1=CC(C(SCC2=CN(CC3=CC=CC=C3)N=N2)C4=CN=CC=C4)=CC=C1	5.95	6.15	5.01	5.54
TC-110	BrC1=CC(C(SCC2=CN(CC3=CC=CC=C3)N=N2)C4=CN=CN=C4)=CC=C1	5.91	6.04	4.94	5.42
TC-111	BrC1=CC=C(C(C2=CC=CC(C)=C2)SCC3=CN(CC4=CC=CC=C4)N=N3)C=C1	6.18	6.3	5.14	5.47
TC-112	ClC1=CC=C(C(C2=CC=CC(C)=C2)SCC3=CN(CC4=CC=CC=C4)N=N3)C=C1	6.17	6.25	5.22	5.57
TC-113	ClC1=CC=C(C(C2=CC=C(C=CC=C3)C3=C2)SCC4=CN(CC5=CC=CC=C5)N=N4)C=C1	6.3	6.07	5.17	5.66
TC-114	BrC1=CC=CC(C(C2=CC=C(NC=C3)C3=C2)SCC4=CN(CC5=CC=CC=C5)N=N4)=C1	6.14	6.07	5.31	5.46
TC-115	BrC1=CC=CC(C(C2=CC3=C(C=CC=C3)N2)SCC4=CN(CC5=CC=CC=C5)N=N4)=C1	6.2	6.05	5.38	5.25
TC-116	BrC1=CC(C(SCC2=CN(CC3=CC=CC=C3)N=N2)C4=COC=N4)=CC=C1	6.03	6.12	5.13	5.42
TC-117	BrC1=CC(C(SCC2=CN(CC3=CC=CC=C3)N=N2)C4=NC=NC=N4)=CC=C1	5.96	6.04	4.94	5.28
TC-118	FC(C=C1)=CC=C1C(SCC2=CN(CC3=CC=CC=C3)N=N2)C4=CC=C(F)C=C4	6.26	6.31	5.09	5.64
TC-119	BrC1=CC(C(SCC2=CN(CC3=CC=CC=C3)N=N2)C4CCCCC4)=CC=C1	6.27	6.25	5.47	5.77
TC-120	BrC1=CC(C(SCC2=CN(CC3=CC=CC=C3)N=N2)C4=CN=CO4)=CC=C1	5.98	6.08	5.14	5.51
TC-121	BrC1=CC=CC(C(C2=CNC3=C2C=CC=C3)SCC4=CN(CC5=CC=CC=C5)N=N4)=C1	6.08	6.06	5.32	5.45
TC-122	BrC1=CC=C(C(CC2=CC=CC=C2)SCC3=CN(CC4=CC=CC=C4)N=N3)C=C1	6.05	6.26	5.27	5.54
TC-123	BrC1=CC=CC(C(CC2=CC=CC=C2)SCC3=CN(CC4=CC=CC=C4)N=N3)=C1	5.99	6.18	5.25	5.54
TC-124	BrC1=CC=CC(C(C2=CC=C(C=CC=C3)C3=C2)SCC4=CN(CC5=CC=CC=C5)N=N4)=C1	6.29	6.02	5.1	5.51

TC-125	BrC(C=C1)=CC=C1C(SCC2=CN(CC3=CC=C(OC)C=C3)N=N2)C4=CC=CC=C4	6.05	6.28	5	5.57
TC-126	BrC(C=C1)=CC=C1C(SCC2=CN(CC3=CC=C(C(O)=O)C=C3)N=N2)C4=CC=CC=C4	6.07	6.19	5.19	5.34
TC-127	BrC(C=C1)=CC=C1C(SCC2=CN(CC3=CC=CC(F)=C3)N=N2)C4=CC=CC=C4	6.14	6.13	5.01	5.56
TC-128	BrC(C=C1)=CC=C1C(SCC2=CN(CC3=CC=C(C4=CC=CC=C4)C=C3)N=N2)C5=CC=CC=C5	6.2	6	5.11	5.59
TC-129	BrC(C=C1)=CC=C1C(SCC2=CN(CC3=C(C=CC4=CC=CC(C=C5)=C46)C6=C5C=C3)N=N2)C7=CC=CC=C7	6.15	5.84	5.37	5.61
TC-130	BrC(C=C1)=CC=C1C(SCC2=CN(CC3=CC=CC(C)=C3)N=N2)C4=CC=CC=C4	6.19	6.26	5.09	5.44
TC-131	BrC(C=C1)=CC=C1C(SCC2=CN(CC3=CC=CC=C3F)N=N2)C4=CC=CC=C4	6.06	6.16	5.07	5.55
TC-132	BrC(C=C1)=CC=C1C(SCC2=CN(CC3=CC=C(C(C)(C)C)C=C3)N=N2)C4=CC=CC=C4	6.15	6.22	5.42	5.63
TC-133	BrC(C=C1)=CC=C1C(SCC2=CN(CC3=CC=CC=C3Cl)N=N2)C4=CC=CC=C4	6.1	6.24	5.2	5.68
TC-134	BrC(C=C1)=CC=C1C(SCC2=CN(CC3=CC=CC=C3C#N)N=N2)C4=CC=CC=C4	6.09	6.22	5.06	5.46
TC-135	BrC(C=C1)=CC=C1C(SCC2=CN(CC3=CC(C(O)=O)=CC=C3)N=N2)C4=CC=CC=C4	6.07	6.2	5.17	5.27
TC-136	BrC(C=C1)=CC=C1C(SCC2=CN(CC3=CC=C(F)C=C3)N=N2)C4=CC=CC=C4	6.17	6.21	5.06	5.65
TC-137	BrC(C=C1)=CC=C1C(SCC2=CN(CC3=CC=C(C)C=C3)N=N2)C4=CC=CC=C4	6.19	6.35	5.11	5.56
TC-138	BrC(C=C1)=CC=C1C(SCC2=CN(CC3=CC=CC=C3C)N=N2)C4=CC=CC=C4	6.17	6.29	5.11	5.51
TC-139	BrC(C=C1)=CC=C1C(SCC2=CN(CC3=CC=C(Cl)C=C3)N=N2)C4=CC=CC=C4	6.22	6.32	5.24	5.74
TC-140	CC(C=C1)=CC=C1C(SCC2=CN(CC3=CC=C(OC)C=C3)N=N2)C4=CC=CC=C4	6.11	6.22	5.02	5.51
TC-141	CC(C=C1)=CC=C1C(SCC2=CN(CC3=CC=C(C(O)=O)C=C3)N=N2)C4=CC=CC=C4	6.18	6.19	5.23	5.41
TC-142	CC(C=C1)=CC=C1C(SCC2=CN(CC3=CC=CC(F)=C3)N=N2)C4=CC=CC=C4	6.14	6.22	5.06	5.56
TC-143	CC(C=C1)=CC=C1C(SCC2=CN(CC3=CC=C(C4=CC=CC=C4)C=C3)N=N2)C5=CC=CC=C5	6.32	6.27	5.25	5.58
TC-144	CC(C=C1)=CC=C1C(SCC2=CN(CC3=C(C=CC4=CC=CC(C=C5)=C46)C6=C5C=C3)N=N2)C7=CC=CC=C7	6.19	6.12	5.44	5.62
TC-145	CC(C=C1)=CC=C1C(SCC2=CN(CC3=CC=CC(C)=C3)N=N2)C4=CC=CC=C4	6.19	6.17	5.1	5.33
TC-146	CC(C=C1)=CC=C1C(SCC2=CN(CC3=CC=CC=C3F)N=N2)C4=CC=CC=C4	6.1	6.22	5.09	5.55
TC-147	CC(C=C1)=CC=C1C(SCC2=CN(CC3=CC=C(C(C)(C)C)C=C3)N=N2)C4=CC=CC=C4	6.27	6.37	5.35	5.5
TC-148	CC(C=C1)=CC=C1C(SCC2=CN(CC3=CC=CC=C3Cl)N=N2)C4=CC=CC=C4	6.17	6.24	5.24	5.54
TC-149	CC(C=C1)=CC=C1C(SCC2=CN(CC3=CC=CC=C3C#N)N=N2)C4=CC=CC=C4	6.07	6.07	5.13	5.47
TC-150	CC(C=C1)=CC=C1C(SCC2=CN(CC3=CC(C(O)=O)=CC=C3)N=N2)C4=CC=CC=C4	6.11	6.12	5.19	5.31
TC-151	CC(C=C1)=CC=C1C(SCC2=CN(CC3=CC=C(F)C=C3)N=N2)C4=CC=CC=C4	6.16	6.3	5.13	5.66
TC-152	CC(C=C1)=CC=C1C(SCC2=CN(CC3=CC=C(C)C=C3)N=N2)C4=CC=CC=C4	6.19	6.31	5.12	5.46
TC-153	CC(C=C1)=CC=C1C(SCC2=CN(CC3=CC=CC=C3C)N=N2)C4=CC=CC=C4	6.15	6.21	5.1	5.42

TC-154	CC(C=C1)=CC=C1C(SCC2=CN(CC3=CC=C(Cl)C=C3)N=N2)C4=CC=CC=C4	6.22	6.35	5.25	5.64
TC-155	COC(C=C1)=CC=C1CN2N=NC(CSC(C3=CC=CC(Br)=C3)C4=CC=CC=C4)=C2	6.04	6.24	5.02	5.55
TC-156	OC(C(C=C1)=CC=C1CN2N=NC(CSC(C3=CC=CC(Br)=C3)C4=CC=CC=C4)=C2)=O	6.09	6.15	5.18	5.35
TC-157	FC1=CC(CN2N=NC(CSC(C3=CC=CC(Br)=C3)C4=CC=CC=C4)=C2)=CC=C1	6.09	6.19	4.99	5.73
TC-158	BrC1=CC(C(SCC2=CN(CC3=CC=C(C4=CC=CC=C4)C=C3)N=N2)C5=CC=CC=C5)=CC=C1	6.2	5.89	5.08	5.59
TC-159	BrC1=CC(C(SCC2=CN(CC3=C(C=CC4=CC=CC(C=C5)=C46)C6=C5C=C3)N=N2)C7=CC=CC=C7)=CC=C1	6.16	5.84	5.38	5.61
TC-160	CC1=CC(CN2N=NC(CSC(C3=CC=CC(Br)=C3)C4=CC=CC=C4)=C2)=CC=C1	6.15	6.27	5.1	5.55
TC-161	FC1=CC=CC=C1CN2N=NC(CSC(C3=CC=CC(Br)=C3)C4=CC=CC=C4)=C2	6.06	6.15	5.08	5.52
TC-162	CC1=CC=CC=C1CN2N=NC(CSC(C3=CC=CC(Br)=C3)C4=CC=CC=C4)=C2	6.16	6.28	5.16	5.44
TC-163	CC(C=C1)=CC=C1CN2N=NC(CSC(C3=CC=CC(Br)=C3)C4=CC=CC=C4)=C2	6.17	6.28	5.11	5.45
TC-164	FC(C=C1)=CC=C1CN2N=NC(CSC(C3=CC=CC(Br)=C3)C4=CC=CC=C4)=C2	6.13	6.15	5.06	5.62
TC-165	O=C(O)C1=CC=CC(CN2N=NC(CSC(C3=CC=CC(Br)=C3)C4=CC=CC=C4)=C2)=C1	6.09	6.21	5.14	5.51
TC-166	BrC1=CC(C(SCC2=CN(CC3=CC=CC=C3C#N)N=N2)C4=CC=CC=C4)=CC=C1	6.14	6.24	5.06	5.46
TC-167	ClC1=CC=CC=C1CN2N=NC(CSC(C3=CC=CC(Br)=C3)C4=CC=CC=C4)=C2	6.07	6.19	5.22	5.62
TC-168	CC(C)(C)C(C=C1)=CC=C1CN2N=NC(CSC(C3=CC=CC(Br)=C3)C4=CC=CC=C4)=C2	6.12	6.14	5.39	5.53
TC-169	ClC(C=C1)=CC=C1CN2N=NC(CSC(C3=CC=CC(Br)=C3)C4=CC=CC=C4)=C2	6.19	6.25	5.22	5.63
TC-170	BrC1=CC(C(SCC2=CN(C3=CC=C(Cl)C=C3)N=N2)C4=CC=CC=C4)=CC=C1	6.19	6.33	5.13	5.85
TC-171	BrC1=CC(C(SCC2=CN(C3=CC(F)=CC=C3)N=N2)C4=CC=CC=C4)=CC=C1	6.06	6.14	4.97	5.59
TC-172	FC(F)(F)C1=CC=CC(CN2N=NC(CSC(C3=CC=CC(Br)=C3)C4=CC=CC=C4)=C2)=C1	6.06	6.08	4.89	5.75
TC-173	BrC1=CC(C(SCC2=NN(C3=CC=CC=C3)N=C2)C4=CC=CC=C4)=CC=C1	6.08	6.4	4.99	5.52
TC-174	ClC(C=C1)=CC=C1N2N=NC(CSC(C3=CC=C(C)C=C3)C4=CC=CC=C4)=C2	6.22	6.3	5.11	5.59
TC-175	FC1=CC=CC(N2N=NC(CSC(C3=CC=C(C)C=C3)C4=CC=CC=C4)=C2)=C1	6.05	6.2	4.94	5.62
TC-176	FC(F)(F)C1=CC=CC(CN2N=NC(CSC(C3=CC=C(C)C=C3)C4=CC=CC=C4)=C2)=C1	6.28	6.18	5.04	5.53
TC-177	CC(C=C1)=CC=C1C(SCC2=NN(C3=CC=CC=C3)N=C2)C4=CC=CC=C4	6.15	6.32	4.9	5.55
TC-178	ClC(C=C1)=CC=C1N2N=NC(CSC(C3=CC=C(Br)C=C3)C4=CC=CC=C4)=C2	6.23	6.32	5.09	5.73
TC-179	FC1=CC=CC(N2N=NC(CSC(C3=CC=C(Br)C=C3)C4=CC=CC=C4)=C2)=C1	6.06	6.13	4.93	5.6
TC-180	FC(F)(F)C1=CC=CC(CN2N=NC(CSC(C3=CC=C(Br)C=C3)C4=CC=CC=C4)=C2)=C1	6.13	6.09	4.99	5.54
TC-181	BrC(C=C1)=CC=C1C(SCC2=NN(C3=CC=CC=C3)N=C2)C4=CC=CC=C4	6.1	6.38	4.92	5.56